SYNTHESIS AND APPLICATIONS OF METATHESIS-DERIVED FUNCTIONAL MONOLITHIC MEDIA

Von der Fakultät Chemie der Universität Stuttgart
zur Erlangung der Würde eines
Doktors der Naturwissenschaften (Dr. rer. nat.) genehmigte Abhandlung

vorgelegt von
Sudheendran Mavila, M.Sc.
aus Kerala/Indien

Erstberichter:	Prof. Dr. Michael R. Buchmeiser
Mitberichter:	Prof. Dr. René Peters
Zusätzlicher Prüfer:	Prof. Dr.-Ing. Elias Klemm
Tag der mündlichen Prüfung:	19/12/2011

Institut für Polymer Chemie
der Universität Stuttgart
2011

To my dear parents.....

Most of what I knew was left untold,
Most of what I spoke was hardly worthy,
While you hate me with half your heart,
Forgive me with the other half;
This is my flesh and blood,
and this is all I have left to offer.

-Balachandran Chullikkad

അറിഞ്ഞതിൽ പാതി പറയാതെ പോയി
പറഞ്ഞതിൽ പാതി പതിരായും പോയി
പകുതി ഹൃത്തിനാൽ വെറുക്കുമ്പോഴെന്നെ
പകുതി ഹൃത്തിനാൽ പൊറുത്തുകൊള്ളുക
ഇതെന്റെ രക്തമാണിതെന്റെമാംസമാണെടുത്തുകൊള്ളുക

ബാലചന്ദ്രൻ ചുള്ളിക്കാട്

(This thesis work was done during June/2008–December/2009 at Leibniz-Institute of Surface Modification e. V. (IOM), Leipzig, Germany and January/2010–December/2011, at the Institute of Polymer Chemistry, University of Stuttgart, under the supervision of ***Prof. Dr. Michael. R. Buchmeiser****)*

Acknowledgements

Let me convey my 'vote of thanks' to all those who helped me to materialize this manuscript.

First and foremost, I am obliged to Prof. Dr. Michael.R. Buchmeiser, for offering me a doctoral position in his workgroup and for the motivation and encouragement he provided during my tenure as a PhD student. I am hugely benefited from the excellent guidance, stimulating suggestions and valuable advises that he conveys to his co-workers.

I am grateful to Prof. Dr. René Peters and Prof. Dr.-Ing. Elias Klemm for their willingness to be my examiners and also for the interesting collaboration projects.

My sincere thanks to Frau Dorothea Zippel at IOM, Leipzig, Dr. Gabriele Hardtmann, Frau Dagmar Schuhmacher, Frau Sandra Ost for helping me out in administrative matters. Frau Panicker-Otto deserves special mention for her immense support and care that made my academic and personal life at ease.

I am grateful to all those who provided the technical and analytical support to complete this thesis work. Dr. Dongren Wang, Dr. Ulrich Decker for NMR, Mrs. Christa Kühnel for GPC.

Many thanks to Herrn Jan Pigorsch for assisting me in ordering the chemicals and other required things. Special thanks to Dr. Rajander Bandari, Guram Venkata Narayan and Dr. Santhosh Kumar for their sincere help throughout my PhD programme.

I would like to thank Simon Eitel, Dr. Alaxander Seifert and Andrea Inan productive discussions and their experimental contribution to the collaboration projects. Many thanks Eric Roeben for his experimental contribution one of my project during his deploma thesis.

Thanks a ton to all my colleagues in Stuttgart and in Leipzig for their support and intimacy on and off the academia. Special thanks to Jörg Unold for the translation of my abstracts and also to Benjamin Autenrieth, Falk Brustmann for their kindness for solving all the official formalities.

I am hugely indebted to my previous research mentors, Prof. Faiz. Ahmed Khan at IIT Kanpur and Dr. Ashish Baren Mandel for their guidance, inspiration and the expertise I gained from their laboratories. I also owe a lot to all my teachers-especially Ramanathan sir and Madhavan sir (higher-secondary), Janaki teacher (bachelors), and Asokan sir (masters)- from schooling to graduation who influenced me to the core and played such an important role in shaping up my career and self.

My very special thanks to all my dear friends, Rajesh Keloth, Naveen Prasad, Kishore Kumar in my hometown. Sreekumar, Krishnamohan, Saju, Sreeraj, Ramesh, Gopan, Sreenivasan and Rajesh komban, friends from my home university deserve a lot for what they are always; selfless, motivating and funny that entertained and enriched my life a lot. Thanks a lot to my friends here in and out of Stuttgart Shaju Albert and wife, Michael Marino, Marina, Gopalakrishnan Frank for the lively social circle and entertainment.

Last but never the least, I express my sincere gratitude to my dear and loving wife Kavitha Sudheendran, my parents, brothers, mother-in-law and sisters-in-law for their life-long love, support and intimacy. I bow to the almighty for strengthening me to follow the destiny.

Contents

List of Abbreviations and Symbols

Å	Angstrom
ACN	Acetonitrile
ATR	Attenuated total reflection
BA	*N*-α-benzoyl-DL-arginine
BAPNA	*N*-α-benzoyl-DL-arginine-*p*-nitroanilide
3-Br-Py	3-Bromo pyridine
Calcd.	Calculated
COE	*cis*-Cyclooctene
d	day(s)
d	Doublet
DCM	Dichloromethane
DEDPM	Dipropargyl diethylmalonate
DMAP	4-Dimethylaminopyridine
DMF	*N*,*N*-Dimethylformamide
DMNH6	1,4,4a,5,8,8a-hexahydro-1,4,5,8-exo-endo-dimethanonaphthalene
DMSO	Dimethylsulfoxide
dr	diastereomeric ratio
ee	enantiomeric excess
ELMI	Electron microscopic image
equiv	Equivalents
ESI	Electrospray ionisation
Et	Ethyl
et al.	And others
Et_2O	Diethyl ether
Et_3N	Triethylamine
EtOAc	Ethyl acetate
EVE	Ethyl vinyl ether
FBIP-Cl	Ferrocen-1,1’-diyl bisimidazoline bis-palladacycles
FT-IR	Fourier transform infrared
g	Gram
GA	Glutaraldehyde
GC-MS	Gas chromatography-mass spectrometry
GPC	Gel permeation chromatography
h	Hours
HEPES	4-(2-Hydroxyethyl)piperazine-1-ethanesulfonic acid
HOAc	Acetic acid
HRMS	High resolution mass spectra
Hz	Hertz
$IMesH_2$	1,3-Dimesitylimidazolin-2-ylidene
ISEC	Inverse size exclusion chromatography
J	Coupling constants in Hertz
ki	Rate of initiation
kp	Rate of propagation
$LiAlH_4$	Lithium aluminium hydride
M	molar
m	Multiplet
m/z	mass/charge

M^+	Molecular ion
MeOH	Methanol
mg	Milligram
MHz	Megahertz (10^6 Hz)
min	Minute
mL	Milliliter
mmol	Millimol
M_n	Number average molecular weight
mol-%	Molar percentage
MS	Mass spectroscopy
mW	milli-Watts
M_w	Weight average molecular weight
NBE	Norborn-2-ene
NHC	N-Heterocyclic carbene
NMR	Nuclear magnetic resonance
$NO^+BF_4^-$	Nitrosyl tetraflourobarate
OLEDs	Organic light emitting diodes
PCy_3	Tricyclohexylphosphine
PDI	Poly dispersity index
Ph	Phenyl
PNA	*p*-Nitro aniline
ppm	Parts per million
PS	Polystyrene
q	Quartet
RCM	Ring-closing metathesis
RP-HPLC	Reverse phase- high-performance liquid chromatography
ROMP	Ring-opening metathesis polymerization
rt	Room temperature
s	Singlet
S/cm	Siemens per centimetre
SEC	Size exclusion chromatography
SPS	Solvent purification system
t	Triplet
TBAB	Tetrabutylammoniumbromide
TEPA	Tetraethylenepentamine
THF	Tetrahydrofuran
TMS	Trimethylsilane
TON	Turn-over number
UV-Vis	Ultra violet-visible
wt.-%	Weight percentage
λmax	Wavelength of maximum optical absorption
µL	Microliter
µmol	Micromol

Specific projects in this thesis have been presented/appeared in:

Publications

- A Continuous Bioreactor Prepared via the Immobilization of Trypsin on Aldehyde Functionalized, Ring-Opening Metathesis Polymerization-Derived Monoliths, **M. Sudheendran**, M. R. Buchmeiser, *Macromolecules* **2010**, *43*, 9601.

- Heterogenization of a Chiral Bimetallic Catalyst on a ROMP-Derived Monolithic Support: Applications in Enantioselective Michael Addition, **M. Sudheendran**, Simon Eitel, R. Peters, M. R. Buchmeiser, (Manuscript in preparation)

- Cyclopolymerization-Derived Conductive Monolithic Media For Continuous Heterogeneous (Electro-) Catalysis, **M. Sudheendran**, E. Roeben, P. S. Kumar, M. R. Buchmeiser, (Manuscript in preparation)

- Cyclopolymerization-Derived Block Copolymers of 4, 4-Bis(octyloxymethyl)-1,6-heptadiyne and Dipropargyl malonodinitrile, **M. Sudheendran**, M. R. Buchmeiser, (Manuscript in preparation)

Poster Presentations

1. Cyclopolymerization-Derived Conductive Monolithic Media. **M. Sudheendran**, P. S. Kumar, M. R. Buchmeiser, *The 3rd EuCheMS Chemistry Congress "Chemistry-the Creative Force"*, August 29-September 2, 2010, Nurnberg, Germany.

2. Cyclopolymerization-Derived Conductive Monolithic Media For Continuous Heterogeneous (Electro-) Catalysis, **M. Sudheendran**, E. Roeben, P. S. Kumar, M. R. Buchmeiser, *The 19th International Symposium on Olefin Metathesis and Related Chemistry* (ISOM XIX), July 10-15, 2011, Rennes, France.

Oral Presentations

1. A Continuous Bioreactor Prepared via the Immobilization of Trypsin on Aldehyde Functionalized, Ring-Opening Metathesis Polymerization-Derived Monoliths, 15. Tag der Organischen Chemie, 14th October 2011, Institut für Organische chemie, Universität Stuttgart.

Zusammenfassung

Mittlerweile haben übergangsmetallkatalysierte Metathesepolymerisationen sowie verwandte Methoden einen hohen Stellenwert in der organischen Synthesechemie und der Polymerchemie erreicht. Folglich ist das Interesse an Metathese-basierten monolithischen Materialien für die heterogene Katalyse sowie für chromatographische Anwendungen beachtlich gestiegen.

Das erste Kapitel der vorliegenden Arbeit gibt einen Überblick über den hohen Stellenwert der Metathese im Arbeitsgebiet Polymer-basierter monolithischer Materialien sowie über die historische Entwicklung der Metathesechemie und die Synthese Metathese-basierter Polymere bis hin zur aktuellen Entwicklung und Anwendung. Im letzten Jahrzehnt konnte eine beeindruckende Entwicklung in der Ring öffnenden Metathesepolymerisation (ROMP) mit Ruthenium-Initiatoren beobachtet werden. Dies kann dem Fortschritt in der Synthese von wohl definierten Katalysatoren zugeschrieben werden. Interessanterweise existieren divergierende Ansichten über die Stabilität von Ruthenium-Initiatoren gegenüber Luft, Wasser, Nitrilen, Aminen usw. Trotzdem wurde bisher der synthetische Nutzen der Umsetzung von Ruthenium-Alkylidenen mit Sauerstoff wenig erforscht.

Konsequenter weise befasst sich das zweite Kapitel dieser Arbeit mit der Untersuchung einer neuen und zweckmäßigen Synthese von Aldehyd-semitelechelen ROMP-Polymeren, wobei die Metathesereaktion lebender Ruthenium-Alkyliden Endgruppen mit Sauerstoff verwendet wird (Abbildung 1). Desweiteren werden die vielfältigen Möglichkeiten der Funktionalisierung von ROMP-hergestellten Polymeren nach Terminierung mit Sauerstoff beschrieben und der Nutzen dieser Reaktion für Materialwissenschaften und Biokatalyse diskutiert. Die ROMP von Norborn-2-en (NBE) und *cis*-Cycloocten (COE) wurde mit definierten Grubbs-Initiatoren wie $RuCl_2(PCy_3)_2(=CHPh)$, $[RuCl_2(PCy_3)(IMesH_2)(CHPh)]$, und $[RuCl_2(3\text{-Br-Py})_2(IMesH_2)(CHPh)]$ ($MesH_2$ = 1,3-bis(2,4,6-trimethylphenyl) imidazolin-2-yliden, PCy_3 = tricyclohexylphosphin, 3-Br-Py = 3-bromopyridin) durchgeführt. Die Synthese von Aldehyd-semitelechelen Polymeren durch die Reaktion von lebenden Polymeren mit Luftsauerstoff konnte in Abhängigkeit vom verwendeten Initiator und Monomer bis zu einer Ausbeute von 80% durchgeführt werden.

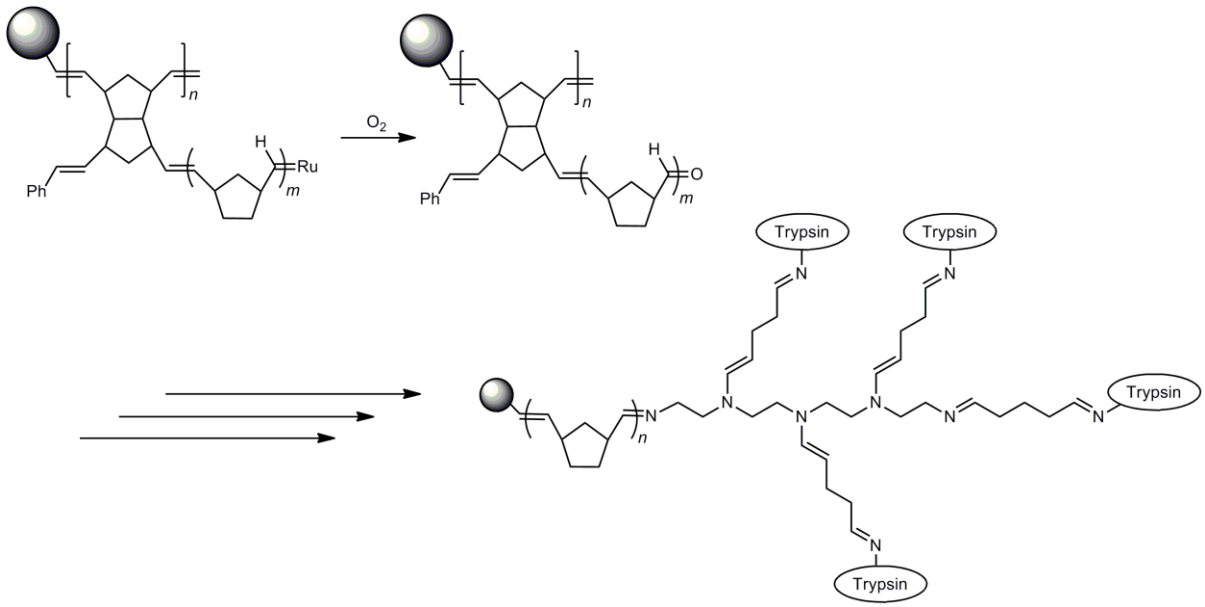

Abbildung 1. Synthese von Aldehyd-telechelen Monolithen und Immobilisierung von Trypsin.

Um die Aldehyd-Bildung zu beweisen, wurden die terminalen Aldehydgruppen in die entsprechenden 2,4-Dinitrophenylhydrazin-Derivate überführt und die Struktur der Hydrazone mittels NMR- und IR-Spektroskopie bestätigt. Diese simple Methode wurde anschließend bei der Funktionalisierung ROMP-basierter Monolithen ausgehend von NBE, 1,4,4a,5,8,8a-hexahydro-1,4,5,8-*exo*-*endo*-dimethanonaphthalin (DMN-H6) und $(NBE\text{-}CH_2O)_3SiCH_3$ angewandt, um Aldehyd-funktionalisierte Monolithe zu erhalten. Die Menge des gebildeten Aldehyds wurde über die Menge an gebildetem Hydrazon bestimmt. Auf diese Weise konnten bis zu 8 μm Aldehydgruppen pro Gramm Monolith erzeugt werden. Schließlich wurden diese Aldehyd-funktionalisierten Monolithe zur Immobilisierung von Trypsin verwendet. Es konnte eine hervorragende proteolytische Aktivität des immobilisierten Enzyms sowohl unter Batch-Bedingungen als auch unter kontinuierlichem Durchfluss beobachtet werden.

Das dritte Kapitel befasst sich mit der Entwicklung eines auf monolithischem Material immobilisierten chiralen bimetallischen Katalysators, der sich unter anderem für enantioselektive Michael-Additionen eignet. Die Immobilisierung von chiralen Katalysatoren hat aufgrund der hohen Kosten des verwendeten Metalls, sowie des chiralen Liganden erhebliche Bedeutung erlangt. Folglich sind Systeme, welche die einfache Abtrennung des teuren chiralen Katalysators von der Reaktionsmischung ermöglichen und eine Produktkontaminierung durch Auswaschen des Metalls verhindern, erstrebenswert und ermöglichen effizientes Recycling.

In diesem Kapitel wird die Anwendbarkeit von monolithischen Trägermaterialien, welche durch ROMP zugänglich sind, für die Immobilisierung solcher Katalysatoren untersucht. Ein geeigneter Zugang für die Immobilisierung wurde durch ROMP mittels Grubbs-Katalysatoren der ersten Generation $RuCl_2(PCy_3)_2(=CHPh)$ geschaffen. Norborn-5-en-2-ylmethylhexafluoro-5-oxohexansäure und Mono(norborn-5-en-2-ylmethyl) hexafluoroglutarat wurden hierbei auf die Oberfläche des Monolithen durch Reaktion mit den lebenden Kettenenden aufpolymerisiert (Abbildung 2).

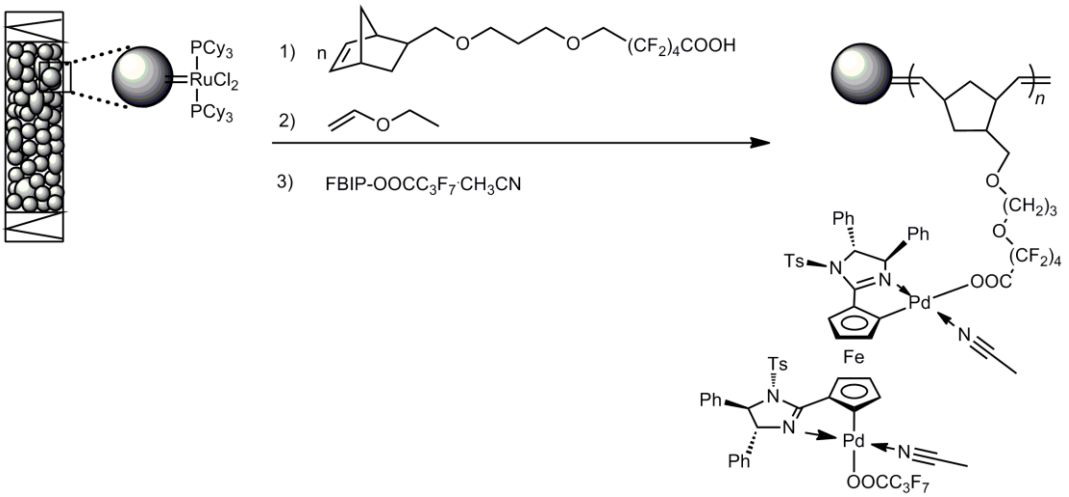

Abbildung 2. Synthese eines Monolith-immobilisierten chiralen bimetallischen Katalysators.

Die Immobilisierung des bimetallischen Katalysators mit entsprechenden Gegenion wurde durch die Reaktion des aktivierten Komplexes mit einem aufgepfropften Polymer, welches freie Säurefunktionalitäten besitzt, erfolgreich durchgeführt. Die auf diese Weise aufgebrachten Katalysatoren wurden anschließend in der enantioselektiven Michael-Addition von *tert*-Butyl 2-cyano-2-phenylacetat an 2-Cyclohexen-1-on am Institut für Organische Chemie, AK Professor Peters, getestet.

Das große Potential redoxaktiver Enzyme organische Reaktionen regio- und stereoselektiv umzusetzen, erklärt die Motivation, neue innovative Strategien im Gebiet der elektrochemischen Biokatalyse auszuarbeiten. Allerdings liegt die größte Schwierigkeit der kommerziellen Anwendung redoxaktiver Katalysatorsysteme in der Notwendigkeit eines kontinuierlichen Elektronenflusses zum Metallzentrum. Zu diesem Zweck wurden leitfähige Polymere als Medium für den Ladungstransport von den Elektroden zu dem elektrochemisch aktiven Bioenzym entwickelt.

Das vierte Kapitel dieser Arbeit beschäftigt sich mit dem bisher unerforschten Ansatz leitfähige, monolithische Materialen mittels Zyklopolymerisation herzustellen, indem Tris(4-methyl-1,6-heptadiin)benzol-1,3,5-tricarboxylat und Bis(4-methyl-1,6-heptadiin)terephthalat als Vernetzer mit 2-Propanol und 1,2-Dichloroethan als Porogene verwendet wurden. *N*-Hydroxysuccinimid-(1,6-heptadiin-4-yl)carboxylat und 4-Trimethylsiloxymethyl-1,6-heptadiin wurden als funktionelle Monomere und [Ru(CF_3COO)$_2$(1,3-dimesitylimidazolin-2-ylidene)(CH-2-(2-PrO)-C_6H_4)] als Katalysator eingesetzt (Abbildung 3). Durch Elementaranalyse wurde bewiesen, dass etwa 77% der funktionellen Monomere auf der Oberfläche der Mikroglobuli aufgebracht werden konnten. Auf diese Weise sind diese für die Reaktion mit redoxaktiven Katalysatoren, über Aminogruppen, leicht zugänglich.

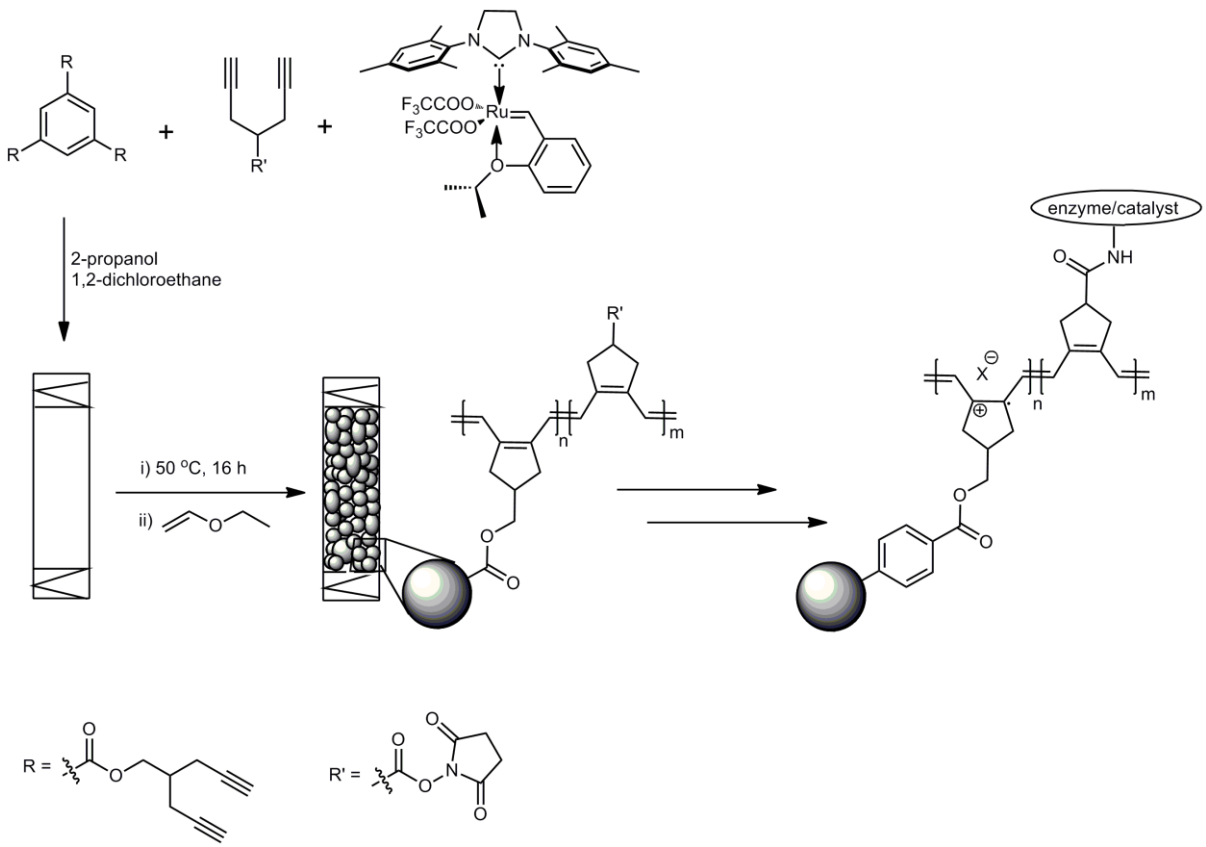

Abbildung 3. Immobilisierung von Enzymen auf Zyklopolymerisation-basierten leitfähigen Monolithen.

Nach Dotierung mit verschiedenen p-Dotierungsmittel in geeigneten Lösungsmitteln, konnte mit diesen Monolithen eine Leitfähigkeit von $6x10^{-4}$ Scm^{-1} erreicht werden. Darüberhinaus konnte Trypsin erfolgreich auf dem dotierten Trägermaterial immobilisiert werden ohne dass eine Schädigung des Enzyms festgestellt wurde. Dies wurde durch die exzellente proteolytische Aktivität des immobilisierten Enzyms gezeigt. Des Weiteren wurden die Synthese,

Charakterisierung und Anwendungsmöglichkeiten dieser neuen monolithischen Materialien in diesem Kapitel beschrieben.

Das Thema des letzten Kapitels ist die Synthese eines telechelen AB-Blockcopolymers von 4,4-Bis(octyloxymethyl)-1,6-heptadiin und Dipropargyl-malonodinitril mittels Metathese-basierter Zyklopolymerisation mit wohldefinierten Molybdän- und Rutheniuminitiatoren. Die Polymerisationen mit Rutheniuminitiatoren führten aufgrund von signifikantem „back biting“ nicht zur Bildung von Blockpolymeren. Daraufhin wurden detaillierte Untersuchungen über den Einfluss der Reaktionsbedingungen auf das Auftreten von „back biting“ für beide Monomere durchgeführt. Es konnten deutliche Verbesserungen in der Unterdrückung des „back bitings“ durch die Verwendung von $[Ru(NCO)_2(IMesH_2)(=CH\text{-}2\text{-}(2\text{-}PrO)\text{-}C_6H_4]$ und $[Ru(NCO)_2(3\text{-}Br\text{-}Py)_2(IMesH_2)(CHPh)]$, ($IMesH_2$ = 1,3-dimesytylimidazolin-2-ylidene, 3-Br-Py = 3-bromopyridine) als Katalysatoren für die Zyklopolymerisation erreicht werden.

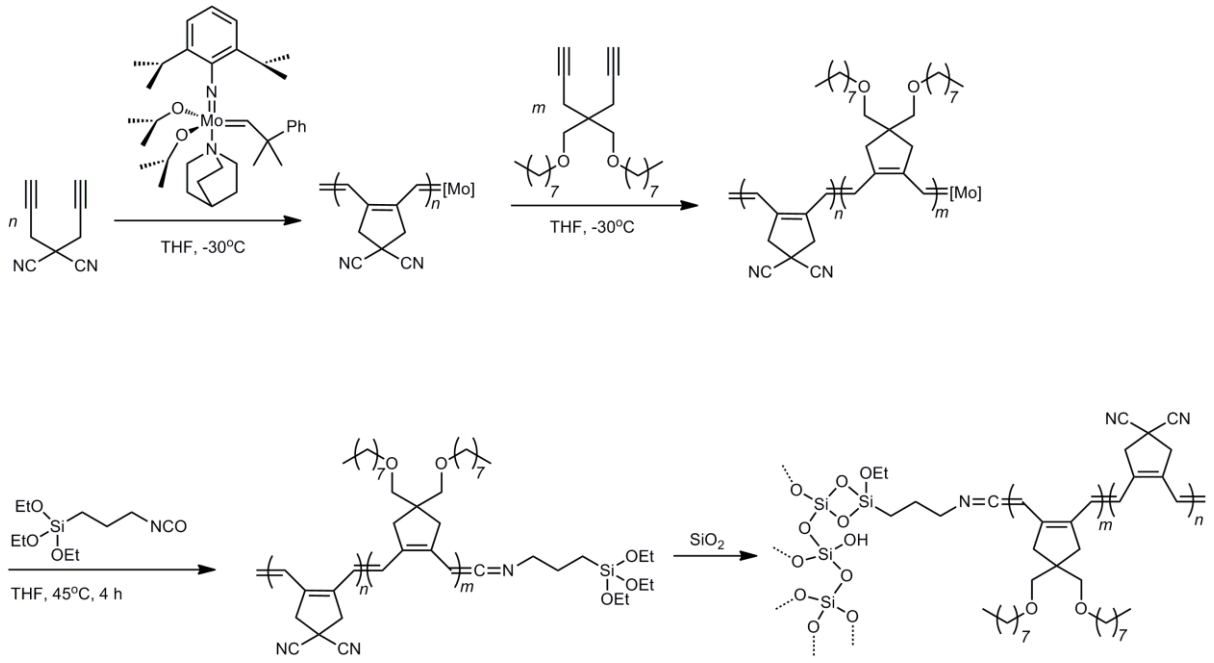

Abbildung 4. Synthese von Triethoxysilyl-Endgruppen-funktionalisierten AB-Block copolymer von 4,4-bis(octyloxymethyl)-1,6-heptadiinund Dipropargyl-malonodinitril.

Die erfolgreiche Synthese dieses Blockcoploymers konnte schließlich durch die Verwendung des optimierten Molybdän-Schrock-Katalysators (*N*-2,6-*i*-$Pr_2C_6H_3$)($CHCMe_2Ph$)($OCH(CH_3)_2$)$_2$ und THF als Lösungsmittel erzielt werden. Daraufhin konnte im Rahmen dieser Untersuchungen die Endgruppenfunktionalisierung des Blockpolymers mit $EtO)_3SiCH_2CH_2CH_2N=C=O$ zur Festphasenanbindung an Kieselgel realisiert werden (Abbildung 4).

Abstract

Among transition metal-catalysed polymerizations, metathesis polymerization and related techniques have gained a strong position in synthetic organic and polymer chemistry. Therefore, the synthesis of metathesis–derived functional monolithic supports for heterogeneous catalysis as well as for separation sciences has received considerable attention.

The first chapter of this thesis deals with an overview on the key discoveries that revealed the pertinence of metathesis in the field of polymeric monolithic materials. The text also offers a short excursion to the historical background of metathesis reactions and metathesis-derived polymeric materials. A few sections are devoted to the recent developments in metathesis-derived polymeric monoliths and their most recent applications.

The last decade witnessed an impressive progress in the ring-opening metathesis polymerization (ROMP), particularly with ruthenium-based initiators. This tremendous popularity is attributed to the progressive development in the discovery of well-defined catalytic system. Interestingly, there exist diverging reports on the stability of Ru-based initiators vs oxygen, water, nitriles, amines etc. However, the synthetic utility of the reaction of Ru-alkylidenes with oxygen remains little-explored. The second chapter of this thesis addresses the exploration of a novel and convenient method for the synthesis of ROMP-derived aldehyde-semitelechelic polymers via the metathesis of living Ru-alkylidenes of ROMP-derived polymers with O_2 (Scheme I).

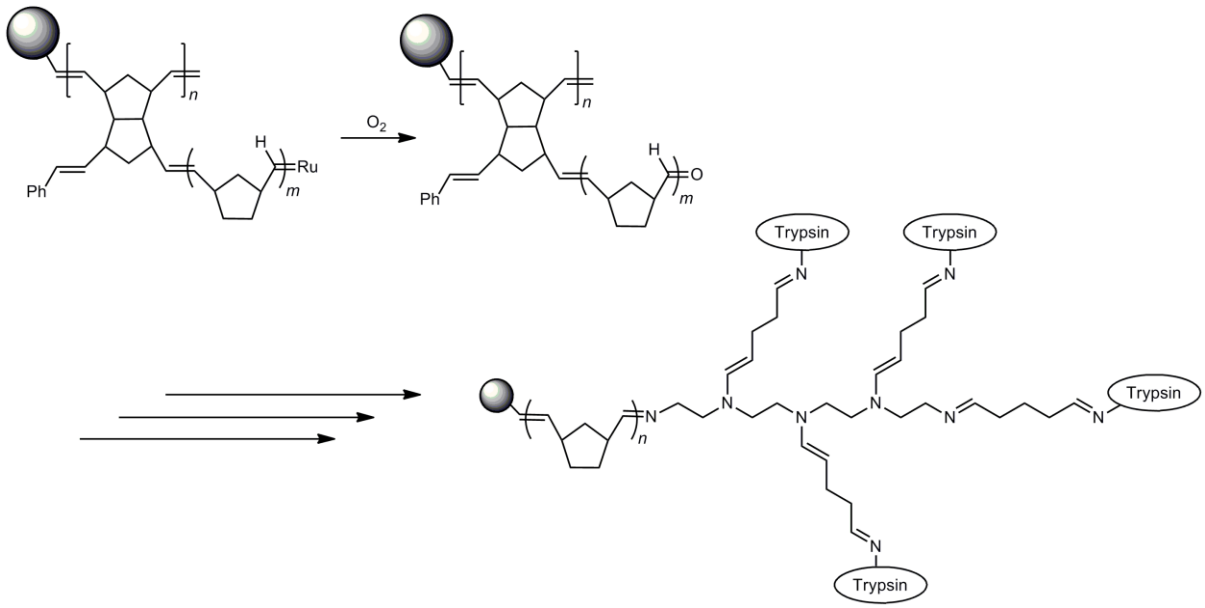

Scheme I. Synthesis of aldehyde-telechelic monoliths and immobilization of trypsin.

This study also describes as to what extent ROMP-derived polymers can be functionalized upon termination with O_2 and in which form this reaction can be useful to material science and biocatalysis. The ROMP of norborn-2-ene (NBE) and *cis*-cyclooctene (COE) was initiated with well-defined Grubbs-type initiators, i.e., $RuCl_2(PCy_3)_2(=CHPh)$, $[RuCl_2(PCy_3)(IMesH_2)(=CHPh)]$, and $[RuCl_2(3\text{-Br-Py})_2(IMesH_2)(CHPh)]$ ($MesH_2$ = 1,3-bis(2,4,6-trimethylphenyl)imidazolin-2-ylidene, PCy_3 = tricyclohexylphosphine, 3-Br-Py = 3-bromopyridine). Reaction of the living polymers with O_2 (air) resulted in the formation of aldehyde-semitelechelic polymers in up to 80% yield, depending on the initiator and monomer used. To proof aldehyde formation, the terminal aldehyde groups were converted into the corresponding 2,4-dinitrophenylhydrazine derivatives, and the structure of the hydrazones was confirmed by NMR and IR spectroscopy. This simple methodology was then used for the functionalization of ROMP-derived monoliths prepared from NBE, 1,4,4a,5,8,8a-hexahydro-1,4,5,8-*exo*-*endo*-dimethanonaphthalene (DMN-H6) and $(NBE\text{-}CH_2O)_3SiCH_3$, to yield aldehyde-funtionalized monoliths. The extent of aldehyde formation was determined by hydrazone formation. Up to 8 μmol of aldehyde groups/g of the monolith could be generated by this approach. Finally, these aldehyde-functionalized monoliths were used for the immobilization of trypsin. Excellent proteolytic activity of the immobilized enzyme was found in both under batch and continuous flow conditions.

The third chapter of this thesis was done in collaboration with Prof. Dr. René Peter's group at Institute of Organic Chemistry, University of Stuttgart. This project focuses on the development of a supported version of a chiral bimetallic catalyst suitable for the enantioselective Michael-additions. The heterogenization of such chiral catalysts has received considerable attention due to the high costs for both the metal and the chiral ligands. Therefore, system that allow for the straightforward separation of expensive chiral catalysts from reaction mixtures and minimum product contamination by metal leaching and efficient recycling are highly desirable. In this chapter, the utility of ROMP-derived monolithic support for the heterogenization of such catalyst is explored. A suitable support for immobilization was prepared via ROMP using the "1st generation Grubbs catalyst", $RuCl_2(PCy_3)_2(=CHPh)$. Norborn-5-ene-2-ylmethyl hexafluoro-5-oxohexanoic acid and mono(norborn-5-ene-2-ylmethyl) hexafluoroglutarate were surface-grafted utilizing the living termini on to the monolithic support via a grafting from approach (Scheme II).

The immobilization of the bimetallic catalyst with a proper counter ion was successfully accomplished by the reaction of the activated complex with free carboxylic acid groups of the graft polymer. The thus prepared supported catalysts were then used for the enantioselective Michael additions of *tert*-butyl 2-cyano-2-phenylacetate to 2-cyclohexen-1-one.

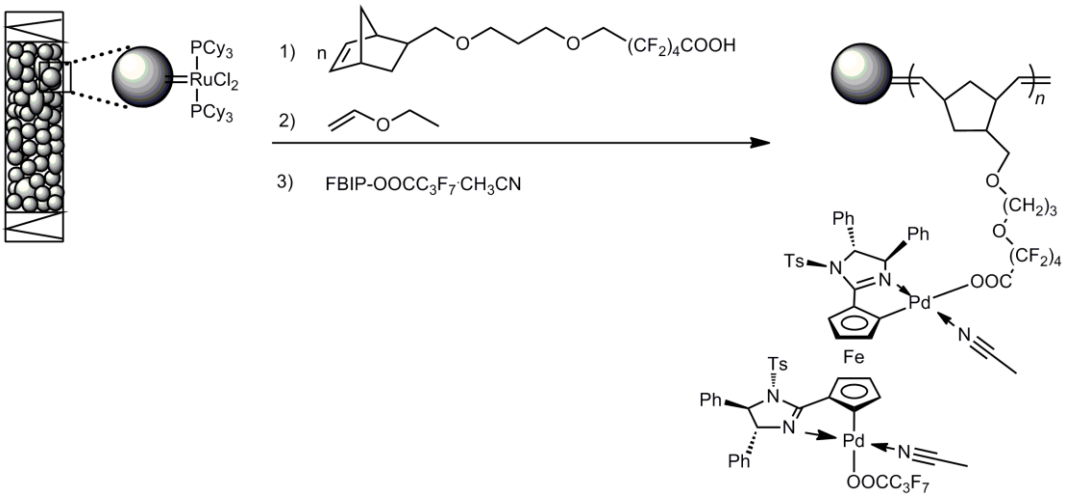

Scheme II. Synthesis of a monolith-supported chiral bimetallic catalyst.

The large potential of redox active enzymes to carry out valuable organic tranformations with very high regio-and stereoselectivity encouraged the scientists towards the search for novel strategies in electrode-driven biocatalysis. However, a major hurdle for implementing such a redox-active catalysis for commercial syntheses is the requirements for a continuous electron supply to the metal center. For this purpose, conductive polymeric materials have received considerable attention as a medium for the charge transfer from the electrode to the electrochemically active bioenzyme. The fourth chapter of this thesis address an unprecedented cyclopolymerization-based approach to conductive monolithic media using tris(4-methyl-1,6-heptadiyne) benzene-1,3,5-tricarboxylate and bis(4-methyl-1,6-heptadiyne) terephthalate as cross-linkers and 2-propanol and 1,2-dichloroethane as porogens. *N*-hydroxysuccinimide-(1,6-heptadiyne-4-yl) carboxylate and 4-trimethylsiloxymethyl-1,6-heptadyine was used as a functional monomer, the polymerization was initiated by [Ru(CF_3COO)$_2$(1,3-dimesitylimidazolin-2-ylidene)(CH-2-(2-PrO)-C_6H_4)] (Scheme III). Approximately 77% of the functional monomers were located at the surface of the microglobules as evidenced by elemental analysis. This way, they are readily accessible to the reaction with redox-active catalysts containing amino groups. Upon doping with various p-dopant in suitable solvents, the thus prepared monoliths displayed a conductivity of 6×10^{-4} $S\cdot cm^{-1}$. Moreover, successful immobilization of the trypsin without any deterioration of the enzyme was achieved on the

doped monolith as shown by the excellent proteolytic activity of the immobilized enzyme. Synthesis, characterization and application possibility of these novel monolithic materials are described in this chapter.

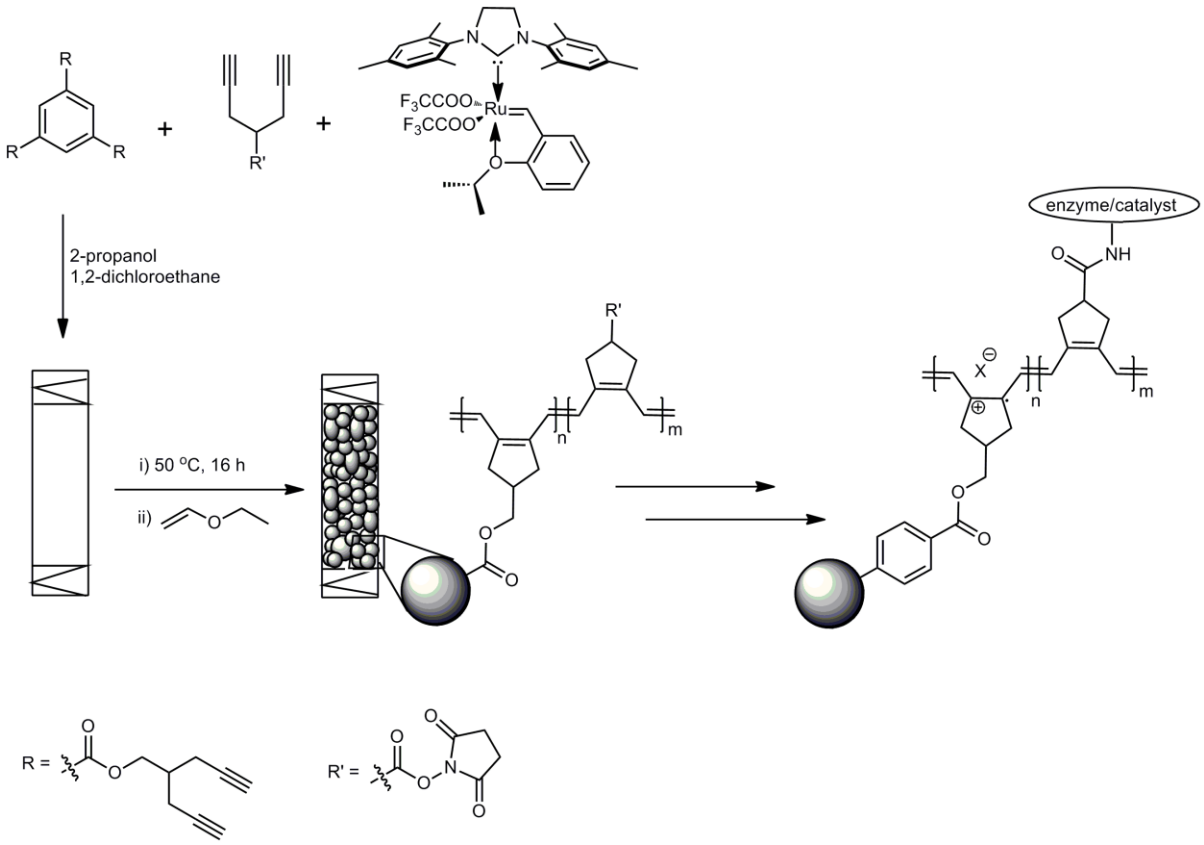

Scheme III. Enzymes immobilized on cyclopolymerization-derived conductive monoliths.

The focal theme of the last chapter is the synthesis of telechelic AB-type block copolymers of 4,4-bis(octyloxymethyl)-1,6-heptadiyne and dipropargyl malonodinitrile via the metathesis–based cyclopolymerization using well-defined molybdenum- and ruthenium-based initiators. Even though, the polymerization using Ru-based initiator did not resulted in block polymers due to significant backbiting, an investigation towards the influence of various reaction conditions on backbiting of these two monomers was accomplished.

A significant improvement in the elimination of backbiting was achieved when the polymerization was carried out with $[Ru(NCO)_2(IMesH_2)(=CH\text{-}2\text{-}(2\text{-}PrO)\text{-}C_6H_4]$ and $[Ru(NCO)_2(3\text{-}Br\text{-}Py)_2(IMesH_2)(CHPh)]$, ($IMesH_2$ = 1,3-dimesitylimidazolin-2-ylidene, 3-Br-Py = 3-bromopyridine) using 3-Br-Py as additive. Nevertheless, a successful synthesis of these block copolymers was accomplished by using the designed Mo-based Schrock-type initiators $Mo(N\text{-}2,6\text{-}i\text{-}Pr_2C_6H_3)(CHCMe_2Ph)(OCH(CH_3)_2)_2$ and THF as solvent.

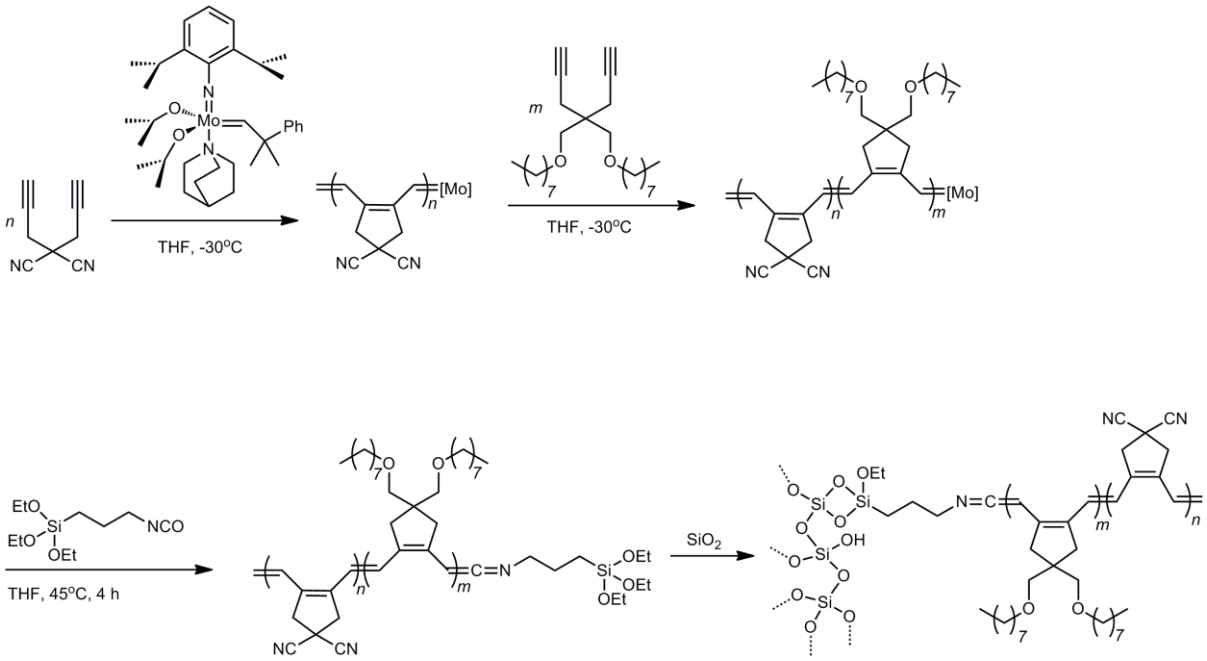

Scheme IV. Synthesis of triethoxysilyl end-functionalized AB-type block copolymers of 4,4-bis(octyloxymethyl)-1,6-heptadiyne and dipropargyl malonodinitrile.

The end-functionalization of these block copolymer using $(EtO)_3SiCH_2CH_2CH_2N=C=O$ afforded $Si(OCH_2CH_3)$-telechelic polymers. Finally, the surface grafting of the thus prepared telechelic polymer on a silica support was also realized as a part of these investigations (Scheme IV).

Goal/Aim

The last decade witnessed the dramatic development in metathesis-derived polymeric materials and is nowadays holds a strong position in organic and polymer chemistry. The discovery of well defined metathesis catalysts possessing high tolerance to the large verity of functional groups smoothened the way to well defined functional polymers and complex architecture. In this context, metathesis-derived functional monolithic materials received considerable attention. A great deal of research has been focussed on exploring the synthetic utilities of these polymeric monoliths in separation sciences. An appreciable extent of many other important applications including heterogeneous catalysis and tissue engineering has also been unveiled. This thesis pursues the line and attempts to explore the synthesis, characterization and the applications of metathesis-derived functional polymers and monolithic materials further.

The first project addresses a simple metathesis-based approach to functionalize ROMP-derived polymers and monolithic materials. The synthetic potential of the metathesis reaction of Ru-alkylidenes with oxygen are demonstrated in the precedence available, but still the utilization of this reaction in the functionalization of ROMP-derived polymeric monoliths remain unexplored. It will be interesting to investigate to what extend the ROMP-derived polymers can be functionalized based on this approach and in which form this reaction can be useful to material science and biocatalysis.

The second project focuses on the immobilization of a chiral bimetallic catalyst on ROMP-derived monolithic support. The main goal for the development of such supported version of the chiral catalyst is to combine the positive aspects of a homogeneous catalyst such as high enantioselectivity, good reproducibility with those of a heterogeneous catalyst such as ease of separation, stability, reusability etc.

The third project of this thesis addresses the unprecedented cyclopolymerization-based approach to conductive monolithic media using 1,6-heptadiyne based cross-linkers and monomers. This project was aimed to develop a conductive polymeric monolithic system which is suitable for the immobilization of redox active enzymes and also to investigate its utility as a medium for the transfer of electrons from electrode to the metal centre of redox active enzyme.

The final project focuses on the synthesis of block copolymers via the metathesis–based cyclopolymerization of 4-substituted 1,6-heptadiynes using well-defined molybdenum- and ruthenium-based initiators. Poly(1,6-heptadiynes) prepared via the cyclopolymerization of 1,6-heptadiynes are suitable for various electronic applications due to their conjugated structure. The main goal of this project was to synthesize a triethoxysilyl-end fuctionalized AB-type block copolymer of 4,4-bis(octyloxymethyl)-1,6-heptadiynes and dipropargyl malanodinitrile suitable to surface-graft onto a silica support.

.

1

Metathesis-Derived Polymers and Monoliths: Historical Perspective and Recent Developments

Metathesis[1] is considered to be one of the most remarkable advancements in both organic and polymer chemistry. The uniqueness of the reorganization of an unsaturated carbon skeleton using efficient and designed catalysts broadened the scope of this reaction in both areas of chemistry. Moreover, the development of well defined catalytic systems during the last three decades led this reaction to be of profound application in synthetic chemistry. Since then this area has been developed to such an extent that it has now become a powerful tool not only for the experts in inorganic, organic and polymer chemistry, but also in many other areas of chemistry. The introductory part of this thesis can only offer a brief overview of the key discoveries that revealed the pertinence of metathesis in the field of polymers and monolithic materials. A few sections are devoted to the recent developments and applications of metathesis in polymers and material sciences.

1.1 Early Stages of Metathesis (1931-1980)

The roots of metathesis can be traced back to the year 1931, when the first observation of metathesis of propene at high temperature was reported.[2] The first metathesis reactions were observed in the 1950's when industrial chemists at Du Pont, Standard Oil and Phillips Petroleum reported that propene was converted to ethylene and 2-butenes when heated with molybdenum (in the form of the metal, oxide or $[Mo(CO)_6]$ on alumina).[3] The first remarkable report on the polymerization of norborn-2-ene by the system $WCl_6/AlEt_2Cl$ was independently reported in 1960 by Eleuterio[4] and Truett *et al.*[5] But it took years to recognize the ring-opening metathesis polymerization (ROMP) and the disproportionation of acyclic olefins were based on the same reaction. The expression metathesis was coined to this reaction by Calderon in 1967[6]. A brief survey over the history of metathesis and metathesis polymerization has been given by Schrock[7] and Eleuterio[4]. In the early stages, all metathesis reactions were accomplished with poorly defined catalyst systems consisting of transition metal salts combined with main group alkylating agents, sometimes deposited on solid supports.[8] However, the requirement of strong Lewis acids and harsh reaction conditions made them incompatible with most of the functional groups. Therefore these catalysts were hardly attractive in advanced organic synthesis and only

found their way in olefin metathesis to the production of non-functionalized polymers. These problems motivated extensive work aiming on a better understanding of metathesis and the underlying mechanism. The mechanistic pathway suggested for this transformation was debatable for a while.[6, 9] Consequently, Y. Chauvin and his student J. -L Herisson developed the most consistent scheme in 1971 with some experimental evidence.[10] The mechanism was further supported by the work of Katz et al[11, 12], later Schrock's work published in 1980[13] clearly established the validity of the Chauvin mechanism, which remains as the generally accepted mechanism today (Scheme 1). Consecutive investigations mainly carried out by Schrock et al.[7, 14, 15] and Grubbs et al.,[16-18]motivated further research on that area. These discoveries were the major breakthrough in metathesis as evident from the amazing popularity of these catalytic systems attained in the following years.

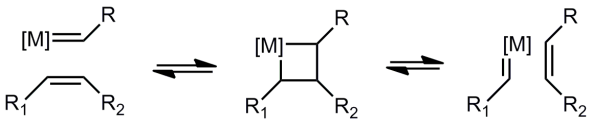

Scheme 1. The principle of olefin metathesis.

1.2 Versatility of Metathesis Reactions

The last few decades witnessed an exponential rise in activity in the area of metathesis. Several new and more efficient catalytic systems based on the metal alkylidenes with high specificity and turnover have been developed and found their applications in different areas of chemistry such as organic chemistry, polymer chemistry and material sciences. The excellent tolerance vs. a large variety of functional groups, combined with their high efficiency, and the ease of handling in air particularly for Grubbs catalysts led to their widespread use in the above mentioned areas. So far, numerous types of metathesis reactions are known, all of them can be catalysed by both Schrock and Grubbs catalysts (Figure 1).[1, 8, 19-23] The most popular metathesis reactions among the organic chemist are ring closing metathesis (RCM) and the cross metathesis, which can be achieved at ambient conditions with high stereo- and regio- selectivity using Ru-or Mo-based catalysts.[24] Recent studies on Mo- and W-based metathesis catalysts that bear stereogenic metal centres provide excellent access to complex natural products.[25-29]

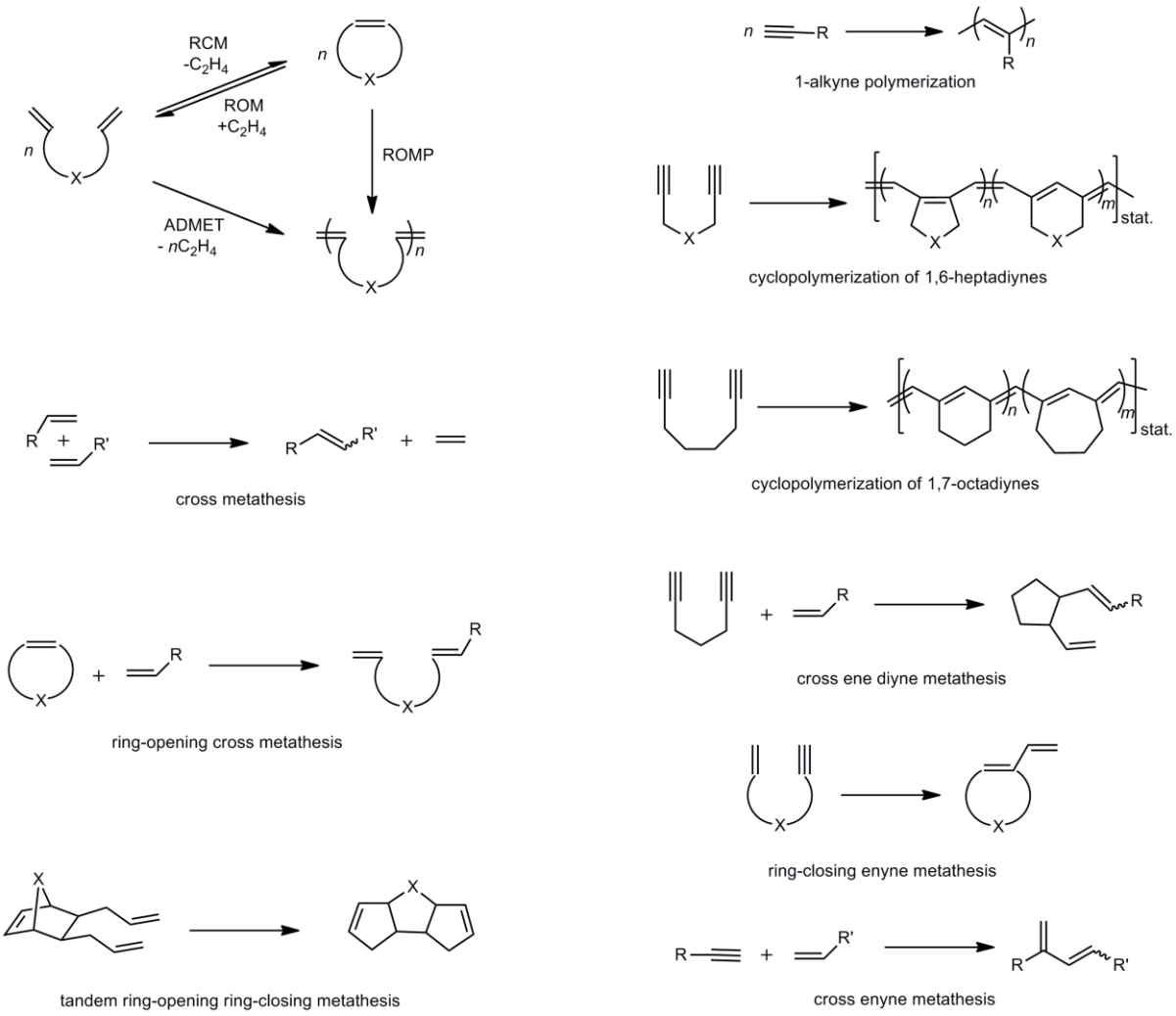

Figure 1. Various types of metathesis reactions.

More recently, Ru-based catalysts also proved their potential in the synthesis of enantioselective transformations.[30, 31] So far, a large variety of biologically and medically important compounds have been synthesized using well defined metathesis catalysts.[24, 26, 32, 33] The testimony of these facts is the mere multitude publications and reviews that came out during this period.

1.3 Metathesis Polymerizations

The progressive development in well defined metathesis catalysts smoothened the way for metathesis-based polymerizations such as ring-opening metathesis polymerization (ROMP), 1-alkyne polymerization, acyclic diene metathesis (ADMET) polymerization and the cyclopolymerization of diynes, and consequently made them attractive for the scientific community. More recently, ROMP and the cyclopolymerization of 1,6-heptadiynes, both a variation of olefin metathesis, emerged as a powerful method for synthesizing polymers with

tunable size, structure and functions. These polymeric materials are now widely used in preparing materials with interesting biological, electronic and mechanical properties. In addition, metathesis polymerization techniques developed as remarkable tools for the synthesis of polymers in a stereo- and regio regular manner.[25, 34-41] Another key feature of metathesis polymerization is its living nature,[23, 42-44] which allows one to add a second monomer after the first is consumed to yield block copolymers.[34, 40] All these features along with an excellent tolerance to various functional groups made this polymerization technique a powerful and broadly applicable method for the synthesis of macromolecular materials.

The following sections will focus on the application of ROMP and cyclopolymerization in the syntheses of functional polymers and monolithic materials.

1.3.1 Livingness

The concept of living polymerization was first introduced by Swarzc in 1956.[45] He defined the living polymerization on the basis of anionic polymerization that proceeds without chain transfer or termination. As Swarzc wrote in his report "The polymer molecule will live for an indefinite period of time, when no termination occurs. However, a 'living' polymer does not grow indefinitely, nor does its molecular weight exceed certain limits. The chain growth is interrupted when all monomer is consumed, and resumes polymer chain growth when additional amount of monomer is added". The key feature of a living polymerization is its ability to afford polymeric materials that generally have very narrow molecular weight distributions (Poly Dispersity Index (PDI) < 1.1). These molecular weight distributions are usually determined following the equation: PDI = M_w/M_n = 1 + 1/DP, where M_w is the weight-averaged molecular weight, M_n is the number-averaged molecular weight, and DP is the degree of polymerization.[43] In fact, there are few essential criteria that should be fulfilled to consider a polymerization 'living and controlled': (1) Fast and complete initiation: The rate of initiation needs to be similar or preferably greater than the rate of propagation, (2) irreversible propagation steps, (3) absence of chain termination and chain transfer, (4) a linear relationship between the degree of polymerization and monomer consumption, and (5) PDI < 1.1. Conventional binary and ternary catalysts were often heterogeneous mixtures that were extremely sensitive towards air and moisture, difficult to characterize, and could thus hardly be subjected to systematic studies or optimization. For these reasons they seldom allow for polymerizations in a well-controlled manner and hardly produced living polymerization setups. The advances in living polymerizations can be attributed to the progressive development of well-defined, functional

group tolerant catalysts amenable to olefin metathesis. This catalytic system enables us to synthesize well-defined polymers with narrow distributions and predictable molecular weights specified by the initial monomer to initiator ratio (M/I).[43] Apparently, these features offers access to synthesize well-defined block-, graft-, and other types of copolymers, end-functionalized (telechelic) polymers, and various other polymeric materials with complex architectures of useful functions.

1.3.2 Ring-Opening Metathesis Polymerization (ROMP)

ROMP is a variation of metathesis, which involves the breaking and reforming of double bonds with simultaneous opening of the unsaturated cycles of the monomer. The double bonds are retained throughout the reaction, resulting in a polymer with repeating double bonds in the polymer backbone.[1] A general example of the ROMP is shown in Scheme 2. The origin of ROMP can be traced back to the mid-1950s. The impetus for extensive research in the field of polymeric materials using metathesis was provided by the work of Truett et al. at Dupont. [4, 5, 46]

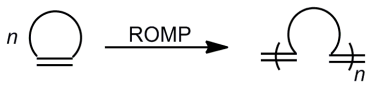

Scheme 2. ROMP of cyclic olefin.

In the early stages ROMP reactions were carried out by catalyst systems based on heterogeneous mixtures, which were often very sensitive to air and moisture. The development of well-defined transition metal catalysts based on the identification and isolation of key intermediates involved in olefin metathesis broadened the scope of this methodology. A detailed survey on living ring-opening metathesis polymerization can be found in ref. [43]By definition, ROMP is a chain growth polymerization processes were a mixture of cyclic olefins is converted into polymeric materials.[43]A general mechanism for ROMP based on Chauvins proposal is shown in Scheme 3. Initiation involves the coordination of a transition metal alkylidene to a cyclic olefin followed by [2+2]-cycloaddition to afford a four-membered metallacyclobutane intermediate. This intermediate then undergoes a cycloreversion reaction to afford a new metalalkylidene. The analogous steps are repeated during the propagation stage until all monomer is consumed. The polymerization is finally terminated by quenching the living end, i.e. the metal alkylidene with a suitable reagent to either remove the transition metal or by installing a new functional group at the end of the polymer chain.[43]

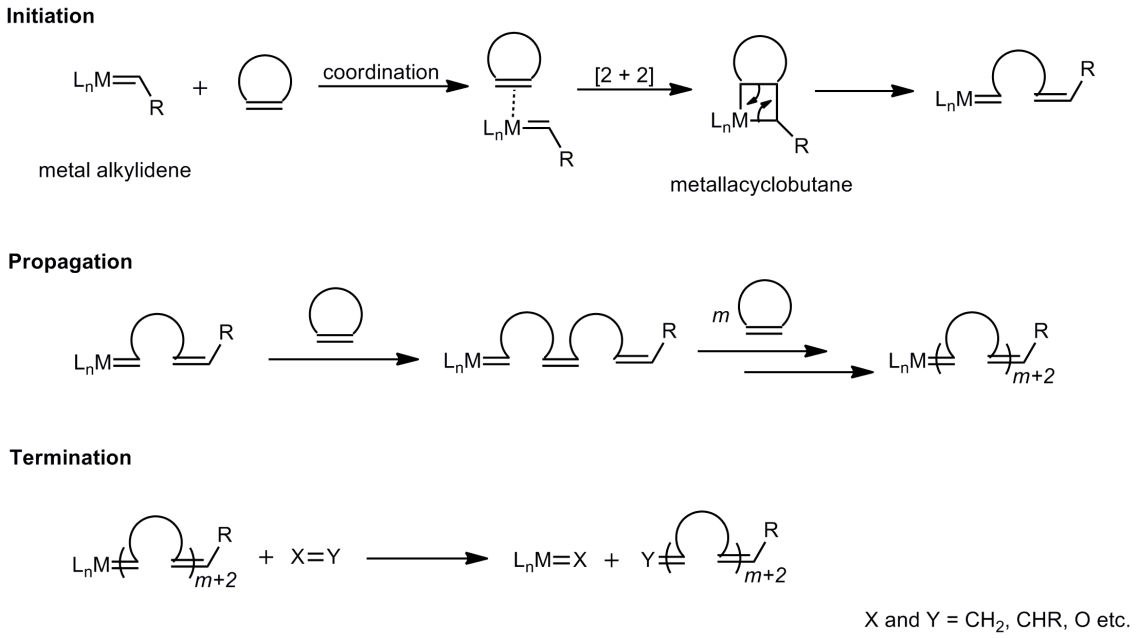

Scheme 3. A general mechanism to a typical ROMP reaction.[43]

Another remarkable feature of ROMP is the rich microstructural possibilities of the polymeric product formed. In contrast to the all other olefinic polymerizations the double bonds that mediate the polymerization reappear in the product.[1] In addition, the polymerization of chiral or prochiral monomers, the tacticity of the polymer arising from the sequence of the chiral atom along the polymer chain, must also be taken into account. Up to the late 1980s, there exist only some scattered reports on structural studies on ROMP-derived polymers prepared by classical metathesis catalysts. The development of Mo- and W-based catalysts with known structure and mode of the reaction have allowed the synthesis of ROMP polymers that have a single micro structure. Schrock et al. very recently reported the utilization of monoaryloxide-pyrrolido-imidoalkylidene (MAP) complexes of Mo for the synthesis of *cis*-syndiotactic polymers of several ROMP-active monomers.[41, 47]They proposed that the *cis*- selectivity arises through addition of the monomer to produce an all-*cis*-metallacyclobutane intermediate, while syndioselectivity and alternating enantiomer structures arise as a consequence of inversion of configuration at the metal center with each metathesis step. The very same feature of these catalysts also prompted organic and polymer chemists to achieve products with defined stereochemistry.

1.3.3 Cyclopolmerization of 1,6-Heptadiynes

Cyclopolymerization (ring forming polymerization) is another type of metathesis reaction based on a chain-growth polymerization that leads to the formation of cyclic structures in a polymer main chain via alternating intramolecular and intermolecular chain propagation.[39, 48] Over the last few years, poly(1,6-heptadyine)s prepared via the cyclopolymerization 1,6-heptadyines have been an area of considerable interest. These polymers possess cyclic structures recurring along the conjugated backbone, thus providing enhanced stability and excellent processability.[49] Usually, this class of polymers displays good solubility in common organic solvents (e.g., benzene, toluene, CH_2Cl_2, $CHCl_3$), good long-term stability towards oxidation, and high effective conjugation lengths. Therefore, they are considered interesting materials in the fields of organic (semi-) conductors, optoelectronics and photonics.[50-57]

In the early stages of conjugated polymers, the studies mainly focused on poly(acetylene).[58] Poly(acetylene)s are highly conductive, when doped, particularly when oriented. However, because of their poor solubility and stability, poly(acetylene)s including poly(1-alkyne)s have never found their way into any application. Consequently, conjugated materials based on poly(thiophene)s, poly(pyrrole)s, poly(thiazole)s, poly(*p*-phenylene)s, PPV and related materials are used.[53, 55] To increase the processability and provide various functionalities to poly(acetylene), different 1-alkynes were polymerized using various transition metal catalysts including Schrock carbenes.[59-63]However, mostly poorly or poorly stable polymers have been obtained. The cyclopolymerization of 1,6-heptadiyne was first reported by J. K. Stille et al. in 1961 using Ziegler-type catalysts.[64] Poly(1,6- heptadiynes) were obtained as dark-red materials, which indicates a high degree of conjugation in the polymer chain, however, no further analyses were performed to determine the structure of those polymers. Later, S. K. Choi et al. used W- or Mo-based catalysts for the cyclopolymerization of various 1,6-heptadiynes and studied the structure as well as the physio-chemical properties of the resulting polymers.[48] In the early 1990, Richard R. Schrock (Chemistry Nobel Laureate 2005), introduced a series of Mo-alkylidene-based metathesis initiators of the general formula $Mo(CHR`)(NAr)(OR)_2$ for the cyclopolymerization of 1,6-heptadiynes and also proposed a mechanistic pathways that gives access to five- or six-membered ring structures along the polymer main chain depending on the mode of insertion (α- or β-) of the monomer into the initiator (Scheme 4).[42] While both polymers are conjugated, it has been shown that particularly those based on five-membered repeat units possess higher effective conjugation lengths and higher conductivity.[65]

For the past decades, the synthetic approaches to poly(ene)s via the cyclopolymerization of 1,6-heptadiynes has reached an extraordinary level of sophistication. Buchmeiser *et al*. developed a series of modified Ru-alkylidene-based Grubbs-Hoveyda type metathesis initiators of the general formula $RuX_2(NHC)(CHAr)$; (NHC = *N*-heterocyclic carbenes; X = fluorocarboxylates), for the cyclopolymerization of 1,6-heptadiynes.[35, 66-68]

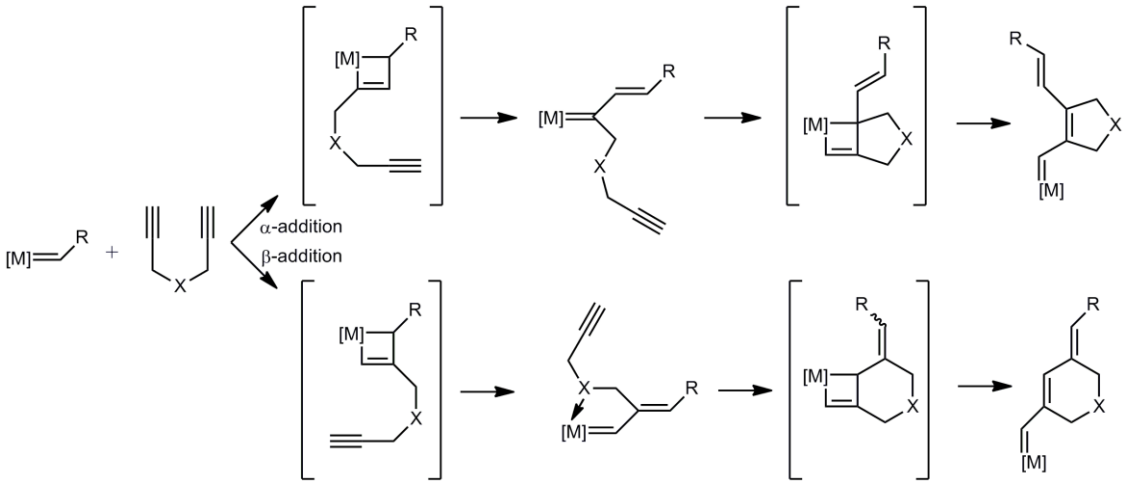

Scheme 4. Polymer structures obtainable via the cyclopolymerisation of 1,6-heptadiynes.

These were successfully used for the cyclopolymerization of 4-substituted1,6-heptadiynes and the resulting poly(ene)s consisted solely (>95%) of five-membered ring structures along the polymer main chain, following the results obtained by the action of newly-designed Mo-based initiators with same monomers.[35, 69-71] In short, both well-defined Mo-based Schrock type catalysts and modified Grubbs type metathesis catalysts may be used for cyclopolymerization. Here, particularly Schrock and in selected cases the modified Grubbs-type initiators allow for controlled or even living polymerizations. Important enough, Schrock-type initiators allow for accomplishing cyclopolymerizations in a stereo- and regio- selective manner, offering access to both five- and six-membered repeat units.[38, 42, 72] Buchmeiser et al. recently reported on the synthesis poly-1,6-heptadiynes consisting of exclusively five-membered repeat units in a controlled living manner using well-defined Mo-based catalysts with quinuclidine.[36] The advent of living and controlled polymerization of 1,6-heptadiynes opened a new era for the synthesis of complex polymeric architecture with conjugated back bones. Quite recently, T. L. Choi and co-workers reported on the synthesis of a diblock polymer having a conjugated backbone with controlled molecular weight and narrow PDI. They also prepared G3-denronized polymers in a living manner via a macro monomer approach.[40]

1.3.4 Applications of Living Metathesis Polymerizations

The capacity of both ROMP and cyclopolymerization to polymerize monomers with various functional groups in a living and controlled manner using well-defined metathesis catalysts allowed for the synthesis of well-defined block-, graft-, and other types of copolymers, telechelic (end-functionalized) polymers, and various other polymeric materials with complex architectures and useful functions.[1] The blocks of both A-B and A-B-A type copolymers can be prepared conveniently by the sequential addition of monomer to the living polymerization system. The first cyclopolymerization-derived block copolymer was reported in 2006 by Buchmeiser et al.[34] Very recently, T. L. Choi et al. reported the synthesis of cyclopolymerization-derived block copolymer using 3rd generation Grubbs catalyst in weakly coordinating solvent such as THF.[40]

1.4 Metathesis-Derived Monolithic Supports

The last two decades witnessed a rapid development in monolithic materials, and nowadays these supports hold an impressively strong position in separation science as well as in heterogeneous catalysis. [20, 73-78]Besides the advantages such as lower back pressure and enhanced mass transfer, the ease of fabrication, many possibilities in structural alteration and functionalization led these innovative materials to emerge in the field of heterogeneous catalysis.

The following sections are devoted to a brief overview on the historical background and the recent developments of metathesis-derived monolithic materials.

1.4.1 A Brief Historical Background

The roots of monolithic materials can be traced back to 1950s, emanating from the theoretical discussions of Nobel laureates Synge, Martin and Tiselius, but soon disappeared from the screen as gel like materials that were available at that time would collapse on hydrostatic pressure.[79, 80] Later Kubin et al. in the 1960s developed 2-hydroxyethyl methacrylate-based hydrogel-type materials with low degrees of crosslinking; its permeability was very poor and therefore allowed only for very low flow rates.[81] A remarkable achievement in the development these materials was the use of columns filled with open pore poly(urethane)-based materials, which allowed more successful, and decent separations in HPLC. However, none of these early technologies lasted long. Another key discovery was the introduction of continuous beds by Hjertén et al. They used a highly swollen cross-linked gel prepared by the polymerization of aqueous solutions of *N*, *N*-methylene bisacrylamide and acrylic acid in the presence of a salt.[82] This

material was compressed within the confines of a chromatographic column and exhibited very good permeability to flow, despite the high degree of compression. In the 1990s, Tanaka et al. provided the next remarkable contribution to modern monolithic materials in collaboration with material scientists in Kyoto.[83] They designed a process that afforded silica-based monoliths with controlled porous properties. However, the in situ preparation of such monoliths for any chromatographic use was restricted owing to their significant shrinkage. Therefore, the monolith was encased within a PEEK tubing to obtain chromatographic columns. Early studies with all these columns clearly demonstrated extremely fast chromatographic separations at high flow rates and at reasonably low back pressure. These advantageous features made monolithic columns particularly suitable for high-throughput applications.

1.4.2 Synthesis and Characterization of Metathesis-Derived Monoliths

Generally, the word 'monolith' applies to any uni-body structure composed of interconnected repeating cell or channels. In the following chapters, the term "monolith" or "rigid rod" shall comprise cross-linked, organic materials that are characterized by a defined porosity and that support interactions/reactions between this solid and the surrounding liquid phase.[84] The early efforts inspired a large number of groups worldwide to innovative research thereby moving the field rapidly forward. So far, a variety of functionalized and non-functionalized monolithic columns based on either organic or inorganic polymers are available. Inorganic monoliths are usually based on silica and may conveniently be prepared via sol-gel techniques. In contrast, the traditional organic continuous beds are based on poly(meth)acrylates or poly(styrene-*co*-divinylbenzene) and are almost exclusively prepared by radical polymerization.[85-88] However, only simple functional groups, such as amino-, alcohol-, phenol-, sulfonic acid-, or carboxylic acid moieties may be introduced in a controlled way. A comprehensive report on the variety of preparation techniques can be found in ref.[78]

The ROMP-based approach to the preparation of monolithic materials has been introduced by Buchmeiser and Sinner in 2000.[73, 89] The possibility to use functional monomers along with the controlled living polymerization mechanism allows a highly flexible yet reproducible polymerization setup. Initial experiments on the synthesis of ROMP derived monolithic supports entailed the copolymerization of norbornene (NBE) with *exo,endo*-1,4,4a,5,8,8a-hexahydro-1,4,5,8-*exo,endo*-dimethanonaphthalene ($DMNH_6$) or tris(norborn-2-ene-5-ylmethylenoxy)methylsilane ($(NBE\text{-}CH_2O)_3SiCH_3$) in the presence of two porogenic solvents, i.e. 2-propanol and toluene, with $RuCl_2(PCy_3)_2(CHPh)$ (**I1**). Usually less oxygen sensitive

metathesis initiators such as 1st generation Grubbs catalysts are preferred for the monolith synthesis and derivatization (Scheme 5).[73, 90]

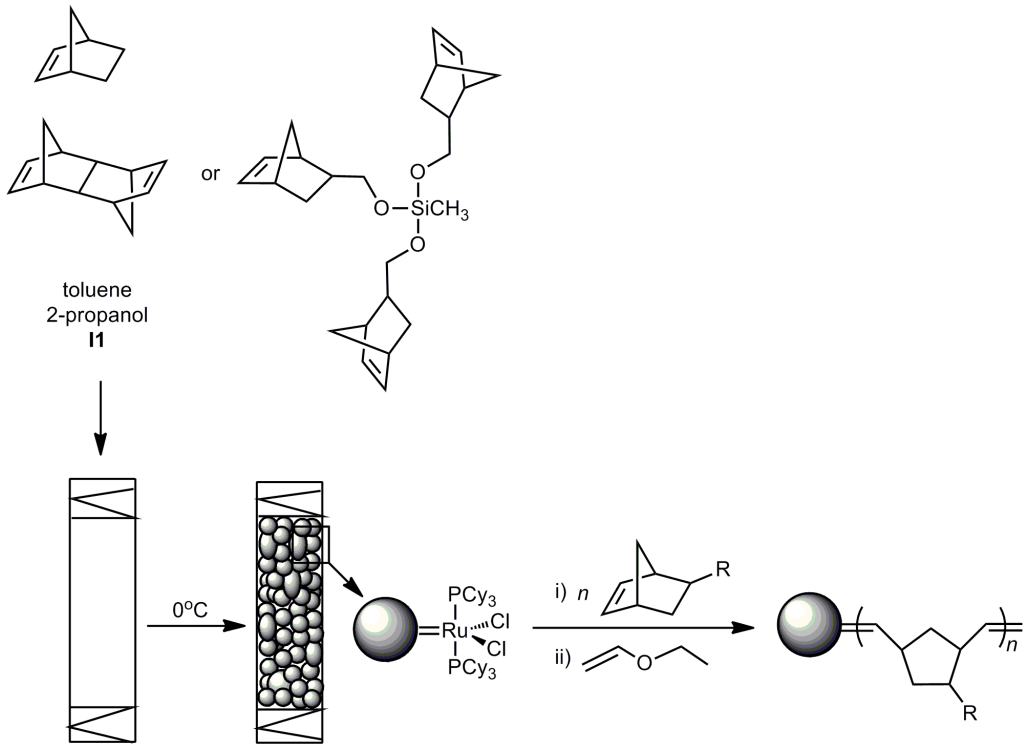

Scheme 5. Synthesis and functionalization of a ROMP-derived monolithic support.

By variation of the polymerization mixture in terms of monomer, crosslinker and porogen content, the porous properties could be successfully varied. A description of the construction of a monolith in terms of microstructure, backbone and relevant abbreviation is shown in Figure 2.[73] In brief, monoliths consist of interconnected microstructure-forming microglobules, which are characterized by a certain mean particle diameter (d_p) and microporosity (ε_p). In addition, the monolith is characterized by an intermicroglobule void volume (ε_z), which is mainly responsible for the back pressure at a certain flow rate. Microporosity (ε_p) and intermicroglobule porosity (ε_z) add up to the total porosity (ε_t), which indicates the porosity as a percentage of all types of pores within the monolith and from which the total pore volume (V_p), expressed in μL/g, can be calculated. The pore size distribution is best calculated from inverse size exclusion chromatography (ISEC) data.[91] In addition, one may calculate the specific surface area (σ), expressed in m^2/g, there from, however, these values should be treated with great care.

The original procedure involving norborn-2-ene derived monomers was later extended to other cyclic monomers such as *cis*-cyclooctene copolymerized with a tris(cyclooct-4-ene-1-yloxy) methylsilane crosslinker.[92] While norborn-2-ene derived monomers result in polymer

structures comprising of *tert*. allylic carbons, which tend to be easily oxidized, thereby resulting in reduced long-term stabilities of monolithic columns, the *cis*-cyclooctene-based monoliths revealed a significantly improved long-term stability, attributed to the *sec*-allylic structures present in each repeat unit.

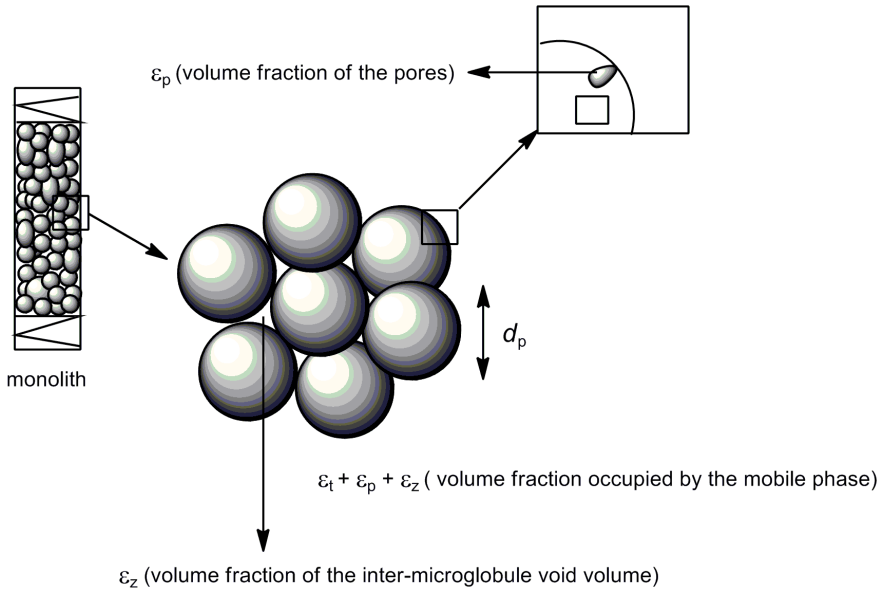

Figure 2. General construction of a monolith.

The most striking feature of cyclooctene-based systems is their structural difference from norborn-2-ene derived ones. Monoliths differ significantly in that the cyclooctene-based structures exhibit significantly reduced values for ε_z, yet higher values for ε_p and V_p compared to their norborn-2-ene-based counterparts.[73, 92]

1.4.3 Application of Metathesis-Derived Functional Monolithic Media

A remarkable feature of the ROMP-based protocol is its capacity for in situ functionalization of the monolith. The living character of the Ru-catalysed polymerization offers a perfect access to functionalization.[73] In fact the active ruthenium-sites can be used for the derivatization after the rod formation is complete. Ru-measurement by inductively coupled plasma optical emission spectroscopy (ICP-OES) investigations revealed that more than 98% of the initiators are located at the surface of the microglobules after the structure-forming process.[73, 93] The possibility of surface grafting from the living Ru-termini offers multiple advantages. Firstly, the structure of the parent monolith is not affected by the nature of the functional monomer used. Secondly, suitable solvents for the functional monomer may be used for the in situ derivatization.[73] These unique features of the metathesis-derived monolithic media led them to emerge in the field of

separation sciences, but also in many other important applications including heterogeneous catalysis and tissue engineering.[20, 84, 94-99]

1.4.3.1 Separation of Biomolecules

The most striking advantages generally ascribed to monolithic supports are a low back pressure, which allows for high flow rates and thus enables fast separations without loss in efficiency.[73, 76, 100] Depending on their porosity and pore size distribution, monoliths have proven to be excellent chromatographic supports for the separation of a large variety of analytes, including small, i.e. low molecular weight molecules,[101, 102]and peptides, proteins and nucleic acid.[103-106]Large biomolecules are more vulnerable than small molecules to structural damage caused from shear forces. Even subtle alterations can compromise recovery, stability and performance of such sensitive biomolecules. The structure of monolith avoids generation of shear forces thereby contributing to high functional recoveries. Non-functionalized monolithic materials prepared by ROMP have been extensively used in the fast separation of biologically relevant molecules such as proteins, double stranded (ds)DNA, oligonucleotides as well as phosphorothioate oligodeoxynucleotides.[103-105, 107]The elution order of oligonucleotides strongly correlates with their molar masses, suggesting that an increase in molar mass directly translates into an increase in the hydrophobic interaction of the corresponding analyte with the monolith. Very recently, the living nature of ROMP has been conveniently utilized in the preparation of monolithic anion exchangers for the fast separation of double-stranded DNA and 5'-phosphorylated oligodeoxythymidylic acids fragments.[105, 106]

1.4.3.2 Heterogeneous Catalysis

The practical application of expensive catalysts and in particular of asymmetric catalysts for valuable organic transformations is severely limited due to the difficulties in separation and recycling. These difficulties arises primarily due to the homogeneous nature of the reaction systems.[108] Another major drawback often associated with homogeneous catalytic processes is that of product contamination by metal leaching; this is particularly unacceptable for the production of fine chemicals and pharmaceuticals. One of the most promising ways to avoid this difficulty is the immobilization of those catalysts on a suitable support. Heterogenization of catalysts allows continuous operations, recycling of the catalyst, and an easy separation of the reaction products, thereby, reducing both waste and costs. Over the past decade, a number of strategies have been developed for heterogenization of such catalysts on inorganic or organic supports. In this regards, the use of metathesis-derived monolithic supports for catalyst

immobilization is an area of considerable interest.[20, 74, 75, 97, 109, 110] Various immobilization techniques used for the immobilization of expensive metathesis catalysts on the polymer support can be found in ref.[20] The most remarkable feature of metathesis-derived monolithic system is the possibility to surface graft the suitable ligand for the immobilization taking advantage of living nature of the catalyst used.

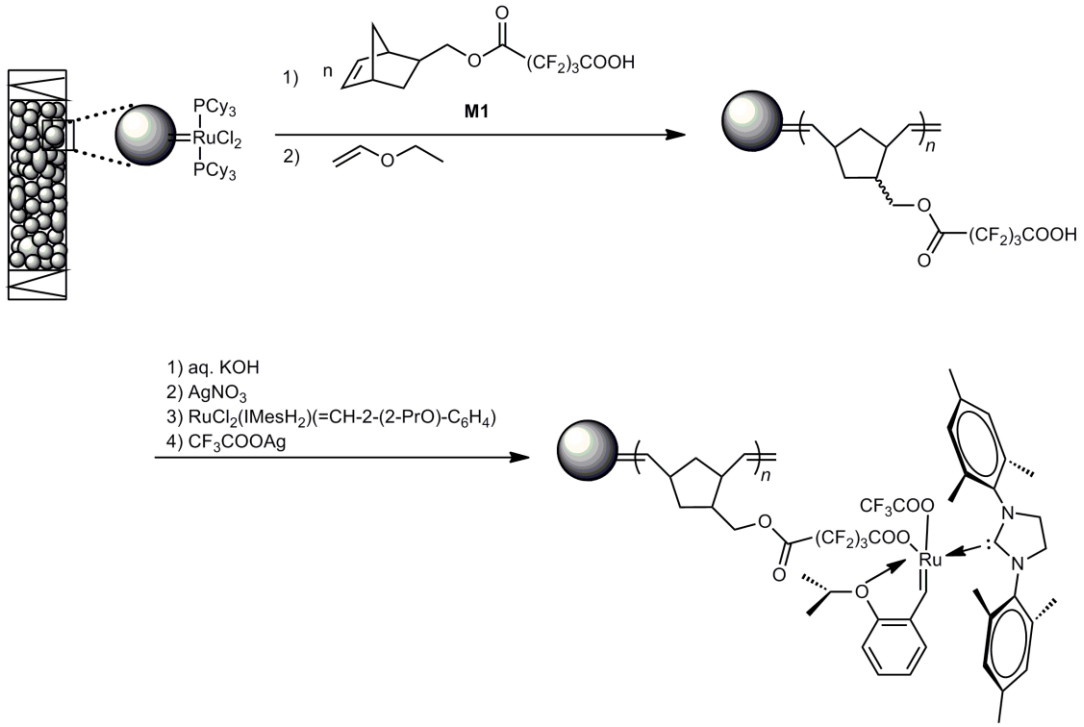

Scheme 6. Synthesis of a monolith-bound 2nd-generation Grubbs-Hoveyda-type catalyst.

Recently Buchmeiser et al. reported the synthesis of supported version of Ru-and Mo-based catalysts on to a ROMP-derived monolithic support with long-term stability and low metal leaching.[98, 99]The ROMP-derived monolithic support was surface grafted with **2** via the living Ru-termini. The free carboxylic acid groups were converted to silver salt and reacted with Grubbs-Hoveyda catalyst to afford the supported version (Scheme 6).[99]

1.4.3.3 Continues Flow Bioreactors

Although monolithic supports were used in the early stages monolithic era for enzyme immobilization,[76, 111, 112] the advent of proteomics has renewed researcher's interests in this aspect. Immobilized enzymes offer several advantages over enzymes in solution. Firstly, the bio-

catalyst could be easily removed from the reaction mixture, thus facilitating the separation of product. Second, the process can be carried out in a continuous flow mode in a designed reactor. The increasing popularity of polymeric monolithic support for enzyme immobilization is attributed to its high chemical stability over a wide range of pH, ease of modification with various functional groups and excellent biocompatibility. In most cases the enzymes immobilized on monolithic supports showed a significant acceleration of the reaction rate for proteolysis.[76] This is probably due to a fast mass transfer of the substrate to the immobilized enzyme and the efficient removal of reaction products by convective flow through the pores of the monolith. Because the enzyme moieties are located at the surfaces of the large pores, macromolecular substrates do not need to be transported via slow diffusion. Dulay et al. observed an increase in the tryptic activity upto 1500-fold for an enzyme immobilized in a photopolymerized sol–gel monolith compared to its counterpart in solution.[113] A technique developed by Kato's group consisted of a thin layer of trypsin encapsulated in tetramethoxysilane gel which was covered on the pore surface of a silica monolith.[114]The utilization of ROMP-derived monoliths for the trypsin has been addressed in this thesis. The immobilization was achieved via the aldehyde functionalities located at the surface of the microglobules (see chapter 2 for more details).[115]

1.4.3.4 Microreactors

Another key feature of meathesis-derived polymeric monolith is its microreactor compatibility. Because of the ease of fabrication of metathesis-derived monolith by in situ polymerization, they are ideally suited for use as components in microchip devices. Performing reactions in microreactor offers several advantages over traditional batch synthesis methods, such as low waste generation, and safer experimental conditions.[116-118] Moreover, the reactor configuration and reaction parameters can be varied systematically. Furthermore, the method can be easily scaled up from laboratory to industrial scale.

1.5 References

[1] R. H. Grubbs, *Handbook of Metathesis*, Wiley-VCH, Weinheim, **2003**.

[2] V. Schneider, P. K. Frolich, *Ind. Eng. Chem.* **1931**, *23*, 1405.

[3] R. L. Banks, G. C. Bailey, *Ind. Eng. Chem. Prod. Res. Dev.* **1964**, *3*, 170.

[4] H. S. Eleuterio, *J. Mol. Catal.* **1991**, *65*, 55.

[5] W. L. Truett, D. R. Johnson, I. M. Robinson, B. A. Montague, *J. Am. Chem. Soc.* **1960**, *82*, 2337.

[6] N. Calderon, H. Y. Chen, K. W. Scott, *Tetrahedron Lett.* **1967**, *8*, 3327.

[7] R. R. Schrock, *J. Organomet. Chem.* **1986**, *300*, 249.

[8] T. M. Trnka, R. H. Grubbs, *Acc. Chem. Res.* **2000**, *34*, 18.

[9] N. Calderon, *Acc. Chem. Res.* **1972**, *5*, 127.

[10] J. -L. Hérisson, Y. Chauvin, *Makromol. Chem.* **1971**, *141*, 161.

[11] T. J. Katz, S. J. Lee, N. Acton, *Tetrahedron Lett.* **1976**, *17*, 4247.

[12] T. J. Katz, J. McGinnis, *J. Am. Chem. Soc.* **1975**, *97*, 1592.

[13] R. Schrock, S. Rocklage, J. Wengrovius, G. Rupprecht, J. Fellmann, *J. Mol. Catal.* **1980**, *8*, 73.

[14] J. H. Oskam, H. H. Fox, K. B. Yap, D. H. McConville, R. O`Dell, B. J. Lichtenstein, R. R. Schrock, *J. Organomet. Chem.* **1993**, *459*, 185.

[15] J. Feldman, J. S. Murdzek, W. M. Davis, R. R. Schrock, *Organometallics* **1989**, *8*, 2260.

[16] P. Schwab, M. B. France, J. W. Ziller, R. H. Grubbs, *Angew. Chem.* **1995**, *107*, 2179; *Angew. Chem. Int. Ed.* **1995**, *34*, 2039.

[17] S. T. Nguyen, L. K. Johnson, R. H. Grubbs, J. W. Ziller, *J. Am. Chem. Soc.* **1992**, *114*, 3974.

[18] S. T. Nguyen, R. H. Grubbs, J. W. Ziller, *J. Am. Chem. Soc.* **1993**, *115*, 9858.

[19] D. Astruc, *New J. Chem.* **2005**, *29*, 42.

[20] M. R. Buchmeiser, *Chem. Rev.* **2008**, *109*, 303.

[21] R. H. Grubbs, S. H. Pine, *In Comprehensive Oragnic Synthesis;* B. M. Trost, I. Fleming, Eds.; Pergamon Press: Oxford, **1991,** *Vol. 5*.

[22] S. Naumann, J. Unold, W. Frey, M. R. Buchmeiser, *Macromolecules* **2011**.

[23] R. R. Schrock, *Acc. Chem. Res.* **1990**, *23*, 158.

[24] A. Fürstner, *Angew. Chem.* **2000**, *112*, 3140; *Angew. Chem. Int. Ed.* **2000**, *39*, 3012.

[25] Y. Zhao, A. H. Hoveyda, R. R. Schrock, *Org. Lett.* **2011**, *13*, 784.

[26] S. J. Meek, R. V. O/'Brien, J. Llaveria, R. R. Schrock, A. H. Hoveyda, *Nature* **2011**, *471*, 461.

[27] S. C. Marinescu, R. R. Schrock, P. Müller, M. K. Takase, A. H. Hoveyda, *Organometallics* **2011**, *30*, 1780.

[28] S. C. Marinescu, D. S. Levine, Y. Zhao, R. R. Schrock, A. H. Hoveyda, *J. Am. Chem. Soc.* **2011**, *133*, 11512.

[29] M. M. Flook, A. J. Jiang, R. R. Schrock, P. MuÌˆller, A. H. Hoveyda, *J. Am. Chem. Soc.* **2009**, *131*, 7962.

[30] B. K. Keitz, K. Endo, M. B. Herbert, R. H. Grubbs, *J. Am. Chem. Soc.* **2011**, *133*, 9686.

[31] A. Kannenberg, D. Rost, S. Eibauer, S. Tiede, S. Blechert, *Angew. Chem.* **2011**, *123*, 3357; *Angew. Chem. Int. Ed.* **2011**, *50*, 3299.

[32] P. K. Maity, A. Rolfe, T. B. Samarakoon, S. Faisal, R. D. Kurtz, T. R. Long, A. Schätz, D. L. Flynn, R. N. Grass, W. J. Stark, O. Reiser, P. R. Hanson, *Org. Lett.* **2011**, *13*, 8.

[33] E. S. Sattely, S. J. Meek, S. J. Malcolmson, R. R. Schrock, A. H. Hoveyda, *J. Am. Chem. Soc.* **2008**, *131*, 943.

[34] M. G. Mayershofer, O. Nuyken, M. R. Buchmeiser, *Macromolecules* **2006**, *39*, 2452.

[35] J. O. Krause, O. Nuyken, M. R. Buchmeiser, *Chem. Eur.J.* **2004**, *10*, 2029.

[36] U. Anders, O. Nuyken, M. R. Buchmeiser, K. Wurst, *Macromolecules* **2002**, *35*, 9029.

[37] S. Kobayashi, L. M. Pitet, M. A. Hillmyer, *J. Am. Chem. Soc.* **2011**, *133*, 5794.

[38] U. Anders, O. Nuyken, M. R. Buchmeiser, *J. Mol. Catal A: Chem* **2004**, *213*, 89.

[39] M. R. Buchmeiser, *Adv. Polym. Sci.* **2005**, *176*, 89.

[40] E.-H. Kang, I. S. Lee, T.-L. Choi, *J. Am. Chem. Soc.* **2011**, *133*, 11904.

[41] M. M. Flook, L. C. H. Gerber, G. T. Debelouchina, R. R. Schrock, *Macromolecules* **2010**, *43*, 7515.

[42] H. H. Fox, R. R. Schrock, *Organometallics* **1992**, *11*, 2763.

[43] C. W. Bielawski, R. H. Grubbs, *Prog. Polym. Sci.* **2007**, *32*, 1.

[44] K. Matyjaszewski, *Macromolecules* **1993**, *26*, 1787.

[45] Szwarc M, *Nature* **1956**, *178*, 1168.

[46] N. Calderon, E. A. Ofstead, J. P. Ward, W. A. Judy, K. W. Scott, *J. Am. Chem. Soc.* **1968**, *90*, 4133.

[47] M. M. Flook, V. W. L. Ng, R. R. Schrock, *J. Am. Chem. Soc.* **2011**, *133*, 1784.

[48] S.-K. Choi, Y.-S. Gal, S.-H. Jin, H. K. Kim, *Chem. Rev.* **2000**, *100*, 1645.

[49] C. C. W. Law, J. W. Y. Lam, Y. Dong, H. Tong, B. Z. Tang, *Macromolecules* **2005**, *38*, 660.

[50] J. H. Burroughes, D. D. C. Bradley, A. R. Brown, R. N. Marks, K. Mackay, R. H. Friend, P. L. Burns, A. B. Holmes, *Nature* **1990**, *347*, 539.

[51] R. H. Friend, R. W. Gymer, A. B. Holmes, J. H. Burroughes, R. N. Marks, C. Taliani, D. D. C. Bradley, D. A. D. Santos, J. L. Bredas, M. Logdlund, W. R. Salaneck, *Nature* **1999**, *397*, 121.

[52] A. J. Heeger, *Angew. Chem.* **2001**, *113*, 2660; *Angew. Chem. Int. Ed.* **2001**, *40*, 2591.

[53] F. Hide, M. A. Diaz-Garcia, B. J. Schwartz, A. J. Heeger, *Acc. Chem. Res.* **1997**, *30*, 430.

[54] A. G. MacDiarmid, *Angew. Chem.* **2001**, *113*, 2649; *Angew. Chem. Int. Ed.* **2001**, *40*, 2581.

[55] J. R. Sheats, Y.-L. Chang, D. B. Roitman, A. Stocking, *Acc. Chem. Res.* **1999**, *32*, 193.

[56] H. Shirakawa, *Angew. Chem.* **2001**, *113*, 2642; *Angew. Chem. Int. Ed.* **2001**, *40*, 2574.

[57] T. A. Skotheim, R. L. Elsenbaumer, J. R. Reynolds, *Handbook of Conducting Polymers*, 2 ed., Dekker, New York, **1997**.

[58] J. L. Brédas, R. J. Silbey, In *Conjugated Polymers*, Kluwer, Dordrecht, **1991**.

[59] C. I. Simionescu, V. Percec, *Prog. Polym. Sci.* **1982**, *8*, 133.

[60] L. S. Meriwether, E. C. Colthup, G. W. Kennerly, R. N. Reusch, *J. Org. Chem.* **1961**, *26*, 5155.

[61] L. B. Luttinger, *J. Org. Chem.***1962**, *27*, 1591.

[62] M. R. Buchmeiser, N. Schuler, G. Kaltenhauser, K.-H. Ongania, I. Lagoja, K. Wurst, H. Schottenberger, *Macromolecules* **1998**, *31*, 3175.

[63] S. Amdur, A. T. Y. Cheng, C. J. Wong, P. Ehrlich, R. D. Allendoerfer, *J. Polym. Sci: Polym. Chem. Ed.* **1978**, *16*, 407.

[64] J. K. Stille, D. A. Frey, *J. Am. Chem. Soc.* **1961**, *83*, 1697.

[65] M. R. Buchmeiser, J. O. Krause, D. Wang, U. Anders, R. Weberskirch, M. T. Zarka, O. Nuyken, C. Jäger, D. Haarer, *Macromol. Symp.* **2004**, *217*, 179.

[66] Y. S. Vygodskii, A. S. Shaplov, E. I. Lozinskaya, P. S. Vlasov, I. A. Malyshkina, N. D. Gavrilova, P. Santhosh Kumar, M. R. Buchmeiser, *Macromolecules* **2008**, *41*, 1919.

[67] T. S. Halbach, J. O. Krause, O. Nuyken, M. R. Buchmeiser, *Macromol. Rapid. Commun.* **2005**, *26*, 784.

[68] J. O. Krause, M. T. Zarka, U. Anders, R. Weberskirch, O. Nuyken, M. R. Buchmeiser, *Angew. Chem. Int. Ed.* **2003**, *42*, 5965.

[69] P. S. Kumar, K. Wurst, M. R. Buchmeiser, *Chem. Asian. J.* **2009**, *4*, 1275.

[70] P. S. Kumar, K. Wurst, M. R. Buchmeiser, *Organometallics* **2009**, *28*, 1785.

[71] P. S. Kumar, K. Wurst, M. R. Buchmeiser, *J. Am. Chem. Soc.* **2009**, *131*, 387.

[72] U. Anders, O. Nuyken, M. R. Buchmeiser, K. Wurst, *Angew. Chem.* **2002**, *114*, 4226.

[73] M. R. Buchmeiser, *Macromol. Rapid. Commun.* **2001**, *22*, 1081.

[74] M. R. Buchmeiser, *J. Mol. Catal. A: Chem.* **2002**, *190*, 145.

[75] M. R. Buchmeiser, *New J. Chem.* **2004**, *28*, 549.

[76] S. Frantisek, *Anal. Chem* **2006**, *78*, 2100.

[77] S. Frantisek, *J. Sep. Sci.* **2008**, *9999*, NA.

[78] F. Svec, *J. Chromatogr. A* **2010**, *1217*, 902.

[79] D. L. Mould, R. L. M. Synge, *Analyst* **1952**, *77*, 964.

[80] D. L. Mould, R. L. M. Synge, *Biochem. J.* **1954**, *58*, 571.

[81] Kubín M, Ŝpček P, C. c. R, *Coll. Czech. Chem. Commun.* **1967**, *32*, 3881.

[82] S. Hjertén, J.-L. Liao, R. Zhang, *J. Chromatogr. A* **1989**, *473*, 273.

[83] H. Minakuchi, K. Nakanishi, N. Soga, N. Ishizuka, N. Tanaka, *Anal. Chem.* **1996**, *68*, 3498.

[84] M. R. Buchmeiser, *Polymeric Materials in Organic Synthesis and Catalysis*, Wiley-VCH, Weinheim, **2003**.

[85] E. C. Peters, F. Svec, J. M. J. Fréchet, *Adv. Mater.* **1999**, *11*, 1169.

[86] C. Viklund, E. Pontén, B. Glad, K. Irgum, P. Hörstedt, F. Svec, *Chem. Mater.* **1997**, *9*, 463.

[87] C. Viklund, F. Svec, J. M. J. Fréchet, K. Irgum, *Chem. Mater.***1996**, *8*, 744.

[88] D. Sýkora, F. Svec, J. M. J. Fréchet, *J. Chromatogr. A* **1999**, *852*, 297.

[89] F. Sinner, M. R. Buchmeiser, *Angew. Chem. Int. Ed.* **2000**, *39*, 1433.

[90] M. R. Buchmeiser, *Polymer* **2007**, *48*, 2187.

[91] I. Halász, K. Martin, *Angew. Chem.* **1978**, *90*, 954; *Angew. Chem. Int. Ed.* **1978**, *17*, 901.

[92] R. Bandari, A. Prager-Duschke, C. Kuhnel, U. Decker, B. Schlemmer, M. R. Buchmeiser, *Macromolecules* **2006**, *39*, 5222.

[93] F. Sinner, M. R. Buchmeiser, *Macromolecules* **2000**, *33*, 5777.

[94] M. R. Buchmeiser, R. Kröll, K. Wurst, T. Schareina, R. Kempe, C. Eschbaumer, U. S. Schubert, *Macromol. Symp.* **2001**, *164*, 187.

[95] F. Weichelt, S. Lenz, S. Tiede, I. Reinhardt, B. Frerich, M. R. Buchmeiser, *Beilstein J. Org. Chem.* **2010**, *6*, 1199.

[96] F. Weichelt, B. Frerich, S. Lenz, S. Tiede, M. R. Buchmeiser, *Macromol. Rapid Commun.* **2010**, *31*, 1540.

[97] M. R. Buchmeiser, *Bioorg. Med. Chem. Lett.* **2002**, *12*, 1837.

[98] M. Mayr, D. Wang, R. Kröll, N. Schuler, S. Prühs, A. Fürstner, M. R. Buchmeiser, *Adv. Syn. Catal.* **2005**, *347*, 484.

[99] J. O. Krause, S. H. Lubbad, O. Nuyken, M. R. Buchmeiser, *Macromol. Rapid Commun.* **2003**, *24*, 875.

[100] M. R. Buchmeiser, R. Bandari, A. Prager-Duschke, A. Löber, W. Knolle, *Macromol. Symp.* **2010**, *287*, 107.

[101] S. H. Lubbad, M. R. Buchmeiser, *J. Chrom. A* **2010**, *1217*, 3223.

[102] S. H. Lubbad, M. R. Buchmeiser, *J. Sep. Sci.* **2009**, *32*, 2521.

[103] S. Lubbad, B. May, M. Mayr, M. R. Buchmeiser, *Macromol. Symp.* **2004**, *210*, 1.

[104] S. Lubbad, B. Mayr, C. G. Huber, M. R. Buchmeiser, *J. Chromatogr. A* **2002**, *959*, 121.

[105] S. H. Lubbad, R. Bandari, M. R. Buchmeiser, *J. Chromatogr. A* **2011**, doi:10.1016/j.chroma.2011.03.003

[106] S. H. Lubbad, M. R. Buchmeiser, *J. Chromatogr. A* **2011**, *1218*, 2362.

[107] R. Bandari, W. Knolle, M. R. Buchmeiser, *J. Chromatogr. A* **2008**, *1191*, 268.

[108] K. Ding, Y. Uozumi, WILEY-VCH Verlag GmbH & Co. KGaA, Weinheim, **2008**.

[109] R. Bandari, T. Höche, A. Prager, K. Dirnberger, M. Buchmeiser, R. , *Chem. Eur. J.* **2010**, *16*, 4650.

[110] M. R. Buchmeiser, K. Wurst, *J. Am. Chem. Soc.* **1999**, *121*, 11101.

[111] T. N. Krogh, T. Berg, P. Højrup, *Anal. Biochem.* **1999**, *274*, 153.

[112] S. Frantisek, *Electrophoresis* **2006**, *27*, 947.

[113] M. T. Dulay, Q. J. Baca, R. N. Zare, *Anal. Chem.* **2005**, *77*, 4604.

[114] M. Kato, K. Inuzuka, K. Sakai-Kato, T. Toyo'oka, *Analytical Chemistry* **2005**, *77*, 1813.

[115] M. Sudheendran, M. R. Buchmeiser, *Macromolecules* **2010**, *43*, 9601.

[116] P. D. I. Fletcher, S. J. Haswell, E. Pombo-Villar, B. H. Warrington, P. Watts, S. Y. F. Wong, X. Zhang, *Tetrahedron* **2002**, *58*, 4735.

[117] K. Jähnisch, V. Hessel, H. Löwe, M. Baerns, *Angew. Chem.* **2004**, *116*, 410; *Angew. Chem. Int. Ed.* **2004**, *43*, 406.

[118] B. P. Mason, K. E. Price, J. L. Steinbacher, A. R. Bogdan, D. T. McQuade, *Chem. Rev.* **2007**, *107*, 2300.

2

A Continuous Bioreactor Prepared via the Immobilization of Trypsin on Aldehyde-Functionalized, Ring-Opening Metathesis Polymerization-Derived Monoliths

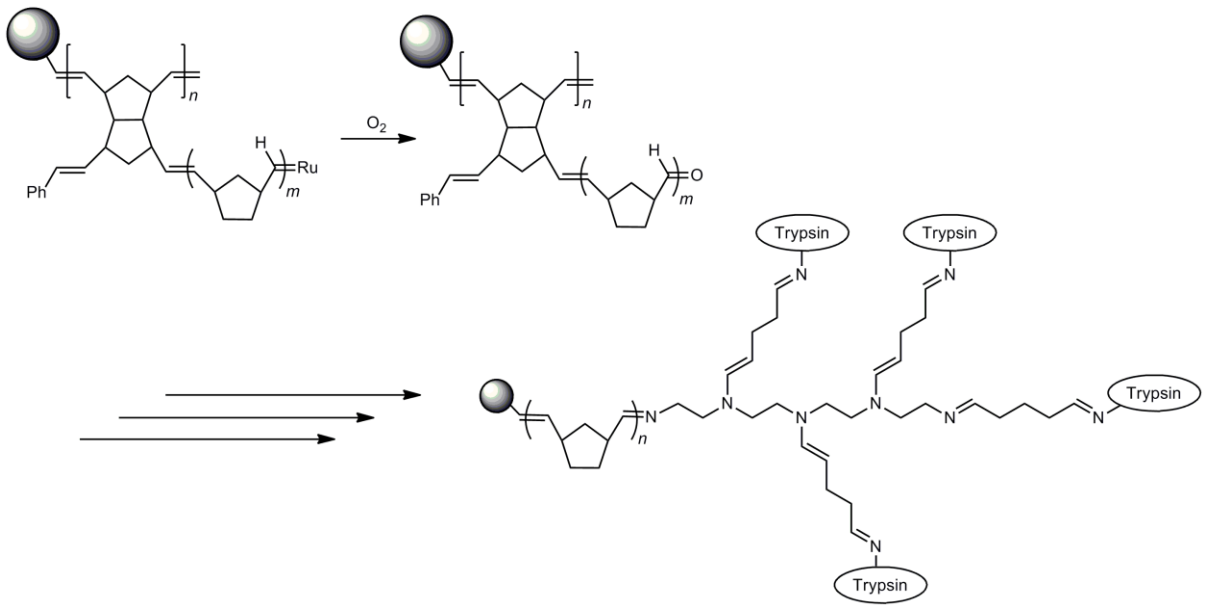

The material covered in this chapter has appeared in

M. Sudheendran, M. R. Buchmeiser, *Macromolecules*, **2010**, *43*, 9601-9607

2.1 Introduction

Ring-opening metathesis polymerization (ROMP) has become a powerful tool for polymer synthesis.[1-4] For this purpose, Ru-based initiators have attracted significant attention. Their ease of use, enhanced stability, high catalytic activity, and their excellent functional group tolerance relative to the other catalysts have broadened their synthetic utility beyond olefin metathesis.[5-7] Interestingly, there exist diverging reports on the stability of Grubbs' type initiators vs oxygen, water, nitriles, amines, etc.[8-13] Gibson et al. were the first to use this reaction for the preparation of semitelchelic ROMP-derived polymers.[14,15] Recent reports show that on exposure to oxygen these initiators can afford Ru-hydride complexes along with organic byproducts.[10,16,17] Thus, reaction of $RuCl_2(CHPh)(PCy_3)_2$ (**I1**) with air in benzene has been reported to result in the formation of benzaldehyde as well as *cis*- and *trans*-stilbene along with various Ru-containing byproducts (Scheme 7).[13,18]

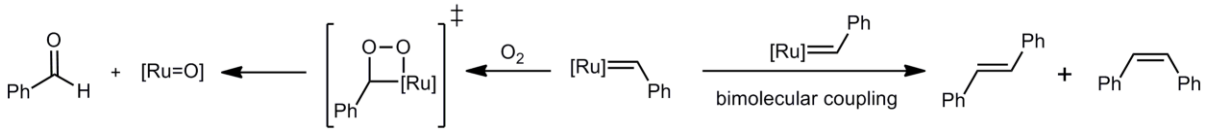

Scheme 7. Proposed pathway for the formation benzaldehyde and of the stilbenes.

For the past decades, several approaches toward the synthesis of telechelic or semi-telechelic polymers have been reported.[19-41] In view of the synthetic potential of the metathesis reaction of Ru-alkylidenes with oxygen, this reaction employed for the preparation of aldehyde-functionalized, ROMP-derived polymeric monoliths. This study describes as to what extent ROMP-derived polymers can be functionalized upon termination with O_2 and in which form this reaction can be useful to material science and biocatalysis.

2.2 Results and Discussion

2.2.1 Reactivity of Ru-Based Initiators vs Air (O_2)

In order to obtain a mechanistic understanding, the initiators **I1**-**I3** were first reacted ($IMesH_2$ = 1,3-bis(2,4,6-trimethylphenyl)imidazolin-2-ylidene, PCy_3 = tricyclohexylphosphine, 3-Br-Py = 3-bromopyridine (Figure 3) with air (O_2) in the absence of any monomer in benzene for 24 h. In accordance with the results of Grubbs et al. on the decomposition products of **I1**,[13] this reaction afforded a mixture of benzaldehyde and *cis*/*trans*-stilbene (Scheme 7, Figure S1-Chapter 6) along with several Ru byproducts, which were not further characterized. The yields of

benzaldehyde and the stilbenes were determined by GC-MS with the aid of an internal standard and reference compounds and are summarized in Table 1.

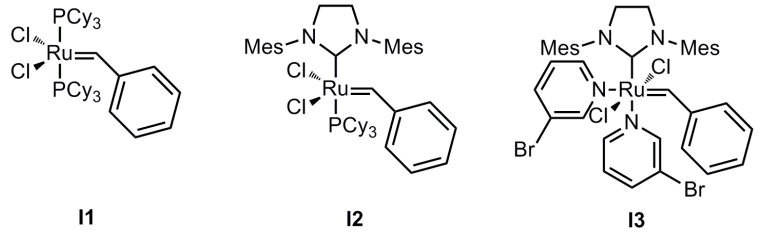

Figure 3. Structures of the first- **(I1)**, second- **(I2)**, and third- generation **(I3)** Grubbs initiators PCy_3=tricyclohexylphosphine, Mes=mesityl.

As can be seen, the benzaldehyde yield increased in the order **I1** > **I2** ~ **I3** while the yield of the stilbenes decreased in the order **I2** > **I1** > **I3**. Particularly the low stilbene yields obtained with **I3** clearly illustrate the reduced propensity of **I3** to react with an aldehyde to give the corresponding stilbene.

Table 1. Results of the reaction of initiators **I1**, **I2** and **I3** with O_2 [a]

initiator	benzaldehyde (%)[b]	stilbenes (%)	*cis* : *trans*
I1	44	7	1 : 4
I2	24	40	0 : 1
I3	29	1	0 : 1

[a] Benzne, room temperature, 24 h. [b]Determined by GC-MS analysis using *n*-dodecane as internal standard.

2.2.2 Reactivity of Living ROMP-Derived Polymers vs O_2

Next, starting with a high-ring strain monomer, i.e., norborn-2-ene, the aldehyde-telechelic polymers were synthesized via the reaction of the living Ru-alkylidene of the ROMP-derived poly(NBE) with O_2 as outlined in Scheme 8. With the three different initiators **I1-I3** used in this study, the desired aldehyde telechelic polymers were formed to a different extent. Thus, in case a ROMP-derived poly(NBE) initiated by **I1** was reacted with air for 16 h, an aldehyde-semitelechelic polymer with one polymer end bearing an aldehyde group was obtained in 80% yield (Table 2) while the termination of living poly(NBE) prepared by the action of **I2** or **I3** with O_2 gave only 47% and 29% of aldehyde-semitelechelic polymers. These data clearly reflect the different chemical stabilities of the initiators vs O_2. Thus, the stability of the living polymer increases in the order **I1** < **I2** < **I3**.

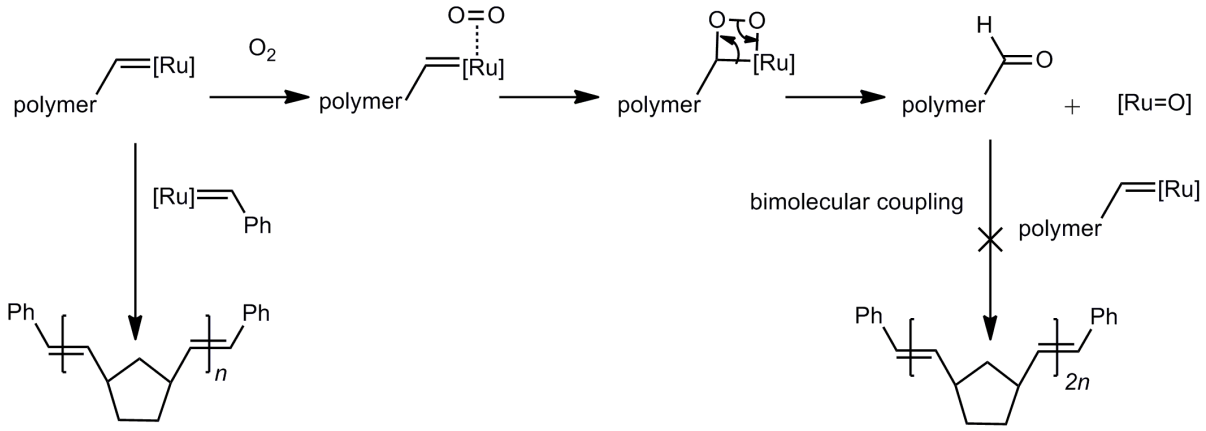

Scheme 8. Synthetic route to aldehyde-semitelechelic ROMP-derived polymers and possible side reactions (exemplified for poly(NBE)).

In the polymers obtained with **I1**-**I3**, the peaks at δ = 9.61 and 203.6 ppm in the ^{1}H and ^{13}C NMR correspond to the aldehyde proton and carbon, respectively (Figures S2 and S3, Chapter 6). Size exclusion chromatography (SEC) revealed monomodal distributions (1.82 < PDI < 1.98).

Table 2. Summary of the ROMP-derived poly(NBE) andpPoly(COE) prepared by the action of **I1**, **I2** and **I3** [a].

#	monomer	initiator	M_n(theor.)[a] *g/mol*	M_n(found) *g/mol*	PDI	yield (%)[b]	CHO-terminated (%)[c]
1		**I1**		7500	1.98	91	80
2		**I2**	2900	8600	1.93	86	47
3		**I3**		8900	1.82	62	29
4		**I1**		8400	1.77	76	15
5		**I2**	3400	5600	1.82	56	61
6		**I3**		6700	1.46	63	55

[a]Polymerizations conditions: benzene, [monomer]$_0$=1 M, monomer:initiator = 30:1; T = 23 °C, t = 1 h. [b]Isolated yield. [c]Determined by ^{1}H NMR spectroscopy.

In principle, this functionalization procedure may be expected to produce a mixture of the aldehyde-semitelechelic polymer via metathesis of the Ru-alkylidene with O_2 as well as a diphenyl-terminated polymer, e.g., via a coupling reaction between a living polymer and an aldehyde-telechelic one (Scheme 8). In such case, the latter polymer should have a molecular weight twice as high as the parent polymer chain. Using **I3** as initiator, a comparison of the size

exclusion chromatography (SEC) results obtained for an ethyl vinyl ether-terminated poly(NBE) (M_n= 6800 g/mol, PDI=1.69) and an O_2-terminated poly(NBE) (M_n = 7100 g/mol, PDI = 1.92) revealed that there was no significant bimolecular coupling among the Ru-alkylidenes of the polymer. An overlay over the SEC traces for these two polymers is shown in Figure 4.

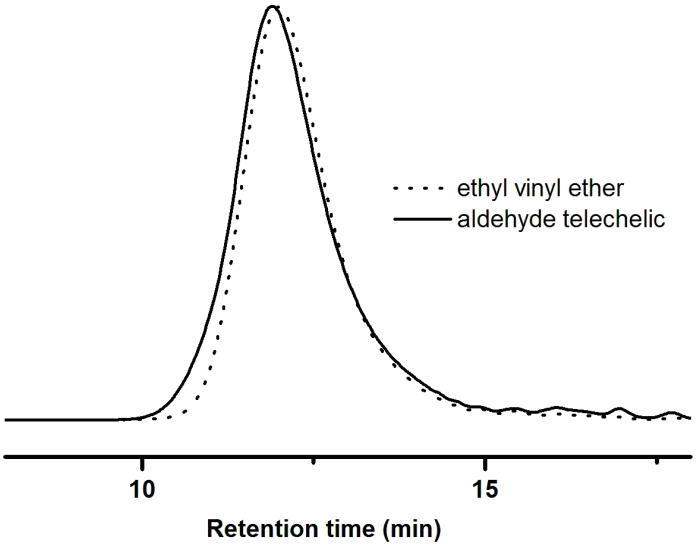

Figure 4. Comparison of the SEC curves between EVE- and O_2-terminated poly(NBE) prepared by the action of **I3**.

Obviously, the by far less oxophilic Ru-alkylidenes are less prone to O_2-triggered bimolecular coupling than the Mo-based Schrock initiators.[42] where almost quantitative bimolecular coupling can be observed in the presence of O_2 In contrast to the initiators, where such a coupling occurs to a significant extent producing substantial amounts of stilbenes, this reaction is less favoured (probable) with entangled polymers, where the chain ends have a lower probability to react.

The investigation was then extended towards less strained monomers such as *cis*-cyclooctene (COE). Again, reaction with O_2 (air) resulted in the formation of aldehyde-telechelic polymers. A maximum aldehyde formation of 61% was obtained with **I2**-derived poly(COE). The peaks at δ = 9.77 and 203.0 ppm in the ^{1}H and ^{13}C NMR support the formation of the aldehyde semitelechelic polymer (Figures S4 and S5, Supporting Information). In contrast, end-group analysis of **I1**- and **I3**-derived poly(COE) prepared under the same conditions showed only 15% and 55% of the aldehyde functionality (Table 2). As observed for the poly(NBE)s, SEC revealed a monomodal yet broad molecular weight distribution (1.46 < PDI < 1.82). To further proof the formation of the aldehyde termini for both poly(NBE) and poly(COE), the aldehyde termini was

converted into the corresponding 2,4-dinitrophenylhydrazine derivatives.[43,44] For that purpose, both aldehyde-semitelechelic poly(NBE) and poly(COE) were treated with a freshly prepared acidic solution of 2,4-dinitrophenylhydrazine to afford yellow precipitates of the corresponding hydrazones (Scheme 9).

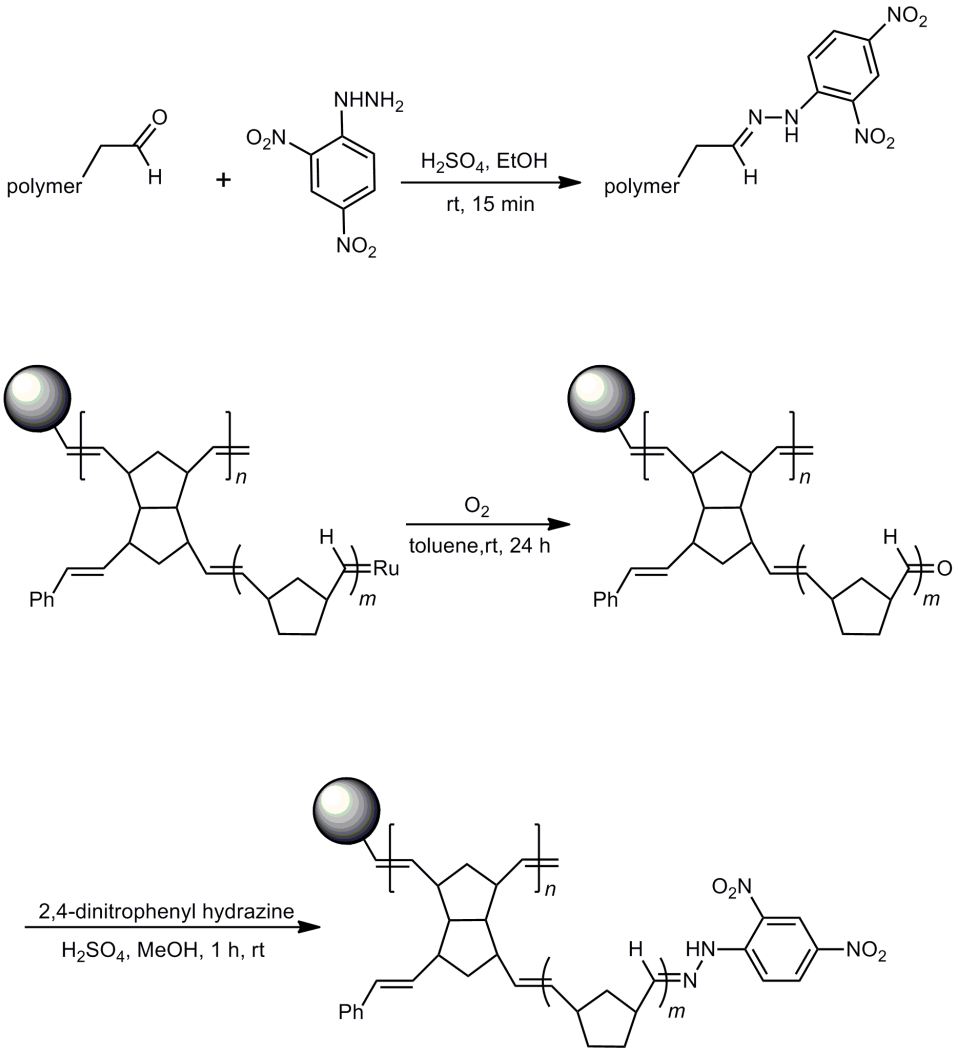

Scheme 9. Reaction of aldehyde-semitelechelic ROMP-derived polymers with 2,4-dinitrophenylhydrazine and schematic illustration of the synthesis of aldehyde- and 2,4-dinitrophenyl hydrazone-functionalized monoliths.

The ^{1}H NMR, ^{13}C NMR, and IR data strongly support the aldehyde functionality in the polymer chain. In the ^{1}H and ^{13}C NMR, the peaks at δ = 9.61 and 203.6 ppm corresponding to the aldehyde group disappeared, and new signals corresponding to the –HC=N- moiety at δ = 7.49 and 155.9 ppm appeared in the ^{1}H and ^{13}C NMR, respectively.

2.2.3 Application: Surface Functionalization of ROMP-Derived Monolithic Supports

The above-described methodology was applied to the functionalization of ROMP-derived monoliths by taking advantage of the truly living character of ROMP.[45,46] Monoliths were prepared from NBE,1,4,4a,5,8,8a-hexahydro-1,4,5,8-exo-endo-dimethanonaphthalene (DMN-H6), 2-propanol, toluene, and **I1** within stainless steel columns according to published procedures.[45,47] Then the initiator was subjected to a metathesis reaction with O_2 (Scheme 9) by flushing the monolith consecutively with toluene and air. Since a rigid polymer is formed, side reactions as described in Scheme 8 may well be expected to occur to a very minor extent, if at all. In fact, as evidenced by FT-IR, aldehyde groups formed at the surface of the structure forming microgobules. To further proof aldehyde formation and to quantify the amount of aldehyde groups, these were again converted into the corresponding hydrazones via reaction with 2,4-dinitrophenylhydrazine. Both the signal at 1725 cm^{-1} in the IR spectrum and the nitrogen content (up to 30 μmol/g) as determined by elemental analysis confirmed the successful functionalization sequence (up to 8 mmol/g).

2.2.4 Immobilization of Trypsin

The use of monoliths for the immobilization of transition-metal-based catalysts or enzymes has been reported by our group[48-51] as well as by Svec and Fréchet.[52-54] Monoliths were prepared from NBE and from $(NBE\text{-}CH_2\text{-}O)_3SiCH_3$ according to a published protocol.[55] The reason for the use of $(NBE\text{-}CH_2\text{-}O)_3SiCH_3$ instead of DMN-H6 is that it provides monoliths with better flow-through characteristics.[55] Introduction of the aldehyde groups was carried out as described above (Scheme 9). The aldehyde functionalized monolithic support was then used for the immobilization of trypsin.[56,57] Because of the steric demands of trypsin, we introduced tetraethylenepentamine (TEPA, Figure 5) as a spacer between the aldehyde-functionalized surface and the protein (Scheme 10).

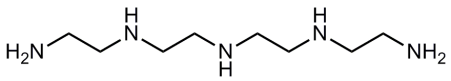

Tetraethylenepentamine (**TEPA**)

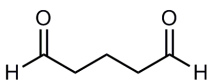

Glutaraldehyde (**GA**)

Figure 5. Reagents used for the immobilization of trypsin on the monolith support.

The primary as well as secondary amino groups were then reacted with glutaraldehyde (GA, Figure 5) to produce a large number of aldehyde functional groups, which were then further used for the reaction with trypsin.

The amount of trypsin bound to the monolithic support was quantified by elemental analysis. There, a nitrogen content of 86 μmol/g of monolith was found. Since the 8 μmol of aldehyde typically found in such monoliths translates upon reaction with TEPA into 40 μmol of N, the additional 46 μmol of N found by elemental analysis is indicative of the successful immobilization of trypsin on the ROMP-derived monolith.

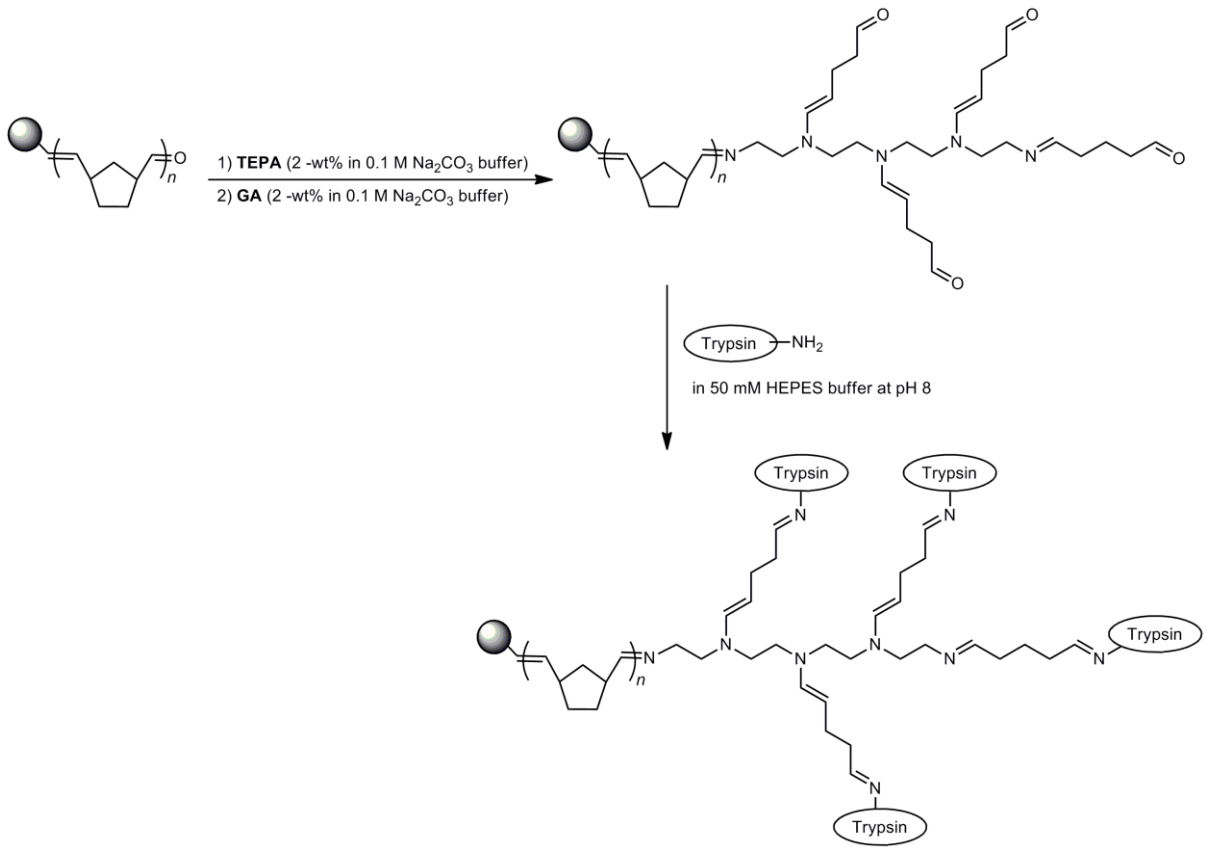

Scheme 10. Schematic illustration for the immobilization of trypsin on a ROMP-derived monolithic support.

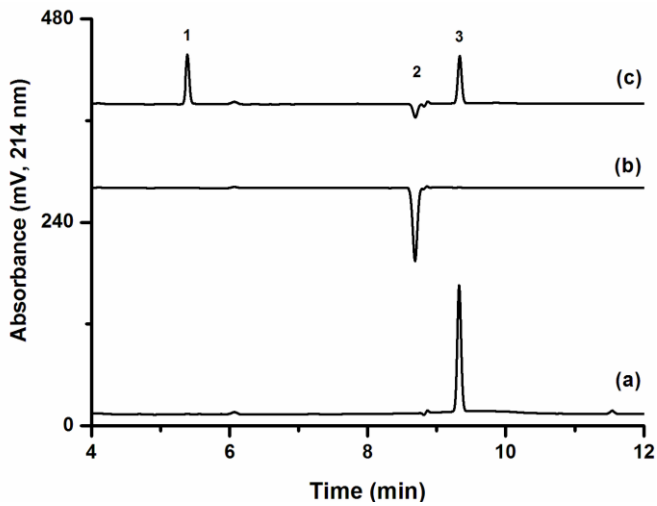

Figure 6. RP-HPLC chromatogram obtained for the tryptic digestion of BAPNA: (a) standard BAPNA, (b) standard PNA, (c) on-column tryptic digest of 0.25 mM BAPNA in 10 min at 37 ^{o}C. Peak 1 is BA product, peak 2 is PNA and peak 3 is undigested BAPNA. Conditions: flow rate 1 mLmin^{-1}; 25 ^{o}C; mobile phases: A: 95% water + 5% acetonitrile (ACN) + 0.1% triflouroacetic acid (TFA), B : 95 % ACN + 5% water + 0.1% TFA; gradient : 0 min 4 % B, 9 min 50% B, 10 min 50% B; UV (214 nm) ; injection volume 20 µL.

After its immobilization, the proteolytic activity of the immobilized protein was quantified by using *N*-α-benzoyl-DL-arginine-*p*-nitroanilide hydrochloride (BAPNA) as substrate, which upon hydrolysis produces *N*-α-benzoyl-DL-arginine (BA) and *p*-nitroaniline (PNA). The product formation and the rate of hydrolysis were monitored by RP-HPLC (Figure 6).

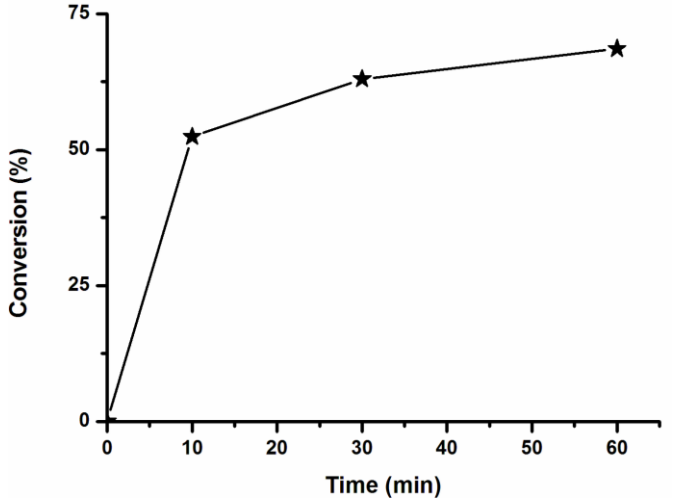

Figure 7. Plot of conversion vs time for the tryptic digest of 0.25 mM BAPNA at different reaction times. Conditions: *T* = 37 ^{o}C; mobile phase of the trypsin monolith was 50 mM HEPES buffer.

The BA that formed was analyzed at λ = 214 nm, whereas the remaining amount of BAPNA was quantified at λ = 310 nm. The hydrolysis yield of BAPNA was determined by comparing the area of BAPNA after hydrolysis to the area of a standard BAPNA solution (0.25 mM). The plot of conversion of BAPNA vs time is shown in Figure 7. As can be seen, a conversion of 65% was accomplished after 60 min.

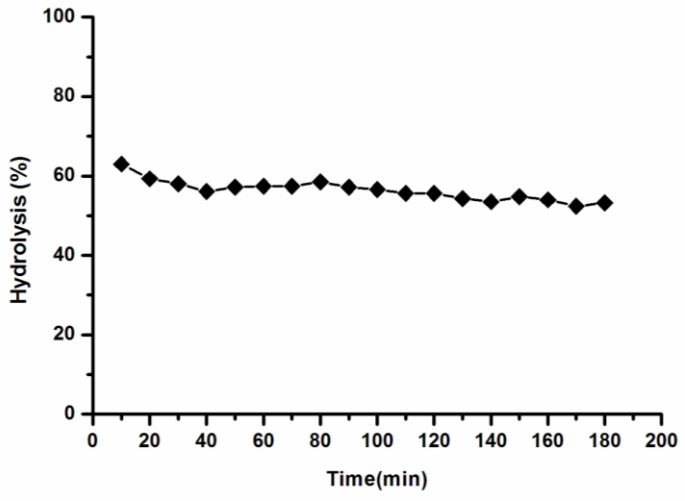

Figure 8. Tryptic activity in a continuous flow experiment. Conditions: on column time 10 min; *T* = 37 °C; mobile phase: 0.25 mM BAPNA in 50 mM HEPES buffer.

We then switched to continuous flow conditions and monitored the hydrolysis rate of BAPNA for 3 h using an on column (residence) time of 10 min. As can be seen (Figure 8), a slow decrease in the conversion of BAPNA with a total loss inactivity of < 20% was observed.

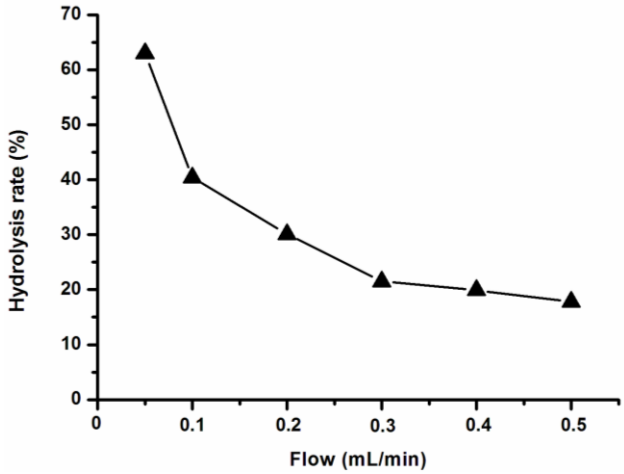

Figure 9. Influence of the flow rate on the hydrolysis of BAPNA. Conditions: *T* = 37 °C; mobile phase: 0.25 mM BAPNA in 50 mM HEPES buffer.

Finally, the influence of the flow rate on BAPNA conversion was examined at 37°C. For this purpose, aliquots were collected at different flow rates and analyzed by RP-HPLC at 310 nm. As expected, lower hydrolysis yields were obtained at higher flow rates, i.e., shorter on column times due to a reduced contact time between substrate and trypsin. A plot for the rate of hydrolysis against the flow rate is shown in Figure 9.

2.3 Conclusion

A novel and convenient method for the synthesis of ROMP-derived aldehyde-semitelechelic polymers via the metathesis of the living Ru-alkylidenes of ROMP-derived polymers with O_2 has been developed. The method was checked for all three Grubbs-type initiators. Up to 80% of aldehyde-semitelechelic poly(NBE) were observed when NBE was polymerized by **I1** and terminated with O_2. Though this simple reaction does not quantitatively yield aldehyde-semitelechelic polymers and therefore appears less suitable for the selective functionalization of linear and soluble polymers, it is of significant synthetic utility for the surface functionalization of insoluble (cross-linked) polymeric materials, e.g., polymeric monoliths, where a significant degree of surface functionalization up to 8 µmol can be achieved. This amount of aldehyde groups allows for the generation of surface bound (branched) oligoaldehydes which finally offer access to the permanent immobilization of enzymes, e.g., trypsin, and for use of the thus-prepared supported enzymes in continuous flow biocatalysis.

2.4 References

[1] M. R. Buchmeiser, *Metathesis Polymerization*; Springer: Berlin, **2005**; *Vol. 176*, p 1

[2] M. R. Buchmeiser, *Ring-Opening Metathesis Polymerization*, 1st ed.; Wiley-VCH: Weinheim, **2009**; p 197.

[3] R. H. Grubbs, *Handbook of Metathesis*, 1st ed.; Wiley-VCH: Weinheim, **2003**; *Vols. 1-3*.

[4] C. W. Bielawski, R. H.Grubbs, *Adv. Polym. Sci.* **2007**, *32*, 1.

[5] A. Fürstner, *Angew. Chem*. **2000**, *39*, 3012.

[6] M. R. Buchmeiser, *Chem. Rev.* **2000**, *100*, 1565.

[7] M. Schuster, S. Blechert, *Angew. Chem., Int. Ed.* **1997**, *36*, 2036.

[8] B. Alcaide, P. Almendros, *Chem.;Eur. J.* **2003**, *9*, 1258.

[9] B. Schmidt, Eur. *J. Org. Chem*. **2004**, *2004*, 1865.

[10] M. B. Dinger, J. C. Mol, *Organometallics* **2003**, *22*, 1089

[11] O. W. Gerald, A. P. Keith,; W. Haim,; R. W. Scott,; R. S.; Nancy, S. M. Jeffrey, *Adv. Synth. Catal.* **2009**, *351*, 1817.

[12] C. Slugovc, S. Demel, F. Stelzer, *Chem.Commun.* **2002**, 2572.

[13] M. Ulman, R. H. Grubbs, *J. Org. Chem.* **1999**, *64*, 7202.

[14] S. C. G. Biagini, R. G. Davies, V. C. Gibson, M. R. Giles, E. L. Marshall, M. North, *Polymer* **2001**, *42*, 6669.

[15] V. C. Gibson, E. L. Mashall, M. North, D. A. Robson, P. J. Williams, *J. Chem. Soc., Chem. Commun.* **1997**, 1095.

[16] B. D. Maarten, C. M. Johannes, *Eur. J. Inorg. Chem.* **2003**, *2003*, 2827.

[17] M. B. Dinger, J. C. Mol, *Eur. J. Inorg. Chem.* **2003**, *2003*, 2827.

[18] H. J. Van der Westhuizen, A. Roodt, R. Meijboom, *Polyhedron* **2010**, *29*, 2776.

[19] C. W. Bielawski, D. Benitez, T. Morita, R. H. Grubbs, *Macromolecules* **2001**, *34*, 8610.

[20] M. A. Hillmyer, R. H. Grubbs, *Macromolecules* **1993**, *26*, 872.

[21] M. A. Hillmyer, S. T. Nguyen, R. H. Grubbs, *Macromolecules* **1997**, *30*, 718.

[22] J. C. Marmo, K. B. Wagener, *Macromolecules* **1993**, *26*, 2137.

[23] J. C. Marmo, K. B. Wagener, *Macromolecules* **1995**, *28*, 2602.

[24] H. R. Allcock, C. R. de Denus, R. Prange, W. R. Laredo, *Macromolecules* **2000**, *34*, 2757.

[25] C. W. Bielawski, J. M. Jethmalani, R. H. Grubbs, *Polymer* **2003**, *44*, 3721.

[26] C. W. Bielawski, O. A. Scherman, R. H. Grubbs, *Polymer* **2001**, *42*, 4939.

[27] K. R. Brzezinska, J. D. Anderson, K. B. Wagener, *Polym. Prepr. (Am. Chem. Soc., Div. Polym. Chem.)* **1998**, *39*, 279.

[28] K. R. Brzezinska, K. B. Wagener, G. T. Burns, J. *Polym. Sci., Part A: Polym. Chem.* **1999**, *37*, 849.

[29] T. C. Chung, M. Chasmawala, *Macromolecules* **1992**, *25*, 5137.

[30] M. A. Hillmyer, R. H. Grubbs, *Polym. Prepr. (Am. Chem. Soc., Div. Polym. Chem.)* **1993**, *34*, 388.

[31] M. A. Hillmyer, R. H. Grubbs, *Macromolecules* **1993**, *26*, 872.

[32] S.Ji, T. R.Hoye, C. W. Macosko, *Macromolecules* **2004**, *37*, 5485.

[33] J. C.Marmo, K. B.Wagner, *Macromolecules* **1993**, *26*, 2137.

[34] J. C.Marmo, K. B.Wagner, *Macromolecules* **1995**, *28*, 2602.

[35] J. B.Matson, R. H. Grubbs, *Macromolecules* **2008**, *41*, 5626.

[36] B. R. Maughon, T. Morita, C.W. Bielawski, R. H. Grubbs, *Macromolecules* **2000**, *33*, 1929.

[37] T. Morita, B. R. Maughon, C. W. Bielawski, R. H. Grubbs, *Macromolecules* **2000**, *33*, 6621.

[38] H. Tamura, N. Maeda, R. Matsumoto, A. Nakayama, H. Hayashi, K. Ikushima, M. Kuraya, *J. Macromol. Sci., Part A: Pure Appl. Chem.* **1999**, *36*, 1153.

[39] H. Tamura, A. Nakayama, *J. Macromol. Sci., Part A : Pure Appl. Chem.* **2002**, *39*, 745.

[40] D. Tao, K. B. Wagener, *Polym. Prepr. (Am. Chem. Soc., Div. Polym. Chem.)* **1993**, *34*, 469.

[41] K. B. Wagener, J. C. Marmo, *Macromol. Rapid Commun.* **1995**, *16*, 557.

[42] W. J. Feast, V. C. Gibson, E. Khosravi, E. L. Marshall, J. P. Mitchell, *Polymer* **1992**, *33*, 872.

[43] R. J. Shriner, R. C. Fuson, D. Y. Curtin, T. C. Merrill, *The Systematic Identification of Organic Compounds*, 6th ed.; Wiley: New York, **1980**.

[44] S. F. Tayyari, J. L. Speakman, M. B. Arnold, Cai, W. Behforouz, M. *J. Chem. Soc., Perkin Trans. 2* **1998**, 2195.

[45] F. Sinner, M. R. Buchmeiser, *Macromolecules* **2000**, *33*, 5777.

[46] F. Sinner, M. R. Buchmeiser, *Angew. Chem., Int. Ed.* **2000**, *39*, 1433.

[47] C. Gatschelhofer, C. Magnes, T. R.Pieber, M. R.Buchmeiser, F. Sinner, M. *J. Chromatogr. A* **2005**, *1090*, 81.

[48] M. Mayr, B. Mayr, M. R. Buchmeiser, *Angew. Chem.* **2001**, *113*, 3957.

[49] M. R. Buchmeiser, S. Lubbad, M. Mayr, K.Wurst, *Inorg. Chim. Acta* **2003**, *345*, 145.

[50] J. O. Krause, S. Lubbad, O. Nuyken, M. R. Buchmeiser, *Adv. Synth. Catal.* **2003**, *345*, 996.

[51] M. Mayr, D. Wang, R. Kröll, N. Schuler, S. Prühs, A. Fürstner, M. R. Buchmeiser, *Adv. Synth. Catal.* **2005**, *347*, 484.

[52] F. Svec, J. M. Fréchet, J. *Science* **1996**, *273*, 205.

[53] S. Xie, F. Svec, J. M. Fréchet, *J. Biotechnol. Bioeng.* **1999**, *62*, 30.

[54] J. Krenkova, N. A. Lacher, F. Svec, *Anal. Chem.* **2009**, *81*, 2004.

[55] S. Lubbad, M. R. Buchmeiser, *Macromol. Rapid Commun.* **2002**, *23*, 617.

[56] Boulares-Pender, A. Prager-Duschke, C. Elsner, M. R. Buchmeiser, *J. Appl. Polym. Sci.* **2009**, *112*, 2701.

[57] E. Calleri, C. Temporini, E. Perani, C. Stella, S. Rudaz, D. Lubda, G. Mellerio, J. L. Veuthey, G. Caccialanza, G. Massolini, *J. Chromatogr. A* **2004**, *1045*, 99.

[58] T. L. Choi, R. H. Grubbs, *Angew. Chem., Int. Ed.* **2003**, *42*, 1743.

[59] J. A. Love, J. P. Morgan, T. M. Trnka, R. H. Grubbs, *Angew. Chem., Int. Ed.* **2002**, *41*, 4035.

[60] J. K. Stille, D. A. Frey, *J. Am. Chem. Soc.* **1959**, *81*, 4273.

3

Heterogenization of Chiral Bimetallic Catalyst on a ROMP-Derived Monolithic Support: Applications in Entantioselective Michael Additions

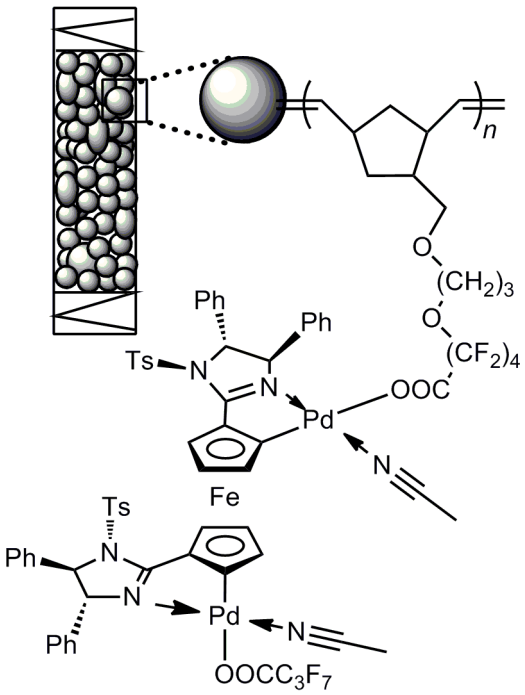

M. Sudheendran, Simon Eitel, René Peters and M. R. Buchmeiser.

This project was done in collaboration with Prof. Dr. René Peter's group at Institute of Organic Chemistry, University of Stuttgart.

3.1 Introduction

Asymmetric synthesis using chiral catalysts is the most efficient way to synthesize optically active compounds and is of great importance for both industrial applications and academic research.[1-3] However, the application of these expensive chiral catalysts in commercial synthesis is severely limited due to the difficulties in separation and recycling. Therefore, a catalytic system that allows for the straightforward separation of an expensive chiral catalysts from the reaction mixture with minimum product contamination by metal leaching and which can be recycled efficiently is highly desirable. Since most of these difficulties are arising primarily due to the homogeneous nature of the catalysts, the heterogenization by the immobilization of homogeneous catalysts on an inorganic or organic support is considered to be the most promising way to overcome these difficulties.[4-10] In this context, monolithic support prepared by ROMP have received considerable attention in recent years.[11-14] This class of monolithic supports having suitable porous properties and functional groups can be prepared easily and have already been identified as excellent carriers for catalytic systems as well as for separation devices.[15-18]The low back pressure, the accessibility of the solely surface-bound catalytic sites as well as the fast mass transfer of the support allow for the running of such devices in a (continuous) flow-through set-up with high TONs and low catalyst leaching.[5] Quite recently, a variety of heterogenization techniques for the immobilization of expensive catalysts and enzymes on a ROMP-derived monolithic support has been reported by Buchmeiser et al.[16, 19-24] This chapter describes the immobilization of a chiral bimetallic catalyst (FBIP-Cl)[25-27] suitable for the enatioselective Michael addition [28, 29] on ROMP-derive monolithic support. The goal of this immobilization technique is to facilitate the efficient recovery and reuse of the expensive catalyst along with the enhanced enantioselectivity than those for their homogeneous counterparts.

3.2 Results and Discussion

3.2.1 Synthesis of Monolithic Supports

The ROMP–derived monolithic support was prepared from NBE and $(NBE–CH_2O)_3SiCH_3$ in a suitable mixture of porogens by using " the 1st generation Grubbs catalyst", $RuCl_2(PCy_3)_2(=CHPh)$ (**I1**), according to a previously published protocol.[11, 22, 30]After rod formation, the 'living' ruthenium termini located at the surface were used for the grafting of the functional monomers. The chiral bimetallic catalyst FBIP-Cl proposed for the immobilization by itself exists as a dimer. The activated form of this complex FBIP-$OOCC_3F_7 \cdot CH_3CN$ can be obtained

by the reaction with silver heptafluorobutyrate and acetonitrile in dichloromethane (Scheme 11). This bimetallic complex offers superior catalytic activity along with enhanced level stereocontrol as a result of highly organized transition state.[29]

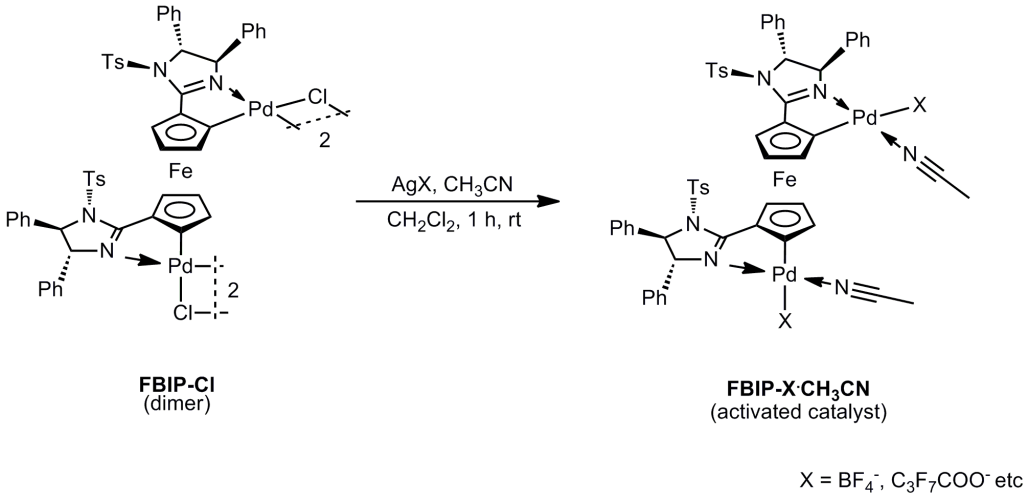

Scheme11. Preparation of activated complex from the precatalyst FBIP-Cl.

Since the activated complex contains a fluorinated carboxylate group, the immobilization can be achieved through a ligand exchange of the complex with carboxylate groups of the grafted polymer. Recently, Buchmeiser et. al. reported a successful immobilization of Ru-based metathesis initiator via the halogen exchange by a fluorinated carboxylate ligand.[22]This approach was more straightforward and convenient as there is no intermediate steps involved. In addition, the unreacted catalyst can be fully recovered.

3.2.2 Synthesis of Supported Catalyst C1 via Surface Grafted M1

We began the immobilization following a previously published procedure,[22] where mono(norborn-5-ene-2-ylmethyl) hexafluoroglutarate (**M1**) was used as the functional monomer. The monomer **M1** can be readily obtained by a simple ring-opening of hexafluoroglutaric anhydride with 5-norbornene-2-methanol (**1**) in dichloromethane (Scheme 12).[22] After the reaction, the solution containing **M1** was used as such without further purification and grafted on to the monolithic surface via the living Ru-termini. The initiator was removed by extensive flushing with a mixture of DMSO:THF:EVE(40:40:20), which results in a ruthenium free monolithic matrix as evidenced by ICP-OES measurements.[11, 13]

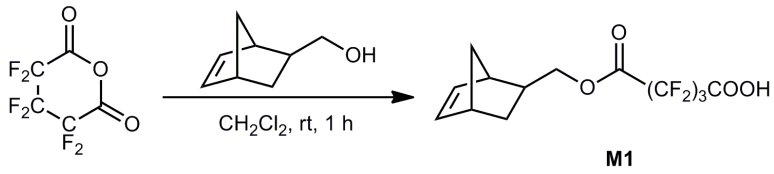

Scheme 12. Synthesis of functional monomer **M1**.

The amount of chemically accessible carboxylate groups of the graft polymer were quantified at this stage by acid-base titration using phenolphthalein as indicator. For this purpose, a known volume of standard KOH solution was injected into the monolith. The amount of carboxylate groups were determined by comparing the concentration of this solution with the one of a standard KOH solution. This way, a carboxylic acid content of 370 µmol/g, was found. The potassium carboxylate groups of the graft polymer were directly utilized for the immobilization of the activated complex FBIP-BF_4·CH_3CN containing the more labile BF_4^- as counter anion. The complex FBIP-BF_4·CH_3CN was in turn obtained by the reaction of the precatalyst FBIP-Cl with silver tetrafluoroborate in acetonitrile.

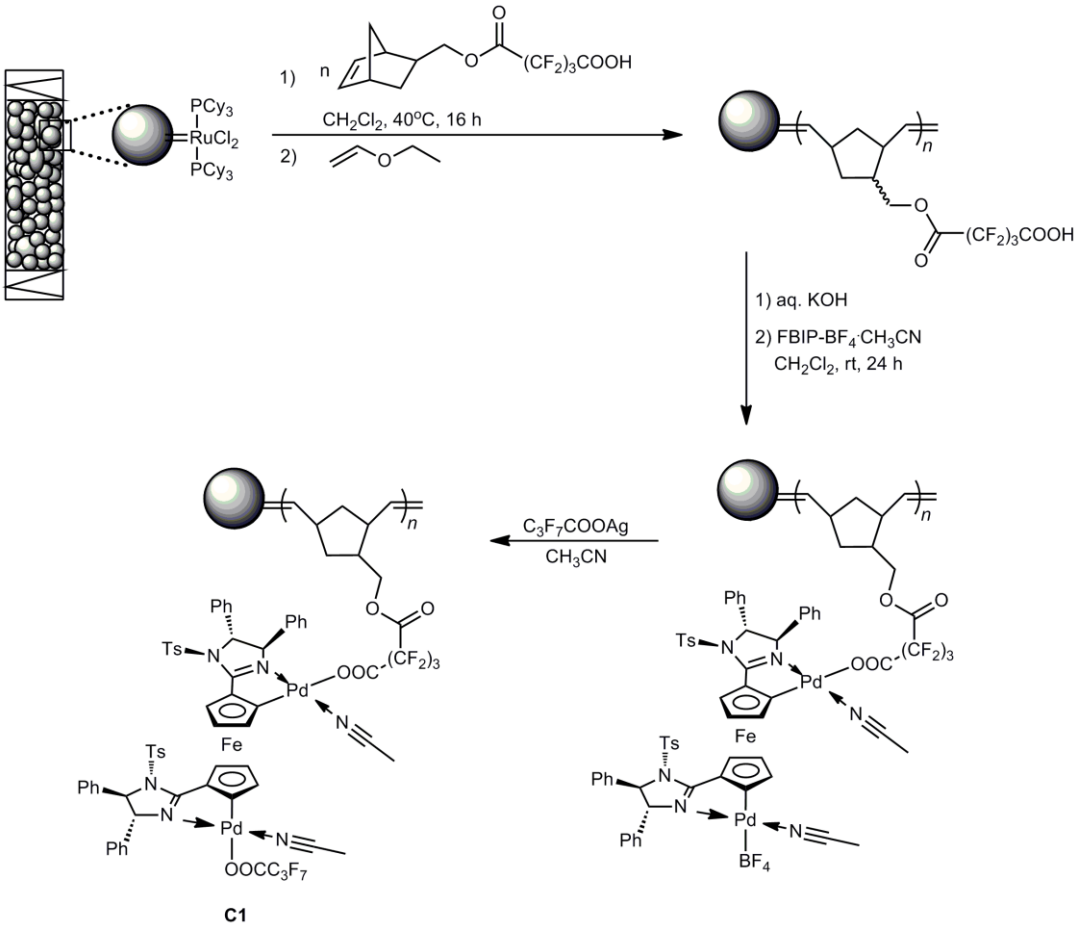

Scheme 13. Synthesis of monolith-supported catalyst **C1**.

The remaining BF_4^- as counter anion was substituted by the addition of another equivalent of silver heptafluorobutyrate. Following this procedure, 20 mg/g of FBIP-BF_4·CH_3CN complex were bound to the support. Any unreacted catalyst can be recovered quantitatively. Since the complex is colored, any leaching of the complex can be easily determined in the solution. To our pleasure, no leaching of the catalyst was observed, indicative for a successful immobilization of the catalyst (Scheme 13).

3.2.3 Catalytic Performance of Supported Catalyst C1

To test the activity of the supported version of FBIP-Cl, the Michael-addition of *tert*-butyl 2-cyano-2-phenylacetate to 2-cyclohexen-1-one was carried out in diglyme at 35°C. The results of these enantioselective Michael-additions are summarized in Table 3. Despite the successful immobilization, however, variations in the results of the four identical experiments (Table 3, entries 2 and 5) in terms of conversion and selectivity indicate that either the catalytic species are not uniformly distributed or that a gradual decomposition of the catalytic species occurs.

Table 3. Results of the Michael addition reactions carried out by using the supported catalysts **C1**[a].

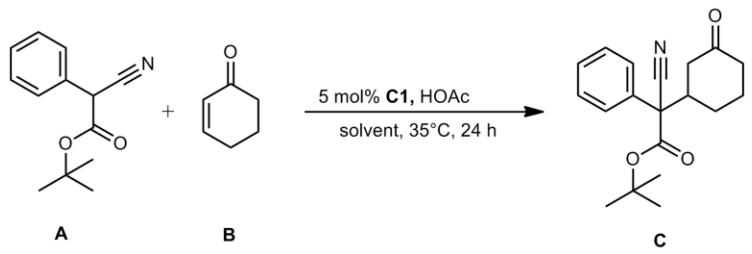

entry	yield [%][b]	$ee_{(R,R)}$ [%][c]	$ee_{(R,R)/(S,R)}$ [%][c]	*dr* [c]
1[d]	95	96	-72	7.7:1
2	41	68	4	1:1.43
3	29	50	-5	1:1.43
4	44	53	4	01:01
5	54	22	-5	1:1.1

Conditions: diglyme, [a]90 µmol of **A**, 10 equiv. of **B**, 0.5 equiv. of HOAc, 0.6 mL of solvent. [b]Determined by ^{1}H NMR spectroscopy. [c]Determined by HPLC. [d] Under optimized homogeneous conditions, 92 µmol of **A**, 2 equiv. of **B**, 1 mol-% of **FBIP-$O_2C_4F_7$**, 0.2 equiv. of HOAc, 0.17 mL of diglyme.

The consistency in the catalytic activity of the supported version was further investigated by performing the reaction in a continuous mode. However, a plot of conversion and selectivity

versus time revealed a large variation in the catalytic activity compared to the homogeneous counterparts (Figure 10). One of the possible reasons for these inconsistencies in catalytic activity are rather attributed to the changing environment of the immobilized catalyst, which is created by different counter ions or even by a slow decomposition of the catalyst or the linker.

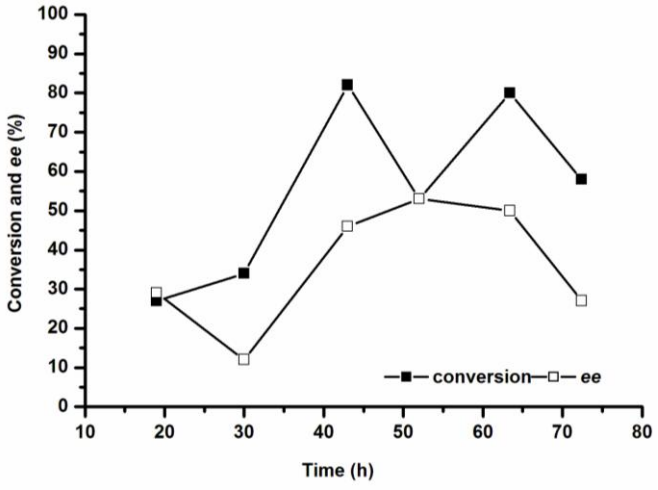

Figure 10. Plot of conversion against time for the Michael addition of **A** and **B** in a continuous flow experiment using the supported catalyst **C1** prepared according to Scheme 13. Conditions: 180 µmol of A, 3.8 mL of dyglyme, flow rate = 0.06 mL/h, room temperature.

3.2.4 Alternative Route to Supported Catalyst C1

In order to overcome the inconsistencies in the catalytic activities of the supported catalyst, the immobilization was carried out via an alternate approach, by which the supported catalyst with the desired counter ion was obtained. Since the Michael-addition occurs in the presence of base, it is reasonable to avoid any traces of basic impurities remaining in the solid matrix after the immobilization. Therefore, the synthesis of the supported catalyst **C1** was alternatively achieved via the substitution of the free acid groups of the graft polymer directly with FBIP-$O_2C_4F_7$.CH_3CN (Scheme 14). The driving forces of this method are different *pKa* values of the carboxylate counter ion (*pKa* ≈ 0.63) and of the carboxylate group of the graft polymer (*pKa* ≈ 0.6). Following this procedure, 23 mg/g of the FBIP-$O_2C_4F_7$·CH_3CN complex used were bound to the support. No catalyst leaching was observed indicative of a successful immobilization of the catalyst with the desired counter ion.

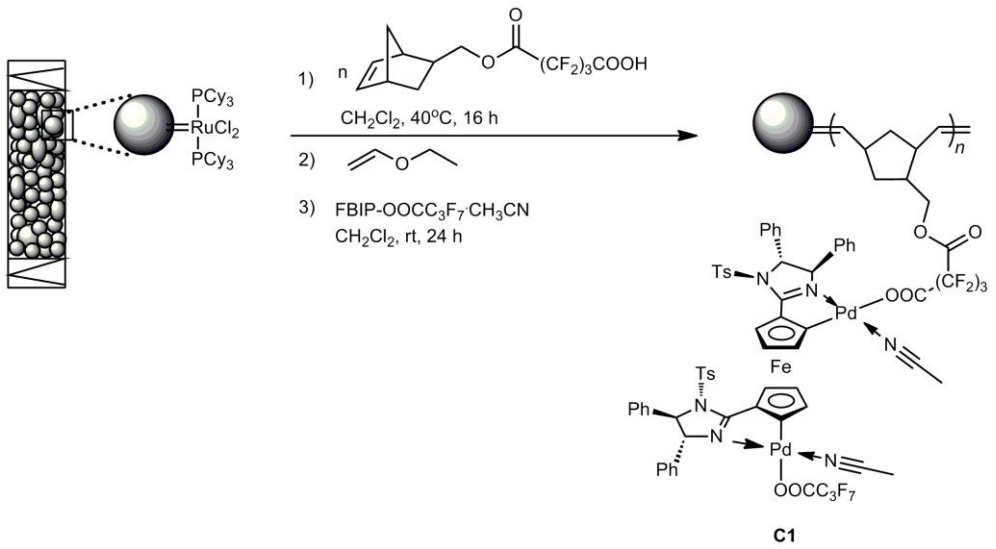

Scheme 14. Alternative route to the supported catalyst **C1**.

In contrast to the previous supported catalyst, no base-catalyzed products can be expected as there is no base used during the immobilization perocess. In addition, the alternative route offers a straightforward and convenient method to afford the supported catalyst with desired counter ion. The results of the enantioselective Michael-additions using this supported catalyst are summarized in Table 4.

Table 4. Results of the Michael addition reactions carried out by using the supported catalyst **C1.**[a]

entry	solvent	yield [%][b]	$ee_{(R,R)}$ [%][c]	$ee_{(R,S)/(S,R)}$ [%][c]	dr[c]
1[d]	diglyme	95	96	-72	7.7:1
2	CH_2Cl_2	18	63	-14	1.2:1
3[e]	diglyme	40	87	5	1.1:1

Conditions: [a] 90 µmol of **A**, 10 equiv. of **B**, 0.5 equiv. of HOAc, 0.6 mL of solvent. [b]Determined by ^{1}H NMR spectroscopy. [c]Determined by HPLC. [d]Under optimized homogeneous conditions, 92 µmol of **A**, 2 equiv. of **B**, 1 mol-% of **FBIP-O$_2$C$_4$F$_7$**, 0.2 equiv. of HOAc, 0.17 mL of diglyme. [e]185 µmol of **A**.

Although the above mentioned results (Table 4, entry 3) is comparable to the parent homogeneous catalysis (Table 4, entry 1), there are few important criteria that an immobilized chiral catalyst should fulfill in order to be applied to a chemical process. Important enough, the heterogenous system should exhibit activity, selectivity and reusability comparable to its homogeneous counterparts. Therefore, it is often necessary to evaluate the supported catalyst in terms of its activity, productivity, enantioselectivity, stability, and reusability. In order to fulfill the above outlined features, the catalyst must be immobilized in such way that the geometry of the optimized homogeneous catalyst should be maintained in the heterogeneous mode. In fact the geometry of an optimized homogeneous catalyst is rather difficult to maintain in the heterogeneous mode due to the interactions with the support and often leads to a negative change in enantioselectivity.[7] At this stage stability and accessibility of the linker ligand should be taken into account. Here the lower catalytic activity assumed to arise from the poor accessibility of the incoming catalytic species. Moreover, the monomer with hydrolysable groups such as ester, amides must be avoided.

3.2.5 Synthesis of Supported Catalyst C2 via Surface-Grafted M2

To overcome the above issues, the fluorinated monomer (**M2**) having a sufficient chain length with no hydrolysable groups was synthesized in six steps.

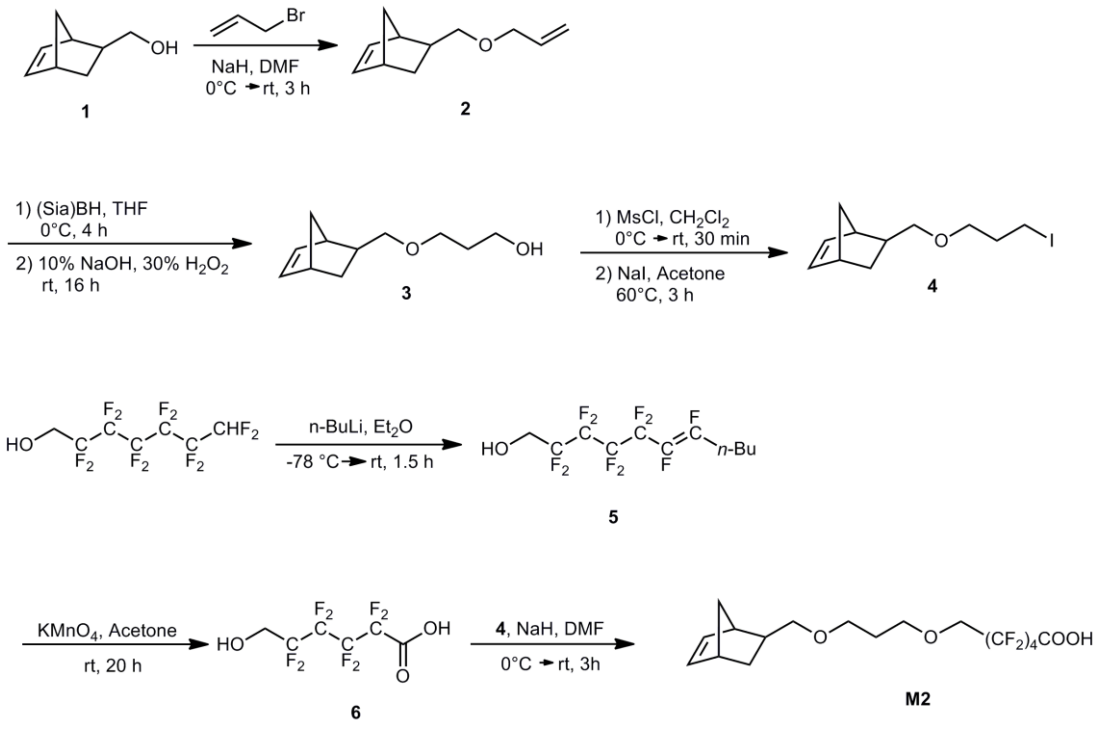

Scheme 15. Synthesis of the functional monomer **M2**.

The synthesis of **M2** entailed the sodium hydride-mediated coupling of the fluorinated hydroxyacid **6** with **4** in DMF (Scheme 15). The intermediate **4**[33] and **6**[31, 32] and was in turn synthesized starting from 5-norbornene-2-methanol (**1**) and 1H,1H,7H-dodecafluoro-1-heptanol, respectively, following a previously published protocol. Monomer **M2** was expected to have a sufficient chain length to connect the complex and the support, so that the complex can move far away from the solid surface and into the liquid phase. This will maintain geometry of the supported catalysts to a better extent similar to the homogeneous system. The absence of any hydrolysable groups in monomer **M2** should improve stability of the linker ligand thereby reducing the leaching of both the metal and ligand. Therefore monomer **M2** should also improve the reusability of the supported-catalysts.

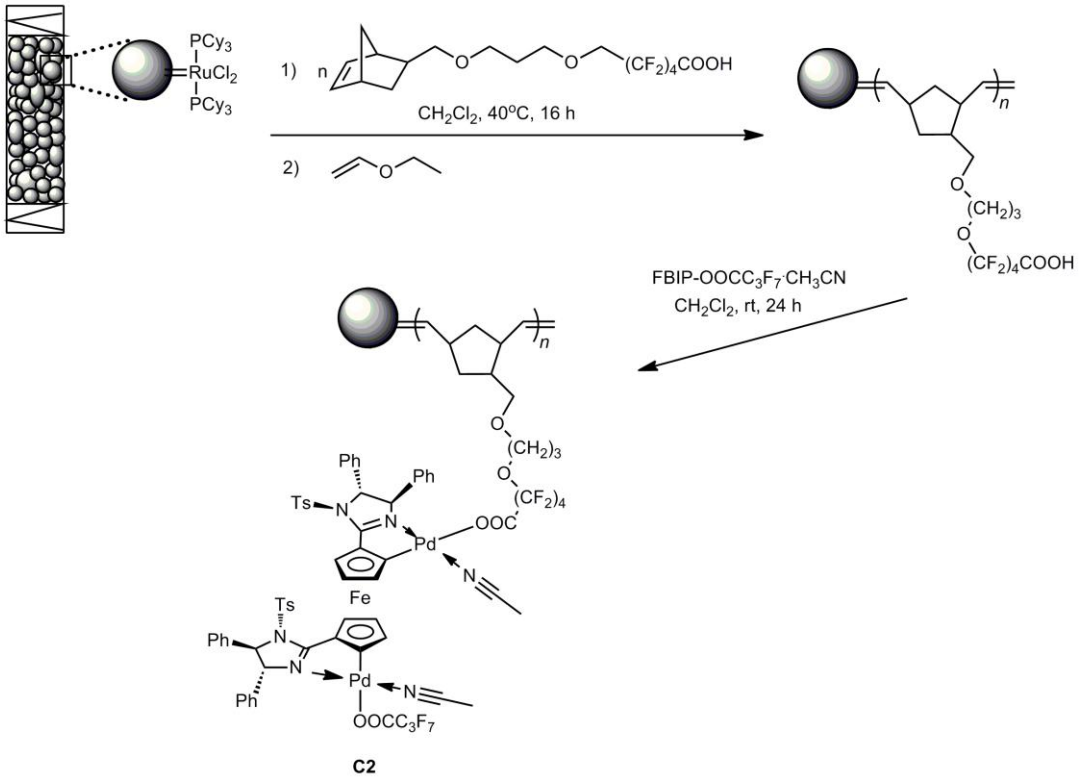

Scheme 16. Synthesis of the monolith-supported catalyst **C2**.

As described above, monomer **M2** was surface-grafted onto the metathesis-derived monolith and then reacted with the activated complex FBIP-$O_2C_4F_7$.CH_3CN to achieve the supported catalyst **C2** (Scheme 16). Immobilization was achieved through the direct substitution of the carboxylic acid groups with the activated complex. This way, 50% (23 mg/g) of the FBIP-

$O_2C_4F_7$·CH_3CN complex used were bound to the support, the remaining 50% were recovered as precatalyst (FBIP-Cl), indicating a successful immobilization.

3.2.6 Catalytic Performance of the Supported Catalyst C2

The catalytic activity of the supported catalyst **C2** in the enantioselective Michael-addition was investigated using *tert*-butyl 2-cyano-2-phenylacetate (**A**) and 2-cyclohexen-1-one as substrates (**B**). The results using 6.5 µmol of the immobilized catalyst under different reaction conditions are summarized in Table 5. Among the various solvents screened, the one carried out in CH_2Cl_2 and diethyl ether showed selectivity comparable to the parent homogenous system (Table 5, entries 4 and 5). However, the conversion of the substrate was found to be much lower when CH_2Cl_2 or $CHCl_3$ were used as solvents (Table 5, entries 5 and 6). Reactions in diglyme showed significantly reduced *ee*s (66%) and conversion compared to the reactions carried out with the supported catalyst **C1**. Nevertheless, the reduced conversions are rather attributed to the different reaction conditions applied here, i.e. unstirred *vs.* stirred batch.

Table 5. Results of the Michael addition reactions carried out by using the supported catalyst **C2.**[a]

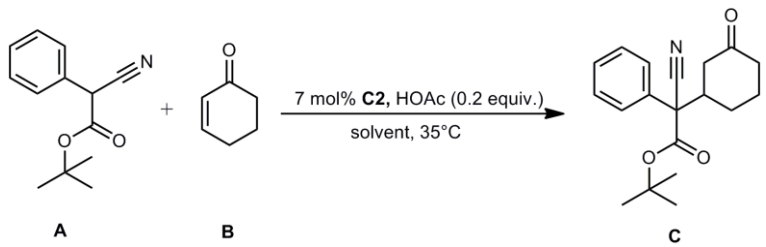

entry	solvent	time	yield [%][b]	$ee_{(R,R)}$ [%][c]	$ee_{(R,S)/(S,R)}$ [%][c]	dr[c]
1[d]	diglyme	20	95	96	-72	7.70:1
2	diglyme	24	29	66	-27	1.67:1
3	diglyme	72	51	23	-8	1.02:1
4	Et_2O	72	15	72	-4	1.44:1
5	CH_2Cl_2	20	2	69	22	2.70:1
6	$CHCl_3$	72	3	57	-10	1.12:1

Conditions : [a]90 µmol of **A**, 10 equiv. of **B**, 0.2 equiv. of HOAc, 0.1 mL of solvent. [b]Determined by ^{1}H NMR spectroscopy. [c]Determined by HPLC. [d]under optimized homogeneous conditions, 92 µmol of **A**, 2 equiv. of **B**, 1 mol-% of **FBIP-$O_2C_4F_7$**, 0.2 equiv. of HOAc, 0.17 mL of diglyme.

On the other hand, the drop in *ee*s can be tentatively attributed to the geometric constrains within the monolithic support. Interestingly, in all cases no observable leaching of metal was

observed. These results promise a stable and reusable heterogeneous chiral catalytic system with very low metal contamination.

3.3 Conclusion

The immobilization of an enatioselective Michael-addition catalyst on a ROMP-derived monolithic support was successfully accomplished via a grafting from approach. Immobilized catalyst bearing proper counter ion ($C_3F_7COO^-$) were realized via the simple substitution of the carboxylate ligand of the activated complex by one of the carboxylic acid groups of the graft polymer. The thus prepared supported catalysts were used in the enantioselective Michael additions of substrates having two stereo-centres. Michael-addition products with *ee*s comparable to the homogenous system were achieved without any metal contamination.

3.4 References

[1] E. N. Jacobsen et al. *Comprehensive Asymmetric Catalysis, Vol. I – III*, Springer, Berlin, **1999**.

[2] R. Noyori, *Asymmetric Catalysis in Organic Synthesis*, Wiley - Interscience, New York, **1994**.

[3] I. Ojima, *Catalytic Asymmetric Synthesis*. 2nd ed., Wiley - VCH Verlag GmbH, New York, **2000**.

[4] C. Baleizão, H. Garcia, *Chem. Rev.* **2006**, *106*, 3987.

[5] M. R. Buchmeiser, *Polymeric Materials in Organic Synthesis and Catalysis*, Wiley-VCH, **2003**.

[6] D. E. De Vos, I. F. J. Vankelecom, P. A. Jacobs, *Chiral Catalyst Immobilization and Recycling*, Wiley - VCH Verlag GmbH, Weinheim, **2000**.

[7] K. Ding, Y. Uozumi, *Handbook of Asymmetric Heterogeneous Catalysis*, WILEY-VCH Verlag GmbH & Co. KGaA, Weinheim, **2008**.

[8] Q.-H. Fan, Y.-M. Li, A. S. C. Chan, *Chem. Rev.* **2002**, *102*, 3385.

[9] J. A. Gladysz, *Chem. Rev.* **2002**, *102*, 3215.

[10] M. Heitbaum, F. Glorius, I. Escher, *Angew. Chem.* **2006**, *118*, 4850; *Angew. Chem. Int. Ed.* **2006**, *45*, 4732.

[11] M. R. Buchmeiser, *Macromol. Rapid Commun.* **2001**, *22*, 1081.

[12] M. R. Buchmeiser, *Polymer* **2007**, *48*, 2187.

[13] F. Sinner, M. R. Buchmeiser, *Macromolecules* **2000**, *33*, 5777

[14] F. Sinner, M. R. Buchmeiser, *Angew . Chem.* **2000,** *112*, 1491; *Angew. Chem. Int. Ed.* **2000**, *39*, 1433.

[15] M. R. Buchmeiser, *J. Mol. Catal. A: Chem.* **2002**, *190*, 145.

[16] M. R. Buchmeiser, R. Bandari, A. Prager-Duschke, A. Löber, W. Knolle, *Macromol. Symp.* **2010**, *287*, 107.

[17] M. R. Buchmeiser, F. M. Sinner, B. Mayr, S. Lubbad, R. Bandari, C. Gatschelhofer, *231st ACS National Meeting, Atlanta, GA, United States* **2006**, *ANYL-394*.

[18] S. Lubbad, B. May, M. Mayr, M. R. Buchmeiser, *Macromol. Symp.* **2004**, *210*, 1.

[19] M. R. Buchmeiser, *Bioorg. Med. Chem. Lett.* **2002**, *12*, 1837.

[20] M. Mayr, B. Mayr, M. R. Buchmeiser, *Angew. Chem.* **2001**, *113*, 3957; *Angew. Chem. Int. Ed.* **2001**, *40*, 3839.

[21] M. R. Buchmeiser, *Chem. Rev.* **2008**, *109*, 303.

[22] J. O. Krause, S. H. Lubbad, O. Nuyken, M. R. Buchmeiser, *Macromol. Rapid Commun.* **2003**, *24*, 875.

[23] R. M. Kroll, N. Schuler, S. Lubbad, M. R. Buchmeiser, *Chem.Commun.* **2003**, 2742.

[24] M. Sudheendran, M. R. Buchmeiser, *Macromolecules*, *43*, 9601.

[25] S. Jautze, P. Seiler, R. Peters, *Chem. Eur. J.* **2008**, *14*, 1430.

[26] S. Jautze, P. Seiler, R. Peters, *Angew. Chem.* **2007**, *119*, 1282; *Angew. Chem. Int. Ed.* **2007**, *46*, 1260.

[27] S. Jautze, S. Diethelm, W. Frey, R. Peters, *Organometallics.* **2009**, *28*, 2001.

[28] S. Jautze, R. Peters, *Synthesis* **2010**, *3*, 365.

[29] S. Jautze, R. Peters, *Angew. Chem.* **2008**, *120*, 9424; *Angew. Chem. Int. Ed.* **2008**, *47*, 9284.

[30] J. O. Krause, S. Lubbad, O. Nuyken, M. R. Buchmeiser, *Adv. Synth. Catal.* **2003**, *345*, 996.

[31] T. Nguyen, M. Rubinstein, C. Wakselman', *Synth. Commun.* **1983**, *13*, 81.

[32] Z. Szlávik, G. Tárkányi, Z. Skribanek, E. Vass, J. Rábai, *Org. Lett.* **2001**, *3*, 2365.

[33] H. Liu, S. Wan, P. E. Floreancig, *J.Org. Chem.* **2005**, *70*, 3814.

4

Cyclopolymerization-Derived Conductive Monolithic Media for Continuous Heterogeneous (Electro-) Catalysis

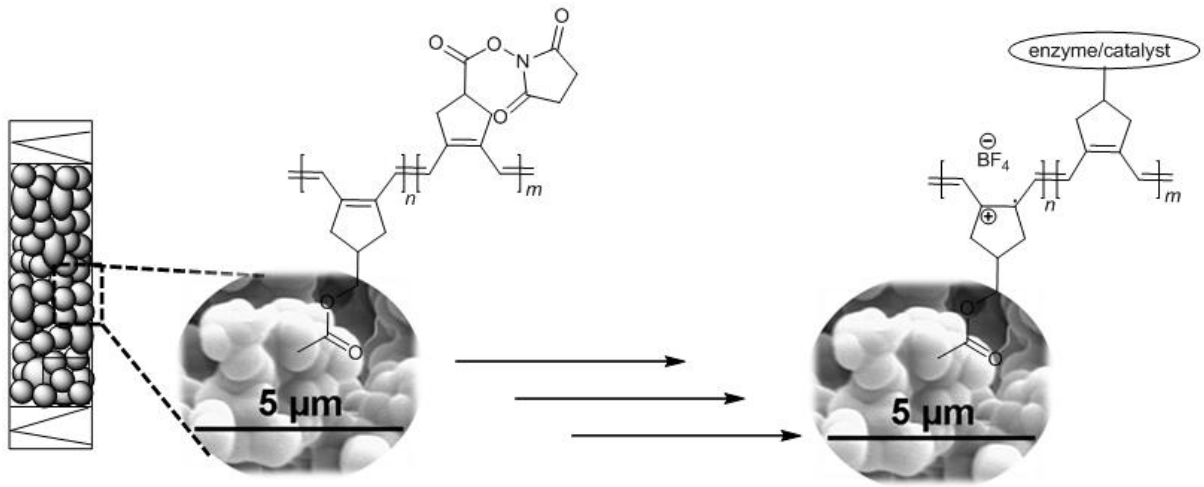

M. Sudheendran, E.Roeben, A.Seifert, A.Inan, P.S. Kumar, E.Klemm and M. R. Buchmeiser.

This project was collaborated with the research group of Prof. Dr.-Ing. Elias Klemm, Institute of Technical Chemistry, University of Stuttgart and Alexander Seifert from Technical Biochemistry, University of Stuttgart.

4.1 Introduction

Conjugated organic polymers play a very important role in material sciences and are used in various electronic applications,[1-9] such as organic light emitting diodes (OLEDs), solar cells, photovoltaic devices and field effect transistors.[4, 5, 7, 8] One of the most remarkable achievements in this field was the discovery of soluble conjugated polymers based on the cyclopolymerization of non-conjugated diynes.[10] For the past decades, poly(1,6-heptadiynes) prepared via the cyclopolymerization of 1,6-heptadiynes have reached an extraordinary level of sophistication.[11-20] They possess good long-term stability toward oxidation, and high effective conjugation lengths. The cyclic structures occur along their conjugated backbone, enhancing their processability.[21] The repeat units of such cyclopolymerization-derived polymers may consist of either five- or six-membered rings, depending on the insertion mode of the monomer into the initiator (α- and β-insertion). Nevertheless, among the two structural variations, those based on five-membered repeat units possess higher effective conjugation lengths and higher conductivity. [22] One of the potential applications of conjugated polymers is in the field of electrochemically-driven biocatalysis. The unbelievable efficiency of various redox enzymes to carry out valuable organic transformations motivates the search for the innovative strategies in electrode-driven biocatalysis.[23-28] There exists scattered reports, were conjugated polymeric materials are used as a medium for the charge transfer from electrode to electrochemically active bioenzyme. The recent studies mainly focuses on the modification of the electrode with an appropriate medium such as polymer, in order to attain native structure and appropriate orientation thereby increasing electron transfer between the enzyme and the electrode.[25-28] One of the most recently studied redox enzyme of this category is cytochome P450. This enzyme is versatile and able to catalyze important reactions with very high regio- and stereoselectivity. However, the utility of this class of enzyme for commercial syntheses is severely limited by the requirements for a continuous electron supply to the heme group. The natural source of electrons for this catalytic system is NAD(P)H, which, is however, too expensive to be used in equimolar concentrations for technical applications. For the last decades several approaches have been made to substitute the natural co-factor NAD(P)H. Very recently, Holtmann et al. reported on the entrapment of catalytically self-sufficient P450 BM-3 in polypyrrole by electrochemical polymerisation to immobilise the active enzyme on electrodes thereby allowing for biocatalytic activity without the use of the native cofactor NADPH.[27] This chapter describes the unprecedented cyclopolymerizaion-based approach to conductive monolithic support, suitable for the immobilization of redox active enzymes for electrocatalysis. Synthesis,

functionalization and the characterization of cyclopolymerization derived-monolithic supports are described in detail.

4.2 Results and Discussion

4.2.1 Monomers, Cross-linkers and Catalysts

In contrast to ROMP-derived monolithic media, in which a 1st generation Grubbs type catalyst is often used to polymerize strained monomers such as norbornenes and its derivatives,[29, 30] the cyclopolymerization-based system requires significant changes in the structure of the catalyst. As a consequence of low reactivity relative to ring-opening metathesis polymerization, a catalyst with enhanced reactivity should be selected in order to cyclopolymerize functionalized 1,6-heptadiynes.

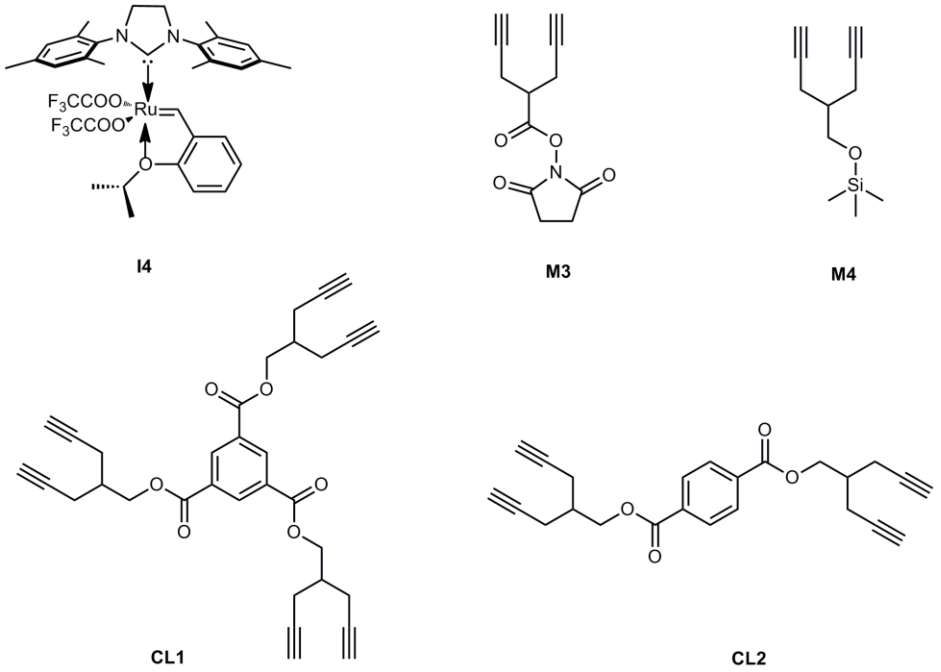

Figure 11. Structure of initiator (**14**), cross-linkers (**CL1** and **CL2**) and monomers (**M3** and **M4**).

In principle, both Schrock and selected modified Hoveyda-Grubbs systems, which are active in cyclopolymerization of diynes, may be applied.[15, 16, 18-20, 31] Quite recently, Buchmeiser et.al. reported the cyclopolymerization of 1,6-heptadiynes in living and stereoregular manner using modified Hoveyda-Grubbs type initiators.[11, 13, 14]

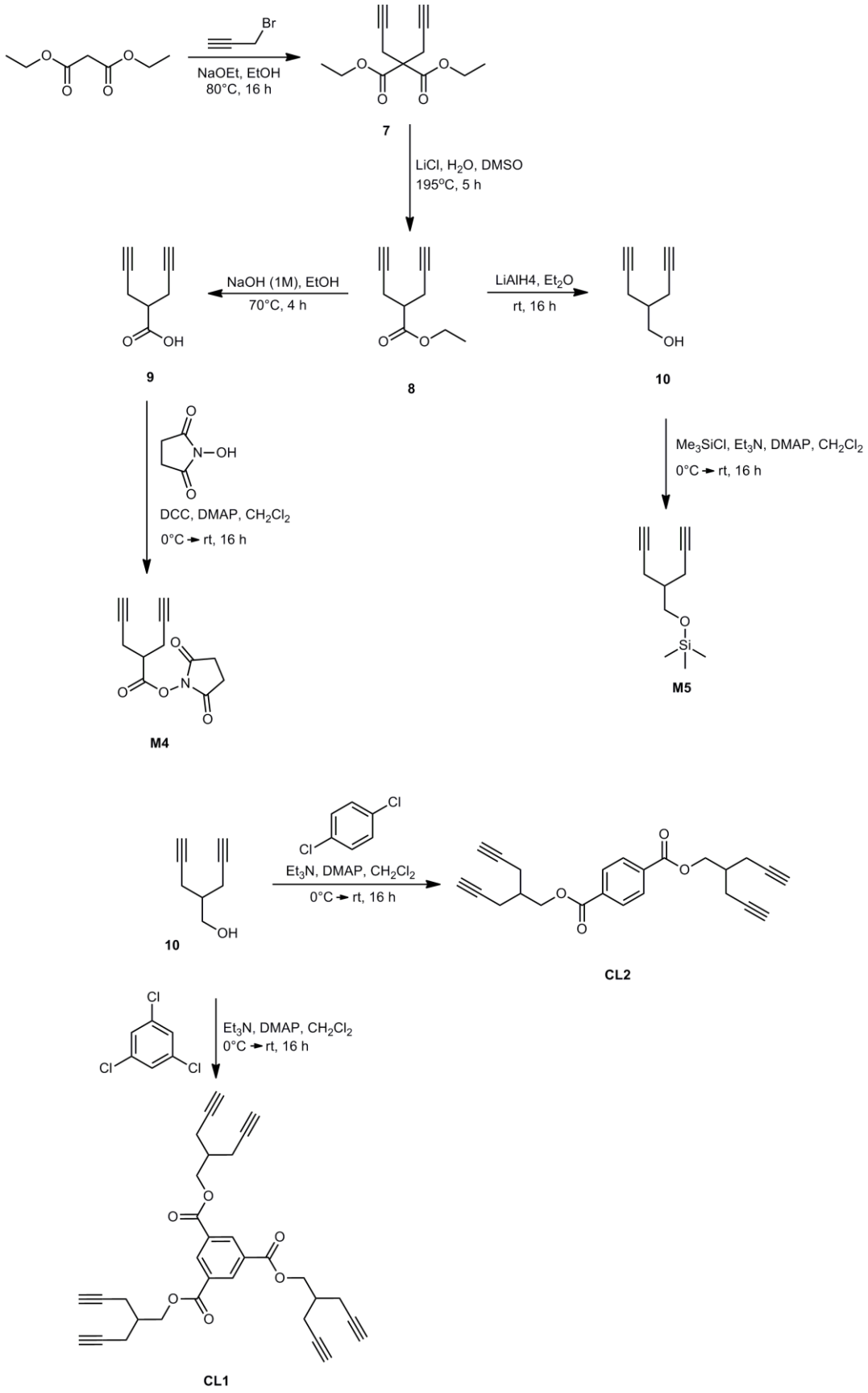

Scheme 17. Synthetic route to the monomers (**M3** and **M4**) and cross-linkers (**CL1** and **CL2**).

Since the preparation of monoliths requires elevated temperature and may not be performed under strict inert atmosphere, a thermally stable and less oxygen-sensitive ruthenium-based initiator [$Ru(CF_3COO)_2(IMesH_2)(=CH\text{-}2\text{-}(2\text{-}PrO)\text{-}C_6H_4)$] (**14**)[14] which is capable of cyclopolymerizing 1,6-heptadiynes, was used.

The basic substrates 4-carboxy-1, 6-heptadiyne (**9**) and 4-(hydroxylmethyl)-1, 6-heptadiyne (**10**) for the synthesis of both functional monomers and cross-linkers were prepared from commercially available diethylmalonate based on a literature protocol (Scheme 17).[14, 32] The synthesis of **M3** entailed the dicyclohexyl carbodiimide-mediated coupling reaction of **9** with *N*-hydroxysuccinimide, whereas the trimethylsilyl-protected monomer **M4** was obtained from the reaction of **10** with trimethylsilyl chloride in the presence of triethylamine and 4-dimethylaminopyridine (DMAP). The synthesis of the cross-linkers **CL1** and **CL2** was fairly simple and entailed the coupling reaction of terephthaloyl dichloride and 1,3,5-benzenetricarboxylicacid chloride, respectively, with **10**. The synthetic route to monomers and cross-linkers are shown in Scheme 17.

4.2.2 Synthesis of Cyclopolymerization-Derived Monoliths

In contrast to ROMP-derived system, the cyclopolymerization of 1,6-diynes using Ru-based initiators often require long reaction time and slightly elevated temperatures. Another key issue is the miscibility of the monomers, cross-linkers and porogenic solvents. Among the various porogenic solvents investigated for their pore-forming properties, 2-propanol was found to be good as in the case of standard ROMP-drived system.[33] Though toluene and 1,2-dichloroethane were found to be capable of forming the desired microstructures in combination with 2-propanol, on the basis of solubility dichloroethene was most suitable. Nevertheless, a slight warming up to 45^{o}C was unavoidable to maintain the polymerization mixture homogeneous. For the preparation of monoliths, different combinations were tested including those reported for the ROMP-derived system for their ability to form the desired, well-defined microstructures. Among the possible combinations, the one consisting of **CL1** or **CL2** (30 wt.-%), 2-propanol (40 wt.-%) as macroporogen, 1,2-dichloroethane (30 wt.-%) as microporogen and **I4** (0.4 wt.-%) as initiator at a polymerization temperature of 45^{o}C worked best.[34] The procedure adopted for the preparation of monoliths was similar to that of standard ROMP-derived systems,[33] however, with a slight modification (Scheme 18).

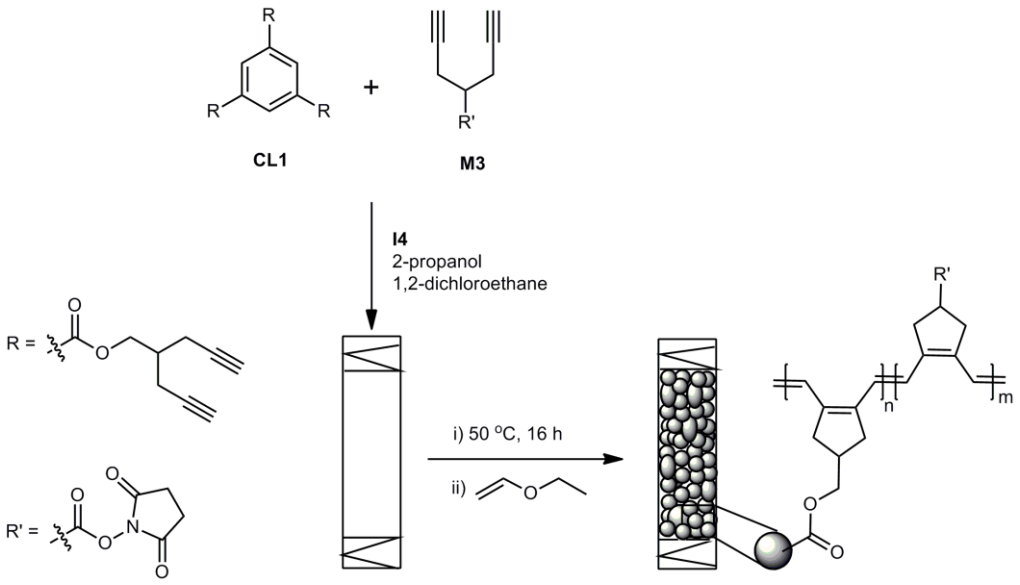

Scheme 18. Schematic illustration of the preparation of a cyclopolymerization derived monolith.

Briefly, two solutions A and B were prepared separately with all the necessary reactants for the polymer synthesis. Solution A consisted of the monomer (**M3** or **M4**) (2 wt.-%), **CL1** or **CL2** (28 wt.-%), 1,2-dichloroethane (20 wt.-%) and 2-propanol (40 wt.-%), solution B consisted of the initiator **I4** (0.4 wt.-%) in 1,2-dichloroethane (10 wt.-%). Solution A was warmed to 45°C to dissolve the monomer and cross-linker completely and it was removed from the bath once all compounds had dissolved. Since the polymerization at this temperature is much faster, the time for the handling of the mixture i.e., transfer into the column is very short. Before solution A had reached room temperature, solution B was added, followed by mixing for a few seconds. The mixture was then immediately transferred to the stainless steel column or microstructured channels closed at one end. The polymerization was allowed to proceed at 45^{o}C for 16 h. The initiator was removed by flushing the monolith with a mixture of DMSO:THF:EVE (40:40:20) at a flow rate of 0.05 mL/min. The dark purple colour of the monolith indicates a highly conjugated backbone.

4.2.3 Microstructure of Cyclopolymerization-derived Monoliths

In order to understand the microstructure of the monolithic supports, the structural data were obtained by means of electron microscopy (ELMI) and by inverse size exclusion chromatography (ISEC).[35] A description of the construction of a monolith in terms of microstructure, backbone and relevant abbreviations is given elsewhere (Figure 12).[33, 36]The porosity and pore size distribution of each monolith was determined by inverse size exclusion

chromatography (ISEC) in $CHCl_3$ using polystyrene (PS) standards. The ISEC calibration curve of monoliths 1-3 (Figure 13) shows the retention volume for a set narrow PS standards with defined molecular masses in the range of 92 (toluene)-2000 000 g/mol. The values for σ, ε_p, ε_z and ε_t were directly calculated from ISEC data following the method reported by Halász et al.[35]

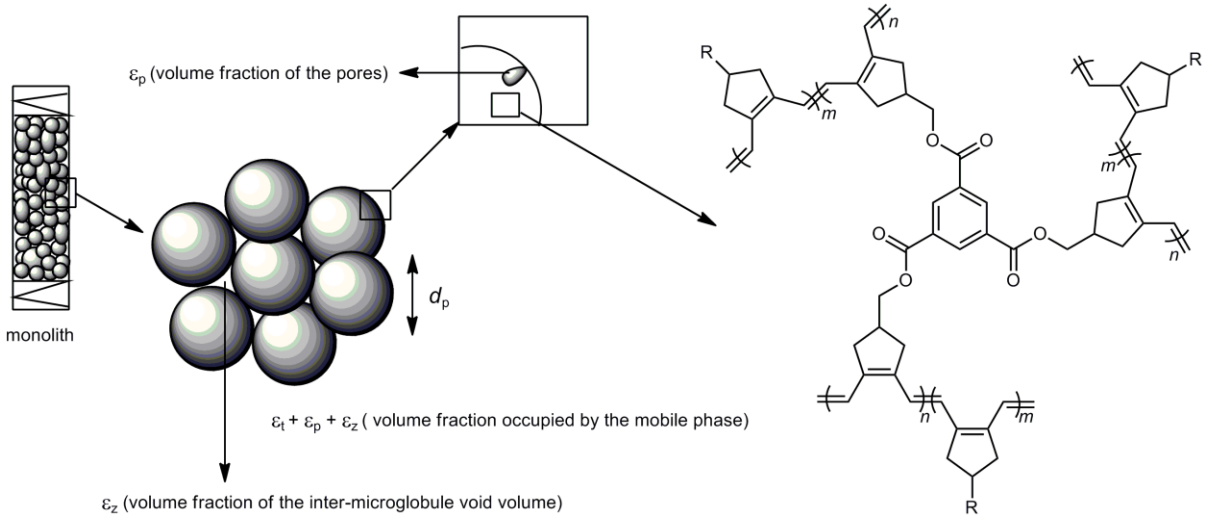

Figure 12. Illustration of the physical meanings of d_p, ε_p, ε_z and ε_t and schematic drawing of the backbone structure. R = functional group.

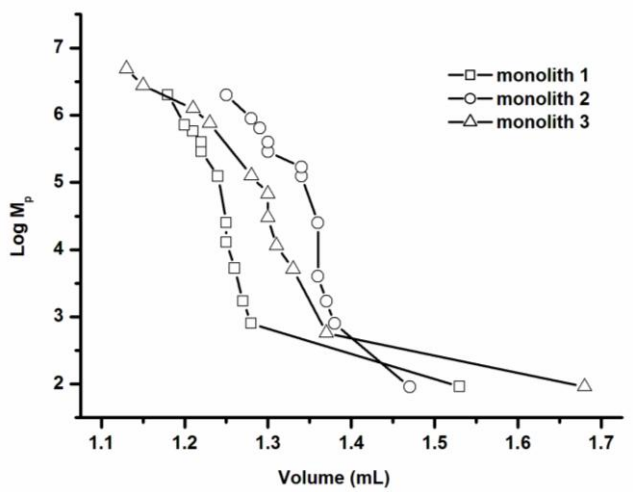

Figure 13. Inverse size exclusion chromatography calibration curve for monoliths 1-3(120 x 2.3 mm i.d.); monlith 1 and 2, flow rate: 0.8 mL/min; monolith 3, flow rate: .1 mL/min; mobile phase, THF; analytes, polystyrene standards and toluene; UV detection, 254 nm.

As can be deduced from Table 6, the volume fraction of the pores (ε_p) and the volume fraction of the inter-microglobule void volume (ε_z) could be varied within 10-28 and 57-64% respectively.

These values resulted in the total porosities (ε_t) within the range of 74-85%. The pore-size distributions of monoliths 1-3 are summarized in Figure 14.

Table 6. Physicochemical Data for Cyclopolymerization-Derived Monoliths **1-3**.

#	CL (%)	M (%)	1,2-DCE (%)	2-PrOH (%)	I4 (%)	σ (m^2g^{-1})	V_p (μLg^{-1})	ε_p (%)	ε_z (%)	ε_t (%)
1	**CL1**/33	**M3**/2	25	40	0.4	64	500	18	59	77
2	**CL2**/28	**M3**/2	30	40	0.4	18	317	10	64	74
3	**CL2**/28	**M4**/2	30	40	0.4	49	916	28	57	85

M: functional monomer **M3** or **M4**, CL: cross-linker **CL1** or **CL2**, 1,2-DCE: 1,2-dichloroethane, 2-PrOH: 2-propanol, T_p: polymerization temperature (45°C), σ: specific surface, V_p: pore volume ε_p: volume fraction of open pores, ε_z: volume fraction of inter microglobule void volume, ε_t: volume fraction occupied by mobile phase.

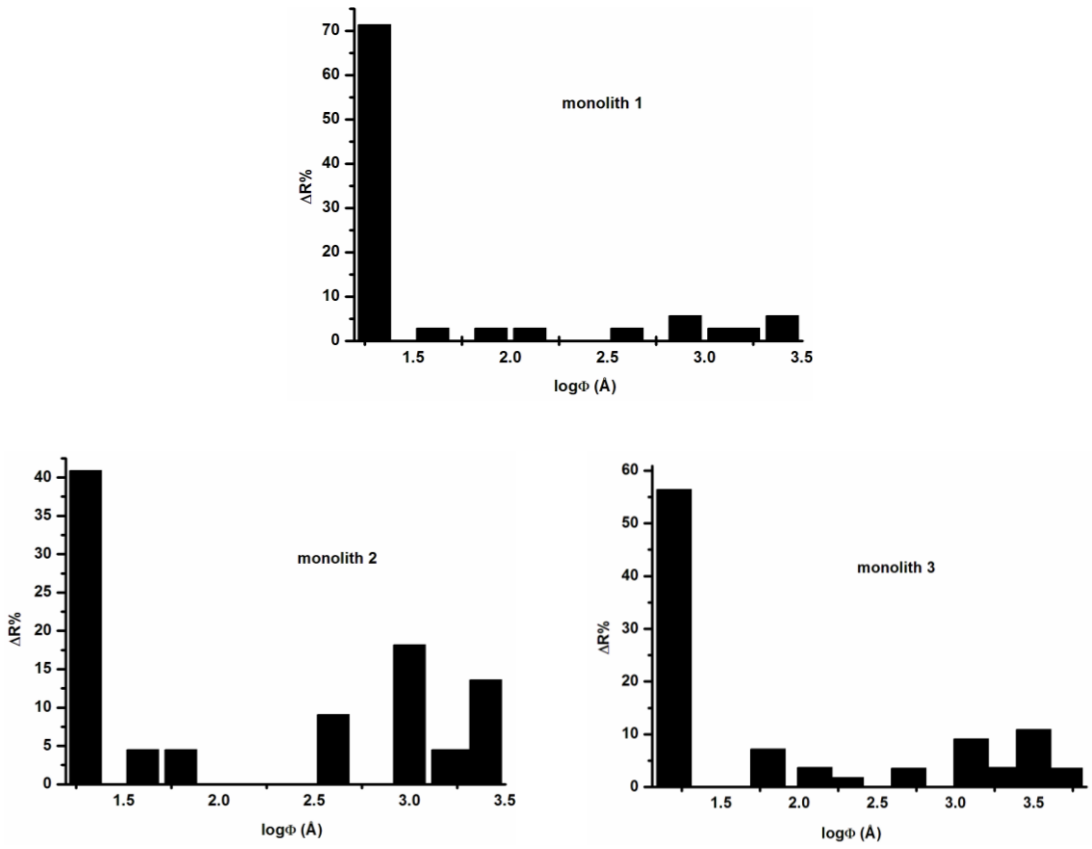

Figure 14. Pore size distribution for cyclopolymerization-derived monolith **1-3**.

Another important parameter, which influences the morphology of the monolith, is the polymerization temperature. The cyclopolymerization-derived system requires a higher polymerization temperature (T_p = 50°C) as compared to standard ROMP-derived systems. This

elevated temperature increases the initiators activity and leads to the formation of larger amounts of growing nuclei and, consequently, to the formation of smaller microglobules. Therefore the mean microglobular diameter (d_p) determined from ELMI was almost 1 ± 1 µm, as is also visualized in Figure 15. Additionally, phase separation is delayed at higher T_p values due to the enhanced solubility of the polymer in the system.

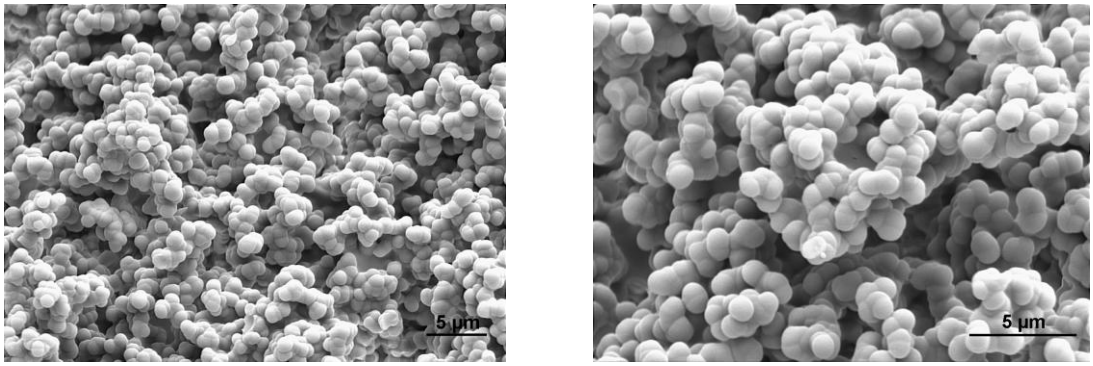

Figure 15. Electron microscope images of cyclopolymerization-derived monolith **1**.

Porous polymeric stationary phases in contact with organic solvents often lack sufficient mechanical strength.[33] To evaluate the mechanical stability of the column material, the pressure-drop across the column was measured by perfusion with various solvents in a wide range of flow rates.

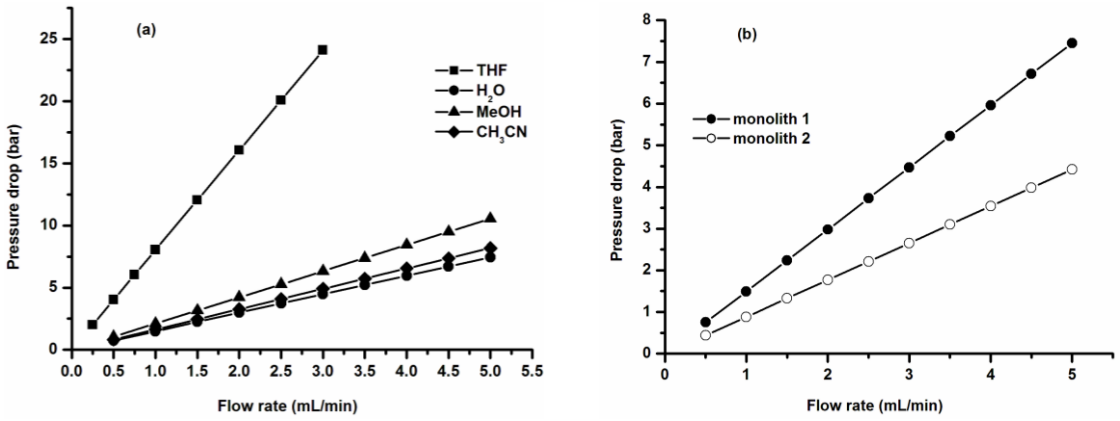

Figure 16. A plot of pressure drop (bar) versus flow rate (mL/min); (a) for monolith **1**; (b) for monolith **1** and **2** applying water as mobile phase.

The pressure drop at different flow rates for four different solvents is summarized in Figure 16. As might be expected, THF, which represents an excellent solvent for polymers causes extensive swelling of the monolithic material; consequently, the back pressure is found to be significantly elevated. The other solvents do not cause any considerable swelling, and consequently gave the

expected order in the back pressure. Most important, all points were linear, indicative for a non-compressible monolithic bed.

4.2.4 Functional Group Accessibility

The monolithic polymeric supports nowadays hold an impressively strong position in separation sciences as well as in the other area of chemistry such as heterogeneous catalysis and bioreactors.[37-49] It is often necessary to functionalize the monolithic support to introduce suitable functional groups for the immobilization of a catalyst or an enzyme. Usual synthetic protocols for functionalization entail the copolymerization of the corresponding functional monomer during the synthesis of the rigid rod. However, by this approach major part of the functional monomers are located at the interior of the rod-forming microglobules, and are thus often difficult to access by an incoming catalyst or enzyme. For the successful realization of the monolithic polymeric structures from monomers and cross-linkers, the polymerization kinetics of the copolymerization was investigated. The polymerization was carried out by using initiator **I4** at 45^{o}C in 1, 2-dichloroethane.

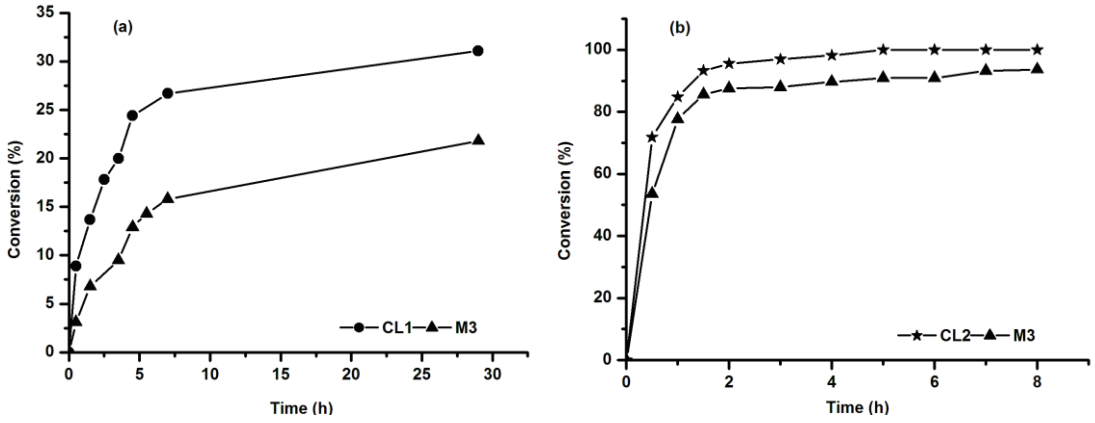

Figure 17. Kinetic plot obtained for the copolymerization of **M3** with **CL1** and **CL2** using initiator **I4** in 1,2-dichloroethane at 45^{o}C.; (a) **M3** with **CL1** (b) **M3** with **CL2**.

The homopolymerization of **M3** and **M4** showed a conversion of >80% within 16 h, whereas conversion reached to 100% within 16 h in the case of **CL2** (Figure S13, Chapter 6). The non-linear nature of the 1st-order plots obtained for this polymerization indicates that the polymerizations are not truly living. Therefore, it is reasonable to conclude that the functionalization via surface-grafting of such monoliths is not a suitable method to achieve functional monolithic media. As can be deduced from the kinetic studies, the conversion of **CL1** and **CL2** proceeded faster compared to the conversion of **M3**, which implies that the majority of

the functional monomer **M3** might be located at the surface of the microglobule (Figure 17) since they are copolymerized at the late stage of the reaction. To further proof the accessibility, active ester functional groups were reacted with taurine in 0.1M $NaHCO_3$ solution at pH = 8 (Scheme 19). The chemically accessible functional groups in the monolith were then quantified by elemental analysis. There, a nitrogen content of 220 µmol/g and a sulfur content of 170 µmol/g of monolith were found.

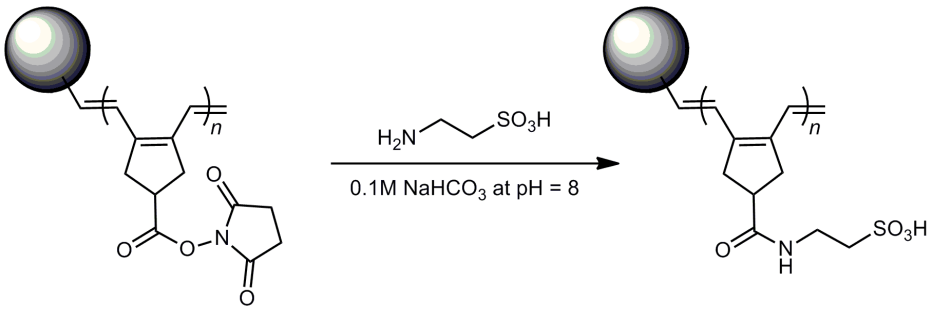

Scheme 19. Reaction of the active ester groups with taurine in a cyclopolymerization-derived monolith.

The nitrogen content indicates the total number of active ester groups in the monolith, where as the sulfur content indicate the number of accessible active ester groups. From the above data it is clear that, approximately 77% of the active ester groups are located at the surface of the microglobule and are chemically accessible. Moreover, the experiment also provided a proof for the stability of the monolith at pH 8, which lies in the preferred pH range of bioenzymes. In contrast, the kinetic study of the copolymerization of **CL2** with **M4** revealed that conversion of **CL2** almost stopped after 30 min and reached a maximum of 54 % after 10 h (Figure S14, Chapter 6). Since the proposed project was targeted to immobilize redox-active catalyst particularly enzymes, monomer **M3** containing active ester group was preferred over **M4.**

4.2.5 Conductivity of Cyclopolymerization–Derived Monolith

Interest in conductive monolithic media derives from its ability to act as a support for electrode-driven-biocatalysis. Although there exist several reports on conductive polymeric materials, conductive monolithic media with defined porous structure prepared via the cyclopoymerization of diynes have never been reported. In addition, they have excellent processability and are stable at the optimum pH range used for the enzyme catalysis. However, in order to find application in electrode-driven catalysis, the conductivity of such monoliths must exceed 10^{-5} $S{\cdot}cm^{-1}$. For this purpose, monoliths were doped with a 5 wt.-% solution of p-dopants in suitable solvent and the

conductivity was measured by using an ohm meter. The observed conductivities of the cyclopolymerization-derived monoliths employing various p-dopants are outlined in Table 7. Since the resistance of the undoped monolith was beyond the limit of detection of the instrument used, the conductivity in this case was taken as zero (Table 7, entry 1). Among the dopants used, $NO^+BF_4^-$ was found to be the best in terms of conductivity and ease of handling. While the monolith doped with I_2 and SbF_5 displayed a conductivity of 7.3 $x10^{-6}$ $S{\cdot}cm^{-1}$and 1.4 $x10^{-6}$ $S{\cdot}cm^{-1}$, repecitvely, (Table 7, entry 5 and 6), the $NO^+BF_4^-$ -doped monolith displayed a conductivity of 5.7 $x10^{-4}$ (Table 7, entry 1).

Table 7. Conductivity of non-doped/doped cyclopolymerization-derived monoliths.

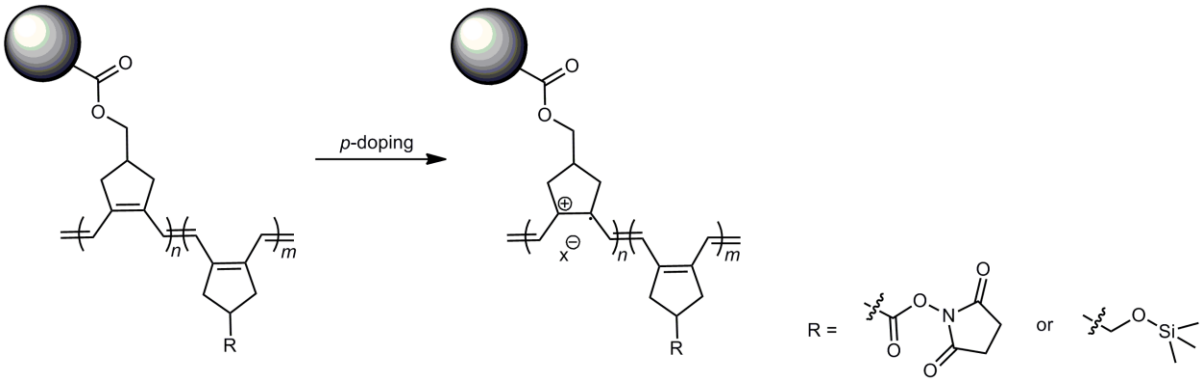

Entry	Monolith	Dopant	Solvent[a]	l (cm)	σ ($S{\cdot}cm^{-1}$)
1	**1** and **2**	undoped	n.m	12	n.m
2	**1**	$NO^+BF_4^-$	THF	12	5.7 $x10^{-4}$
3	**1**	$NO^+BF_4^-$	MeOH	5	1.4 $x10^{-4}$
4	**2**	$NO^+BF_4^-$	THF	0.8	3.4 $x10^{-6}$
5	**2**	I_2	CH_2Cl_2	0.6	7.3 $x10^{-6}$
6	**2**	SbF_5	THF	0.6	1.4 $x10^{-6}$

[a]solvent used for doping, l = length of the monolith, area of cross section (A) = 0.13 cm^2. σ = conductivity. n.m – not measured.

Since the enzymatic reactions are planned to be conducted in a buffer medium, it is also interesting to note the conductivity of such monoliths in the presence of buffer solutions. In contrast to the undoped monolith which displayed a conductivity of 6.3 x 10^{-6} $S{\cdot}cm^{-1}$in 0.1 M HEPES buffer solution at pH = 9.2, the doped monolith displayed a conductivity of 5.9$x10^{-4}$ $S{\cdot}cm^{-1}$ under the same buffer conditions.

4.2.6 Immobilization of Trypsin on a Cyclopolymerization-Derived Monolith[50]

Next, we aimed to examine the stability of various enzymes immobilized onto a monolithic support in both a doped and an undoped environment. This is supposed to be the crucial part before applying the monolith for electrode-driven biocatalysis. The use of monoliths for the immobilization of transition-metal-based catalysts or enzymes has been reported by our group[50-54] as well as by Svec and Fréchet.[55-57]Since the electrocatalysis was proposed to be carried out in a doped system the stability of the enzyme under these conditions should also be taken into account. For this purpose we chose to immobilize trypsin on a doped cyclopolymerization-derived monolith. Since the doping procedure might result in a total deterioration of the immobilized enzyme, the monolith was doped with $NO^+BF_4^-$ before the immobilization of trypsin. Excess dopant was completely removed by flushing with THF. Finally, the immobilization of trypsin was achieved via the accessible active ester functionalities of the monolith (Scheme 20).

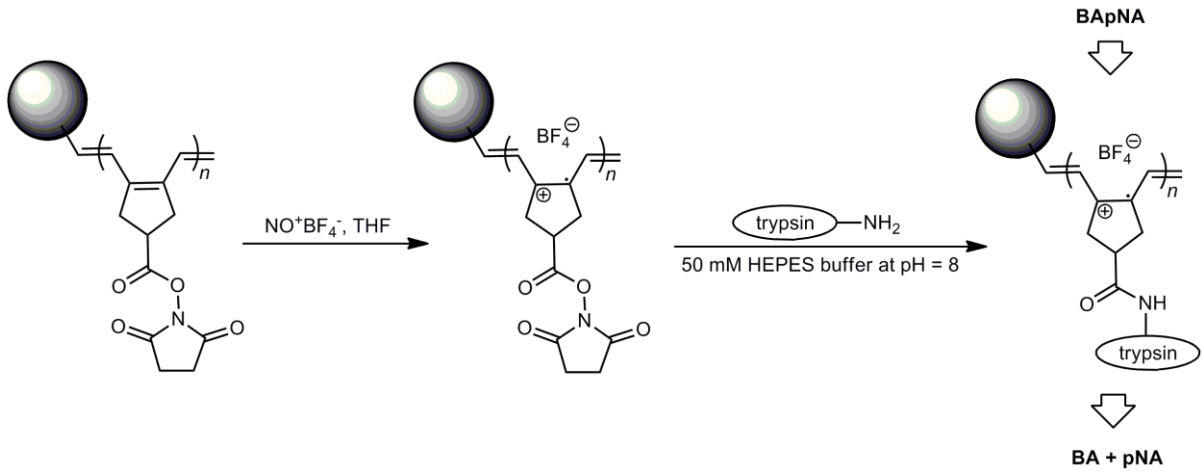

Scheme 20. Schematic illustration for the immobilization of trypsin on a doped cycloplymerization-derived monolith.

After its immobilization, the proteolytic activity of the immobilized enzyme was quantified by using *N*-α-benzoyl-DL-arginine-p-nitroanilide hydrochloride (BAPNA) as substrate as described in Chapter 2. Figure 18 summarizes the product formation and the rate of hydrolysis as monitored by RP-HPLC.

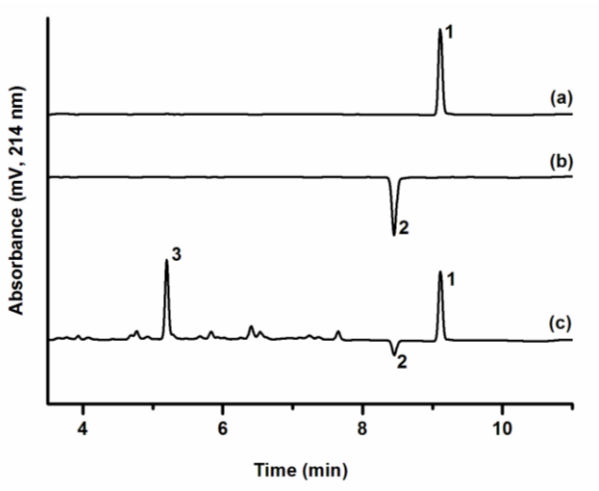

Figure 18. RP-HPLC chromatogram obtained for the tryptic digestion of BAPNA in a monolith doped with $NO^+BF_4^-$: (a) standard BAPNA, (b) standard PNA, (c) on-column tryptic digest of 0.25 mM BAPNA in 10 min at 37 ^oC. Peak 1 is BAPNA, peak 2 is PNA, and peak 3 is BA. Conditions: flow rate 1 mL min^{-1}; 25^oC; mobile phases: A: 95% water + 5% acetonitrile (ACN) +0.1 % trifluoroacetic acid (TFA); B: 95 % ACN + 5 % water + 0.1 % TFA; gradient: 0 min 4 % B, 9 min 50 % B, 10 min 50 % B; UV(214 nm); injection volume 20 μL.

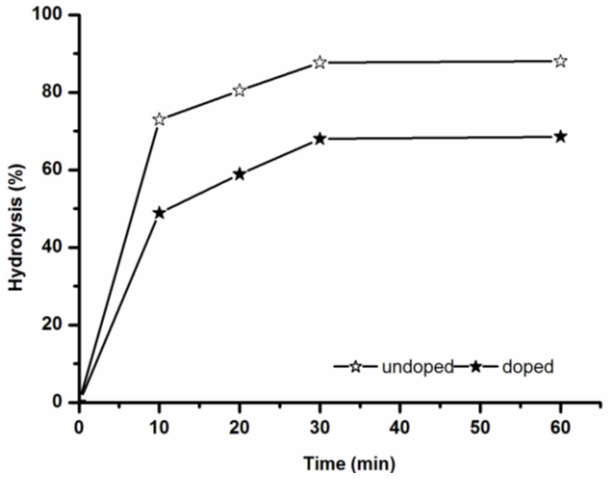

Figure 19. A comparison of the conversion *vs* time for the tryptic digest of 0.25 mM BAPNA at different reaction times using a doped and an undoped monolith. Conditions: T = 37^oC; mobile phase: 50 mM HEPES buffer.

The hydrolysis product *N*-α-benzoyl-DL-arginine (BA) that formed was analyzed at λ=214 nm, whereas the remaining amount of BAPNA was quantified at λ= 310 nm. The hydrolysis yield of BAPNA was determined by comparing the area of BAPNA after hydrolysis to the area of a standard BAPNA solution (0.25 mM). A comparison of the plots of conversion *vs* time for the tryptic hydrolysis of BAPNA in both doped and undoped monolith is shown in Figure 19. As

can be seen from Figure 19, a slight decrease in the activity was observed for the enzyme immobilized in the doped monolith. However, it is interesting to note that the enzyme was still active when immobilized to a doped monolith.

4.2.7 Applications

The above experiments promise an access to the permanent immobilization of enzymes on a conductive monolith without deterioration of the enzyme under doped conditions. The main intention of the conductive monolithic media was to design a stable support for the immobilization of such enzymes with a proper supply of electrons to catalytic site to enable reactions in a continuous flow mode. For our experiments, we chose cytochrome P450 monooxygenases as the enzyme for the proposed electrode-driven biocatalysis. These classes of enzymes are versatile biocatalysts, catalyzing important reactions such as the regio- and stereospecific hydroxylation of non-activated carbon-hydrogen bonds by inserting one oxygen atom from O_2 into the substrate.[23-27]The proposed electrode driven catalytic cycle is shown in Scheme 21. Its unique oxygenation chemistry and its substrate specificity offer the opportunity to develop enzymatic systems for synthesizing fine chemicals of great industrial importance.

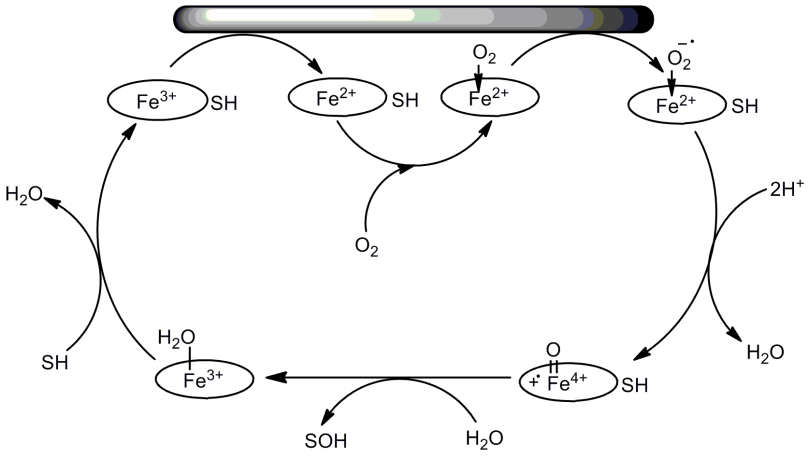

Scheme 21. Proposed catalytic cycle for electrode driven biocatalysis. SH is the substrate.

A key issue of the catalytic applications of such system is the demand for the continuous electron supply to the catalytic site. In this context, the cyclopolymerization-derived conductive monolithic media offers a better platform for the heterogenization of redox active enzymes suitable for eletrocatalysis.

4.2.7.1 Microreactor Compatibility of Cyclopolymerization-Derived Monolithic Materials

Because of low waste generation and safer experimental conditions, the microreactor technology has received considerable attention in the recent years. This technology offers several advantages over traditional batch synthesis methods.[58-60] Moreover, the reactor configuration and reaction parameters can be varied systematically. Furthermore, the method can be easily scaleup from laboratory to industrial scale. The dual channel microreactor setup for the proposed electrocatalysis consisted two goldplated copper blocks with microchannels 1 mm, 0.5 mm, in width, depths, and 980 mm in length all etched on one side. The two plates with micro-structured channels were separated by a thin teflon foil and were firmly compressed with the aid of screws between two stainless steel chucks (Figure 20). Among the two channels, one channel can be used for the monolith-supported enzyme, while the other channel can be used for the continuous supply of oxygen-rich buffer solution. The synthesis, functionalization and doping of the cyclopolymerization-derived monolith inside the micro reactor were accomplished following the protocol described above for the immobilization of trypsin.

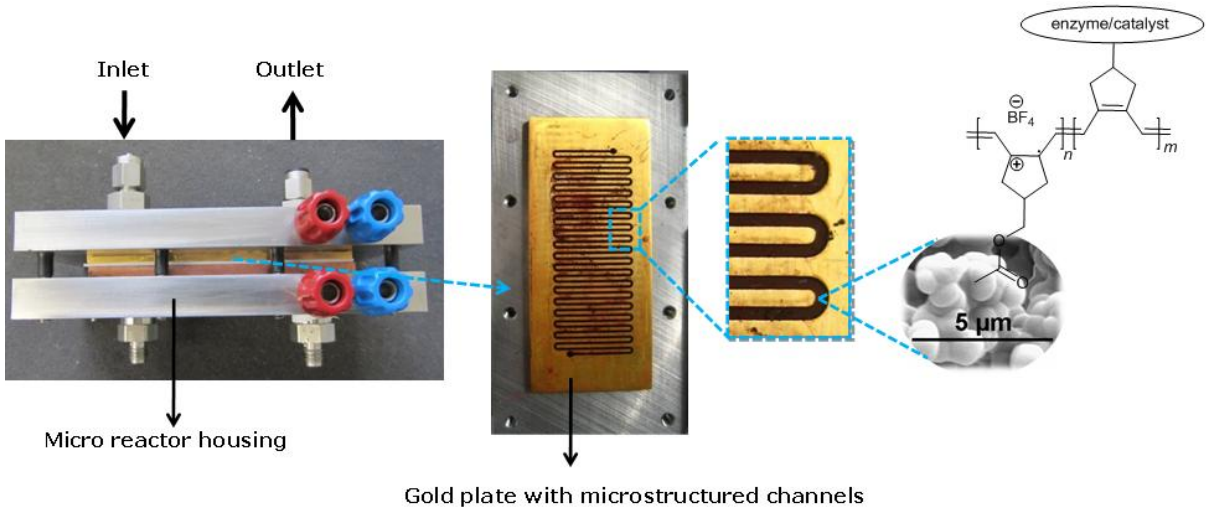

Figure 20: Schematic illustration of the cyclopolymerization-derived monolith fabricated inside microreactor platform.

4.3 Conclusions

An entirely new class of monolithic supports bearing a conjugated backbone prepared via the cyclopolymerization of 1,6-heptadiyne-based monomers and cross-linkers has been presented. Upon doping with $NO^+BF_4^-$, the thus prepared monoliths displayed conductivity in

the range of 10^{-6} to 10^{-4} $S \cdot cm^{-1}$. Monomers bearing functional groups suitable for the immobilization of catalyst or enzymes were introduced by an *in situ* copolymerization. Approximately 77% of the functional monomers were located at the surface of the microglobules, which are readily accessible to enzymes or catalysts. Moreover, the successful immobilization of trypsin without any deterioration of the enzyme was achieved on the doped monolith as shown by the excellent proteolytic activity of the immobilized enzyme. This class of monolithic media offer access to the permanent immobilization of redox-active catalysts containing amino groups and for use of the thus-prepared supported enzymes in continuous flow electrocatalysis. Moreover, the approach is suitable for fabricating the monolith in a microreactor platform.

4.4 References

[1] T. A. Skotheim, R. L. Elsenbaumer, J. R. Reynolds, *Handbook of Conducting Polymers*, 2 ed., Dekker, New York, **1997**.

[2] H. Shirakawa, *Angew. Chem.* **2001**, *113*, 2642; *Angew. Chem. Int. Ed.* **2001**, *40*, 2574.

[3] A. G. MacDiarmid, *Angewandte Chemie* **2001**, *113*, 2649; *Angew. Chem. Int. Ed.* **2001**,*40*,2591.

[4] A. J. Heeger, *Angewandte Chemie* **2001**, *113*, 2660; *Angew. Chem. Int. Ed.* **2001**, *40*, 2591.

[5] R. H. Friend, R. W. Gymer, A. B. Holmes, J. H. Burroughes, R. N. Marks, C. Taliani, D. D. C. Bradley, D. A. D. Santos, J. L. Bredas, M. Logdlund, W. R. Salaneck, *Nature* **1999**, *397*, 121.

[6] R. W. Dyson, M. Goosey, *Speciality Polymers*, New York, **1987**.

[7] S.-H. Chi, J. M. Hales, C. Fuentes-Hernandez, S.-Y. Tseng, J.-Y. Cho, S. A. Odom, Q. Zhang, S. Barlow, R. R. Schrock, S. R. Marder, B. Kippelen, J. W. Perry, *Adv. Mater.* **2008**, *20*, 3199.

[8] J. H. Burroughes, D. D. C. Bradley, A. R. Brown, R. N. Marks, K. Mackay, R. H. Friend, P. L. Burns, A. B. Holmes, *Nature* **1990**, *347*, 539.

[9] J. L. Brédas, R. J. Silbey, In *Conjugated Polymers*, Kluwer, Dordrecht, **1991**.

[10] J. K. Stille, D. A. Frey, *J. Am. Chem. Soc.* **1961**, *83*, 1697.

[11] P. S. Kumar, K. Wurst, M. R. Buchmeiser, *J. Am. Chem. Soc.* **2009**, *131*, 387.

[12] J. O. Krause, O. Nuyken, K. Wurst, M. R. Buchmeiser, *Chem. Eur. J.* **2004**, *10*, 777.

[13] J. O. Krause, O. Nuyken, M. R. Buchmeiser, *Chem. Eur. J.* **2004**, *10*, 2029.

[14] T. S. Halbach, J. O. Krause, O. Nuyken, M. R. Buchmeiser, *Macromol. Rapid Commun.* **2005**, *26*, 784.

[15] H. H. Fox, M. O. Wolf, R. O'Dell, B. L. Lin, R. R. Schrock, M. S. Wrighton, *J. Am. Chem. Soc.* **1994**, *116*, 2827.

[16] H. H. Fox, R. R. Schrock, *Organometallics* **1992**, *11*, 2763.

[17] S.-K. Choi, Y.-S. Gal, S.-H. Jin, H. K. Kim, *Chem. Rev.* **2000**, *100*, 1645.

[18] M. R. Buchmeiser, *Adv. Polym. Sci.* **2005**, *176*, 89.

[19] U. Anders, O. Nuyken, M. R. Buchmeiser, K. Wurst, *Angew. Chem.* **2002**, *114*, 4226.

[20] U. Anders, O. Nuyken, M. R. Buchmeiser, *J. Mol. Catal. A: Chem.* **2004**, *213*, 89.

[21] C. C. W. Law, J. W. Y. Lam, Y. Dong, H. Tong, B. Z. Tang, *Macromolecules* **2005**, *38*, 660.

[22] M. R. Buchmeiser, J. O. Krause, D. Wang, U. Anders, R. Weberskirch, M. T. Zarka, O. Nuyken, C. Jäger, D. Haarer, *Macromol. Symp.* **2004**, *217*, 179.

[23] F. Rubinson Judith, In *Conducting Polymers and Polymer Electrolytes, Vol. 832*, American Chemical Society, **2002**, pp. 2.

[24] V. Reipa, M. P. Mayhew, V. L. Vilker, *Proc. Natl. Acad. Sci.* **1997**, *94*, 13554.

[25] S. Krishnan, D. Wasalathanthri, L. Zhao, J. B. Schenkman, J. F. Rusling, *J. Am. Chem. Soc.* **2011**, *133*, 1459.

[26] S. Krishnan, J. B. Schenkman, J. F. Rusling, *J. Phy. Chem. B* **2011**, *115*, 8371.

[27] D. Holtmann, K.-M. Mangold, J. Schrader, *Biotech. Lett.* **2009**, *31*, 765.

[28] G. Chang, K. Morigaki, Y. Tatsu, T. Hikawa, T. Goto, H. Imaishi, *Anal. Chem.* **2011**, *83*, 2956.

[29] F. Sinner, M. R. Buchmeiser, *Macromolecules* **2000**, *33*, 5777.

[30] F. Sinner, M. R. Buchmeiser, *Angew. Chem. Int. Ed.* **2000**, *39*, 1433.

[31] U. Anders, M. Wagner, O. Nuyken, M. R. Buchmeiser, *Macromolecules* **2003**, *36*, 2668.

[32] L. Q. Xu, F. Yao, G.-D. Fu, L. Shen, *Macromolecules* **2009**, *42*, 6385.

[33] M. R. Buchmeiser, *Macromol. Rapid Commun.* **2001**, *22*, 1081.

[34] E. Roben, Diploma Thesis, University of Stuttgart (Stuttgart), **2011**.

[35] I. Halász, K. Martin, *Angew. Chem.* **1978**, *90*, 954; *Angew. Chem. Int. Ed.* **1978**, *17*, 901.

[36] M. R. Buchmeiser, *Ring-Opening Metathesis Polymerization, in Handbook of Ring-Opening Polymerization (eds P. Dubois, O. Coulembier and J.-M. Raquez)*, Wiley-VCH Verlag GmbH & Co. KGaA, Germany, **2009**.

[37] R. Bandari, W. Knolle, M. R. Buchmeiser, *J. Chromatogr. A* **2008**, *1191*, 268.

[38] R. Bandari, A. Prager-Duschke, C. Kuhnel, U. Decker, B. Schlemmer, M. R. Buchmeiser, *Macromolecules* **2006**, *39*, 5222.

[39] M. R. Buchmeiser, *J. Mol. Catal. A: Chem.* **2002**, *190*, 145.

[40] M. R. Buchmeiser, *Polymer* **2007**, *48*, 2187.

[41] M. R. Buchmeiser, *Chem. Rev.* **2008**, *109*, 303.

[42] S. Frantisek, *Electrophoresis* **2006**, *27*, 947.

[43] S. Frantisek, *Anal. Chem.* **2006**, *78*, 2100.

[44] M. Kato, K. Inuzuka, K. Sakai-Kato, T. Toyoóka, *Anal. Chem* **2005**, *77*, 1813.

[45] S. Lubbad, B. May, M. Mayr, M. R. Buchmeiser, *Macromol. Symp.* **2004**, *210*, 1.

[46] S. H. Lubbad, R. Bandari, M. R. Buchmeiser, *J. Chromatogr. A* **2011**, doi:10.1016/j.chroma.2011.03.003

[47] S. H. Lubbad, M. R. Buchmeiser, *J. Sep. Sci.* **2009**, *32*, 2521.

[48] S. H. Lubbad, M. R. Buchmeiser, *J. Chromatogr. A* **2010**, *1217*, 3223.

[49] S. H. Lubbad, M. R. Buchmeiser, *J. Chromatogr. A* **2011**, *1218*, 2362.

[50] M. Sudheendran, M. R. Buchmeiser, *Macromolecules* **2010**, *43*, 9601.

[51] J. O. Krause, S. Lubbad, O. Nuyken, M. R. Buchmeiser, *Adv. Syn. Catal.* **2003**, *345*, 996.

[52] J. O. Krause, S. H. Lubbad, O. Nuyken, M. R. Buchmeiser, *Macromol. Rapid Commun.* **2003**, *24*, 875.

[53] M. Mayr, B. Mayr, M. R. Buchmeiser, *Angew. Chem.* **2001**, *113*, 3957.

[54] M. Mayr, D. Wang, R. Kröll, N. Schuler, S. Prühs, A. Fürstner, M. R. Buchmeiser, *Adv. Syn. Catal.* **2005**, *347*, 484.

[55] J. Krenkova, N. A. Lacher, F. Svec, *Anal. Chem.* **2009**, *81*, 2004.

[56] F. Svec, J. M. J. Fréchet, *Science* **1996**, *273* 205.

[57] S. Xie, F. Svec, J. M. J. Fréchet, *Biotechn. Bioeng.* **1999**, *62*, 30.

[58] P. D. I. Fletcher, S. J. Haswell, E. Pombo-Villar, B. H. Warrington, P. Watts, S. Y. F. Wong, X. Zhang, *Tetrahedron* **2002**, *58*, 4735.

[59] K. Jähnisch, V. Hessel, H. Löwe, M. Baerns, *Angew. Chem.* **2004**, *116*, 410; *.Angew. Chem. Int. Ed.* **2004**, *43*, 406.

[60] B. P. Mason, K. E. Price, J. L. Steinbacher, A. R. Bogdan, D. T. McQuade, *Chem. Rev.* **2007**, *107*, 2300.

5

Cyclopolymerization-Derived Block Copolymers of 4, 4-Bis(octyloxymethyl)-1,6-heptadiyne and Dipropargyl malonodinitrile

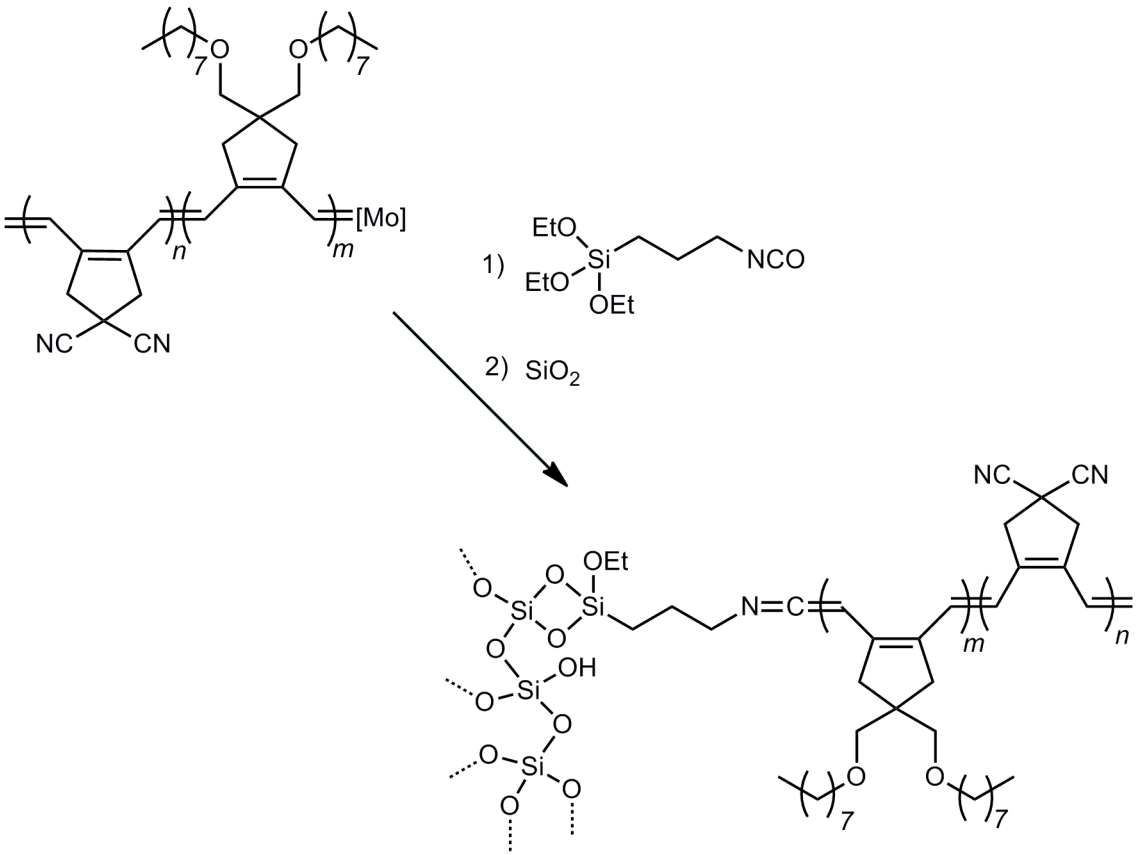

M. Sudheendran and M. R. Buchmeiser

5.1 Introduction

Soluble organic polymers having a conjugated π system in the main chain have been extensively studied for the past decades.[1-10] Polymers having such conjugated backbones show unique properties such as electrical conductivity, photo- and electroluminescence.[6, 8-10] Owing to these properties, they are used in several electronic applications, such as organic light emitting diodes (OLEDs), solar cells, photovoltaic devices, lasers, all-plastic full-color image sensors, and field effect transistors.[3-5, 9, 10] The simplest representative of this class of polymers, poly(acetylene), suffers from insolubility, lack of processability and inefficient moisture and oxygen stability. For those reasons, the characterization of polyacetylene has not been fully investigated, and frequently hampered the applications of polyacetylene due to poor functionality peculiar to its simple chemical structure. Consequently, conjugated materials based on poly(thiophene)s, poly(pyrrole)s, poly(thiazole)s, poly(*p*-phenylene)s, PPV and related materials are used in mostly technical applications.[2, 3, 11] In this regard, soluble conjugated polymers prepared by the cyclopolymerization of (substituted) 1,6-heptadiynes with the help of metathesis catalysts represents powerful alternatives to these polymers. For the past decades, the synthetic approaches to poly(ene)s via the cyclopolymerization of 1,6-heptadiynes has reached an extraordinary level of sophistication.[12-22] These polymers possess cyclic structures recurring along the conjugated backbone, thus providing enhanced stability and excellent processability.[23] Usually this class of polymers displays good solubility in common organic solvents depending on the substituent at 4-position, good long-term stability toward oxidation, and high effective conjugation lengths.

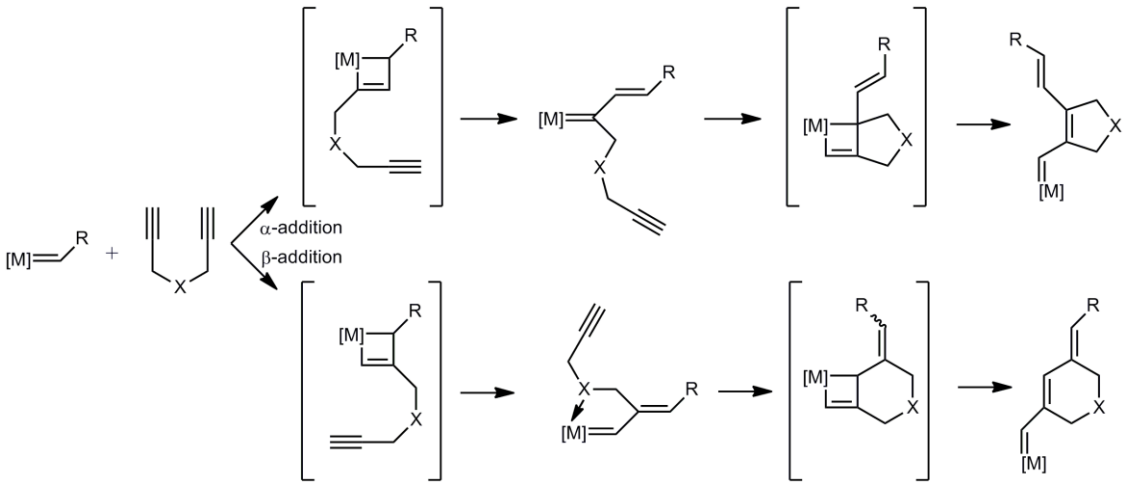

Scheme 22. Polymer structures obtainable via the cyclopolymerization of 1,6-heptadiynes.

The repeat units of such cyclopolymerization-derived polymers may consist of either five- or six-membered rings, depending on the insertion mode of the monomer into the initiator (Scheme 22). Usually, one refers to these two different insertion modes as α- and β-insertion (addition), respectively. While both polymers are conjugated, it has been shown that particularly those based on five-membered repeat units possess higher effective conjugation lengths and higher conductivity.[24] Both well-defined Mo-based Schrock type catalysts and modified Grubbs type metathesis catalysts may be used for cyclopolymerization. Here, particularly Schrock and in selected cases the modified Grubbs-type initiators allow for controlled or even living polymerizations. Important enough, Schrock-type initiators allow for accomplishing cyclopolymerizations in a stereo- and regio- selective manner, offering access to both five- and six-membered repeat units.[16, 18-21] Recently Buchmeiser et al reported the synthesis poly(1,6-heptadiyne)s consisting exclusively of five-membered repeat units in a controlled living manner using well-defined Mo-based catalysts with quinuclidine.[18] They also reported on the living stereo and regioselective cyclopolymerization of selected 1,6-heptadiynes by various Mo-derived Schrock catalysts and extend this chemistry to modified Ru-based metathesis catalysts as well.[12-14, 16-19, 22, 25-27] Recently T.L.Choi and co-workers reported the living cyclopolymerization of 1,6-heptadiynes using a 3rd generation Grubbs catalyst.[28] The reason for the excellent control over the molecular weight and PDI was attributed to the stability of the propagating species in a weakly coordinating solvent like THF. They also synthesized the diblock polymer having a conjugated backbone with controlled molecular weight and narrow PDI. Here, we report the synthetic approach to an Si(OCH_2CH_3)-telechelic AB-type block copolymer of 4,4-bis(octyloxymethyl)-1,6-heptadiyne (**M5**) and dipropargyl malonodinitrile (**M6**) by taking the advantage of the living nature of these polymers by using designed Ru and Mo-based initiators. In addition, we investigated various methods to reduce the backbiting during the course of polymerization.

5.2 Results and Discussion

5.2.1 Synthesis of Monomers and Initiators

Initiators **I5** and **I6** were synthesized from [$RuCl_2(PCy_3)(IMesH_2)(=CHPh)$] and [$RuCl_2(IMesH_2)(=CH\text{-}2\text{-}(2\text{-}PrO)\text{-}C_6H_4$] following previously published procedures.[13, 29, 30] The isocyanate-modified 3rd-generation Grubbs initiator [$Ru(N=C=O)_2(3\text{-}Br\text{-}Py)_2(IMesH_2)(CHPh)$] (**I7**) was accessible via the reaction of [$Ru(3\text{-}Br\text{-}Py)_2(PCy_3)(IMesH_2)(CHPh)$] (**I5**) with silver cyanate. The Mo-based Schrock-type initiator **I8** was prepared according to the literature.[31-33] A summary of the monomers and initiators that have been used is given in Figure 21.

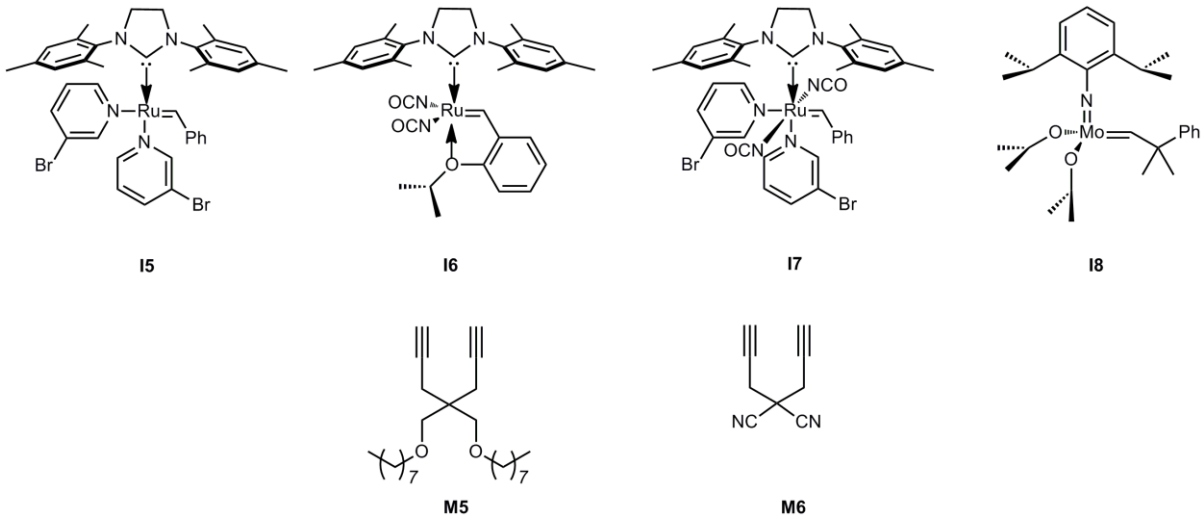

Figure 21. Structure of initiators **I5-I8** and monomers **M5** and **M6**.

The synthesis of **M5** entailed the reduction of diethyl dipropargylmalonate with $LiAlH_4$ followed by the alkylation of the resulting diol with 1-bromooctane.[34] After its synthesis, **M5** was distilled under reduced pressure and transferred to the glove box. Monomer **M6** was synthesized in quantitative yield by a solvent-free reaction of malonodinitrile with propargylbromide in the presence of tetrabutylammonium bromide (TBAB) as phase transfer agent.[35] The synthetic route to these monomers is outlined in Scheme 23.

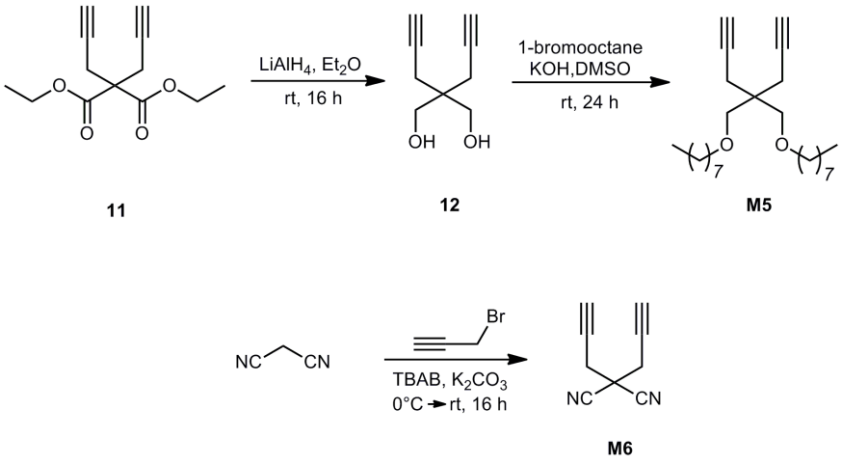

Scheme 23. Synthetic route to monomers **M5** and **M6**.

5.2.2 Polymerization of M5 and M6 using Ru-Based Initiators

Since the polymerizations of substituted 1,6-heptadiynes using Ru-based initiators normally require elevated temperatures, the non-coordinating solvent 1,2-dichloroethane was chosen for

the polymerization of **M5** and **M6**. Few reactions were also tried in weakly coordinating solvents such as THF.

First, the reactivity of **M1** and **M2** was examined using **I2**, a Grubbs Hoveyda type initiator modified by our group which is capable of cyclopolymerizing 1,6-heptadiynes efficiently.[13] The kinetic studies using *n*-dodecane as internal standard revealed that both **M5** and **M6** were polymerized by the action of **I6.** While the polymerization using 2 mol-% of **I6** resulted in 90 and 60% conversion of **M5** and **M6,** respectively, in 6h, the conversion reached >95% within 2 h when 4 mol-% **I6** were employed. Among the two monomers, **M6** was polymerized much faster than **M5** by the action of **I6** as indicated by kinetic studies (Figure 22). However, the reaction mixture of **M6** with **I6** in 1,2- dichloroethane immediately became dark red and the polymer was precipitated**.** No further improvement in conversion was observed after 6 h. The resulting polymer is essentially insoluble in all solvents. The insolubility of this polymer precluded obtaining its NMR spectrum and any GPC data.

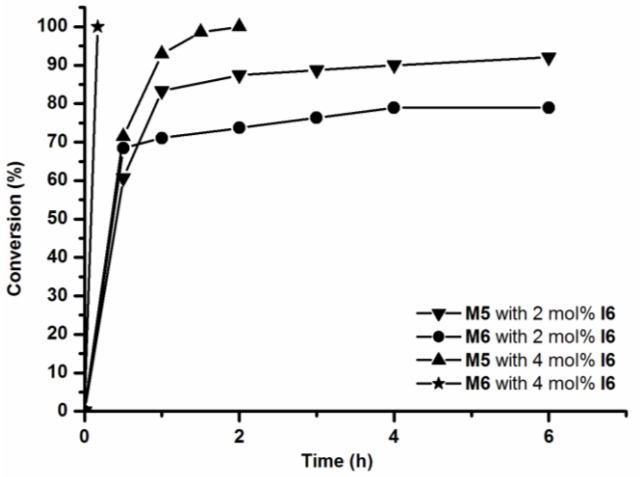

Figure 22. Kinetic plots obtained for the homopolymerization of **M5** and **M6** by the action of **I6** at 50^{o}C in 1,2-dichloroethane.

Even though poly(**M6**) was completely insoluble, poly(**M5**) displayed good solubility in common organic solvents (e.g., THF, CH_2Cl_2, $CHCl_3$), obviously due to the long alkyl chain at the 4-position. In view of these findings, we focused our attention on the synthesis of a block copolymer from **M5** and **M6**. An attempt to synthesize poly(**M5**)-*b*-poly(**M6**) did not give any promising result. While the conversion of **M5** reached >99% in 2h, the conversion of **M6** reached >99% in 20 h indicating lack of livingness. A kinetic plot of the conversion of **M5** vs. time is shown in Figure S16 (Chapter 6). Although, monomer conversion was >99% with a linear first order plot, the broad polydispersity indexes (PDIs) in the range of 3-3.5 revealed that

none of these polymerizations was truly living. The ^{13}C-NMR study of poly(**M5**) revealed that the polymerization proceeded via selective α-insertion to yield five-membered repeat units throughout the polymer chain (Figure S19, Chapter 6). Apart from the two carbon signals representative of the olefinic carbons of five membered poly(**M5**) at δ = 123.5 and 138.6 ppm, we observed further six well-defined carbon signals at δ = 142.1, 139.9, 136.8, 128.8, 127.5 and 124.2 ppm (Figure 23). A comparison of the ^{1}H and ^{13}C NMR signals of the model compounds with those of poly(**M5**)-*b*-poly(**M6**) failed to give any significant evidence for these extra peaks in the polymer. However, a closer observation of these well defined signals revealed that, these signals belongs to the dimer **11** formed as a result of backbiting (Figure 23).

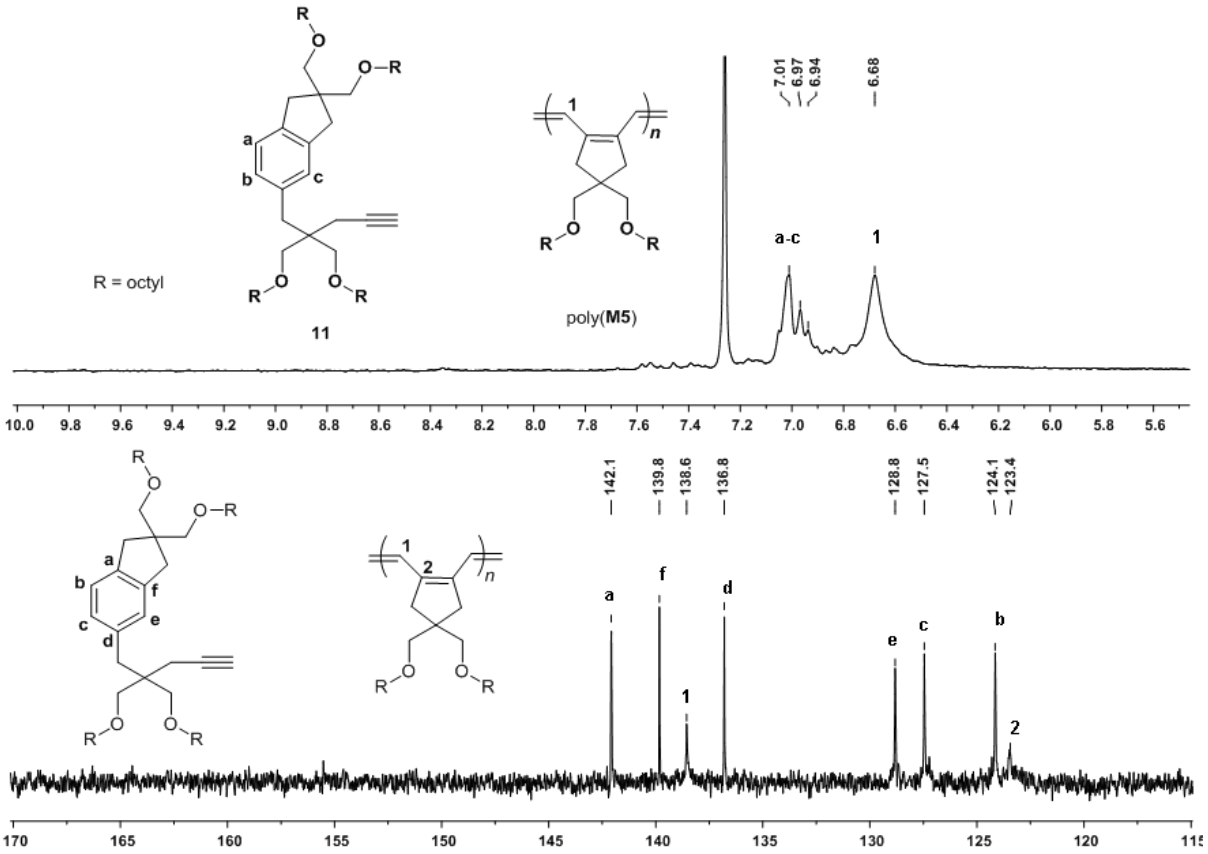

Figure 23. ^{1}H and ^{13}C NMR in $CDC1_3$ of poly(**M5**)$_{25}$ synthesized by the action of catalyst **I6**, showing the existence of **11** as a result of backbiting.

This dimer was isolated by reprecipitating the polymer in acetone and was characterized by ^{1}H and ^{13}C NMR spectroscopy. In fact, the isolated yield of the polymer prepared by the action of **I6** was only 25%, while the rest was pure dimer **11** (Table 9, entry 2 and Table 10, entry 4). The reduced yield with respect to the complete conversion of the monomer is due to the formation of **11**, which results in the complete shutdown of the polymerization after the first two insertion of

the monomer (Scheme 24). Since the initiator is regenerated in the course of this process, this also accounts for the broad PDIs.

Table 9. Summary of the results of the cyclopolymerization of **M5** using **I5- I7.**

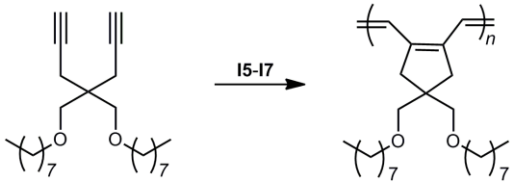

entry	initiator	[M]/[I]	M_n(theor.) [g/mol][a]	M_n(found) [g/mol][b]	PDI	λ_{max} [nm][c]	yield [%][d]
1	**I5**	50	18800	51800	3.5	550	83
2	**I6**	25	9400	12300	3.1	549	25
3	**I6**	25	9400	62800	3.8	552	68 [e]
4	**I7**	25	9400	179400	3.4	549	34
5	**I7**	50	18800	82200	3.2	550	84
6	**I7**	25	9400	83700	4.2	550	56 [e]

Polymerization conditions: 1,2-dichloroethane except entries 1 and 5 in THF, T = 50 °C entries 1 and 5 at 0 °C, t = 24h, [a]including end groups, [b]determined by SEC vs. polystyrene standard, [c] in $CHCl_3$, [d]isolated yields, [e] initiator with 10 equiv. 3-Br-Py.

5.2.3 Back biting

Though this kind of backbiting was already observed with 1,6-heptadiynes containing *tert*-amines at the 4-postition,[17] the above -mentioned results indicate that backbiting is also possible with 1,6-heptadiynes lacking any coordinating substituents like ethers or amines at the 4-position but contain ethers or nitriles at other positions (Scheme 24).

Next, the investigation was focussed to reduce the backbiting by using suitable catalysts and reaction conditions. First, the polymerization was examined using **I7**, an isocyanate modified catalyst prepared from the 3rd-generation Grubbs catalyst by exchanging the two chlorides by two isocyanates. Initiator **I7** has an added advantage in that the 3-bromopyridine that decoordinates during the polymerization stabilizes the metal center against intramolecular coordination, thereby reducing backbiting. It is interesting to note that by using **I7** the back

biting was significantly reduced from 67% to 22% under same polymerization conditions as before (Table 10, entry 7).

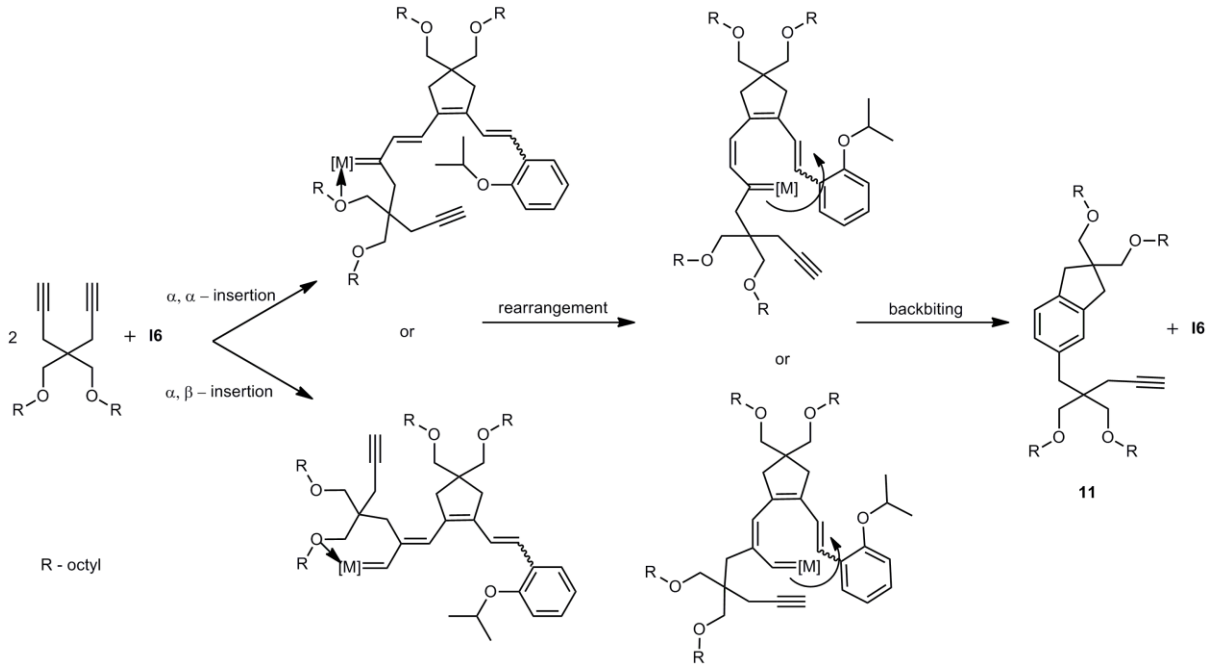

Scheme 24. Reaction of **M5** with **I6** and the formation of **11** via backbiting.

During these investigations it was also realized that the back biting is depended on the reaction temperature as well. Thus, polymerizations conducted at 40^{o}C using **I7** showed a slight but significant improvement in the backbiting compared to cyclopolymerization carried out at T = 50^{o}C. The backbiting was product found in this case was only 19% (Table 10, entry 8).

Inspired by recent work by T.L.Choi and co-workers,[28] the cyclopolymerization of **M5** and **M6** was also tried using the highly active initiator **I5** at 0°C. As reported, the polymerizaion was completed in one hour in the case of **M5**. Interestingly, no backbiting was observed and the polymer was isolated in 83% yield. However, the polymer displayed a PDI of 3.5 indicative for a non-living nature of the polymerization (Table 9, entry 1, Table 10, entry 1). In contrast, the polymerization carried out with **I6** in THF at 45^{o}C again resulted in 20% of backbiting (Table 10, entry 3).

Next, the influence of an excess of 3-bromopyridine in the reaction mixture on backbiting was examined. This way, backbiting was completely suppressed as indicated by the ^{1}H NMR of the crude polymer mixture. The kinetic plots of these polymerizations are shown in Figure S17 (Experimental and Spectroscpic data). Although the polymerizations of **M5** using **I6** and **I7** in presence of 3-bromopyridine significantly reduced backbiting, no improvement in the

conversion as well as the living nature of the polymerization was observed. The results of the cyclopolymerizations employing Ru-based initiators **I5-I7** are summarized in Table 9 and Table 10.

Table 10. Influence of various reaction conditions on polymerization of **M5** using **I5-I7**.

entry	initiator	[M]/[I]	solvent	*T* [°C]	conversion[%][a]	**11[**%][b]
1	**I5**	50	THF	0	> 99	-
2	**I5**	50	1,2-DCE	50	35	12
3	**I6**	50	THF	45	> 95	20
4	**I6**	25	1,2-DCE	50	> 99	67
5	**I6** + 3-Br-Py	25	1,2-DCE	50	> 99	-
6	**I7**	50	THF	0	> 99	-
7	**I7**	25	1,2-DCE	50	50	22
8	**I7**	25	1,2-DCE	40	46	19
9	**I7** + 3-Br-Py	25	1,2-DCE	50	72	-

Polymerization conditions: 1,2-dichloroethane, [a]determined by kinetic studies using *n*-dodecane as internal standard, [b]determined by ^{1}H NMR spectroscopy.

In order to gain a better understanding about the large variations in molecular weight and the broad PDIs, the values for the ratio of the rate constant of polymerization (k_p) over the rate constant of initiation (k_i), k_p/k_i, was determined by ^{1}H NMR.[36] In order to gain perfect control over molecular weights, value for k_p/k_i <1 are preferred. The k_p/k_i value of 190 determined for the system **M5**/**I6** system in presence of 3-bromo pyridine by ^{1}H NMR is thus clearly indicative of the lack of control over the molecular weight and high PDI values.

5.2.4 Polymerization of M5 and M6 using Mo-Based Initiators.

Since the polymerizations of **M5** and **M6** using Ru-based initiators failed in achieving control over molecular weights and PDIs, we turned our attention on well-defined Mo-based initiators. Among the initiators tried for **M5** and **M6** at different reaction conditions, initiator **I8** containing 2-propyloxy ligands was found to be more suitable for our purpose as judged on the basis of lower PDIs (Table 11). Buchmeiser et.al. already reported the selective synthesis of poly(1,6-diyne)s consisting of >95% five membered repeat units using designed Mo-based catalysts containing quinuclidine as base.[18] The results of the polymerization of **M5** and **M6** carried out

under various reaction conditions aiming at >95%, five membered repeat units along the polymer chain employing **I8** are summarized in Table 11.

Table 11. Summary of the results of the cyclopolymerization of **M5** using **I8.**

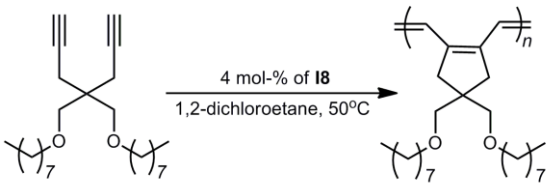

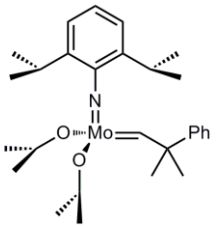

I8

entry	additive	T [°C]	M_n(theor.) [g/mol][a]	M_n(found) [g/mol][b]	PDI	λ_{max} [nm][c]	yield [%][d]
1	quinuclidine	-	18800	197000	2.4	546	96
2	-	-30	18800	181000	2.7	546	94
3	quinuclidine	-30	18800	58800	2.4	551	93
4	quinuclidine	-30	18800	13900	2.4	551	87

Polymerization conditions: CH_2Cl_2 (for enties 1-3), THF for entry 4, [M]/[I] = 50, $[M]_o$ =1M, t = 1h, [a] including end groups, [b]determined by $CHCl_3$ SEC vs. polystyrene standard, [c] in $CHCl_3$, [d] isolated yields.

All polymerizations showed >95% conversion and the polymers were isolated >90% yields. Though the polymerization using 4 mol-% of **I8** in CH_2Cl_2 was relatively better than with Ru-based intiators, a decent PDI also better control over M_n was attained when the polymerization was carried out in a weakly coordinating solvent THF (Table 11, entry 4). The reason for the improved PDI in THF could be attributed to the stabilization of the propagating species during the course of polymerization.

5.2.5 Synthesis of Block Copolymers

*Synthesis of poly(**M5**)-b-poly(**M6**)*

Owing to the insolubility of poly(**M6**) in common polymeric solvents, the synthesis of poly(**M5**)-*b*-poly(**M6**) starting with **M5** as the first block was tried first. This allowed us for determining the degree of polymerization of each block separately. The kinetic study of **M5** at -30°C in the presence of quinuclidine revealed a complete conversion within 30 min followed by complete conversion of the second monomer **M6** within 1.5 h.

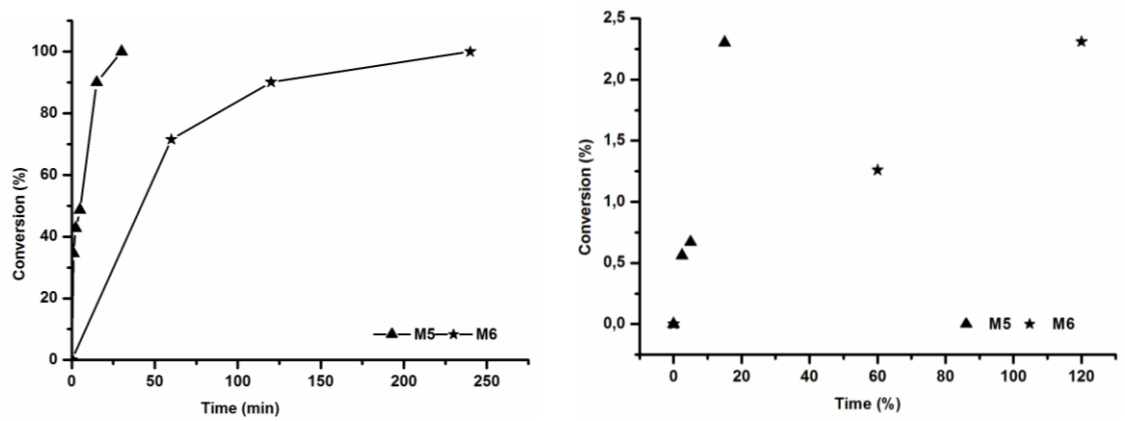

Figure 24. Kinetic plot obtained for the synthesis of poly(**M5**)-*b*-poly(**M6**) using **I8** (Left), 1st order plot (Right).

The first order plot and the comparably low PDIs in the range of 1.30-1.73 obtained for the polymers suggest a living nature of these polymerizations (Figure 24). The SEC results revealed the successful synthesis of poly(**M5**)-*b*-poly(**M6**) with a degree of polymerization of 58 and 36, respectively, for poly(**M5**) and poly(**M6**). The overlay of the SEC traces and results for poly(**M5**)-*b*-poly(**M6**) are shown in Figure 25 and Table 12, respectively.

Table 12. Results for poly(**M5**)-*b*-poly(**M6**) synthesized by the action of **I8.**

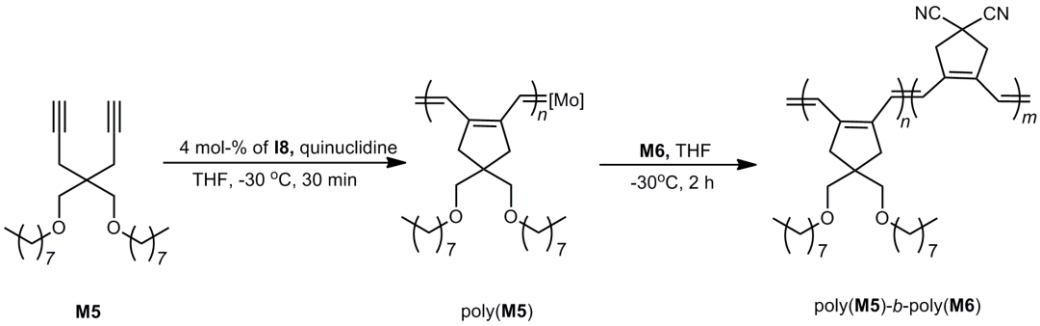

Polymer	M_n (calcd.) [g/mol][a]	M_n (found) [g/mol][b]	PDI	DP (calcd.)		DP (found)	
				M5	**M6**	**M5**	**M6**
Poly(**M5**)	9400	21900	1.3	25	---	58	--
Poly(**M5**)-*b*-poly(**M6**)	12900	27000	1.73	25	25	58	36

Polymerization conditions: THF, [a]including end groups, [b]determined by $CHCl_3$ SEC vs. polystyrene standard.

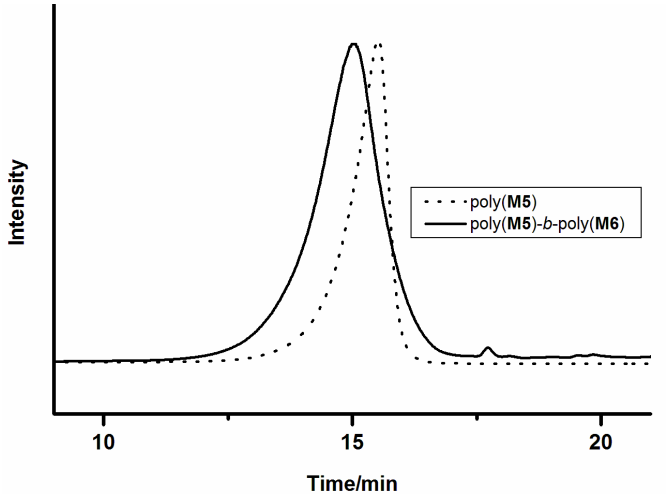

Figure 25. Overlay of SEC curves obtained for poly(**M5**) and poly(**M5**)-*b*-poly(**M6**) prepared by the action of **I8**.

*Synthesis of poly(**M6**)-b-poly(**M5**)*

Encouraged by the successful synthesis of poly(**M5**)-*b*-poly(**M6**), the synthesis of poly(**M6**)-*b*-poly(**M5**) starting with **M6** as the first block was tried next. The ratio of the monomer to initiator was **M6**:**M5**:**I8** (25:25:1).

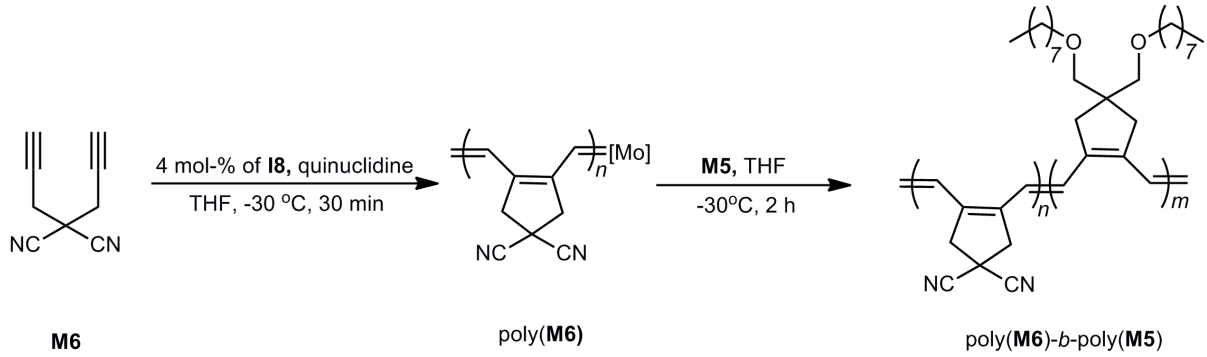

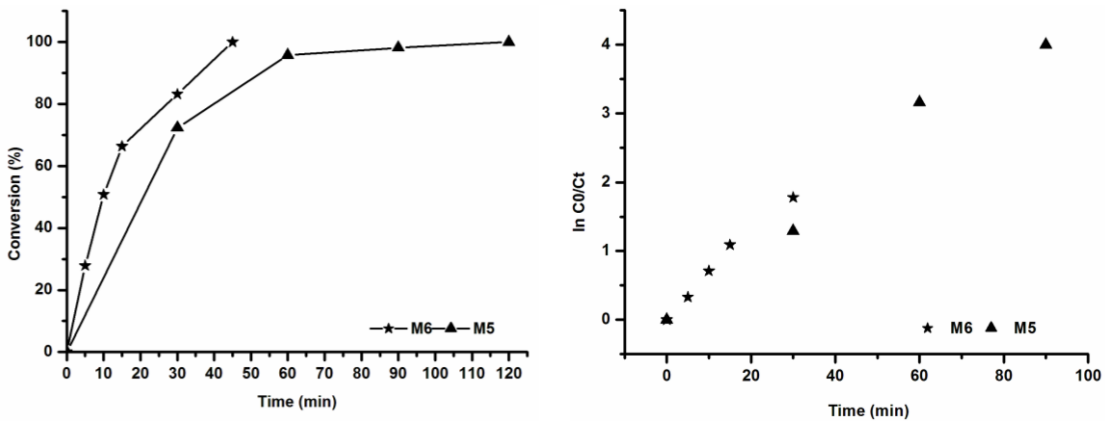

Figure 26. Kinetic plot obtained for the synthesis of poly(**M6**)-*b*-poly(**M5**) using **I8** (left), 1st order plot (right)

The insolubility of poly(**M6**) in all solvents precluded any determination of the degree of polymerization of each block. The kinetic plots obtained for the synthesis of poly(**M6**)-*b*-poly(**M5**) showed >99% conversion of each monomer and linear first order plots indicating a living nature of the polymerization (Figure 26). The resulting dark violet polymer was essentially insoluble in CH_2Cl_2, $CHCl_3$ or DMF and had limited solubility in THF. However, ^{1}H and ^{13}C NMR spectra of sufficient quantity could be obtained in THF-*d8* (Figure S21 and S22, Chapter 6). Any attempt to improve the solubility of the block polymer by changing the ratio of monomer to initiator by **M6**:**M5**:**I8** (15:25:1) did not result in any soluble polymer.

5.2.6 Synthesis of Telechelic Poly(M6)-*b*-poly(M5)

Next, the investigation was extended to introduce a triethoxysilyl endgroup at the end of the polymer chain. This way a telechelic polymer suitable for the immobilization on to a silica support can be achieved. Recently, Buchmeiser et al. reported the synthesis of such a telechelic oligomer via the endcapping the living polymer chain with 3-isocyanatopropyltriethoxysilane.[38] They have successfully utilized those telechelic oligomers for the immobilization of 2nd-generation Grubbs catalyst on a silica support. Following a similar protocol, the endcapping of poly(**M6**)-*b*-poly(**M5**) was attempted (Scheme 25).

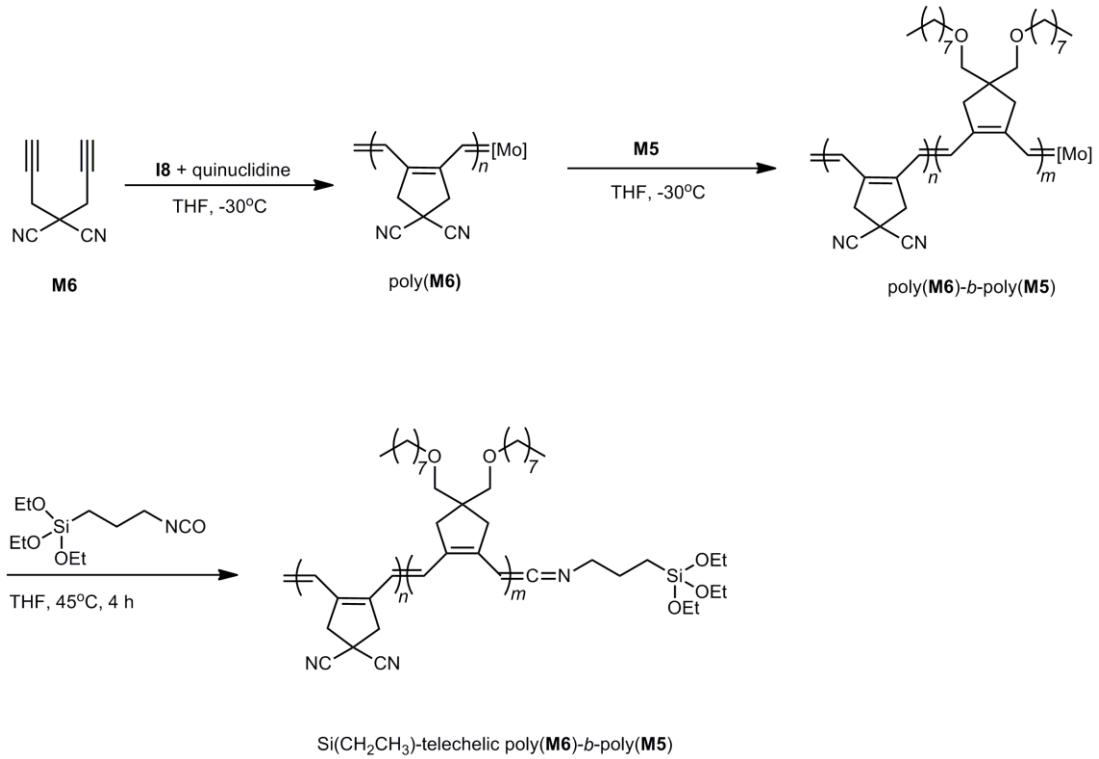

Scheme 25. Syntheis of triethoxysilyl-telechelic poly(**M6**)-b-poly(**M5**).

For this purpose, poly(**M6**)-*b*-poly(**M5**) was synthesized using a monomer to initiator of **M6**:**M5**:**I8** (10:30:1) and was then reacted with ten fold excess of the 3-isocyanatopropyltriethoxysilane to yield triethoxysilyl-telechelic blockcopolymer. The endgroup analysis using ^{1}H NMR spectroscopy indicates the formation of telechelic polymer. The peaks at δ = 3.78 and 1.18 in the ^{1}H NMR correspond to the -OCH_2 and -CH_3 protons respectively (Figure S23, Chapter 6).

5.2.7 Grafting of the Telechelic Poly(M5)-b-poly(M6) onto Silica Surface

The Si(CH_2CH_3)-telechelic poly(**M6**)-b-poly(**M5**) was reacted with silica 60 inorder to graft onto the surface of the silica (Scheme 26). The polymer grafted on the silica was quantified by elemental analysis. There a carbon content of 0.823 mmol/g clearly illustrates the successful grfting of this telechelic polymer.

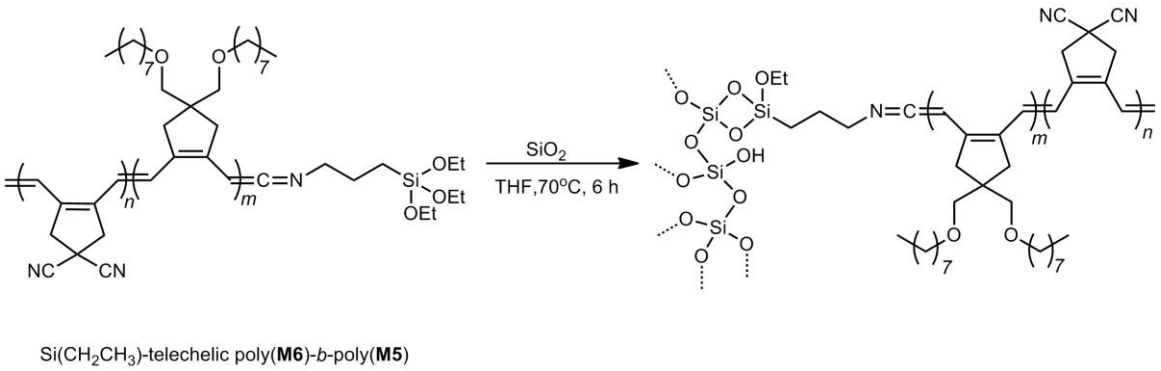

Scheme 26. Grafting of triethoxysilyl- telechelic poly(**M6**)-b-poly(**M5**) on to silica.

5.3 Conclusion

The synthesis of cyclopolymerization-derived block copolymers of **M5** and **M6** was successfully accomplished using a well defined Schrock type initiator (**I8**). The living block copolymer was successfully endcapped using 3-isocyanatopropyltriethoxysilane to yield triethoxysilyl-telechelic blockcopolymers, and was surface grafted onto a silica support. Although, despite the successful kinetic studies on the block copolymerization of these two monomers using Ru-based initiator, a complete shutdown of the polymerization was observed, due to backbiting. Nevertheless, an investigation towards the influence of various reaction conditions on backbiting was accomplished. The backbiting was most pronounced, when the polymerization was carried out using **I6** in 1,2-dichloroethane at 50^{o}C and could be minimized by using suitable additives.

5.4 References

[1] T. A. Skotheim, R. L. Elsenbaumer, J. R. Reynolds, 2 ed., Dekker, New York, **1997**.

[2] M. A. Fox, *Acc. Chem. Res.* **1999**, *32*, 201.

[3] J. R. Sheats, Y.-L. Chang, D. B. Roitman, A. Stocking, *Acc. Chem. Res.* **1999**, *32*, 193.

[4] S.-H. Chi, J. M. Hales, C. Fuentes-Hernandez, S.-Y. Tseng, J.-Y. Cho, S. A. Odom, Q. Zhang, S. Barlow, R. R. Schrock, S. R. Marder, B. Kippelen, J. W. Perry, *Advanced Materials* **2008**, *20*, 3199.

[5] A. J. Heeger, *Angew. Chem.* **2001**, *113*, 2660; A. J. Heeger, *Angew. Chem. Int. Ed.* **2001**, *40*, 2591.

[6] A. G. MacDiarmid, *Angew. Chem.* **2001**, *113*, 2649; A. G. MacDiarmid, *Angew. Chem. Int. Ed.* **2001**, *40*, 2581.

[7] H. Shirakawa, *Angew. Chem.* **2001**, *113*, 2642; H. Shirakawa, *Angew. Chem. Int. Ed.* **2001**, *40*, 2574.

[8] J. L. Br´edas, R. J. Silbey, in *Conjugated Polymers*, Kluwer, Dordrecht, **1991**.

[9] J. H. Burroughes, D. D. C. Bradley, A. R. Brown, R. N. Marks, K. Mackay, R. H. Friend, P. L. Burns, A. B. Holmes, *Nature* **1990**, *347*, 539.

[10] R. H. Friend, R. W. Gymer, A. B. Holmes, J. H. Burroughes, R. N. Marks, C. Taliani, D. D. C. Bradley, D. A. D. Santos, J. L. Bredas, M. Logdlund, W. R. Salaneck, *Nature* **1999**, *397*, 121.

[11] F. Hide, M. A. Diaz-Garcia, B. J. Schwartz, A. J. Heeger, *Acc. Chem. Res.* **1997**, *30*, 430.

[12] M. R. Buchmeiser, *Adv. Polym. Sci.* **2005**, *176*, 89.

[13] P. S. Kumar, K. Wurst, M. R. Buchmeiser, *Chem. Asian. J.* **2009**, *4*, 1275.

[14] J. O. Krause, O. Nuyken, M. R. Buchmeiser, *Chem. Eur.J.* **2004**, *10*, 2029.

[15] S.-K. Choi, Y.-S. Gal, S.-H. Jin, H. K. Kim, *Chem. Rev.* **2000**, *100*, 1645.

[16] H. H. Fox, M. O. Wolf, R. O'Dell, B. L. Lin, R. R. Schrock, M. S. Wrighton, *J. Am. Chem. Soc.* **1994**, *116*, 2827.

[17] P. S. Kumar, K. Wurst, M. R. Buchmeiser, *J. Am. Chem. Soc.* **2009**, *131*, 387.

[18] U. Anders, O. Nuyken, M. R. Buchmeiser, K. Wurst, *Macromolecules* **2002**, *35*, 9029.

[19] U. Anders, M. Wagner, O. Nuyken, M. R. Buchmeiser, *Macromolecules* **2003**, *36*, 2668.

[20] M. S. Ryoo, W. C. Lee, S. K. Choi, *Macromolecules* **1990**, *23*, 3029.

[21] H. H. Fox, R. R. Schrock, *Organometallics* **1992**, *11*, 2763.

[22] P. S. Kumar, K. Wurst, M. R. Buchmeiser, *Organometallics* **2009**, *28*, 1785.

[23] C. C. W. Law, J. W. Y. Lam, Y. Dong, H. Tong, B. Z. Tang, *Macromolecules* **2005**, *38*, 660.

[24] M. R. Buchmeiser, J. O. Krause, D. Wang, U. Anders, R. Weberskirch, M. T. Zarka, O. Nuyken, C. Jäger, D. Haarer, *Macromol. Symp.* **2004**, *217*, 179.

[25] U. Anders, O. Nuyken, M. R. Buchmeiser, K. Wurst, *Angew. Chem.* **2002**, *114*, 4226.

[26] U. Anders, O. Nuyken, M. R. Buchmeiser, *J. Mol. Catal A: Chem* **2004**, *213*, 89.

[27] T. S. Halbach, J. O. Krause, O. Nuyken, M. R. Buchmeiser, *Macromol. Rapid. Commun.* **2005**, *26*, 784.

[28] E.-H. Kang, I. S. Lee, T.-L. Choi, *J. Am. Chem. Soc.* **2011**, *133*, 11904.

[29] T.-L. Choi, R. H. Grubbs, *Angew. Chem. Int. Ed.* **2003**, *42*, 1743.

[30] J. A. Love, J. P. Morgan, T. M. Trnka, R. H. Grubbs, *Angew. Chem. Int. Ed.* **2002**, *41*, 4035.

[31] H. H. Fox, K. B. Yap, J. Robbins, S. Cai, R. R. Schrock, *Inorg. Chem.* **1992**, *31*, 2287.

[32] R. R. Schrock, J. S. Murdzek, G. C. Bazan, J. Robbins, M. DiMare, M. O'Regan, *J. Am. Chem. Soc.* **1990**, *112*, 3875.

[33] J. H. Oskam, H. H. Fox, K. B. Yap, D. H. McConville, R. O`Dell, B. J. Lichtenstein, R. R. Schrock, *J. Organomet. Chem.* **1993**, *459*, 185.

[34] T. Sanji, T. Kanzawa, M. Tanaka, *J. Organomet. Chem.* **2007**, *692*, 5053.

[35] E. Diez-Barra, A. de la Hoz, A. Moreno, P. Sanchez-Verdu, *J. Chem. Soc., Perkin Trans. 1* **1991**, 2589.

[36] G. C. Bazan, E. Khosravi, R. R. Schrock, W. J. Feast, V. C. Gibson, M. B. O'Regan, J. K. Thomas, W. M. Davis, *J. Am. Chem. Soc.* **1990**, *112*, 8378.

[37] L. Q. Xu, F. Yao, G.-D. Fu, L. Shen, *Macromolecules* **2009**, *42*, 6385.

[38] M. Mayr, M. R. Buchmeiser, K. Wurst, *Adv. Syn. Catal.* **2002**, *344*, 712.

6

Experimental and Spectroscopic Data

6.1 General Remarks

Chemicals and Solvents

All manipulations were performed under a dinitrogen atmosphere in a glovebox (LabMaster 130, MBraun Garching, Germany) or by standard Schlenk techniques unless specified otherwise. Purchased starting materials and other chemicals or reagents from Aldrich, Fluka, ABCR, Merck, and KMF were used without any further purification. $CDCl_3$ was distilled from CaH_2 and stored over molecular sieves (4Å). CH_2Cl_2, THF, diethyl ethaer, toluene and pentane was dried by an MBraun solvent purification system (SPS).

Nuclear Magnetic Resonance Spectroscopy (NMR)

NMR measurements were recorded on a Bruker Avance 250 or Bruker Avance III 400 spectrometer in the indicated solvent at 25°C and are listed in parts per million downfield from TMS as an internal standard for proton and carbon.

Gas-Chromatogram Mass Spetroscopy (GC-MS)

GC-MS data were recorded on an Agilent Technologies device consisting of a 7693 autosampler, a 7890A GC and a 5975C quadrupole MS. Dodecane was used as internal standard. A SPB-5 fused silica column (34.13 m x 0.25 mm x 0.25 µm film thickness) was used. The injection temperature was set to 150°C. The column temperature ramped from 45°C to 250°C within eight minutes, and was then held for further five minutes. The column flow was 1.05 mL per minute.

UV-Visible Spectroscopy

UV/Vis measurements were carried out in $CHCl_3$ on a Perkin Elmer Lambda 2.

Infrared Spectroscopy

IR spectra were measured on an IFS 28 (Bruker) using ATR technology or NaCl cuvettes.

Size Exclusion Chromatography (SEC)

Molecular weights and polydispersity indexes (PDIs) of the polymers were determined by size exclusion chromatography (SEC) on Polymer Laboratories columns (PLgel 10 mm MIXEDB, 7.5 X 300 mm) in $CHCl_3$ at 30°C vs. polystyrene (PS) using an autosampler and a 484 UV detector (254 nm, all Waters Corp.). The flow rate was set to 1 mL min^{-1}. Narrow PS standards were purchased from Waters Corp., USA. Prior to measurements, polymer solutions were filtered through Millipore 0.20 μm filters.

Inverse Size Exclusion Chromatography (ISEC)

For ISEC measurements, a G1314B UV detector (Agilent 1200 series) and a G1310A isopump (Agilent 1200 series) equipped with an Agilent instant pilot G4208A and a manual sample injection system were used.

Elemental Aanalysis

Elemental analysis was done in a Carlo Erba elemental analyzer (1106) at the Institute of Organic Chemistry, University of Stuttgart, Germany.

Conductivity Measurements

Conductivity measurements were performed inside a glove box (MBraun, Garching, Germany) under a N_2 atmosphere by using FLUK 76 True RMS Multimeter (JOHN FLUK MFG.CO.INC, USA).

Reverse Phase-High Performance Chromatography (RP-HPLC)

RP-HPLC analyses were carried out by an Agilent Technology HPLC system (Germany). The system consisted of a binary HPLC pump, a diode array UV-vis detector, an autosampler, a column oven, and a sample thermostat. The products were analyzed by RP-HPLC using an Agilent-Eclipse XDB-C18 column (5 μm, 4.6 × 150 mm i.d., Zorbax RX-SIL).

6.2 A Continuous Bioreactor Prepared via the Immobilization of Trypsin on Aldehyde-Functionalized, Ring-Opening Metathesis Polymerization-Derived Monoliths

$RuCl_2(PCy_3)_2(=CHPh)$ (**I1**), $[RuCl_2(PCy_3)(IMesH_2)(CHPh)]$ (**I2**) (PCy_3 = tricyclohexylphosphine; $IMesH_2$ = 1,3-dimesitylimidazolin-2-ylidene), norborn-2-ene (NBE), 5-norbornene-2-methanol, methyltrichorosilane, tetraethylenepentamine (TEPA), trypsin from

bovine pancreas (EC 3.4.21.4), *N*-α-benzoyl-DL-arginine-*p*-nitroanilide hydrochloride (BAPNA), phosphate buffered saline tablets, Tween®20, and deionized water were obtained from Aldrich Chemical Co. (Germany). Glutaraldehyde (GA, 25% in aqueous solution) was purchased from ABCR GmbH and Co. KG (Karlsruhe, Germany). HEPES was purchased from Carl Roth GmbH (Germany). $(NBE\text{-}CH_2O)_3SiCH_3$ was prepared according to the literature. $[RuCl_2(3\text{-}Br\text{-}Py)_2(IMesH_2)(CHPh)]$ (**I3**)[1, 2] and 1,4,4a,5,8,8a-hexahydro-1,4,5,8-exo-endo-dimethanonaphthalene (DMN-H6)[3] were prepared according to the literature.

$(NBE\text{-}CH_2O)_3SiCH_3$[4]

Methyltrichlorosilane (1.2 g, 8.0 mmol) was added dropwise to a solution of 5-norbornene-2-methanol (3.0g, 24mmol) and triethylamine (4 mL) in CH_2Cl_2 (20 mL) at 0°C under argon. The reaction mixture was stirred at 0°C for 30 min and stirring was continued for another 2 h at room temperature. After 2 h, the reaction mixture was then diluted with CH_2Cl_2 (50 mL), washed with 10% acetic acid (25 mL), saturated Na_2HCO_3, water (25 mL), brine (15 mL), dried over anhydrous $MgSO_4$ and then evaporated *in vacuo* to afford the desired product as colorless, viscous liquid. Yield: 3.4 g (94%). ^{1}H NMR ($CDCl_3$): δ= 6.12-5.96 (m, 6H, C*H*=C*H*), 3.84-3.22 (m, 6H), 2.93 (s, 2H), 2.77 (m, 4H), 2.32 (m, 2H), 1.82-1.76 (m, 2H), 1.64 (m, 1H), 1.44-1.40 (m, 2H), 1.30-1.22 (m, 4H), 0.49-0.42 (m, 2H), 0.13, 0.11, 0.08 (s, C*H*$_3$Si). ^{13}C NMR ($CDCl_3$): δ = 137.2, 136.8, 136.7, 132.6 (*C*=*C*), 67.0, 66.1(*C*H_2O), 49.5, 44.9, 43.8, 43.4, 42.3, 41.6, 41.4 (CH), 29.4, 28.9 (CH_2), -7.1 (*C*H_3Si); GC-MS calcd. for $C_{25}H_{36}O_3Si$: *m/z*=412.24; found: 412 ($M^{\cdot+}$)

Preparation of Aldehyde-Semitelechelic Polymers

A 5 mL Schlenk flask was charged with 1 (29.0 mg, 0.035 mmol) in 1mL of benzene and a stir bar. In a separate vial, NBE (100 mg, 1.06 mmol) was dissolved in benzene (1 M solution). The solution was then added to the catalyst solution via a syringe under vigorous stirring. After 1 h, the solution was purged with air under stirring for 16 h. The reaction mixture was then poured into a large excess of methanol (25 mL), and the precipitated polymer was filtered off. The polymer obtained was then precipitated from a 1:9 mixture of CH_2Cl_2 and methanol. It was collected by filtration and dried *in vacuo*. CHO-semitelechelic poly(NBE): 80% aldehyde formation; SEC: M_n = 7500 g/mol, PDI = 1.98. ^{1}H NMR ($CDCl_3$): δ = 9.61 (s, 1H, CHO), 7.34-7.17 (m, 5H, *J*=7.2 Hz, phenyl), 6.35 (d, 1H, *J*=15.6 Hz, Ph-C*H*=CH), 6.21-6.17 (dd, 1H, *J*=15.6, 7.8 Hz, Ph-CH=C*H*), 5.35 (bm, -CH=CH *trans*), 5.21 (bm, -CH=CH *cis*), 2.78 (bs, -CH *cis*), 2.43 (bs, -CH *trans*), 1.87-1.85 (bm, -CH_2), 1.76 (bm, -CH_2), 1.35 (bm, -CH_2), 1.08-1.02

(bm, -CH_2). ^{13}C NMR ($CDCl_3$): δ = 203.6 (CHO), 138.3, 137.9, 135.6, 134.0, 133.1, 128.6, 126.5, 126.0, 52.0, 43.5, 43.2, 42.2, 41.5, 38.5, 33.0, 32.3. IR (ATR mode): 2940 (m), 2862 (m), 1712 (vs), 1444 (w), 1260 (m), 1026 (w), 965 (s), 908 (s), 732 (s), 699 (w), 648 cm^{-1} (w). CHO semitelechelic poly(COE): 15% aldehyde formation; SEC: M_n = 8400 g/mol, PDI=1.77. ^{1}H NMR ($CDCl_3$): δ = 9.77 (s, 1H, CHO), 7.35-7.17 (m, 5H, *J*=7.2 Hz, phenyl), 6.37 (d, 1H, *J*=16.2 Hz, Ph-C*H*=CH), 6.25-6.20 (dd, 1H, *J*=13.8, 6.6 Hz, Ph-CH=C*H*), 5.39 (bm, -CH=CH *trans*), 5.35 (bm, -CH=CH *cis*), 2.42 (bm, -CH), 2.21 (bm, -CH), 2.02-1.97 (bm,-CH), 1.65-1.62 (bm, -CH), 1.48-1.45 (bm, -CH), 1.34 (bm, -CH_2), 1.28 (bm, -CH_2). ^{13}C NMR ($CDCl_3$): δ = 203.0 (CHO), 138.0, 131.5, 130.5, 130.0, 129.8, 128.6, 126.8, 126.0, 114.2, 44.0, 33.2, 32.7, 29.8, 27.3. IR (ATR mode): 2916 (m), 2849 (m), 2360 (vs), 2341 (vs) 1727 (vs), 1467 (vs), 1437 (w), 1284(m), 1070 (w), 965 (s), 717 (s), 691 cm^{-1} (w).

General Procedure for the Preparation of 2,4-Dinitrophenylhydrazine Derivatives

0.25 g of 2,4-dinitrophenylhydrazine was suspended in 5 mL of ethanol, and then 0.5 mL of concentrated sulfuric acid was added cautiously. The warm solution (0.5 mL) was then added to a solution of aldehyde-functionalized polymer suspended in 0.5 mL of a mixture of CH_2Cl_2 and methanol (1:1). The mixture was stirred for 15 min and poured into methanol (25 mL). The precipitate was filtered and washed with methanol to afford the corresponding hydrazones. Poly(NBE)-hydrazone: ^{1}H NMR ($CDCl_3$): δ = 11.00 (s, 1H), 9.13 (m, 1H), 8.29 (m, 1H), 7.92 (m, 1H), 7.49 (d, 1H) 7.35-7.17 (m, 5H, *J*=7.2 Hz, phenyl), 6.37 (d, 1H, *J* = 15.6 Hz, Ph-C*H*=CH), 6.22-6.18 (dd, 1H, *J*=15.6, 7.8 Hz, Ph-CH=C*H*), 5.35 (bm, -CH=CH *trans*), 5.21 (bm, -CH=CH *cis*), 2.78 (bs, -CH *cis*), 2.43 (bs, -CH *trans*), 1.88-1.77 (bm, -CH_2),1.36 (bm, -CH_2), 1.09-1.03 (bm,-CH_2). ^{13}C NMR ($CDCl_3$): δ = 155.9 (-H*C*=N-), 145.2, 138.0, 135.6, 134.0, 133.1, 130.1, 128.0, 126.9, 126.0, 123.7, 43.5, 43.2, 42.2, 41.5, 38.5, 33.0, 32.3. IR (ATR mode): 2941 (m), 2862 (m), 1616 (vs), 1591 (vs), 1518 (vs), 1464 (vs), 1445 (s), 1335 (vs), 1215 (s), 1041 (s), 964 (s), 832 (w), 755 cm^{-1}(s). Poly(COE)-hydrazone: ^{1}H NMR ($CDCl_3$): δ = 11.02 (s, 1H), 9.13 (m, 1H), 8.29 (m, 1H), 7.92 (m, 1H), 7.52 (t, 1H), 7.34-7.17 (m, 5H, *J*=7.2 Hz, phenyl),6.37 (d, 1H, *J*=15.6 Hz, Ph-C*H*=CH), 6.25-6.20 (m, 1H, *J*=15.6, 7.2 Hz, Ph-CH=C*H*), 5.38 (bm, -CH=CH *trans*), 5.35 (bm, -CH=CH *cis*), 2.02-1.96 (bm, -CH), 1.33 (bs, -CH_2), 1.28 (bm, -CH_2). ^{13}C NMR ($CDCl_3$): δ = 152.7 (-H*C*=N-), 138.1, 130.5, 130.0, 128.6, 126.9, 126.0, 116.6, 37.7, 32.8, 29.8, 29.2, 27.4. IR (ATR mode): 2917 (m), 2849 (m), 1617 (vs), 1593 (vs), 1509 (vs), 1466 (vs),1333 (w), 1214 (w), 1069 (w), 965 (s), 756 (s), 719 cm^{-1} (w).

Synthesis of Aldehyde-Functionalized Monoliths

Monoliths were prepared in stainless steel columns (250 × 3 mm) according to a previously published protocol.[5] Two solutions A and B were prepared and cooled to -20°C. Solution A (NBE:$DMNH_6$:2-propanol = 25:25:40 and solution B (toluene:**I1** = 10:1 (all in wt %) were mixed and rapidly transferred to the stainless steel column. The column was kept at 0°C for 30 min, and then the polymerization was allowed to complete at room temperature for 1 h. After 1 h, the monolith was flushed with toluene for 15 min at a flow rate of 0.2 mL/min to remove any unattached catalyst. The monolith was then flushed consecutively with toluene and air for 16 h and then kept at room temperature. After 24 h, the monolith was flushed with THF to remove any Ru-byproducts. IR (ATR mode): 2938 (m), 2861 (m), 1725 (νCO, m), 1649 (m), 1448 (s), 1341 (m), 1148 (w), 963 (s),831 (w), 731 cm^{-1} (s).

Quantification of the Aldehyde Group

The chemically accessible aldehyde groups in the monolith were quantified via conversion into the corresponding 2,4-dinitrophenylhydrazones. For this purpose, the monolith was taken out of the column, ground up and dried *in vacuo* overnight. 100 mg of the sample were suspended in 2 mL of methanol and stirred with 2 mL freshly prepared 2,4-dinitrophenylhydrazine reagent (*vide supra*). After 1 h, the monolith was filtered, washed with methanol and then dried *in vacuo*. Quantification of the hydrazone groups was accomplished by elemental analysis. IR(ATRmode): 2936 (m), 2862 (m), 2165 (m), 1648 (m), 1617 (m), 1592 (m), 1447(s), 1408 (m), 1337 (m), 1143 (w), 964 (s), 837 (w), 733 (s), 688 (m)cm^{-1}. Elemental analysis: C, 88.3; H, 9.51; N, 0.06.

Monoliths for Trypsin Immobilization

Monoliths were prepared in stainless steel columns (100 × 4.6 mm i.d.) according to a previously published protocol.[4] Briefly, two solutions A and B were prepared. Solution A consisted of NBE:$(NBE\text{-}CH2\text{-}O)_3$-$SiCH_3$:2-propanol (20:20:45.7 wt %), solution B consisted of 0.4 wt% of **1** in 13.9 wt % of toluene. Both solutions were cooled to -20°C, mixed for ~1 min, and then rapidly transferred into the stainless steel column. The column was kept at 0°C for 30 min, and then the polymerization was allowed for another 30 min at room temperature. The monolith was flushed with toluene for 30 min at a flow rate of 0.2 mL/min to remove any nonreacted monomers. Then the monolith was consecutively flushed with toluene and air at room temperature for 24 h. Finally, the support was washed with THF to remove any Ru-byproducts.

Modification of Aldehyde-Functionalized Monoliths with Tetraethylenepentamine (TEPA)[6] and Immobilization of Trypsin

A 2 wt % solution of TEPA in 0.1 M Na_2CO_3 buffer solution (pH 9.2) and 10 vol-% of THF was introduced into the aldehyde functionalized monolith at a flow rate of 0.05 mL/min. Then the reaction was allowed for 2 h at room temperature. The monolith was flushed with 10% THF in deionized water followed by absolute ethanol to remove any unattached TEPA. A 2 wt % solution of glutaraldehyde in Na_2CO_3 buffer (20 vol-% THF) at pH 9.2 was then introduced into the monolith at a flow rate of 0.05 mL/min. The monolith was then sealed and kept at room temperature for another 2 h. Finally, the monolith was flushed with 10 vol-% THF in deionized water followed by absolute ethanol to remove any unattached GA. The glutaraldehyde-functionalized monolith was then flushed with 50 mM HEPES buffer solution at pH 8 to remove any organic solvent in the monolith that might interfere with the trypsin derivatization. A fresh solution of trypsin (3 mg/mL) in 50 mM HEPES buffer (100 mM NaCl, 10 mM $CaCl_2$) was prepared and injected into the monolith at a flow rate of 0.05 mL/min. The monolith was then sealed and kept for 2 h at room temperature. Finally, the monolith was flushed with 0.1M phosphate buffer solution containing 0.01 wt % Tween®20 and then with phosphate buffered saline (PBS) solution. After the immobilization the monolith was stored at 4°C.

Proteolytic Activity of the Immobilized Trypsin (Batch Experiment)

The proteolytic activity of the immobilized trypsin was monitored by measuring the hydrolysis products of a standard solution of *N*-α-benzoyl-DL-arginine-p-nitroanilide (BAPNA), i.e., *N*-α-benzoyl-DL-arginine (BA) and *p*-nitroaniline (PNA). A 0.25 mM standard solution of BAPNA in 50 mM HEPES buffer solution at pH 8 was introduced into the monolith at 37°C. After 10 min, the reaction mixture was eluted at a flow rate of 0.05 mL/min for 10 min. The conversion of BAPNA was calculated by comparing the area of BAPNA after proteolysis to the area of the standard BAPNA.

Proteolytic Activity of the Immobilized Trypsin (Continuous Flow)

The activity of immobilized trypsin was monitored under continuous flow conditions for 3 h as follows. A standard solution of BAPNA (0.25 mM) in 50mM HEPES buffer at pH 8 was pumped through the bioreactor at a flow rate of 0.05 mL/min at37°C. Aliquots were collected in 10 min intervals and analyzed by RP-HPLC at 310 nm. For the separation conditions refer to (Chapter 2, Figure 6). The extent of hydrolysis of BAPNA was calculated by comparing the area

of BAPNA of each 10 min aliquot to the area of a standard BAPNA. No perceptible loss in activity was observed for at least 3 h.

Supporting Information

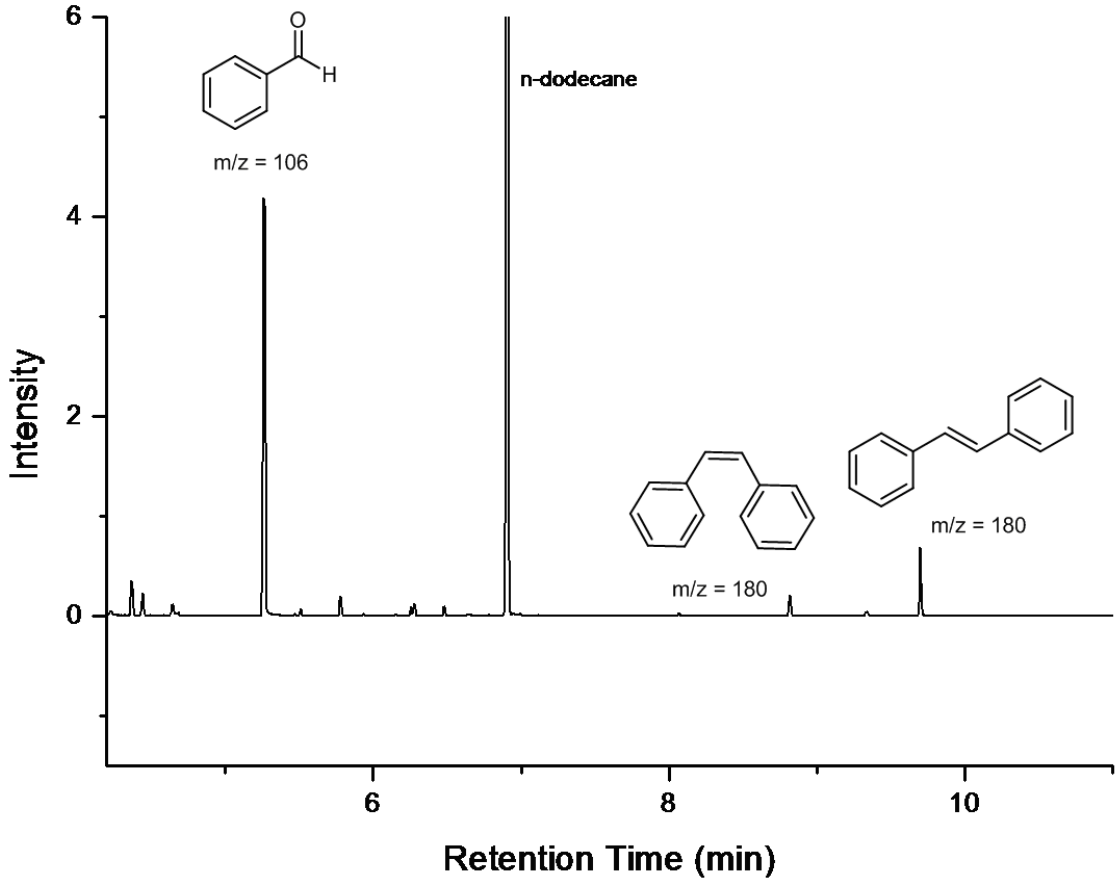

Figure S1. Gas chromatogram with mass labels obtained from the mass spectrum upon exposure of **I1** in benzene to air.

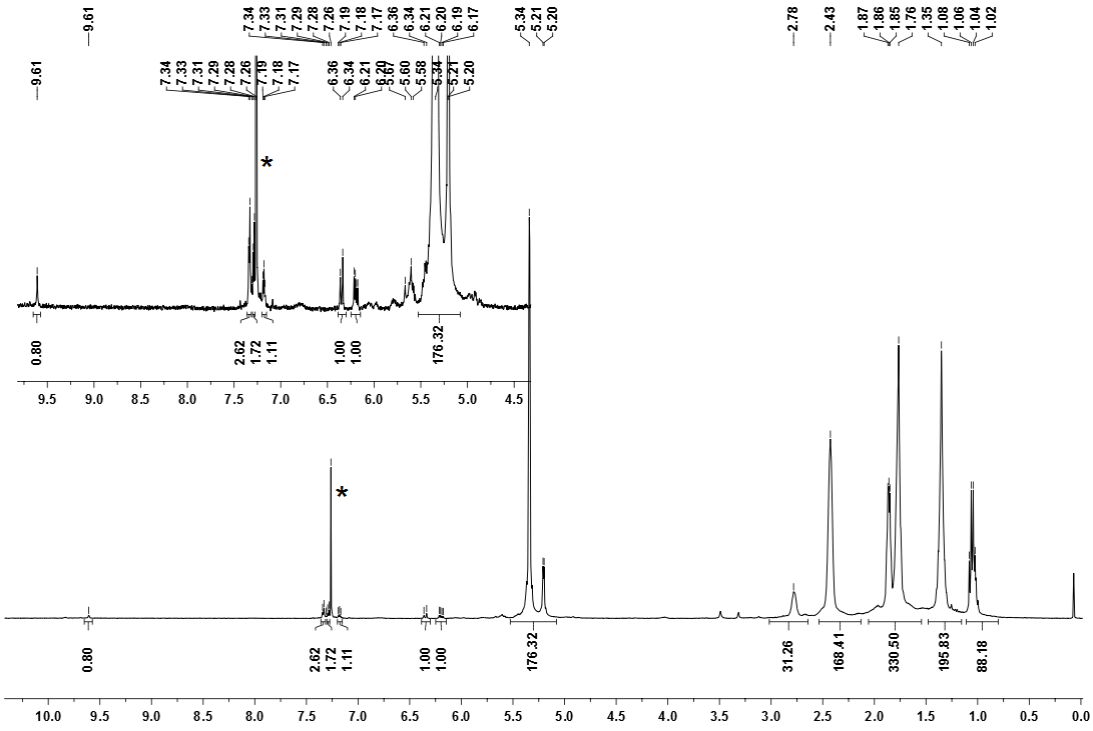

Figure S2. ^{1}H NMR spectrum of aldehyde-semitelechelic poly(NBE) in $CDC1_3$ prepared by the action of initiator **1** (*denotes $CDCl_3$).

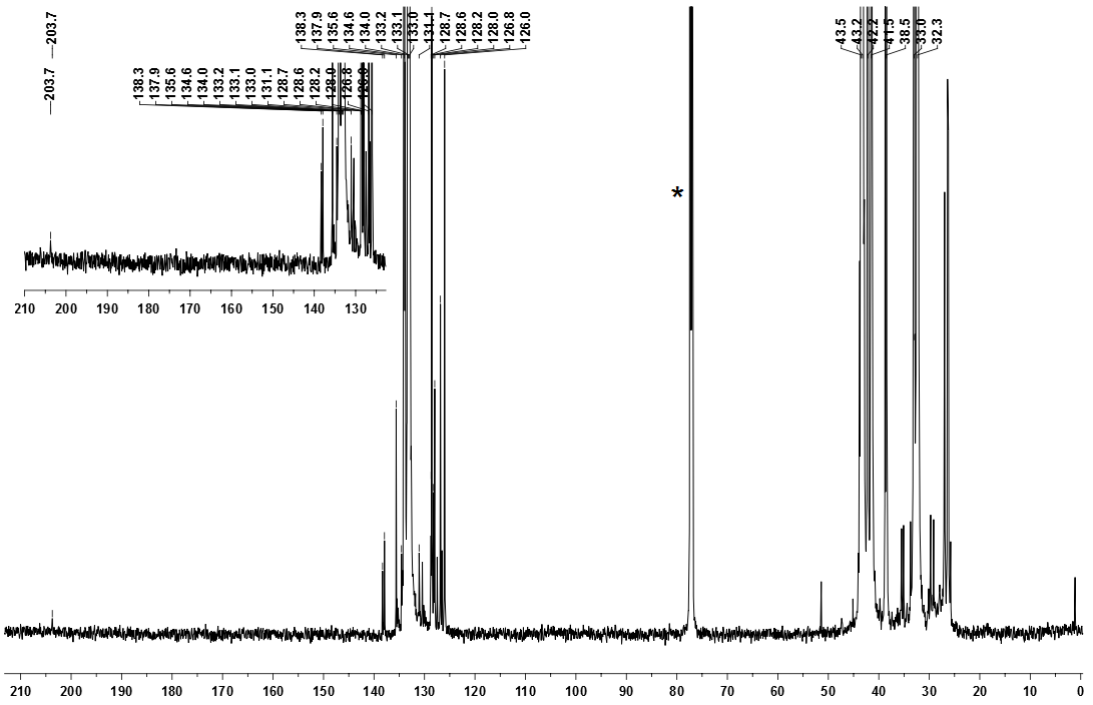

Figure S3. ^{13}C NMR spectrum of aldehyde-semitelechelic poly(NBE) in $CDC1_3$ prepared by the action of initiator **I1**(*denotes $CDCl_3$).

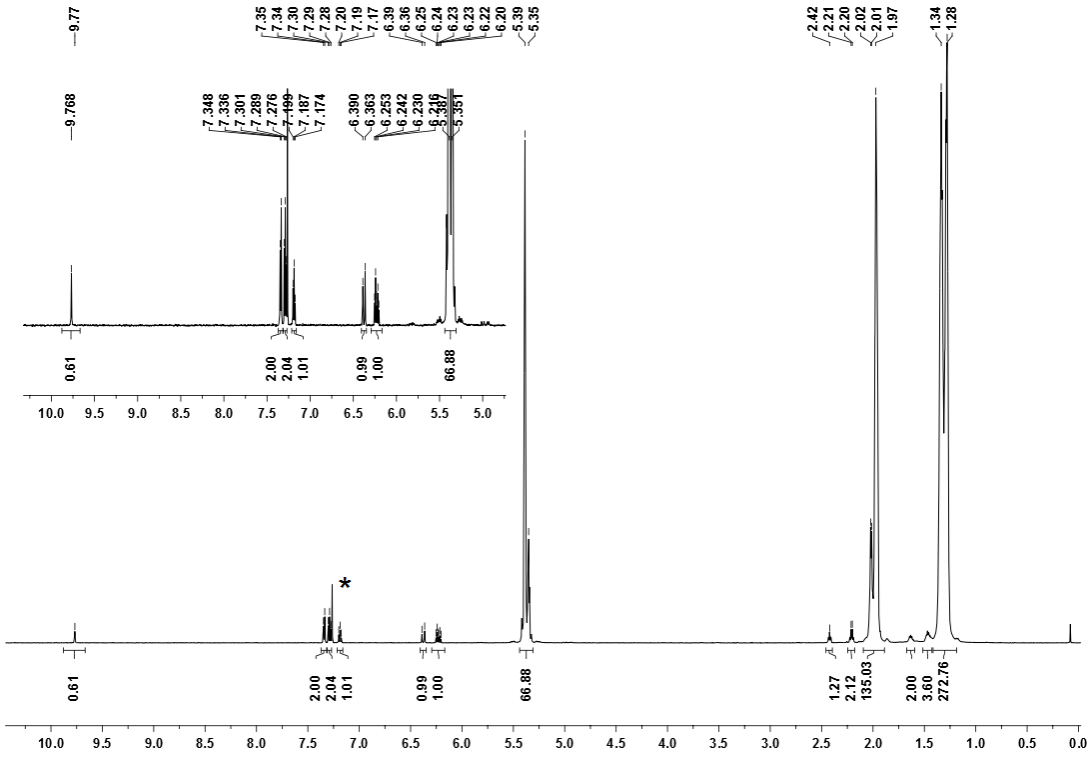

Figure S4. ^{1}H NMR spectrum of aldehyde semi-telechelic poly(COE) in $CDC1_3$ prepared by the action of initiator **I2** (*denotes $CDCl_3$).

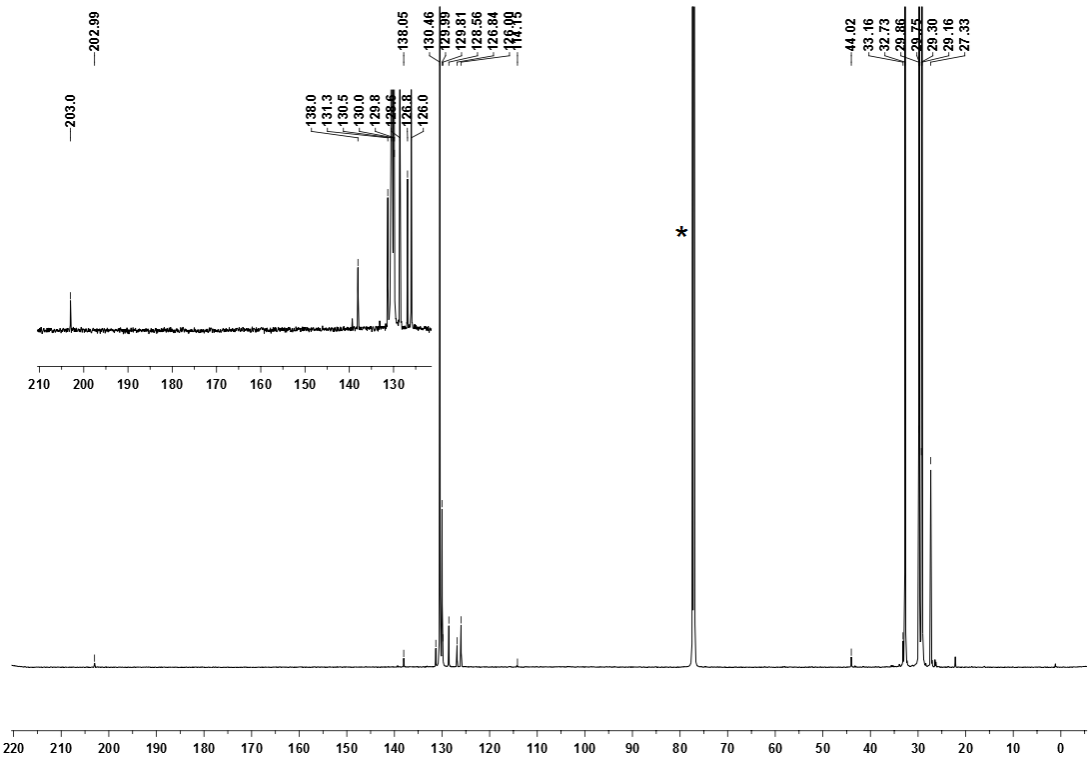

Figure S5. ^{13}C NMR spectrum of aldehyde-semitelechelic poly(COE) in $CDC1_3$ prepared by the action of initiator **I2** (*denotes $CDCl_3$).

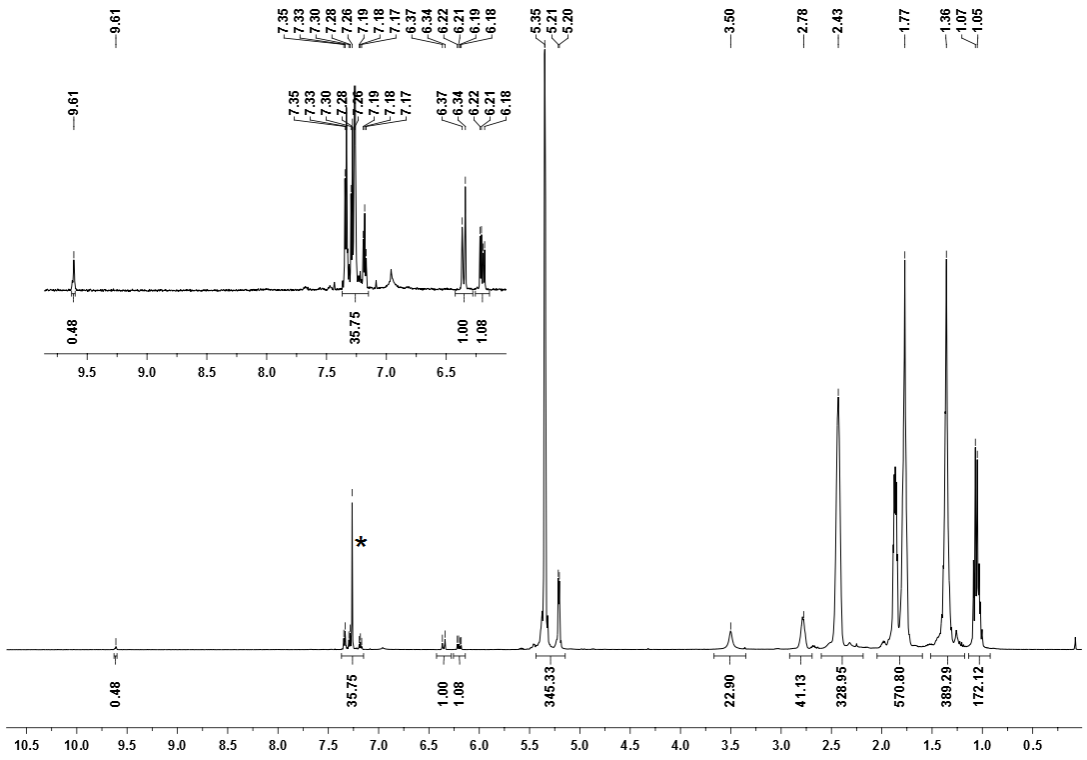

Figure S6. ^{1}H NMR spectrum of aldehyde-semitelechelic poly(NBE) in $CDC1_3$ prepared by the action of initiator **I2** (*denotes $CDCl_3$).

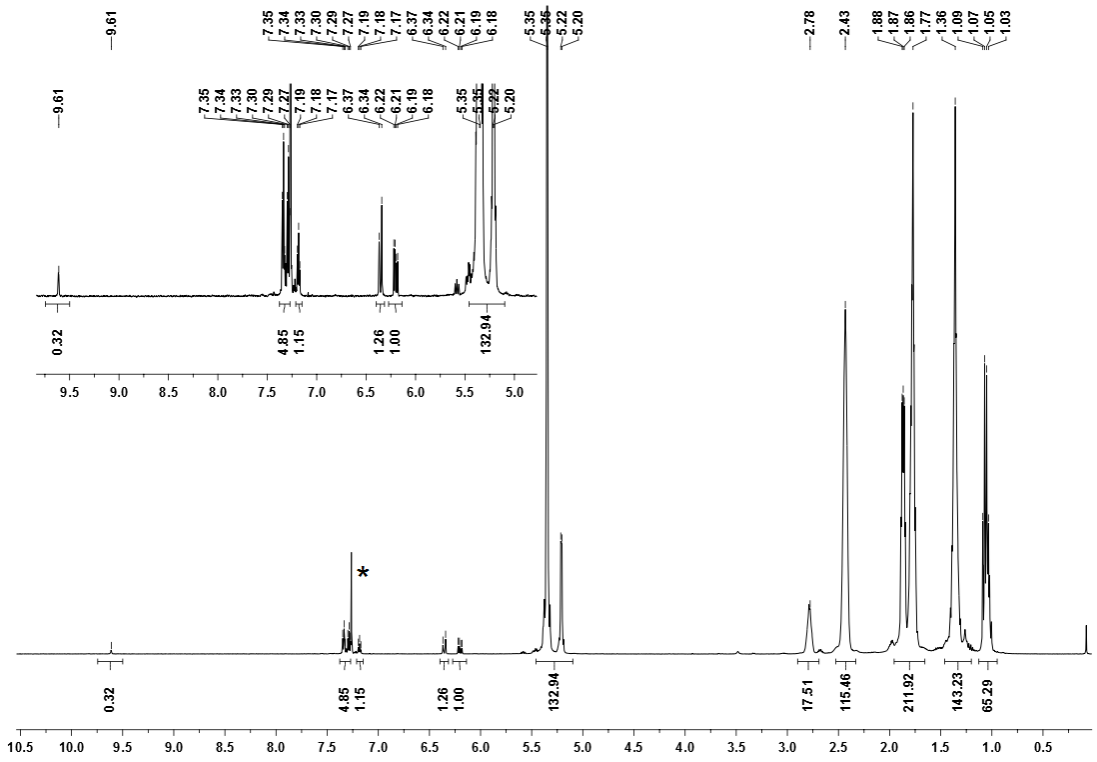

Figure S7. ^{1}H NMR spectrum of aldehyde-semitelechelic poly(NBE) in $CDC1_3$ prepared by the action of initiator **I3** (*denotes $CDCl_3$).

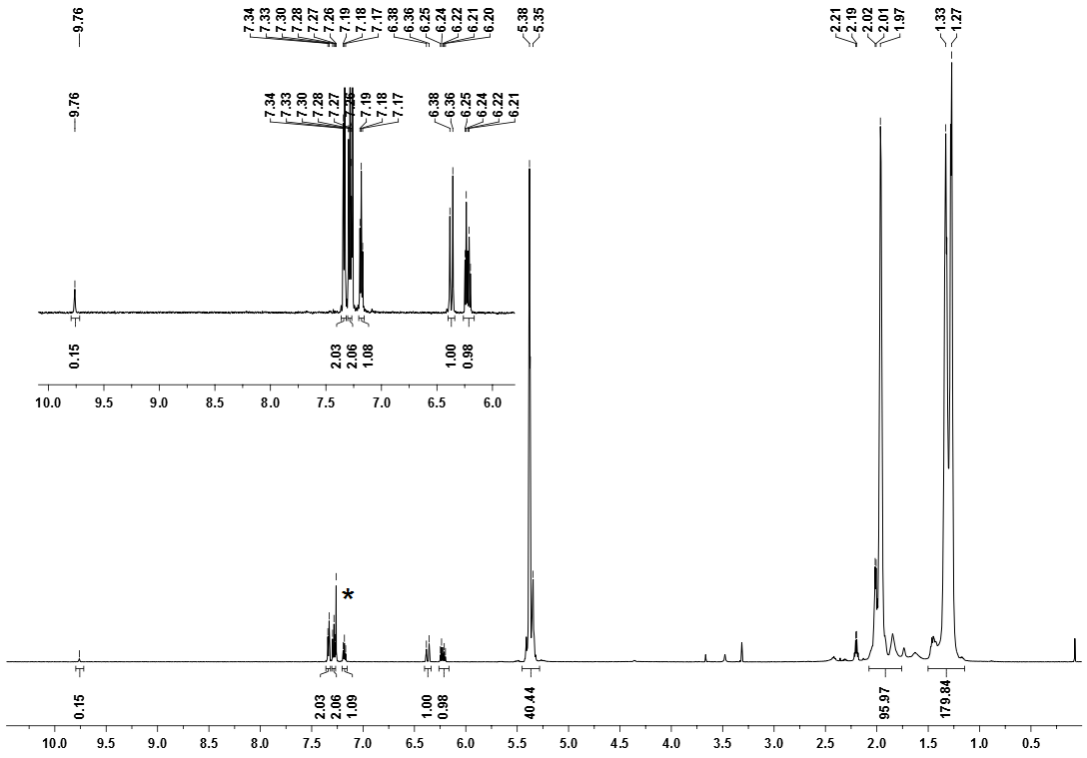

Figure S8. ^{1}H NMR spectrum of aldehyde semitelechelic poly(COE) in $CDC1_3$ prepared by the action of initiator **I1** (*denotes $CDCl_3$).

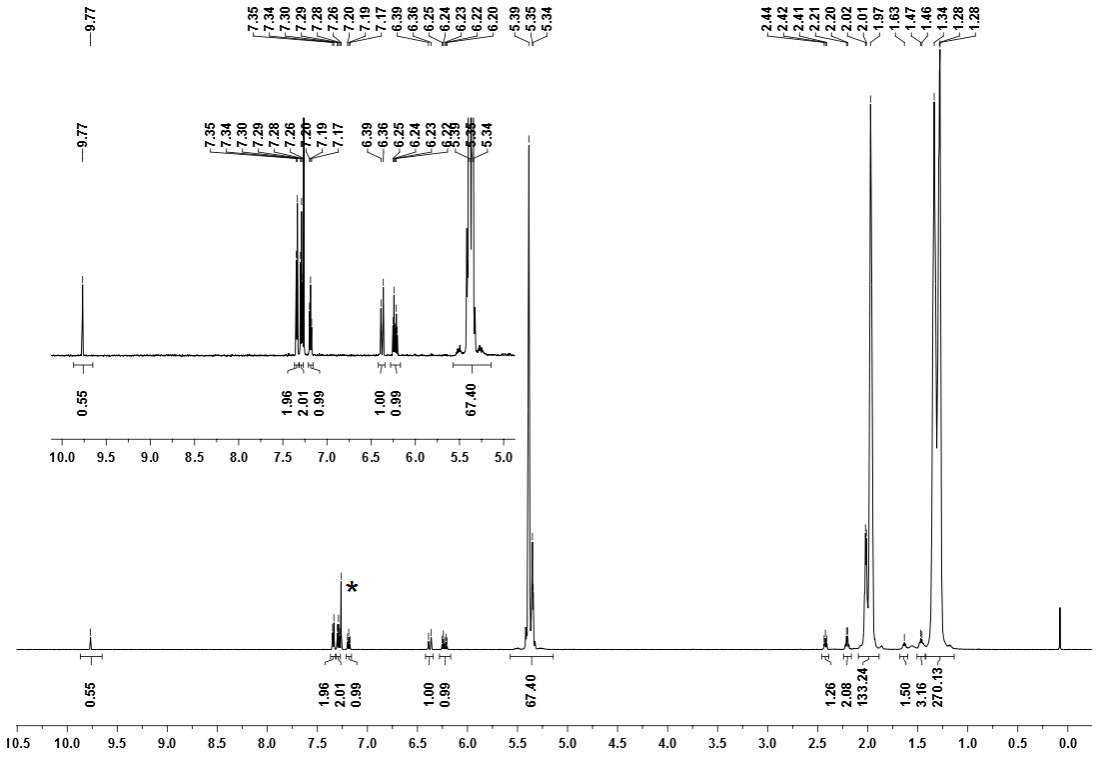

Figure S9. ^{1}H NMR spectrum of aldehyde semitelechelic poly(COE) in $CDC1_3$ prepared by the action of initiator **I3** (*denotes $CDCl_3$).

6.3 Heterogenization of Chiral Bimetallic Catalyst on a ROMP-Derived Monolithic Support: Applications in Entantioselective Michael Additions

The Ru-based initiators $RuCl_2(PCy_3)_2(=CHPh)$, (PCy_3=tricyclohexylphosphine) and norborn-2-ene (NBE), methyltrichorosilane, allyl bromide, allyl alcohol and dicyclopentadiene, 2-methyl-2-butene, BH_3•THF, mesylchloride, *n*-buthyllithium were obtained from Aldrich Chemical Co. (Germany). Hexafluoroglutaric anhydride and 1H,1H,7H-dodecafluoro-1-heptanol were purchased from ABCR GmbH and Co. KG (Karlsruhe, Germany). The synthesis of the activated complexes of FBIP-Cl, their immobilization and the enatioselective Michael-addition reactions and characterization of the products were done by **Simon Eitel** from the Institute of Organic Chemistry, University of Stuttgart.

*5-Norbornene-2-methanol(**1**0)*[7]

A mixture of allyl alcohol (75.0 g, 1.29 mol), cyclopentadiene (94.0 g, 1.42 mol), and a small amount of hydroquinone was heated in an autoclave at 180°C for 16 h. The resulting mixture was distilled under reduced pressure at 80°C to afford **5** as colorless liquid. Yield: 112 g (70%). ^{1}H NMR ($CDCl_3$): δ = 6.14-5.92 (m, 2H, C*H*=C*H*), 3.71-3.18 (m, 2H, CH_2O), 2.91 (s, 1H), 2.79 (s, 1H), 2.34-2.16 (m, 1H), 1.84-1.75 (m, 2H), 1.45-1.41 (m, 1H), 1.30-1.06 (m, 2H), 0.53-0.46 (m, 1H), ^{13}C NMR ($CDCl_3$): δ= 137.5, 136.9, 136.6, 132.2 (*C*=*C*), 67.5, 66.5 (*C*H_2O), 49.6 (CH_2), 45.0, 43.6, 43.3, 42.3, 41.7 (CH), 29.6, 28.9 (CH_2). GC-MS calcd. for $C_8H_{12}O$: *m/z*=124.09; found: 124 ($M^{\cdot+}$)

*5-Allyloxymethylbicyclo[2.2.1]hept-2-ene (**2***[7]

Sodium hydride (3.90 g, 160 mmol) was added to a solution 5-norbornene-2-methanol (5 g, 40 mmol) in DMF (200 mL) at 0°C. The reaction mixture was stirred for 5 min, then allyl bromide (19.4 g, 160 mmol) was added. The reaction mixture was then allowed to stir at room temperature overnight. The reaction was quenched by adding water (50 mL) and extracted with pentane (3 x 100 mL). The combined organic layers were washed with brine, dried over Na_2SO_4 and then evaporated *in vacuo*. The resulting residue was purified by silica-gel column chromatography using 10% Et_2O in pentane as eluent yield the product as pale yellow liquid. Yield: 5.3 g (80%). ^{1}H NMR ($CDCl_3$): δ= 6.13-5.92 (m, *J* = 5.6, 3.0 Hz, 2H), 5.93-5.85 (m, 1H), 5.28-5.14 (m, 2H), 4.00-3.88 (m, 2H), 3.15 (dd, *J* =9.2, 6.6 Hz, 1H), 3.04 (t, *J* = 9.1 Hz, 1H), 2.92 (br, 1H), 2.76 (br, 1H), 2.35 (m, 1H), 1.81 (ddd, *J* = 11.6, 9.2, 3.8 Hz, 1H), 1.44-1.40 (m, 1H), 1.32-1.09 (m, 1H), 0.49 (m, 1H). ^{13}C NMR ($CDCl_3$): *δ* = 137.3, 136.8, 135.4, 132.6, 116.8,

75.1, 74.2, 72.1, 49.6, 45.1, 44.1, 42.3, 39.1, 29.3. GC-MS calcd. for $C_{11}H_{16}O$: *m/z* =164.12; found: 163.9 ($M^{\cdot+}$).

*3-(Bicyclo[2.2.1]hept-5-en-2ylmethoxy)propan-1-ol(**3**)*[7]

To 2-methyl-2-butene (3.1 g, 44 mmol) in THF (200 mL) at –10°C was added BH_3•THF (22 mL, 1.0 M, 22 mmol) dropwise. The reaction mixture was stirred at 0°C for 1 h, then allyloxynorbornene (3.0 g, 18 mmol) was added and stirring was continued at 0°C. After 4 h, the mixture was quenched by adding water and a solution of 10 wt-% solution of NaOH (40 mL), and 30% H_2O_2 (40 mL) were added. The reaction mixture was then stirred overnight at room temperature and extracted with EtOAc (2x100 mL). The combined organic layers were washed with water, brine, dried over Na_2SO_4 and then evaporated *in vacuo*. The resulting residue was purified by silica-gel column chromatography using 20% EtOAc in pentane as eluent to yield the product as colourless liquid. Yield: 2.6 g (78%). ^{1}H NMR ($CDCl_3$): δ= 6.12-5.90 (m, *J* = 5.7, 3.0 Hz, 2H), 3.76 (m, 2H), 3.62-3.53 (m, 2H), 3.15 (dd, *J* = 9.2, 6.7 Hz, 1H), 3.04 (m, 1H), 2.85 (bs, 1H), 2.77 (bs, 1H), 2.63 (bs, 1H), 2.32 (m, 1H), 1.83-1.76 (m, 3H), 1.42-1.06 (m, *2*H), 0.48 (m, 1H); ^{13}C NMR ($CDCl_3$): *δ* = 137.3,132.4, 75.1, 70.7, 62.6, 49.5, 44.1, 41.6, 38.8, 32.1, 29.2; GC-MS calcd. for $C_{11}H_{18}O_2$: *m/z* =182.13; found: 182.1($M^{\cdot+}$).

*5-(3-Iodopropoxymethyl)bicyclo[2.2.1]hept-2-ene (**4**)*[7]

To a mixture of norbornenyl alcohol (1.0 g, 5.5 mmol) and Et_3N (2.2 g, 22 mmol) in CH_2Cl_2 (30 mL), mesyl chloride (0.95 g, 8.3 mmol) was added dropwise at 0°C over a period of 5 min. The reaction mixture was stirred for 30 min and then quenched by adding water (10 mL). The aqueous was extracted with CH_2Cl_2 (2x100 mL). The combined organic layers were washed with saturated aqueous $NaHCO_3$, dried over Na_2SO_4 and evaporated *in vacuo*. The residue (mesylate) was dissolved in acetone (30 mL) then NaI 2.5 g, 16.5 mmol) was added. The mixture was refluxed for 3 h. After cooling, the mixture was diluted with diethyl ether (150 mL) and washed with 10wt-% $Na_2S_2O_3$ and water. The organic layer was dried over Na_2SO_4 and evaporated *in vacuo*. The residue was purified by silica-gel column chromatography using 20% Et_2O in pentane as eluent to afford the product as pale yellow liquid. Yield: 1.4 g (86%). ^{1}H NMR ($CDCl_3$): δ= 6.13-5.93 (m, *J* = 5.6, 3.0 Hz, 2H), 3.51-3.38 (m, 2H), 3.33-3.27 (m, 2H), 3.16 (dd, *J* = 9.2, 5.9 Hz, 1H), 2.02(m, 1H), 2.89 (bs, 1H), 2.78 (bs, 1H), 2.33 (m, 1H), 2.02-1.99 (m, 2H), 1.80 (ddd, *J* = 9.9, 8.6, 3.8 Hz, 1H), 1.41 (m, 1H), 1.31-1.23 (m, 1H), 0.48 (m,1H); ^{13}C NMR ($CDCl_3$): *δ* = 137.3, 132.6, 74.9, 70.1, 49.5,44.1, 42.3, 38.9, 33.6, 29.2, 3.8; GC-MS calcd. for $C_{11}H_{17}IO$: *m/z* =292.03; found: 292.0 ($M^{\cdot+}$).

*2,2,3,3,4,4,5,5,6,7-Decafluoroundec-6-en-1-ol (**5**)*[8]

1H,1H,7H-Dodecafluoro-1-heptanol (3.0 g, 9.0 mmol) was dissolved in Et_2O (60 mL). A solution of *n*-buthyllithium in hexanes (19.2 mL, 1.60 M, 30.7 mmol) was added drop-wise over 30 min-78°C. The mixture was stirred for 1.5 h at room temperature and then the reaction was quenched by the addition of a diluted 1 M aqueous HCl. The organic phase was separated, washed with water (2x20 mL), and dried over Na_2SO_4, then solvent was evaporated *in vacuo*. The residue was distilled under reduced pressure (110-120°C bath temperature, approximately 10 mm Hg) to yield the product as colourless liquid**.** Yield: 1.9 g (61%). ^{1}H NMR ($CDCl_3$): δ= 4.08 (t, 2H), 2.53-2.36 (m, 2H), 1.97 (bs, 1H), 1.63-1.55 (m, 2H), 1.44-1.35(m, 2H), 0.93 (m, 3H); ^{19}F NMR ($CDCl_3$): δ = -115.1, -115.3, -117.1, -122.6, -124.2, -137.3, -156.3, -171.3; ^{13}C NMR ($CDCl_3$): δ = 160.3, 157.5, 138.3, 115.6, 114.1, 109.3, 60.9, 27.2, 21.9, 13.7; GC-MS calcd. for $C_{11}H_{12}F_{10}O$: *m/z* =350.07; found: 330.0 (M-HF).

*2,2,3,3,4,4,5,5-Octafluoro-6-hydroxyhexanoic acid (**6**)*[9]

To a stirred solution of 2,2,3,3,4,4,5,5,6,7-decafluoroundec-6-en-1-ol (0.8 g, 2.3 mmol) in acetone (20 mL) was added $KMnO_4$ (0.8 g, 5.1 mmol). The temperature of the reaction was maintained at 20-30°C. After 20 h, the reaction mixture was clarified with aqueous $NaHSO_3$ solution and acidified with dilute sulphuric acid. The clear solution was saturated with NaCl and extracted with diethyl ether (2x50 mL). The combined organic layers were washed with brine, dried over Na_2SO_4 and then evaporated *in vacuo*. The residue was recrystallized from warm $CHCl_3$ to afford the desired product as a white solid. Yield: 0.32 g (50%). ^{1}H NMR (DMSO-*d6*): δ= 3.95; ^{19}F NMR ($CDCl_3$): δ = -118.4, -121.0, -123.0; ^{13}C NMR ($CDCl_3$): δ = 159.6, 116.4, 113.9, 110.7, 108.1, 58.9.

*6-(3-Bicyclo[2.2.1]hept-5-en-2-ylmethoxy)propoxy)-2,2,3,3,4,4,5,5-octafluorohexanoic acid (**M2**)*

Sodium hydride (60% dispersion in oil, 38.3 mg, 1.09 mmol) was added to a solution of 2,2,3,3,4,4,5,5-octafluoro-6-hydroxyhexanoic acid (100 mg, 0.36 mmol) in anhydrous DMF (5 mL) at 0°C. After stirring for 15 min **4** (159 mg, 0.54 mmol) was added drop-wise. The reaction mixture was then stirred at room temperature. After 3h the reaction was quenched by adding water (20 mL) and washed with pentane twice. The aqueous layers were acidified with a dilute 1M HCl and extracted with diethyl ether (3x50 mL). The combined organic extracts were washed with brine, dried over Na_2SO_4 and evaporated *in vacuo* to afford the product as pale

yellow viscous liquid. Yield: 110 mg (70%). ^{1}H NMR ($CDCl_3$): δ= 9.66 (bs, 1H), 6.14-5.89 (m, *J* = 5.7, 3.1 Hz, 2H), 4.08 (t, 4H), 3.92 (t, 2H), 3.68 (t, 4H), 3.60-3.52 (m, 2H), 3.21 (dd, *J* = 9.2, 5.9 Hz, 1H), 3.12(t, 1H), 2.02(m, 1H), 2.88 (bs, 1H), 2.79 (bs, 1H), 2.35 (m, 1H), 1.99-1.78 (m, 3H), 1.44-1.41 (m, 1H), 1.29-1.07 (m, 2H), 0.48 (m,1H); ^{19}F NMR ($CDCl_3$): δ = -119.2, -119.9, -122.6, -123.0, -123.4, -123.6; ^{13}C NMR ($CDCl_3$): δ = 160.6, 137.6, 132.3, 115.7, 112.3, 108.8, 108.5, 76.0, 75.0, 69.9, 68.1, 67.4, 60.8, 49.6, 44.1, 42.3, 38.5, 29.6, 29.3; HRMS (ESI) calcd. for $C_{17}H_{20}F_8O_4$ (MH^+): = 441.1307; found: 441.1302.

Synthesis and Functionalization of ROMP-Derived Monolithic Supports

The monolith was prepared inside a PEEK column according to previously published procedures.[10] Briefly, two solutions A and B were prepared. Solution A consisted of NBE:$(NBE–CH_2O)_3SiCH_3$: 2-propanol (20:20:45.7 wt.-%), solution B consisted of 0.4 wt.-% of $RuCl_2(CHPh)(PCy_3)_2$ in 13.9 wt.-% of toluene. Both solutions were cooled to -20^{o}C, mixed and rapidly transferred to the column. The column was kept at 0^{o}C for 30 min, then the polymerization was allowed to proceed for another 30 min at room temperature. The column was flushed with freshly distilled toluene for 30 min at a flow rate of 0.2 mL/ min. Argon was passed through the monolith for 10 min to elute the solvent. A solution of **M2** (55 mg, 0.125 mmol) in 1.5 mL of CH_2Cl_2 was introduced into the monolith at a flow rate of 0.1 mL/min. The column was then sealed and kept at 40^{o}C overnight. The following day, the monolith was flushed with a mixture of DMSO:THF:EVE(40:40:20) to remove the initiator and then with THF each for 30 min. Finally the monolith was flushed with CH_2Cl_2 for 30 min at a flow rate of 0.1 mL/min. The grafted monolith was then directly used for the immobilization.

For the grafting of **M1**, hexafluoroglutaric anhydride (660 mg, 2.98 mmol) was added drop wise to a solution of 5-nobornene-2-methanol (310 mg, 2.50 mmol) in 6 mL of dichloromethane under argon. The mixture was stirred at ambient temperature for 1h. After 1 h, the reaction mixture containing **M1** was used as such without purification for grafting.

Procedure for the Immobilization of FBIP-BF_4^-·CH_3CN via a Potassium Salt of a Monolith Functionalized Carboxylic Acid.

An aqueous solution of KOH (10 mL, 5.2 mM) was introduced to the monolith grafted with **M1** at a flow rate of 0.1 mL/min and flushed with water until reaching neutral washings. The column was then flushed with methanol followed by CH_2Cl_2, each for 30 min at a flow rate of 0.2 mL/min. A solution of 4.4 µmol *FBIP-BF_4^-·CH_3CN* (prepared *in situ*) in 1 mL of dry CH_2Cl_2 was

injected to the monolith by using luer syringe technique at a flow rate of 0.05 mL/min. The column was then sealed and kept at room temperature overnight. The following day, the silver heptafluorobutyrate in 1.5 mL of anhydrous CH_3CN was introduced into the monolith, which was again sealed and kept at room temperature for 1 h. Finally, the monolith was flushed with dichloromethane until the effluent was colourless.

Immobilization of FBIP-$O_2C_4F_7$·CH_3CN (via alternative route)

A solution of 4.4 µmol *FBIP-$O_2C_4F_7$·CH_3CN (*prepared *in situ*) in 1 mL of dry CH_2Cl_2 was introduced to the monolith (grafted with **M1** or **M2)** at a flow rate of 0.1 mL/min. The column was then sealed and kept at room temperature. After 24 h, the column was flushed with dry CH_2Cl_2 at a flow rate of 0.1 mL/min for 30 min.

Quantification of Carboxylate Groups.

The amount of carboxylate groups in the monolith was determined by acid-base titration. For this purpose, the functional monolith was flushed with water for 30 min at a flow rate of 0.2 mL/min. A known volume of an aqueous KOH solution (10 mL, 5.2 mM) was passed through the monolith at a flow rate of 0.1 mL/min, followed by water until reaching neutral washings. The amount of carboxylate groups was then quantified by comparing the molarity of flow through solution with standard KOH solution. The molarities of both the solutions were determined by titrating against standard HCl solution (1 mM) using phenolphthalein as indicator.

Supporting Information

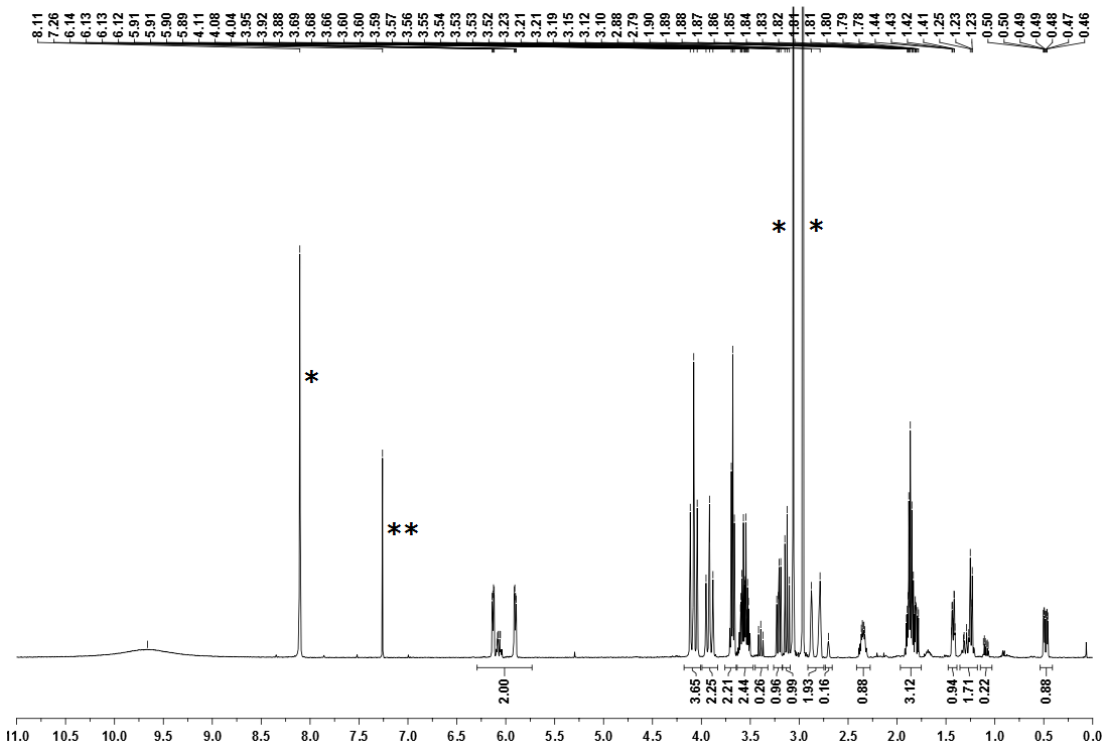

Figure S10. ^{1}H-NMR spectrum of **M2**, **denotes $CDCl_3$ and *denotes DMF.

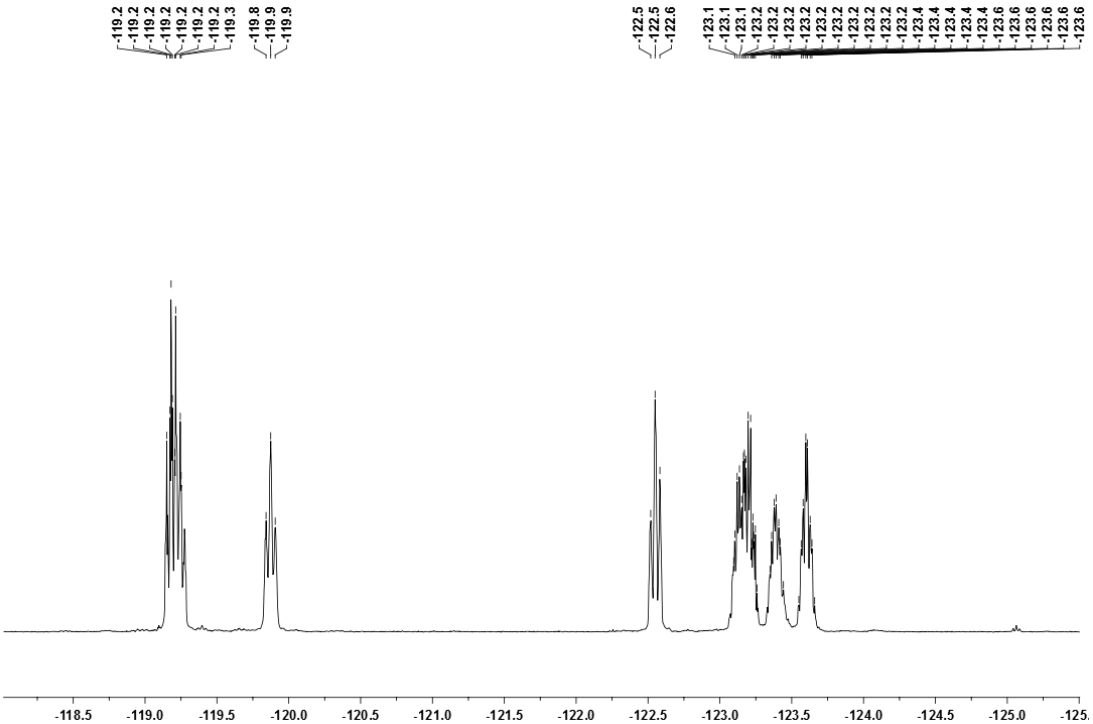

Figure S11. ^{19}F-NMR spectrum of **M2**.

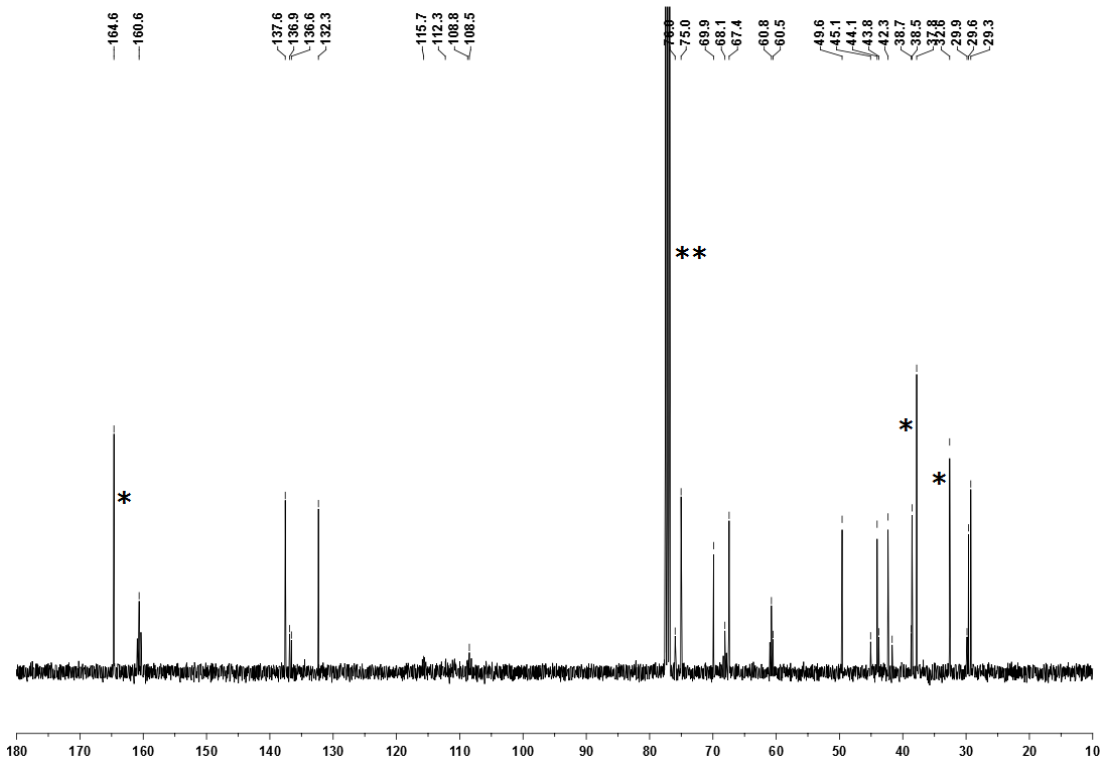

Figure S12. ^{13}C-NMR spectrum of **M2**, **denotes $CDCl_3$ and *denotes DMF.

6.4 Cyclopolymerization-Derived Conductive Monolithic Media for Continuous Heterogeneous (Electro-) Catalysis

The Ru-based initiators $[RuCl_2(IMesH_2)(=CH\text{-}2\text{-}(2\text{-}PrO)\text{-}C_6H_4]$ ($IMesH_2$=1,3-bis(2,4,6-trimethylphenyl)imidazolin-2-ylidene), *N*-hydroxy succinimide, chlorotrimethylsilane, diethyl malonate, $LiAlH_4$, dicyclohexyl carbodiimide, *N*,*N*-dimethylaminopyridine, triethylamine, 2-propanol, I_2, $NO^+BF_4^-$, SbF_5, trypsin from bovine pancreas (EC 3.4.21.4), *N*-α-benzoyl-DL-arginine-p-nitroanilide hydrochloride (BAPNA), phosphate-buffered saline tablets, Tween20, and deionized water were obtained from Aldrich Chemical Co. (Germany). Propargyl bromide, terephthaloyl dichloride, 1,3,5-benzenetricarboxylic acid chloride, DMSO, NaOH were purchased from Acros Organics (Germany). Diethyldipropargyl malonate, 4-(carboxyethyl)-l,6-heptadiyne, 4-(hydroxymethyl)-1,6-heptadiyne, 4-carboxy-1,6-heptadyine as well as the Ru-based initiator $[Ru(CF_3COO)_2(IMesH_2)(=CH\text{-}2\text{-}(2\text{-}PrO)\text{-}C_6H_4)]$ (**I4**), were prepared according to published procedures.[11]

*Diethyldipropargyl malonate (**7**)*[12]

Diethylmalonate (20.0 g, 0.125 mol) was added to a solution of sodium ethoxide (17.0 g, 0.25 mol) in dry ethanol (150 mL). After 30 min, propargyl bromide (29.7 g, 0.25 mol) was added

drop wise to the reaction mixture at room temperature. Then the reaction mixture was refluxed for 16 h. After the removal of alcohol, the residue was diluted with water (500 mL) and extracted with diethyl ether (2 x 500 mL). The combined organic extracts were dried over anhydrous $MgSO_4$ and evaporated *in vacuo*. The pale yellow solid obtained was recrystallised from pentane. Yield 20.5 g (70 %). ^{1}H NMR ($CDCl_3$): δ = 4.17 (q, 4H, OC*H*$_2$Me), 2.92 (d, 4H, C*H*$_2$C≡CH), 2.02 (t, 2H, C≡C*H*), 1.21 (t, 6H, C*H*$_3$); ^{13}C-NMR ($CDCl_3$): δ = 168.9 (*C*OOCH$_2$), 78.7 (*C*≡CH), 72.0 (C≡*C*H), 62.3 (COO*C*H$_2$), 56.5 (CH$_2$*C*HCH$_2$), 22.8 (CH*C*H$_2$-C≡CH), 14.3 (CH$_2$*C*H$_3$),). IR (ATR mode): 3270 (s), 2984 (m), 1726 (vs), 1299 (vs), 1192 (vs), 1002 (m), 852 (w), 671 (m) cm^{-1}.

*4-(Carboxyethyl)-l,6-heptadiyne (**8**)*[13] A solution of diethyldipropargyl malonate (15.0 g, 0.064 mol), H_2O (1.1 mL, 0.064 mol), and LiCl (5.40 g**,** 0.127 mol) in DMSO (110 mL) was heated to reflux under an argon atmosphere. After 5 h, the solution was cooled and diluted with water (400 mL). The aqueous phase was then extracted with hexane (3 x 250 mL). The combined organic phases were consecutively washed with water (200 mL), brine (100 mL) and dried over $MgSO_4$. The solvent was evaporated to leave the crude product as brown liquid. Distillation under high vacuum (20 mmHg) at 80^{o}C afforded the product as a yellow liquid. Yield: 6.0 g (58%); ^{1}H NMR ($CDCl_3$): δ = 4.16 (q, 2H, OC*H*$_2$Me), 2.71 (m, 1H, (CH$_2$)$_2$C*H*CH$_2$), 2.60 (dd, 4H, C*H*$_2$C≡CH), 1.99 (t, 2H, C≡C*H*), 1.25 (t, 3, C*H*$_3$); ^{13}C-NMR ($CDCl_3$): δ = 172.5 (*C*OOCH$_2$), 80.7 (*C*≡CH), 70.8 (C≡*C*H), 61.3 (COO*C*H$_2$), 43.2 (CH$_2$*C*HCH$_2$), 20.1 (CH*C*H$_2$-C≡CH), 14.4 (CH$_2$*C*H$_3$).

*4-Carboxy-1,6-heptadyine (**9**)*[14]

4-(Carboxyethyl)-1,6-heptadiyne (5.00 g, 0.030 mol) was dissolved in 100 mL of ethanol and 1 M aqueous NaOH solution (60 mL, 0.060 mol) was added. The solution was heated to 70^{o}C for 4 h. After 4 h, the ethanol was removed from the reaction mixture. The residue was diluted with water (50 mL) and washed with diethyl ether (50 mL). The diethyl ether solution was discarded. The aqueous phase was acidified to pH=1 using 1M HCl solution and extracted twice with 100 mL of diethyl ether. The organic phase was washed with brine (50 mL) and dried over anhydrous $MgSO_4$ and then evaporated *in vacuo*. The crude product was recrystalised from diethyl ether to yield 4-carboxy-1,6-heptadyine as white solid. Yield: 3.3 g (82 %). ^{1}H NMR ($CDCl_3$): δ = 11.71 (s, 1H, COO*H*), 2.82 (m, 1H, (CH$_2$)$_2$C*H*COO), 2.67 (m, 4H, C*H*$_2$C≡CH), 2.05 (t, 2H, C≡C*H*); ^{13}C-NMR ($CDCl_3$): δ = 179.2 (*C*OOH), 80.4 (*C*≡CH), 71.2 (C≡*C*H), 43.1 (CH$_2$*C*HCH$_2$), 19.8 (CH*C*H$_2$-C≡CH).

*4-(Hydroxymethyl)-1,6-heptadiyne (**10**)*[14]

A solution of 4-(carboxyethyl)-l,6-heptadiyne (7.5 g, 0.046 mol) in 100 mL of dry diethyl ether was added dropwise to a suspension of $LiAlH_4$ (3.5 g, 0.091mol) in 150 mL of dry diethyl ether. The solution was stirred for 16 h at room temperature. After 16 h the reaction was quenched by the dropwise addition of water. The reaction mixture was filtered through a small bed of celite and washed with diethyl ether. The filtrate was then dried over anhydrous $MgSO_4$ and evaporated *in vacuo*. Distillation of the crude under reduced pressure gave **5** as colorless oil. Yield: 5.2 g (93%). ^{1}H NMR ($CDCl_3$): δ = 3.70 (d, 2H, C*H*$_2$OH), 2.36 (dd, 4H, C*H*$_2$C≡CH), 2.13 (s, 1H, CH_2O*H*), 2.01-1.91 (m, 3H, C≡C*H*, $(CH_2)_2$C*H*CH_2); ^{13}C-NMR ($CDCl_3$): *δ* = 82.1 (*C*≡CH), 70.4 (C≡*C*H), 64.1 (*C*H_2OH), 39.3 (CH_2*C*HCH_2), 19.9 (CH*C*H_2-C≡CH).

*N-(1,6-Heptadiyn-4-yl-carbonyloxy)succinimide (**M3**).*

To a solution of **1** (3.0 g, 0.022 mol) in CH_2Cl_2 (50 mL) at 0^{o}C was added dicyclohexyl carbodiimide (6.8 g, 0.033 mol) in one portion under argon. After stirring for 15 min, N-hydroxy succinimide (3.8 g, 0.033 mol) was added at the same temperature followed by a catalytic portion of 4-dimethylaminopyridine (DMAP). The reaction mixture was stirred overnight at room temperature, then filtered through celite. The solvent was evaporated *in vacuo.* The residue was redissolved in CH_2Cl_2 and filtered through a bed of silica. The filtrate was evaporated *in vacuo* to leave **M3** as white solid. Yield: 3.5 g (70 %). ^{1}H NMR ($CDCl_3$): δ = 3.11 **(**m, 1H, $(CH_2)_2$C*H*COO), 2.83 (s, 4H, N(COC*H2*C*H2*CO)$_2$), 2.77 **(**m, 4H, (C*H*$_2$)$_2$CHCOO), 2.11(s, 2H, C≡C*H*); ^{13}C NMR ($CDCl_3$): δ = 169.0 (CH*C*OO), 168.2 (N*C*OCH_2), 79.2 (*C*≡CH), 71.9 (C≡*C*H), 41.1 (($CH_2)_2$CHCH_2)), 25.9 (NCO*C*H_2), 20.1 (*C*H_2C≡CH),). IR (ATR mode): 3289 (s), 2933 (m), 1796 (s), 1779 (s), 1743 (s), 1420 (m), 1199 (s), 1101 (m), 672 (m) cm^{-1}. $^{\cdot+}$). Elemental Analysis: calcd for $C_{12}H_{11}NO_4$: C, 61.80; H, 4.75; N, 6.01, found: C, 61.79; H, 4.73; N, 5.98.

*4-Trimethylsiloxymethyl-1,6-heptadyine (**M4**).*

To a solution of **2** (1.8 g, 0.015 mol) and triethyl amine (4.0 mL, 0.029 mol) in CH_2Cl_2 (75 mL) was added a solution of chlorotrimethylsilane (2.4 g, 0.022 mol) in dry CH_2Cl_2 (25 mL) at 0^{o}C. The reaction mixture was then stirred at room temperature. After 16 h the mixture was diluted with CH_2Cl_2 (100 mL) washed with water (50 mL), brine (50 mL) and then dried over anhydrous $MgSO_4$ and evaporated *in vacuo*. The crude product was dissolved in CH_2Cl_2 and filtered through a bed of silica. The solvent was removed *in vacuo* to afford **M4** as a pale yellow

liquid. Yield: 2.4 g (84 %). ^{1}H NMR ($CDCl_3$): δ = 3.61 **(**d**,** 2H, OC*H*$_2$), 2.33 (dd, 4H, C*H*$_2$C≡CH), 1.98-1.87 (m, 3H, C≡C*H*, $(CH_2)_2$C*H*CH_2), 0.11 (s, 9H, $SiMe_3$); ^{13}C NMR ($CDCl_3$): δ = 82.4 (*C*≡CH), 70.1 (C≡*C*H), 63.7 (O*C*H_2), 39.7 ($(CH_2)_2$*C*HCH_2), 19.8 (*C*H_2C≡CH) , 0.2 ($SiMe_3$).). IR (ATR mode): 3583 (s), 3280 (m), 2528 (m), 2287 (w), 1587(m), 1203 (m), 655 (m) cm^{-1}. MS: (EI +ve ion) calcd. for $C_{11}H_{18}OSi$: 194.1; found: 193.1

*Tris(4-methyl-1,6-heptadiyne) benzene-1,3,5-tricarboxylate (**CL1**).*

1,3,5-benzenetricarboxylic acid chloride (1.30 g, 4.97 mmol) was dissolved in 10 mL of CH_2Cl_2. A solution of **2** (2.00 g, 16.4 mmol) and triethylamine (6.03 g, 59.6 mmol) in CH_2Cl_2 (15 mL) was added dropwise to the acid chloride solution at 0^{o}C over a period of 1h followed by a catalytic portion of 4-dimethylaminopyridine (DMAP). The resulting pale yellow solution was stirred overnight at room temperature. Then saturated aqueous $NaHCO_3$ solution was added to the reaction mixture until bubbling ceased. The organic layer was separated, washed with water (25 mL), brine (10 mL) and dried over anhydrous $MgSO_4$, then the solvent was evaporated *in vacuo*. The resulting crude product was redissolved in CH_2Cl_2 and filtered through silica, the solvent was evaporated *in vacuo* to leave **CL1** as a white solid. Yield: 2.4 g (92 %). ^{1}H-NMR ($CDCl_3$): *δ* = 8.85 (s, 3H, ArH), 4.48 (d, 6H, COOC*H*$_2$), 2.51-2.48 (dd, 12H, C*H*$_2$-C≡C*H*), 2.40-2.28 (m, 4H, CH_2C*H*CH_2-C≡C*H*), 2.07 (t, 6H, C≡C*H*), ^{13}C-NMR ($CDCl_3$): *δ* = 164.7 (*C*OOCH_2), 134.8 (Ph), 131.3 (Ph), 80.8 (*C*≡CH), 70.9 (C≡*C*H), 66.7 (COO*C*H_2), 36.4 (CH_2*C*HCH_2), 20.3 (CH*C*H_2-C≡CH) Elemental Analysis: calcd for $C_{33}H_{30}O_6$: C, 75.84; H, 5.79, found: C, 75.66; H, 5.69.

*Bis(4-methyl-1,6-heptadiyne) terephthalate (**CL2**).*

Terephthaloyl dichloride (11.9 g, 0.0590 mol) was dissolved in 100 mL of CH_2Cl_2. A solution of **2** (15.0 g, 0.123 mol) and triethylamine (49.7 g, 0.492 mol) in CH_2Cl_2 (125 mL) was added dropwise to the acid chloride solution at 0^{o}C over a period of 1h followed by a catalytic portion of 4-dimethylaminopyridine (DMAP). The resulting pale yellow solution was stirred overnight at room temperature. Saturated aqueous $NaHCO_3$ solution was added to the reaction mixture until bubbling ceased. The organic layer was separated, washed with water (100 mL), brine (50 mL) and dried over anhydrous $MgSO_4$ and evaporated *in vacuo*. The resulting crude product was redissolved in CH_2Cl_2 and filtered through silica, then the solvent was evaporated *in vacuo* to leave **CL2** as a white solid. Yield: 20.0 g (90 %). ^{1}H-NMR ($CDCl_3$): *δ* = 8.10 (s, 4H, ArH), 4.44 (d, 4H, COOC*H*$_2$), 2.48 (dd, 8H, C*H*$_2$-C≡C*H*), 2.32 (m, 2H, CH_2C*H*CH_2-C≡C*H*), 2.04 (t, 4H, C≡C*H*), ^{13}C-NMR ($CDCl_3$): *δ* = 165.7 (*C*OOCH_2), 134.2 (Ph), 129.9 (Ph), 80.1 (*C*≡CH),

71.0 (C≡*C*H), 66.5 (COO*C*H_2), 36.7 (CH_2*C*HCH_2), 20.3 (CH*C*H_2-C≡CH), IR (ATR mode): 3421 (s), 3298 (s), 3098 (w), 2943 (m), 2391 (w), 1692 (s), 1262 (m), 1075 (s), 633 (s) cm^{-1}. Elemental Analysis: calcd for $C_{24}H_{22}O_4$: C, 76.99; H, 5.92, found: C, 76.99; H, 5.89.

General Procedure for the Preparation of Cyclopolymerization-Derived Monolith

Monoliths were prepared within stainless steel columns (150 x 4.6 mm). The columns were cleaned, rinsed and sonicated in 1:1 mixture of ethanol and acetone. After drying for 2 h *in vacuo*, one end of the column was closed with frits and end fittings. Separately, two solutions A and B were prepared. Solution A consisted of the monomer (**M3** or **M4**) (2 wt.-%), **CL1** or **CL2** (28 wt.-%), 1,2-dichloroethane (20 wt.-%) and 2-propanol (40 wt.-%) solution B consisted of a solution of the initiator **I4** (0.4 wt.-%) in 1,2-dichloroethane (10 wt.-%). Solution A was warmed to 45°C so that the monomer and cross-linker dissolved completely. While cooling to room temperature, solution B was added and the resulting mixture was stirred for few seconds. The mixture was then immediately transferred to the column closed at one end. After filling the column with polymerization mixture, the column was closed and kept at 45°C for 16 h. To remove the initiator and excess of monomer and cross-linker, columns were provided with new frits and flushed with a mixture of ethyl vinyl ether in DMSO and THF (20:40:40) for 2 h at a flow rate of 0.1 mL/min. Finally, they were flushed with $CHCl_3$ for 4 h at a flow rate of 0.2 mL/min. The synthesis of monoliths inside the glass reactor was accomplished via the same procedure as described above.

Quantification of Accessible Active Ester Groups

The chemically accessible active ester groups in the cyclopolymerization-derived monoliths were determined via the reaction of the active ester groups in the monolith with taurine. For this purpose, the monolith was conditioned with 0.1 M $NaHCO_3$ solution for 30 min at a flow rate of 0.1 mL/min. After that a solution of taurine (5% v/v) in 0.1 M $NaHCO_3$ was introduced into the monolith at a flow rate of 0.1 mL/min. The column was then sealed and kept at room temperature overnight. The following day the monolith was flushed consecutively with water and methanol and then dried *in vacuo*. Quantification of the accessible active ester groups was then accomplished by elemental analysis. Elemental analysis: found: C, 74.45; H, 5.87; N, 0.31; S, 0.55. Active ester: 0.22 mmol/g and accessible groups: 0.17 mmol/g.

Procedure for Doping and Conductivity Measurements

The monolith was prepared as described above in a stainless steel column. After flushing the monolith with CH_2Cl_2 for 30 min at a flow rate of 0.1 mL/min, the end fittings of the column were removed. The monolith was then dried *in vacuo* and transferred to the glove box. The weight of the monolith was noted. After providing the end fittings, a 5 wt.-% solution of the dopant in a suitable solvent (CH_2Cl_2 for I_2 and SbF_5, THF for $NO^+BF_4^-$) was injected into the monolith using luer syringe techniques. The monolith was then kept at room temperature. After 15 min the monolith was washed with the solvent used for doping. The end fitting of the column was removed and the monolith was then dried *in vacuo* to evaporate the solvent. The weight of the monolith was again noted. Resistance (R) of the monolith was measured by using a multimeter connected to both ends of the doped monolith. After measuring the resistance, the monolith was removed from the glove box and then the length (l) and area of cross-section (A) were noted. From these data the conductivity (σ) was calculated in $S \cdot cm^{-1}$ using the following equation.

$$\sigma = 1/\rho$$

$$\rho = RxA/l \qquad \rho \text{ is the resistivity}$$

Where, ρ is the resistivity in Ω.cm, R is the resistance in Ω, A is the area of cross-section in cm^2 and l is the length of the monolith in cm.

Immobilization of Trypsin

The cyclopolymerization-derived monolith was flushed with 50 mM HEPES buffer solution at pH 8 to remove any organic solvent in the monolith that might interfere with trypsin derivatization. A fresh solution of trypsin (3 mg/mL) in 50 mM HEPES buffer (100 mM NaCl, 10 mM $CaCl_2$) was prepared and injected into the monolith at a flow rate of 0.05 mL/min. The monolith was then sealed and kept for 4 h at room temperature and for another 24 h at 4°C. Finally, the monolith was flushed with 0.1M phosphate buffer solution containing 0.01 wt% Tween®20 and then with phosphate buffered saline (PBS) solution. After the immobilization the monolith was stored at 4°C.

Proteolytic Activity of the Immobilized Trypsin.

The proteolytic activity of the immobilized trypsin was monitored by measuring the hydrolysis products of a standard solution of *N*-α-benzoyl-DL-arginine-*p*-nitroanilide (BAPNA), i.e., *N*-α-benzoyl- DL-arginine (BA) and *p*-nitroaniline (PNA). A 0.25 mM standard solution of BAPNA in 50 mM HEPES buffer solution at pH 8 was introduced into the monolith at 37°C. After 10 min, the reaction mixture was eluted at a flow rate of 0.05 mL/min for 10 min. The conversion of BAPNA was calculated by comparing the area of BAPNA after proteolysis to the area of the standard BAPNA.

Supporting Information

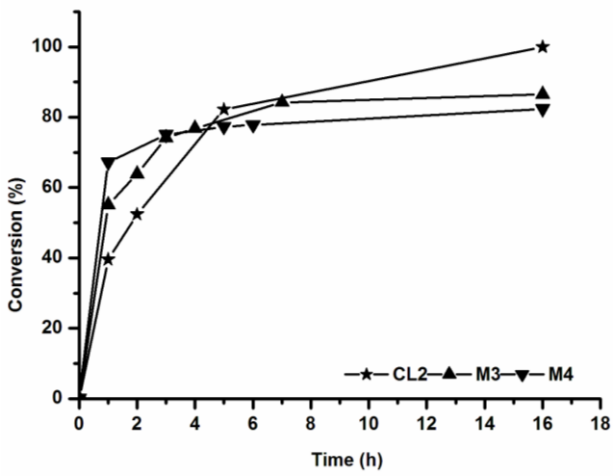

Figure S13. Kinetic plot obtained for the homopolymerizations of **M3, M4** and **CL2** using initiator **1** in 1,2-dichloroethane at 45°C.

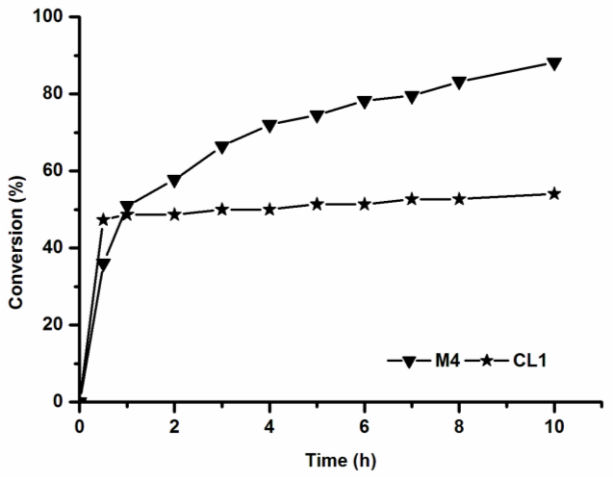

Figure S14. Kinetic plot obtained for the copolymerization of **M4** with **CL2** using initiator **I4** in 1,2-dichloroethane at 45°C.

6.5 Cyclopolymerization-Derived Block Copolymers of 4, 4-Bis(octyloxymethyl)-1,6-heptadiyne and Dipropargyl malonodinitrile

The Ru-based initiators $[RuCl_2(IMesH_2)(=CH\text{-}2\text{-}(2\text{-}PrO)\text{-}C_6H_4]$, $[RuCl_2(PCy_3)(IMesH_2)(CHPh)]$ ($IMesH_2$=1,3-bis(2,4,6-trimethylphenyl)imidazolin-2-ylidene), (PCy_3=tricyclohexylphosphine), tetrabutylammonium bromide (TBAB), potassium carbonate, 3-bromopyridine, quinuclidine and N,N-dimethylformamide were obtained from Aldrich Chemical Co. (Germany). Malanonitrile, propargyl bromide, 1-bromooctane, 4-bromo-1-butene, potassium hydroxide were purchased from Acros Organics (Germany). $[RuCl_2(3\text{-}Br\text{-}Py)_2(IMesH_2)(CHPh)]$ (**I5**),[1, 2] $[Ru(NCO)_2(IMesH_2)(=CH\text{-}2\text{-}(2\text{-}PrO)\text{-}C_6H_4]$(**I6**),[15]Mo(N-2,6-*i*-$Pr_2C_6H_3)(CHCMe_2Ph)(OCH(CH_3)_2)_2$ (**I8**)[16-18] were prepared according to the literature.

*$[Ru(N=C=O)_2(3\text{-}Br\text{-}Py)_2(IMesH_2)(CHPh)]$ (**I7**)*

$[RuCl_2(3\text{-}Br\text{-}Py)_2(IMesH_2)(CHPh)]$ (**I5**) **(**150 mg, 0.170 mmol**)** was dissolved in CH_2Cl_2 (3 mL). A slightly turbid solution of AgOCN (51 mg, 0.34 mmol, 2 equiv.) in DMF (1 mL) was added slowly and the mixture was stirred for 90 min. The precipitated AgCl was filtered off and the filtrate was evaporated to dryness. The residue was then redissolved in CH_2Cl_2 and flashed over a pad of alumina. The solvent was concentrated to approximately 0.5 mL. Then pentane was carefully layered over the solution, and cooled in the freezer overnight. The supernatant solution was decanted and the dark yellow solid was filtered and washed with pentane. Afterward, it was dried in vacuo to give **I7** (100 mg, 67%). ^{1}H NMR ($CDCl_3$): δ = 19.16 (Ru=C*H*), 8.58 (s, 2H), 8.2-8.32(m, 2H), 7.71(m, 1H), 7.29-7.52 (m, 3H), 7.18 (m, 2H), 6.75-6.81 (m, 4H), 6.49(m, 2H), 4.10 (m, 4H), 2.95 (s, 3H), 2.10- 2.51 (m, 14H).

*4,4-Bis(hydroxymethyl)-1,6-heptadiyne (**12**)*[13]

A solution of diethyl dipropargylmalonate (10 g, 42 mmol) in diethyl ether (100 mL) was added dropwise to a suspension of $LiAlH_4$ (3.2 g, 84 mmol) in 250 mL of diethyl ether at room temperature. The reaction mixture was stirred for 16 h at room temperature. After 16 h water was added dropwise to the reaction mixture till the effervescence ceased. The reaction mixture was then filtered through a shot pad of celite. The filtrate was dried over anhydrous $MgSO_4$ and ether removed *in vacuo* to give **12** as a white solid. (5.4 g, 85%): ^{1}H NMR ($CDCl_3$): δ = 3.71 (q, 4H, OC$\underline{H}_2$Me), 2.71 (brs, 2H, O$\underline{H}$), 2.35 (d, 4H, C$\underline{H}_2$-C≡CH), 2.04 (t, 2H, C≡C$\underline{H}$); ^{13}C NMR ($CDCl_3$): δ = 80.3 ($\underline{C}$≡CH), 71.3 (C≡$\underline{C}$H), 66.3 (O$\underline{C}H_2$), 42.1 ($CH_2\underline{C}HCH_2$), 21.7 (CH$\underline{C}H_2$-

C≡CH). IR (ATR mode): 3279 (s), 2934 (w), 1429 (w), 1318 (w), 1106 (w), 1023 (vs), 979 (w), 868 (w) cm^{-1}. GC-MS calcd. for $C_9H_{12}O_2$: *m/z*=152.19; found: 152 (M^{+})

*4,4-Bis(octyloxymethyl)-1,6-heptadiyne (**M5**).*

To a mixture of 4,4-bis(hydroxymethyl)-1,6-heptadiyne (1.5 g, 9.8 mmol) and KOH (2.2 g, 40 mmol) in DMSO (25 mL) was added 1-bromooctane (4.80 g, 24.8 mmol). The reaction mixture was stirred at room temperature for 24 h. After 24 h, water was added and the mixture was extracted with diethyl ether (3 × 50 mL). The combined organic layers were successively washed with water (50 mL) and brine (25 mL) and then dried over anhydrous $MgSO_4$. Finally, the solvent was evaporated *in vacuo*. The residue was distilled to give **M5** (2.6 g, 70%) as colourless viscous liquid. ^{1}H NMR ($CDCl_3$): δ = 3.42 (d, 4H, OC*H*$_2$CH$_2$), 3.37 (s, 4H, OC*H*$_2$C), 2.36 (d, 4H, (C*H*$_2$-C≡CH), 1.96 (t, 2H, C≡C*H*) 1.53 (m, 4H, OCH$_2$C*H*$_2$), 1.27 (bm, 20H, C*H*$_2$), 0.88 (t, 6H, C*H*$_3$); ^{13}C NMR ($CDCl_3$): *δ* = 81.2 (*C*≡CH), 71.7 (O*C*H$_2$C), 71.4 (C≡*C*H), 70.3 (O*C*H$_2$CH$_2$), 41.9 (CH$_2$*C*HCH$_2$), 32.0 (OCH$_2$*C*H$_2$), 29.7, 29.6, 29.5, 26.3, 22.8 (*C*H$_2$), 22.0 (CH*C*H$_2$-C≡CH), 14.3(*C*H$_3$). IR (ATR mode): 3313 (s), 2924 (vs), 2856 (s), 2119 (w), 1465 (m), 1376 (m), 1105 (vs), 722 (w) cm^{-1}. Elemental Analysis: calcd for $C_{25}H_{44}O_2$: C, 79.73; H, 11.78, found: C, 79.86; H, 11.78.

*Dipropargyl malonodinitrile (**M6**)*[19]

In a two necked flask equipped with reflux condenser, a mixture of malononitrile (10 g, 151.5 mmol), propargylbromide (39.50 g, 333.3 mmol) and TBAB (2.0 g, 6.2 mmol) were stirred at room temperature. After 30 min, anhydrous K_2CO_3 (46.00 g, 332.8 mmol) was added slowly at 0^{o}C by Schlenk techniques. The reaction mixture was then stirred at room temperature for 16 h. After 16 h the crude reaction mixture was dissolved in water (150 mL) and extracted with CH_2Cl_2 (2 × 100 mL). The combined organic extracts were washed with water (50 mL), brine (50 mL) and dried over anhydrous $MgSO_4$, then the solvent was evaporated *in vacuo*. The crude product was purified by silica gel column chromatography using 10% EtOAc in hexane as eluent to afford **M6** (16.6 g, 78%) as white solid. ^{1}H NMR ($CDCl_3$): δ = 3.06 (d, 4H, C*H*$_2$-C≡CH), 2.43 (t, 2H, C≡C*H*); ^{13}C NMR ($CDCl_3$): *δ* = 113.6 (*C*N), 75.9 (*C*≡CH), 74.0 (C≡*C*H), 36.0 (CH$_2$*C*HCH$_2$), 27.4 (CH*C*H$_2$-C≡CH). IR (ATR mode): 3289 (s), 2200 (w), 1423 (m), 1272 (m), 688 (vs), 661 (vs) cm^{-1}. Elemental Analysis: calcd for $C_9H_6N_2$: C, 76.04; H, 4.25; N, 19.71, found: C, 76.01; H, 4.22; N, 19.70.

Cyclopolymerization using Ru-based initiators

All polymerizations with initiators **I5-I7** was carried out under a N_2 atmosphere using Schlenk techniques. A typical polymerization procedure using Ru-based initiators was as follows:

A 25 mL Schlenk flask was charged with **M5** (100 mg, 0.266 mmol) dissolved in 9 mL of 1, 2-dichloroethane. In a separate vial, **I7** (3.4 mg, 0.0050 mmol) was dissolved in 1, 2-dichloroethane (1 mL). The catalyst solution was then injected to the monomer solution via a syringe under vigorous stirring. The reaction was carried out at 50^{o}C under N_2 atmosphere. Conversion of the monomer was monitored by GC-MS using *n*-dodecane (75 µL) as an internal standard. After the completion of the reaction, 0.5 mL of ethyl vinyl ether was added and the mixture was stirred for another 30 min. The solvent was removed *in vacuo*, and then 10 mL of methanol were added. After exposure to ultrasonic conditions, the product was centrifuged and dried *in vacuo* to afford poly(**M5**) as dark violet solid in 43% yield. ^{1}H NMR ($CDCl_3$): δ = 6.68 (bm, 2H, C*H*=C*H*), 3.47-3.38 (bm, OCH_2), 2.65 (bm, 2H, CqCH_2), 1.61-1.58 (bm, OCH_2CH_2), 1.27 (bm, CH_2), 0.87 (bm, CH_3); ^{13}C NMR ($CDCl_3$): δ = 138.6 (*C*H=C), 123.5 (CH=*C*), 74.5 (OCH_2C), 71.7 (OCH_2CH_2), 44.9 (C=CCH_2C), 40.4 (Cq), 32.0 (OCH_2CH_2), 29.8, 29.7, 29.5, 26.3, 22.8 (CH_2), 14.3 (CH_3). IR (ATR mode): 2924 (s), 2852 (s), 2360 (w), 1464 (s), 1376 (w), 1223 (s), 1108 (vs), 947 (s), 721 (w), 628 (w) cm^{-1}

5-(2,2-Bis((octyloxy)methyl)pent-4-yn-1-yl)-2,2-bis((octyloxy)methyl)-2,3-dihydro-1H-indene (11). This compound was formed as a result of backbiting and was isolated from the polymer by washing with acetone. ^{1}H NMR ($CDCl_3$): δ = 7.07-6.98 (m, 3H, Ar-H), 3.44-3.37 (m, 12H, OCH_2), 3.23-3.14 (m, 4H, OCH_2), 2.80 (s, 4H, Ar-CH_2), 2.67 (s, 2H, Ar-CH_2), 2.15 (d, 2H, CH_2-C≡CH), 2.03 (t, 1H, C≡CH), 1.56 (m, 8H, CH_2), 1.29 (m, 40H, CH_2), 0.89 (t, 12H, CH_3); ^{13}C NMR ($CDCl_3$): δ = 142.3, 140.2, 135.6 , 128.7, 127.2, 124.3 (Ar), 82.2 (C≡*C*H), 73.9, 71.6, 71.4, 71.3(OCH_2C), 70.4(*C*≡CH) 48.3, 42.9, 38.9, 38.8, 36.8, 32.0, 29.8, 29.8, 29.6, 29.5, 26.5, 26.4, 22.8 (CH_2), 14.3 (CH_3).

Cyclopolymerization using Mo-based initiators

All polymerizations with initiators **I8** was carried out under N_2 atmosphere in a glove box. A typical polymerization procedure using Mo-based initiators was as follows. Initiator **I8** (3.8 mg, 0.0070 mmol) was dissolved in 3 mL of THF. Quinuclidine (0.86 mg, 0.0070 mmol) was added to the solution and stirred at room temperature. After 20 min the vial was cooled to -30^{o}C. A solution of **M6** (50 mg, 0.352 mmol) in 2 mL THF was added all at once to the vigorously

stirred solution. After 2 h, ferrocene aldehyde (16.5 mg, 0.0770 mmol) was added and stirred for another hour at room temperature. The mixture was concentrated and acetone was added. After exposure to ultrasonic conditions, the product was centrifuged and dried *in vacuo* to afford poly(**M6**)$_{50}$ as dark red solid in 31 mg (61% yield). IR (ATR mode): 2962 (w), 2853 (w), 2337 (w), 2251 (s) 1702 (w), 1434 (s), 1138 (s), 1240 (s), 1083 (w) 956 (vs), 763 (w), 620 (w) cm^{-1}.

*Synthesis of poly(**M5**)-b-poly(**M6**) using **I8***

A typical procedure for the synthesis of the AB-type block copolymer using Mo-based initiators is as follows. In a 25 mL Schlenk flask initiator **I8** (5.5 mg, 0.011 mmol) was dissolved in 3 mL of THF. Quinuclidine (1.8 mg, 0.016 mmol) was added to the solution and the mixture was stirred at room temperature. After 20 min, the vial was cooled to -30^{o}C. A solution of **M6** (22.0 mg, 0.155 mmol) in 2 mL of THF was added all at once to the vigorously stirred solution. After the consumption of **M5** (monitored by GC-MS), a – 30 ^{o}C solution of **M5** (100 mg, 0.266 mmol) in 3 mL of THF was injected using a syringe. The reaction was then stirred for another 2 h. Ferrocenealdehyde (34.0 mg, 0.106 mmol) was added and the mixture was stirred for another hour at room temperature. The mixture was then concentrated and acetone was added. After exposure to ultrasonic conditions, the product was centrifuged and dried *in vacuo* to afford poly(**M6**)$_{15}$-b-poly(**M5**)$_{25}$ as a dark violet solid in 118 mg (86% yield). ^{1}H NMR (THF-*d8*): δ = 6.75 (bm, 2H, C*H*=C*H*), 3.42-3.37 (bm, OC*H*$_2$), 2.62 (bm, 2H), 1.58 (bm, OCH$_2$C*H*$_2$), 1.32 (bm, C*H*$_2$), 0.89(bm, C*H*$_3$); ^{13}C NMR ($CDCl_3$): δ = 139.5(*C*H=C), 124.4(CH=*C*), 118.2 (-*C*N), 75.6 (O*C*H$_2$C), 72.3 (O*C*H$_2$CH$_2$), 46.1, 40.9 (Cq), 30.6, 30.5, 27.4, 23.8, , 14.1 (*C*H$_3$). IR (ATR mode): 2925 (s), 2853 (s), 2334 (w), 2250 (m) 1777 (w), 1459 (s), 1373 (s), 1225 (s), 1106 (vs), 949 (s), 804 (w), 629 (s) cm^{-1}

*Poly(**M5**)-b-poly(**M6**) containing R-Si(OCH$_2$CH$_3$)$_3$ end group*

For synthesizing telechelic polymer, **I8** (4.6 mg, 9 µmol) was dissolved in 1 mL of THF. Quinuclidine (1.8 mg, 0.016 mmol) was added to the solution and the mixture was stirred at room temperature. After 20 min, the vial was cooled to -30^{o}C. A solution of **M6** (12.6 mg, 0.090 mmol) in 2 mL of THF was added all at once to the vigorously stirred solution. After the consumption of **M5** (monitored by GC-MS), a – 30^{o}C solution of **M5** (100 mg, 0.266 mmol) in 2 mL of THF was injected using a syringe. The reaction was then stirred for another 2 h. A solution of 3-isocyanatopropyltriethoxysilane (22.3 mg, 0.090 mmol) was added and the mixture was stirred at 45^{o}C for 6 hours. The mixture was then concentrated and acetone was added. After exposure to ultrasonic conditions, the product was centrifuged and dried *in vacuo* to afford

the telechelic poly(**M6**)$_{15}$-b-poly(**M5**)$_{25}$ as a dark violet solid in 104 mg (93% yield). ^{1}H NMR (THF-*d8*): δ = 6.76 (bm, 2H, C*H*=C*H*), 3.43-3.37 (bm, OCH_2), 2.62 (bm, 2H), 1.58 (bm, OCH$_2$CH_2), 1.32 (bm, CH_2), 0.89(bm, CH_3); triethoxysilyl end group: δ = 3.78 (OCH_2) and 1.18(CH_3).

*Grafting of the telechelic poly(**M5**)-b-poly(**M6**) onto silica surface*

The Si(OCH$_2$CH$_3$)$_3$-telechelic poly(**M5**)-*b*-poly(**M6**) was loaded on silica 60 surface following a previously published procedure.[20] For this purpose, silica 60 was dried under vaccum at 20°C for two days. Si(OCH$_2$CH$_3$)$_3$-telechelic poly(**M5**)-*b*-poly(**M6**) 100 mg was dissolved in anhydrous THF and added to 3.0 g of silica 60. The reaction mixture was then refluxed at 70°C. After 6 h, the silica was filtered off, washed with THF and dried *in vacuo*. Analysis found. C 1.065% (0.89 mmol/g).

Supporting Information

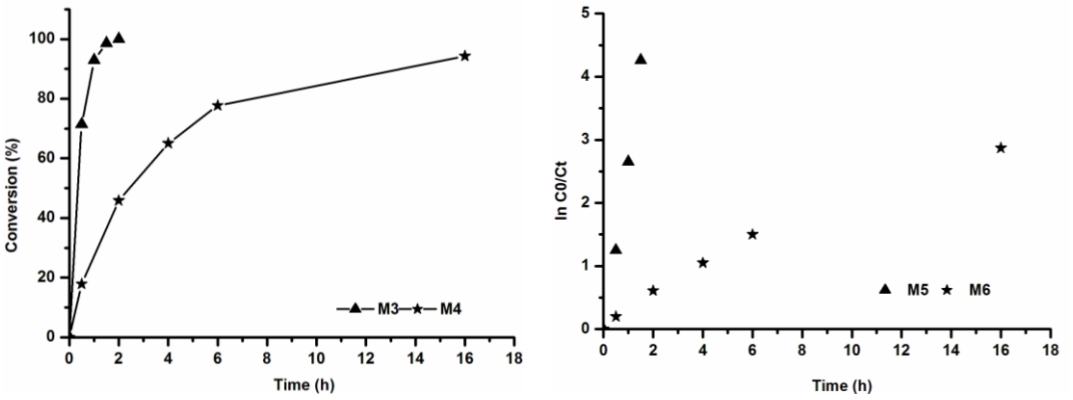

Figure S15. Kinetic plot obtained for the synthesis of poly(**M5**)-*b*-poly(**M6**) using **I6** (left), 1st order plot (right).

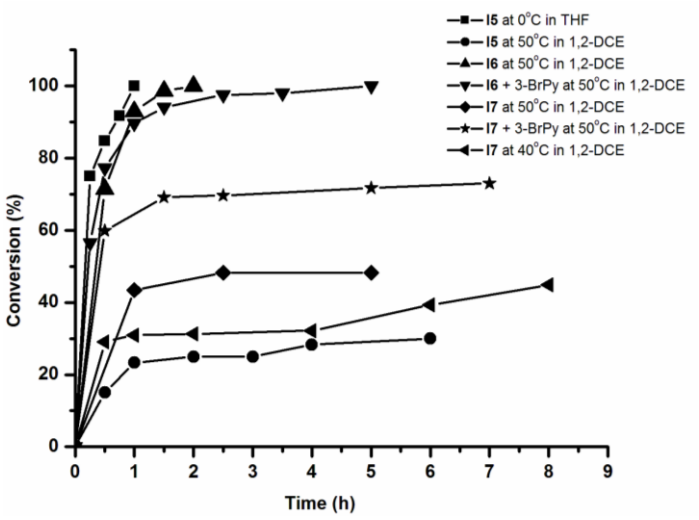

Figure S16. Kinetic plot obtained for the polymerization of **M5** using **I5-I7** at different reaction conditions.

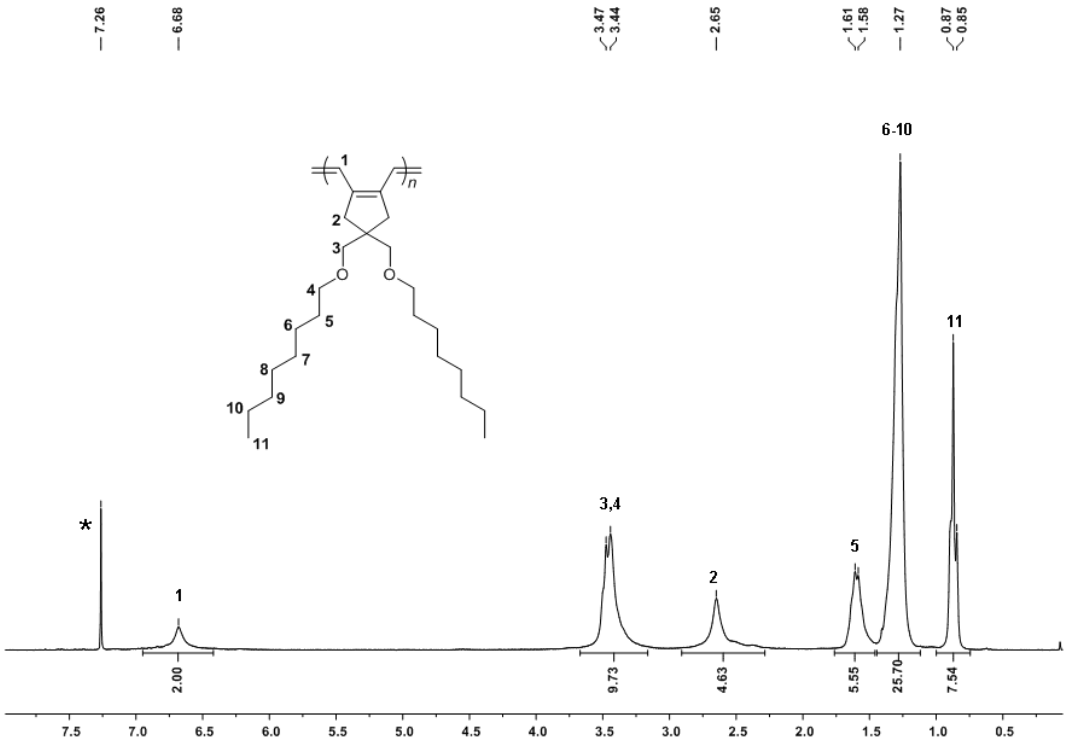

Figure S17. ^{1}H NMR spectrum of poly(**M5**)$_{25}$ synthesized by catalyst **I6** (*denotes $CDC1_3$).

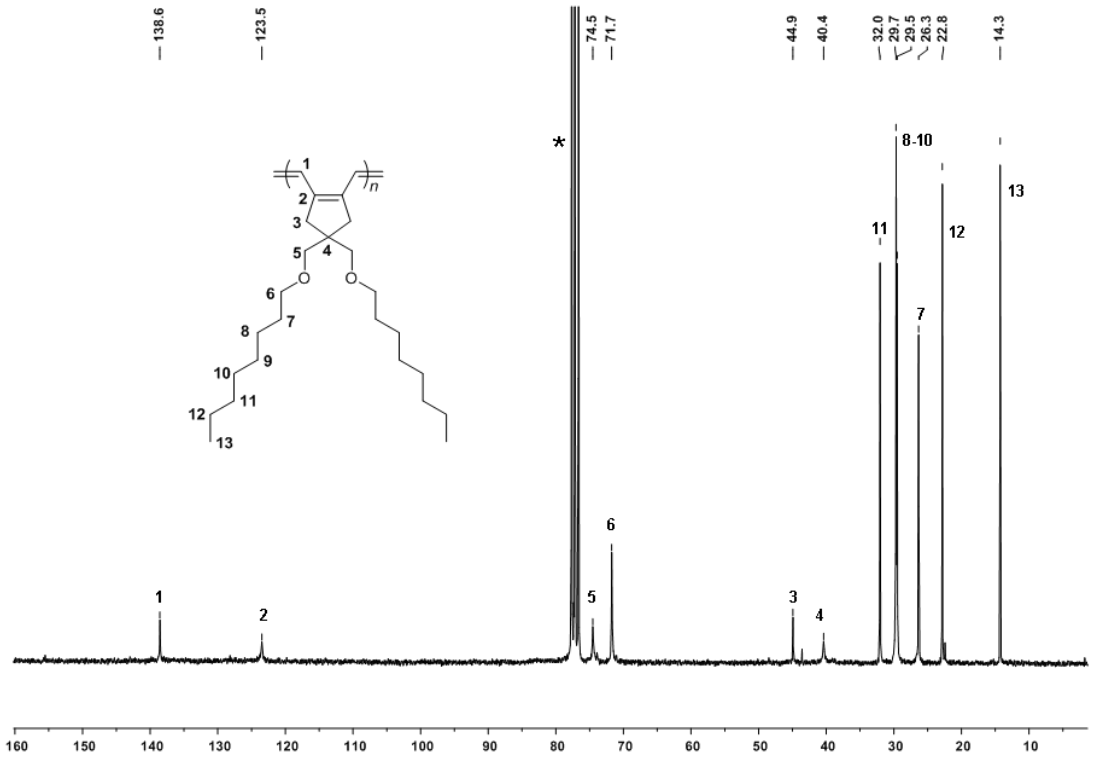

Figure S18. ^{13}C NMR spectrum of poly(**M5**)$_{25}$ synthesized by catalyst **I6** (*denotes $CDC1_3$).

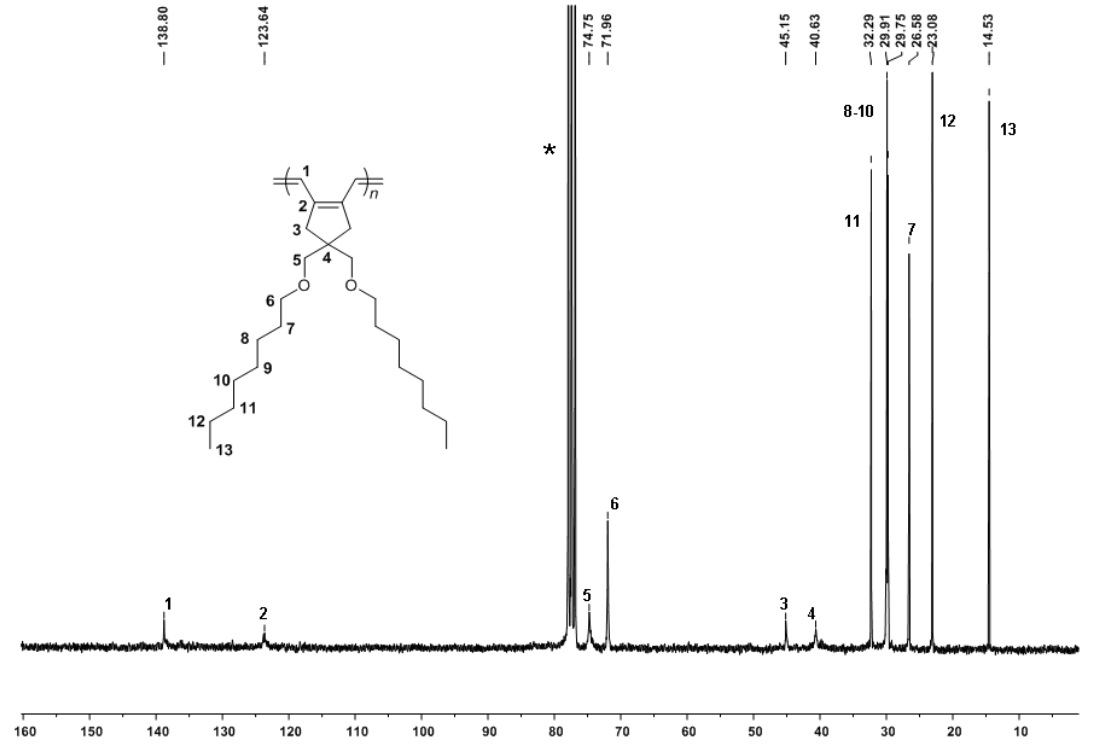

Figure S19. ^{13}C NMR spectrum of poly(**M5**)$_{25}$ synthesized by catalyst **I8** in presence of quinuclidine (*denotes $CDC1_3$).

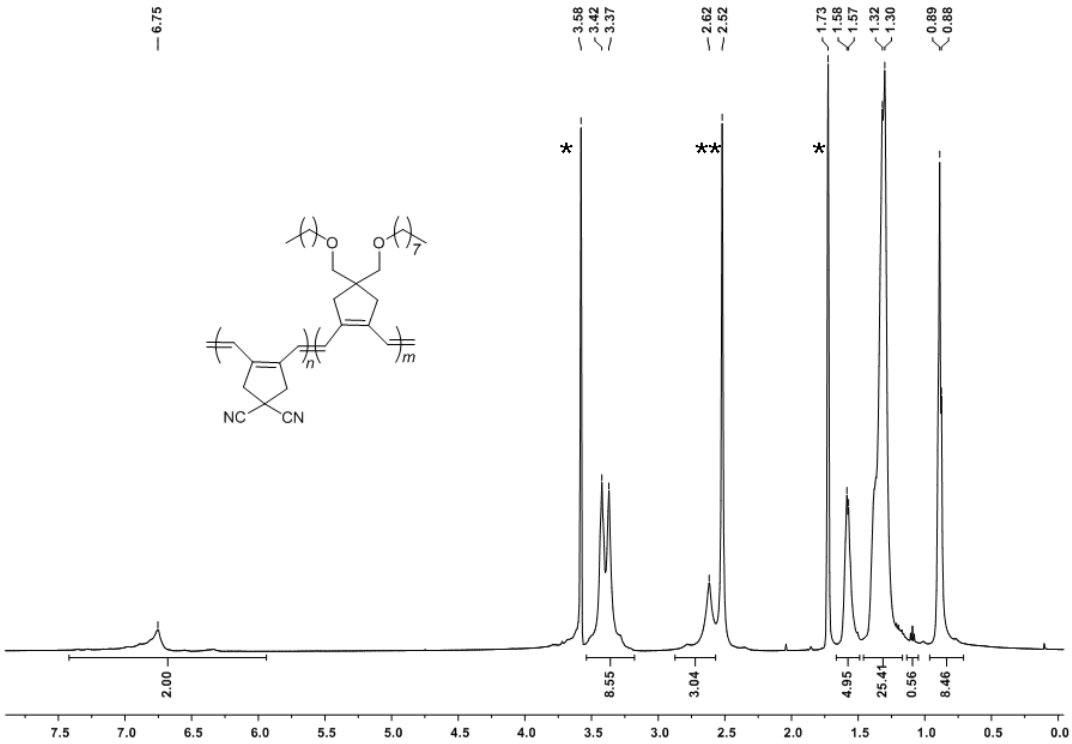

Figure S20. ^{1}H NMR spectrum of poly(**M6**)$_{15}$-*b*-poly(**M5**)$_{25}$ synthesized by catalyst **I8** in presence of quinuclidine (*denotes THF-*d8* and **denotes water).

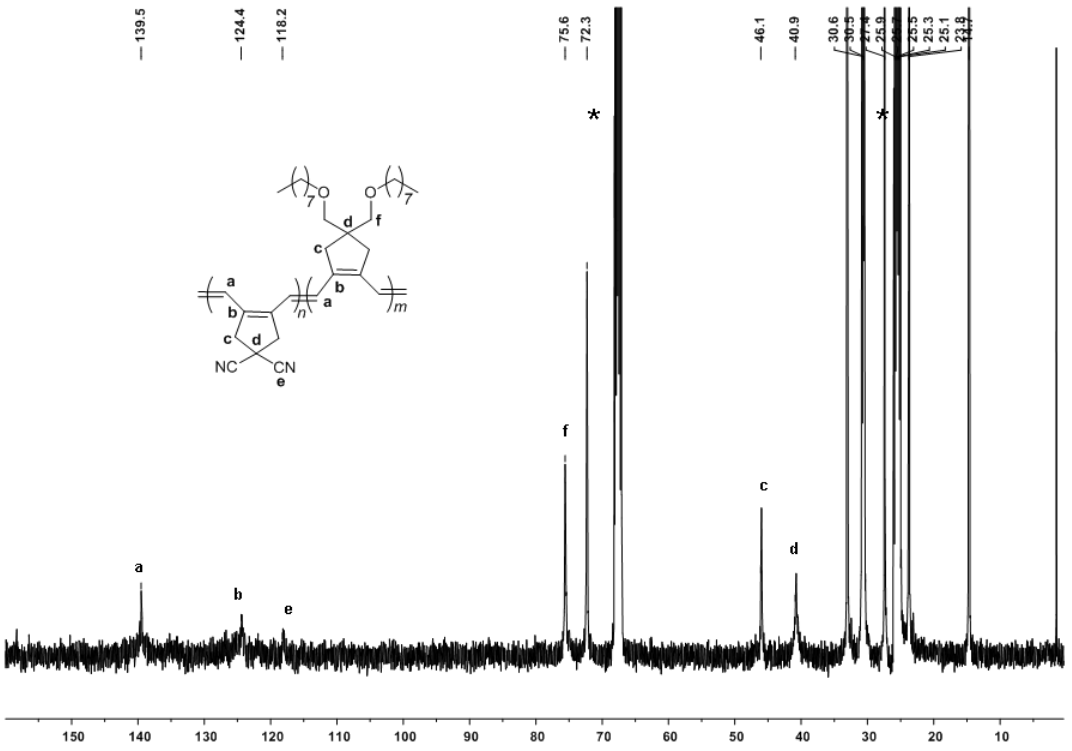

Figure S21. ^{13}C NMR spectrum of poly(**M6**)$_{15}$-*b*-poly(**M5**)$_{25}$ synthesized by catalyst **I8** in presence of quinuclidine (*denotes THF-*d8*).

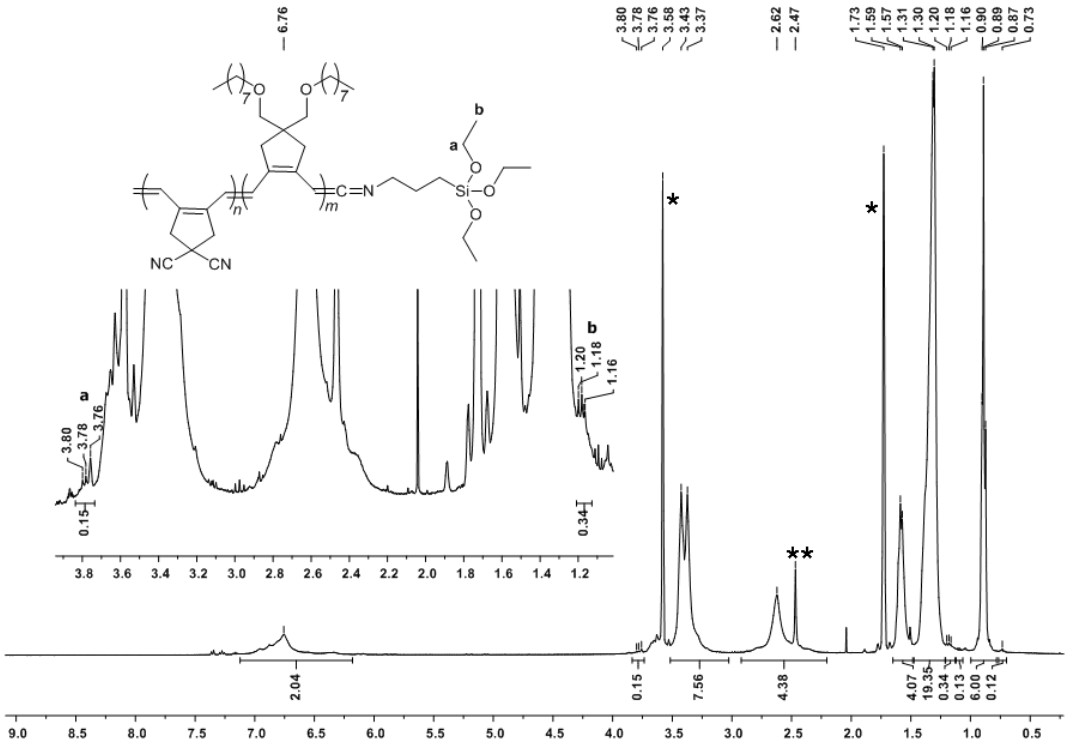

Figure S22. ^{1}H NMR spectrum of telechelic-poly(**M6**)$_{10}$-*b*-poly(**M5**)$_{30}$ synthesized by catalyst **I4** in presence of quinuclidine (*denotes THF-*d8* and **denotes water).

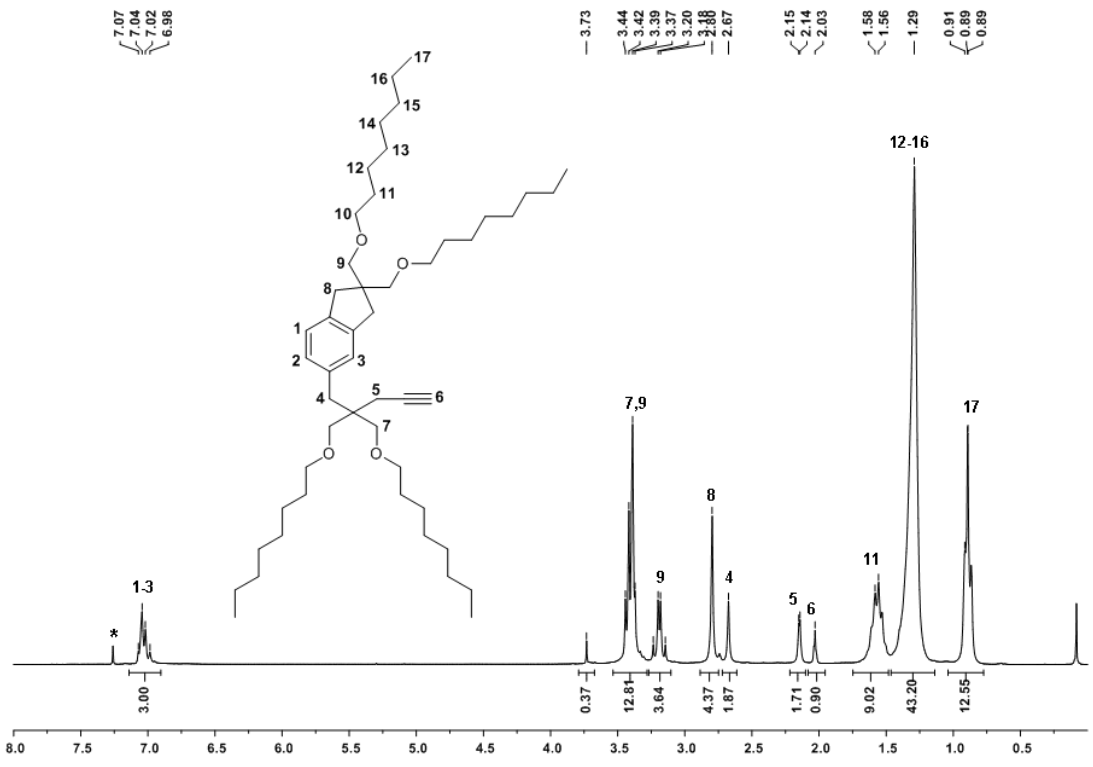

Figure S23. ^{1}H NMR spectrum of of dimmer **11** (*denotes $CDC1_3$).

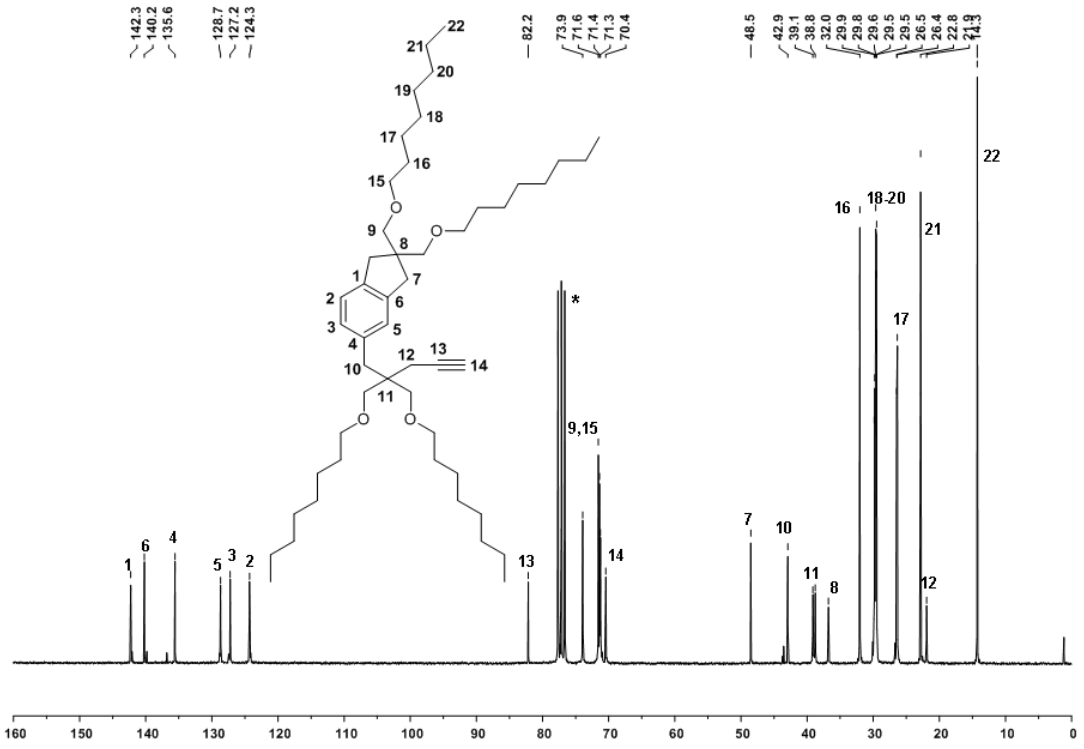

Figure S24. ^{13}C NMR spectrum of dimmer **11** (*denotes $CDC1_3$).

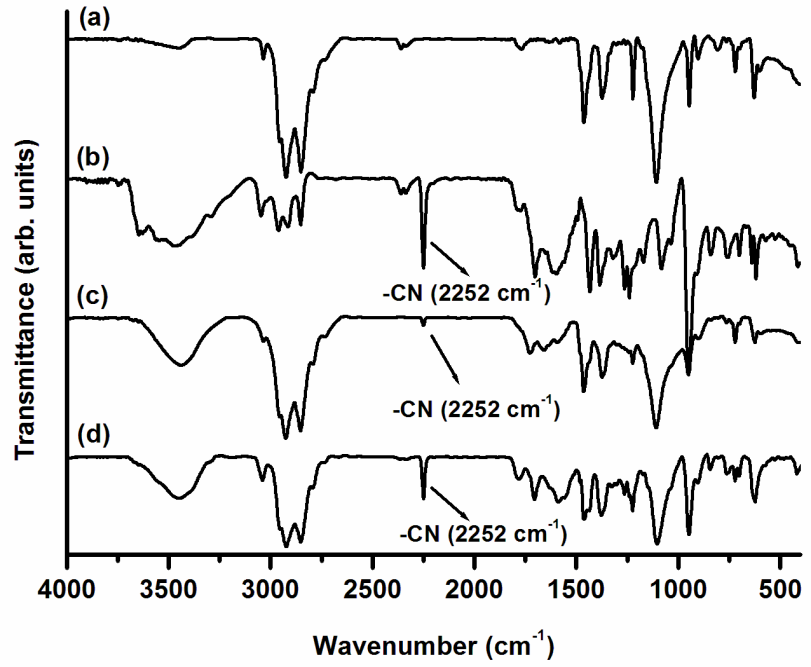

Figure S25. IR spectra of the homo and block polymers of **M5** and **M6** in ATR mode. (a) poly(**M5**), (b) poly(**M6**), (c) poly(**M5**)-*b*-poly(**M6**), (d) poly(**M6**)-*b*-poly(**M5**).

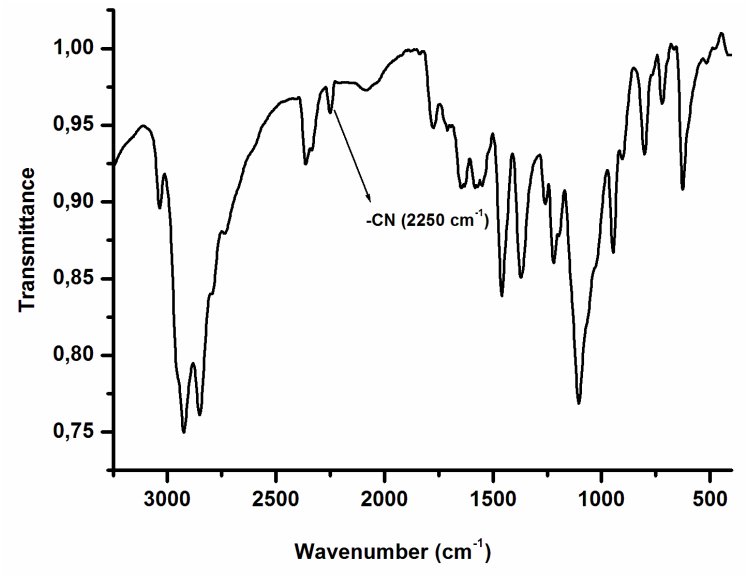

Figure S26. IR spectrum of the telechelic- poly(**M6**)-*b*-poly(**M5**) in ATR mode.

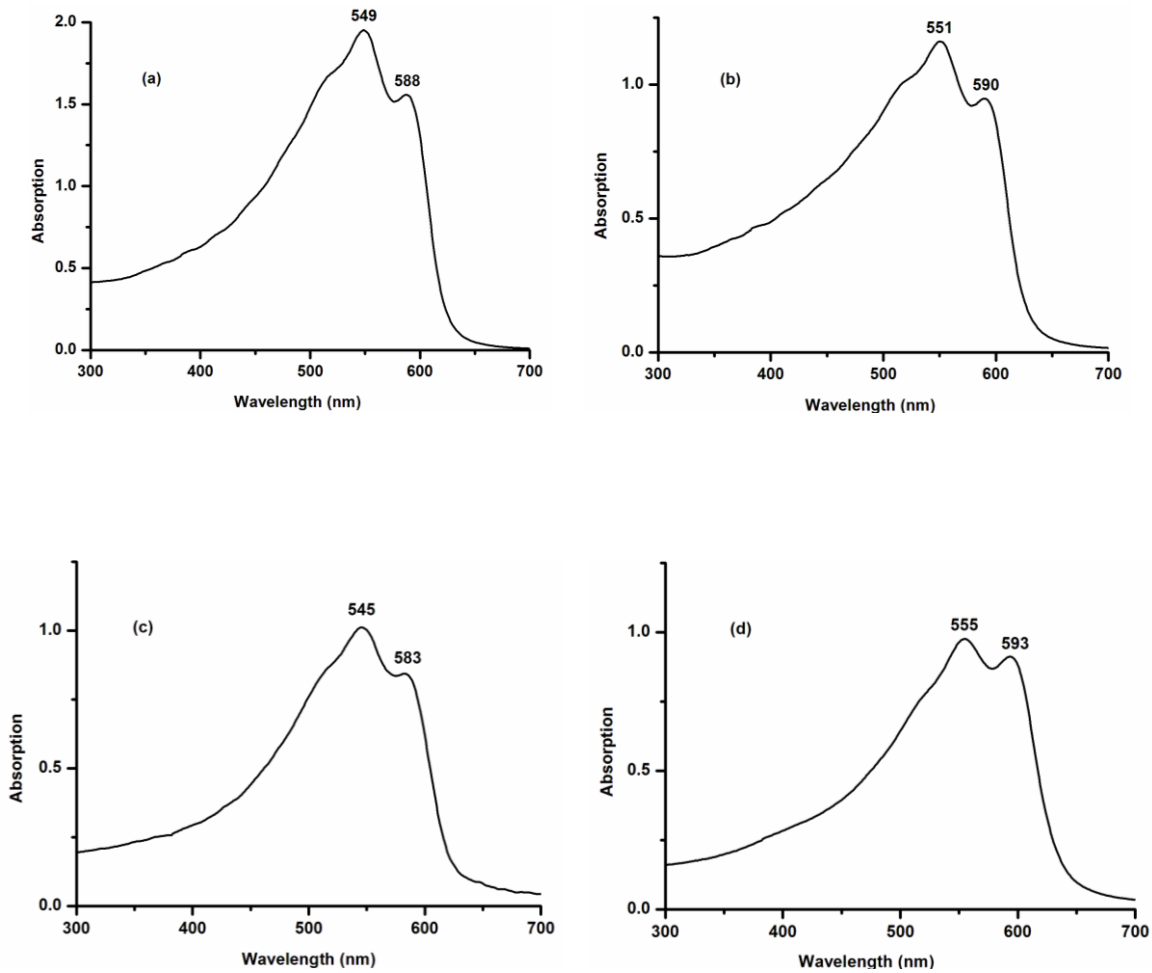

Figure S27. UV-visible spectra of the homo and block polymers in $CHCl_3$. (a) poly(**M5**) prepared by **I6**, (b) poly(**M5**) prepared by **I8**, (c) poly(**M5**)-*b*-poly(**M6**) prepared by **I8**, (d) poly(**M6**)-*b*-poly(**M5**) prepared by **I8**.

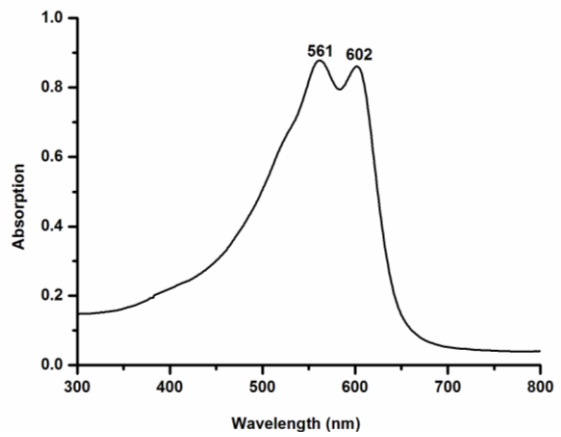

Figure S28. UV-visible spectra of the telechelic- poly(**M6**)-*b*-poly(**M5**) in $CHCl_3$.

6.6 References

[1] T. L. Choi, R. H. Grubbs, *Angew. Chem. Int. Ed.* **2003**, *42*, 1743.

[2] J. A. Love, J. P. Morgan, T. M. Trnka, R. H. Grubbs, *Angew. Chem. Int. Ed.* **2002**, *41*, 4035.

[3] J. K. Stille, D. A. Frey, *J. Am. Chem. Soc.* **1959**, *81*, 4273.

[4] S. H. Lubbad, M. R. Buchmeiser, *Macromol. Rapid Commun.* 2002, *23*, 617.

[5] F. Sinner, M. R. Buchmeiser, *Macromolecules* 2000, *33*, 5777.

[6] A. Boulares-Pender, A. Prager-Duschke, C. Elsner, M. R. Buchmeiser, *J. Appl. Poly. Sci.* 2009, *112*, 2701.

[7] H. Liu, S. Wan, P. E. Floreancig, *J.Org. Chem.* **2005**, *70*, 3814.

[8] Z. Szlávik, G. Tárkányi, Z. Skribanek, E. Vass, J. Rábai, *Org. Lett.* **2001**, *3*, 2365.

[9] T. Nguyen, M. Rubinstein, C. Wakselman', *Synth. Commun.* **1983**, *13*, 81.

[10] J. O. Krause, S. H. Lubbad, O. Nuyken, M. R. Buchmeiser, *Macromol. Rapid Commun.* **2003**, *24*, 875.

[11] J. O. Krause, O. Nuyken, M. R. Buchmeiser, *Chem. Eur.J.* **2004**, *10*, 2029.

[12] L. Q. Xu, F. Yao, G.-D. Fu, L. Shen, *Macromolecules* 2009, *42*, 6385.

[13] H. H. Fox, M. O. Wolf, R. O'Dell, B. L. Lin, R. R. Schrock, M. S. Wrighton, *J. Am. Chem. Soc.* **1994**, *116*, 2827.

[14] T. S. Halbach, J. O. Krause, O. Nuyken, M. R. Buchmeiser, *Macromol. Rapid. Commun.* **2005**, *26*, 784.

[15] P. S. Kumar, K. Wurst, M. R. Buchmeiser, *Chem. Asian. J.* **2009**, *4*, 1275.

[16] H. H. Fox, K. B. Yap, J. Robbins, S. Cai, R. R. Schrock, *Inorg. Chem.* **1992**, *31*, 2287.

[17] . H. Oskam, H. H. Fox, K. B. Yap, D. H. McConville, R. O`Dell, B. J. Lichtenstein, R. R. Schrock, *J. Organomet. Chem.* **1993**, *459*, 185.

[18] R. R. Schrock, J. S. Murdzek, G. C. Bazan, J. Robbins, M. DiMare, M. O'Regan, *J. Am. Chem. Soc.* **1990**, *112*, 3875.

[19] E. Diez-Barra, A. de la Hoz, A. Moreno, P. Sanchez-Verdu, *J. Chem. Soc., Perkin Trans. 1* **1991**, 2589.

[20] M. Mayr, M. R. Buchmeiser, K. Wurst, *Adv. Syn. Catal.* **2002**, *344*, 712.

7

Curriculum Vitae

Sudheendran Mavila

Date of birth: 07.12.1978

Nationality: Indian

Education

- June/**2008**-December/**2011**: PhD in Polymer Chemistry, Institut für Polymer chemie, Universität Stuttgart, Stuttgart, Germany.
- October/**2000**- March/**2003**: Masters in Organic Chemistry (70%), School of Chemical Sciences, Mahatma Gandhi University, Kerala, India
- March/**1996**-March/**1999**: Bachelors in Chemistry (71%), Govt. Brennen College, Kannur University, Kerala, India.

Employment/positions

- Feb/**2004**-May/**2008**: **Senior Scientist-Synthetic Organic Chemistry** at Syngene International Ltd. (The Research and Development division of Biocon India Ltd), Bangalore, India.
- Aug/**2002**-Dec/**2002**: Research Project Student at Indian Institute of Technology, Kanpur, India/ Research project Supervisor: **Prof. Dr. F. A. Khan**/ Project thesis title: "Investigation of alkylation and nucleophilic reactions to 1, 4, 5, 6- tetrabromo-7, 7-dimethoxy [2, 2, 1] bicyclo-hept-5-ene-2-one".

Academic achievements

- Nov/**2008**-Dec/**2009**: Graduate Student in BuildMoNa Graduate School of Excellence, University of Leipzig, Germany, funded within the German Excellence Initiative.
- Qualified **Graduate Aptitude Test in Engineering (GATE)-2003**, For Junior Research Fellowship conducted by the Indian Institute of Technology (IITs) and Indian Institute of Science (IISc.), India with a percentile score of **85.4%**

List of Publications

1. A Continuous Bioreactor Prepared via the Immobilization of Trypsin on Aldehyde Functionalized, Ring-Opening Metathesis Polymerization-Derived Monoliths, **M. Sudheendran**, M. R. Buchmeiser, *Macromolecules* **2010**, *43*, 9601.

2. Heterogenization of a Chiral Bimetallic Catalyst on a ROMP-Derived Monolithic Support: Applications in Enantioselective Michael Addition, Simon Eitel, **M. Sudheendran**, R. Peters, M. R. Buchmeiser, (Manuscript in preparation, 2011).

3. Cyclopolymerization-Derived Conductive Monolithic Media For Continuous Heterogeneous (Electro-) Catalysis, **M. Sudheendran**, E. Roeben, P. S. Kumar, M. R. Buchmeiser, (Manuscript in preparation, 2011).

4. Cyclopolymerization-Derived Block Copolymers of 4,4-Bis(octyloxymethyl)-1,6-heptadiyne and Dipropargyl malonodinitrile, **M. Sudheendran**, M. R. Buchmeiser, (Manuscript in preparation, 2011).

5. Conductivity of p-Doped, Cyclopolymerization-Derived Poly(ene)s, P. S. Kumar, A. Freyer, **M. Sudheendran**, W. Knolle, and M. R. (Submitted).

Posters and International Conferences

1. Cyclopolymerization-Derived Conductive Monolithic Media. **M. Sudheendran**, P. S. Kumar, M. R. Buchmeiser, *The 3rd EuCheMS Chemistry Congress "Chemistry-the Creative Force"*, August 29-September 2, 2010, Nurnberg, Germany.

2. Cyclopolymerization-Derived Conductive Monolithic Media For Continuous Heterogeneous (Electro-) Catalysis, **M. Sudheendran**, E. Roeben, P. S. Kumar, M. R. Buchmeiser, *The 19th International Symposium on Olefin Metathesis and Related Chemistry* (ISOM XIX), July 10-15, 2011, Rennes, France.

Oral Presentations

- A Continuous Bioreactor Prepared via the Immobilization of Trypsin on Aldehyde Functionalized, Ring-Opening Metathesis Polymerization-Derived Monoliths, 15. Tag der Organischen Chemie, 14th October 2011, Institut für Organische chemie, Universität Stuttgart.